TOPOGRAPHIC AND SURFACE CHEMICAL ASPECTS OF THE ADHESION OF STRUCTURAL EPOXY RESINS TO PHOSPHORUS OXO ACID TREATED ALUMINUM ADHERENDS

Gary Alan Nitowski

Dissertation submitted to the Faculty of the Virginia Polytechnic Institute and State University in partial fulfillment of the requirements for the degree of

Doctor of Philosophy
in
Materials Engineering Science

John G. Dillard, Co-Chair
Karl Wefers, Co-Chair
David A. Dillard
William T. Reynolds
Thomas C. Ward
James P. Wightman

August 26, 1998

Blacksburg, Virginia

Keywords: Aluminum Surface Treatment, Phosphorous Acid, Vinylphosphonic Acid, Epoxy, Adhesive Bonding, Joint Durability

TOPOGRAPHIC AND SURFACE CHEMICAL ASPECTS OF THE ADHESION OF STRUCTURAL EPOXY RESINS TO PHOSPHORUS OXO ACID TREATED ALUMINUM ADHERENDS

Gary Alan Nitowski

(ABSTRACT)

Structural adhesive bonding offers several advantages over other types of joining. These include improved stress distribution and increased design flexibility. Adhesive bonding is important in aerospace, automotive, and packaging applications. However, the full potential of the technology has not been exploited because the understanding of the basic mechanisms of adhesion and adhesion failure is incomplete.

This investigation elucidates the chemical and mechanical mechanisms responsible for durable adhesion of epoxy resins to phosphorus oxo acid treated aluminum alloys. By systematically altering the adherend surface chemistry, surface topography, and adhesive formulation, combined with accelerated testing, the chemical and mechanical factors that influence the properties of adhesively bonded aluminum are isolated and assessed.

It is postulated that a combination of two factors determines the strength and environmental durability of epoxy-bonded aluminum. One is the formation of hydrolytically stable, primary bonds between the adhesive and the adherend, and the second is the hydrolytic stability of the surface oxide, which is always present on the surface of aluminum and aluminum alloys.

These conditions can best be met by chemical pretreatment of the oxide surface, which renders the oxide insoluble and creates, at the same time, functional surface sites. These sites can form chemical bonds with reactive components of the adhesive.

Morphological and mechanical alteration of the metal surface oxide through hydroxide formation

requires liquid water. Liquid water can only form by capillary condensation in interfacial gaps from molecularly diffusing water. A hydrolytically stable oxide will prevent bond failure due to mechanical weakening of the substrate surface, while a high density of hydrolytically stable surface bonding sites will minimize the occurrence of capillary gaps at the interface, thus decreasing the formation of liquid water. It is shown that highly chemically active, although not inherently stable, oxide surfaces can provide environmentally stable adhesive bonds. Conversely, certain highly stable oxide surfaces with few chemically active sites provide no environmental stability to adhesive joints, regardless of the topography of the surface.

Grant Information

This work was made possible by the Aluminum Company of America (ALCOA), through the sponsorship of Dr. Karl Wefers (retired). With a commitment to fundamental research, a new understanding of the adhesive bonding and the corrosion inhibition of aluminum were obtained.

Dedication

This dissertation is dedicated to the memory of Dr. Pam Davar Basu. Her enthusiasm for science was a motivating force in pursuing this effort. Her friendship lifted my spirits during difficult times. Her mentoring enabled me to grow professionally. Her companionship is truly missed.

Author's Acknowledgments

Acknowledgments of assistance and support for completion of this dissertation seem endless. I must express gratitude to Co-Chair, Professor John. G. Dillard and to Dr. Karl Wefers for their assistance, persistence, and particularly for their patience in finishing this document. Without their sponsorship and knowledge, this dissertation would not be possible.

My deepest appreciation is also extended to Professor Peter N. Henrikson, University of Akron, for teaching me the theory and practice of Inelastic Electron Tunneling Spectroscopy. His knowledge, together with the knowledge and assistance of Mr. Russell "Rusty" Coast and Mr. Matthew Pikus, were invaluable for this dissertation.

My current and former Alcoa colleagues' contributions to this work must be emphasized:
Dr. Larry F. Wieserman for FT-IR and surface treatment discussions, Dr. Neal R. Dando for providing and interpreting the NMR spectra of phosphorous oxo acid anodized aluminum, Dr. Brian Strohmeier for his consultation with regards to X-ray photoelectron spectra, Dr. Angela M. Ahern for providing and interpreting SERS spectra, and Dr. Alfred C. Miller for obtaining ARXPS spectra and XPS sensitivity factors. Invaluable assistance was provided by: Mr. Raymond J. Colbert, Mr. Elio DaPos, Mr. Joseph P. Harenski, Mr. John Ptasienski, and Ms. Dorothy Schrall.

The assistance of Mr. Geno Iannaccone, of Analytical Services, Virginia Tech is sincerely appreciated. The provided NMR data were instrumental in the dissertation conclusions.

Lastly, my wife Vicki, and my children Tony, Joshua, and Elizabeth, are truly wonderful for putting up with my periods of inscrutability and irascibility during this writing process. I love you all.

Table of Contents

List of Figures

List of Tables

Chapter 1. INTRODUCTION

Adhesive bonding offers several advantages over other types of joining. These include improved stress distribution and increased design flexibility. Therefore, adhesive bonding is used extensively in aerospace, automotive, and packaging applications.[1] Structural adhesives are based on monomer compositions that polymerize on curing to yield a high strength adhesive, producing a strong load-bearing joint. However, the full potential of the technology has not been exploited because an understanding of the basic mechanisms of adhesion, and of the mechanisms of adhesion failure is incomplete. Without a thorough understanding of the mechanisms of adhesion and adhesion failure, the quantitative prediction of the life of an adhesively bonded system has not been possible.

Slow progress in the development of adhesion science may be because the science encompasses various disciplines. These include surface chemistry, polymer chemistry, rheology, physics, and fracture mechanics. In the past, there were few organizations that integrated the contributions from researchers in these fields. Also, most of the earlier adhesion research was empirical in nature, with the investigations being limited to testing joint strength by one of the standard mechanical testing procedures, and the joint durability after exposure to a variety of harsh environmental conditions. An understanding of the interfacial interactions between the adhesive and the adherend, at the molecular level, was not obtainable by this approach.

Recent advances in surface analysis, however, provide deeper insight into molecular aspects of adhesion. By providing information such as: the chemical composition of first few atomic layers of the adherend surface, the topography of the adherend surface, and the mode of failure of the adhesively bonded system, the use of surface analysis measurements is enabling researchers to

---

1. J. D. Minford, "*Handbook of Aluminum Bonding Technology and Data*," Marcel Dekker, Inc., NY (1993) pp. 1-10, 558-584.

study fundamental interactions occurring at the molecular level in the adhesive bonding process. This facilitates improvements in adhesive resin formulation and optimization of surface pretreatments. These advances in the understanding of the chemistry of adhesion, together with a more thorough erudition of fracture mechanics and polymer rheology, should allow precise predictions of the life of adhesively bonded systems under service conditions. Design engineers could then confidently expand the use of structural adhesive bonding to capitalize on the advantages of this joining technology.

However, a complete understanding of the elementary chemical and mechanical interactions controlling adhesion has still not been achieved. A factor that hinders the complete understanding of adhesion mechanisms, and the subsequent prediction of joint life, is that the regions of an adhesively bonded joint that typically influence adhesion and durability are buried interfaces. The interfaces between the adhesive and the adherends are not easily accessible to *in situ* chemical or morphological analyses. Breaking the adhesive joint, to attempt to analyze the interfacial regions, runs the risk of inducing changes in the chemical and physical properties of these regions that render any analyses not representative of the intact joint.

A confounding factor in studying the composition and properties of the interfacial regions is that two-dimensional interfaces rarely exist in real-life adhesively bonded systems. For example, the surface oxide on a metal may be porous. The adhesive or primer may penetrate the pores of the surface oxide. Therefore, the transitional region between the adhesive and the adherend is a composite region of oxide and polymer. The mechanical properties of this composite zone should be different than those of monolithic materials. In addition, from thermodynamic considerations, the presence of a surface alters the number of conformations available to a polymeric adhesive. Thus, the morphology of the polymer near the adherend surface is expected to be different from the bulk polymer structure not confined by a surface. This region of transition was termed the *interphase*.[2] The interphase is a three-dimensional region of transition

---

2. L. H. Sharpe, *J. Adhes.*, ***4*** (1972) 51.

of composition and properties in the adhesive joint, and has been represented schematically by Drzal, as shown in Figure 1.1.[3] One cannot, therefore, rely exclusively on the properties of the bulk adherend and the adhesive in predicting joint strength and joint life. The composition and properties of the interphase must also be considered.

While the determination of the actual structure and mechanical properties of an interphase is elusive, the effects of changing the chemistry or the morphology of the interphase, on the lifetime and failure modes of adhesively bonded systems are more readily determined. It is the scope of the work presented herein to elucidate the chemical and mechanical mechanisms responsible for the durable adhesion of epoxy adhesive resins to phosphorus oxo acid treated aluminum alloy adherends. By systematically altering the adherend surface chemistry, surface topography, and the adhesive formulation, combined with accelerated adhesive joint durability tests, the contributions of chemical and mechanical factors that influence the properties of adhesively bonded joints are isolated and assessed.

---

3. L. T. Drzal, M. J. Rich, and P. F. Lloyd, *J. Adhes.*, ***16*** (1984) 1, with permission.

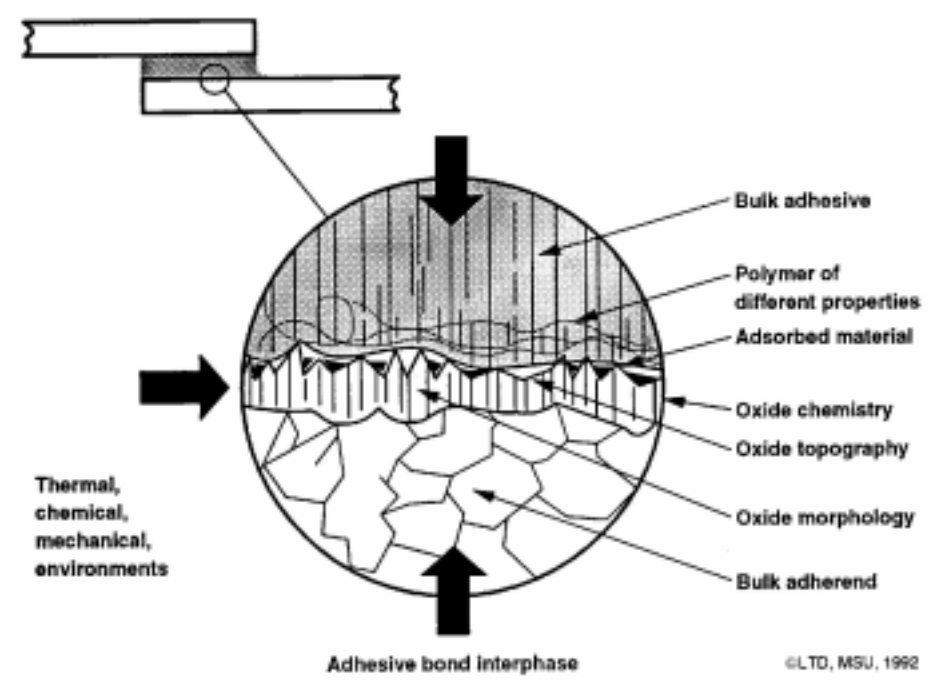

Figure 1.1. Schematic Representation of the Adhesive Bond Interphase[3]

Chapter 2. LITERATURE REVIEW

A. Adhesion Mechanisms

The type of interaction that occurs between the adhesive and the substrate directly influences joint strength and durability. Interactions occurring across an interface vary in nature, ranging from weak physical dispersion forces to hydrogen, covalent, and ionic bonding. In addition, surface roughness can allow for a mechanical contribution to the observed joint strength. The type of interaction(s) occurring in a system depends upon the chemical make-up of the adhesive and the substrate, and the topography of the adherend surface. The following mechanisms of adhesion are emphasized in the literature.[1]

1. Mechanical Interlocking

The theory of mechanical interlocking proposes that adhesion occurs as a result of adhesive penetration into surface irregularities. Subsequent mechanical *keying* or *interlocking* of the adhesive is the major source of joint strength.[4,5,6,7,8,9] Although a number of examples relating joint strength and durability to increased surface roughness exist in the literature, the theory is not universally applicable since good adhesion occurs between smooth surfaces, such as the adhesion that occurs between wet glass microscope slides. Also, it has been observed that increased roughness can result in lower joint strengths.[9]

---

4. T. S. Sun, J. M. Chen, G. D. Davis, and J. D. Venables, "Effects of Surface Morphology and Chemical Composition on the Durability of Adhesively Bonded Aluminum Structures," *Tech. Rep. MML TR-81-45c, AFSOR-TR-81-0725*, (1981).
5. J. D. Venables, D. K. McNamara, J. M. Chen, T. S. Sun, and R. L. Hopping, *Appl. Surf. Sci.*, ***3*** (1979) 88.
6. W. J. van Ooij, *Physiochem. Aspects Polym. Surf. Proc. Int. Symp.*, ***2,*** Plenum Press, New York, NY (1983) 1035.
7. A. J. Kinloch, *J. Mater. Sci.*, ***15*** (1980) 2141.
8. K. W. Allen, *J. Adhes.*, ***21*** (1987) 261.
9. K. W. Allen, *Int. J. Adhes. Adhes.*, ***13*** (1993) 67.

Mechanical interlocking can make a significant contribution towards the joint strength if the adherend surface geometry is specifically fabricated to enhance adhesive penetration. It is still debatable whether the increase in joint strength can be directly related to a mechanical interlocking mechanism or to secondary mechanisms such as an increase in specific surface area for chemical bonding or improved kinetics of wetting.[9] Adhesion by mechanical interlocking requires that the adhesive penetrates geometric irregularities on the adherend surface. Evidence of thermosetting adhesive penetration into the pores of an anodic oxide was presented by Hennemann and Brockmann.[10,11,12] A phenolic resin replica of a sulfuric acid anodized aluminum surface showed a negative image of the metal oxide surface. Arrowsmith and Moth demonstrated that an acrylic adhesive completely penetrated the pores of a sulfuric acid anodized aluminum alloy.[13] Penetration of the pores on aluminum anodic oxide surfaces by thermoplastic adhesives has also been demonstrated.[14,15] After dissolution of the phosphoric acid anodized Al / Li alloy used by Ko, et al.,[14,15] a negative image of the porous oxide was found on the polysulfone adhesive. In another study,[16] penetration of a primer into the pores of a phosphoric acid anodized aluminum surface was confirmed by electron energy loss spectroscopy (EELS) of a cross-sectioned sample. A carbon signal was observed in the spectrum from various spots in the pore structure when a primer was applied to the surface. Carbon could not be detected on samples without the primer. For an aluminum 6061 alloy sample anodized in phosphoric acid,

---

10. O. -D. Hennemann and W. Brockmann, *J. Adhes.*, ***12*** (1981) 297.
11. W. Brockmann, *Adhes. Aspects Polym. Coat. Proc. Symp.*, ***1***, Plenum Press, New York, NY (1983) 265.
12. W. Brockmann, O. -D. Hennemann, H. Kollek, and C. Matz, *Int. J. Adhes. Adhes.*, ***6*** (1986) 115.
13. D. J. Arrowsmith and D. A. Moth, *Trans. Inst. Met. Finish.*, ***64*** (1986) 163.
14. C. U. Ko, E. Balcells, T. C. Ward, and J. P. Wightman, *J. Adhes.*, ***28*** (1989) 247.
15. C. U. Ko, "*Effect of Surface Treatment on the Mechanical Properties of the Polysulfone-Al/Li Bonded System Including Thin Film Studies of Moisture Intrusion and The Viscoelastic Response of the Interphase Region*," Ph.D. Dissertation in Materials Engineering Science, Virginia Polytechnic Institute and State University, Blacksburg, VA (1988).
16. W. Brockmann, O. -D. Hennemann, and H. Kollek, in "*Adhesive Joints*," K. L. Mittal, ed., Plenum Press, NY (1984) p. 469.

and then primed, Davis and Venables[17] showed that the primer penetrated the porous oxide completely, leaving no voids or empty regions. Evidence for this came from a cross-section of the metal / primer interface, examined by scanning electron microscopy (SEM).

Penetration of the polymer into the oxide pores depends upon the wettability of the surface and the shape of the pore. Pore filling occurs until the pressure of the trapped gases equals the capillary pressure. Packham suggests that the shape of the pore (cylindrical versus ink bottle) is a crucial factor in controlling the pore filling process.[18] Penetration of the adhesive into pores on the surface can contribute significantly towards high joint strengths, since it is believed that the failing of ligaments of the adhesive or primer that enter the pores requires considerable plastic deformation, and thus high fracture energy.[18] More recently, Packham and Johnston[19] were able to vary the porosity of a ceramic by varying the firing temperature, and showed that the bonding strength of polyethylene to the fired ceramic was a function of the degree of porosity of the ceramic. In the same work, the authors concede that mechanical adhesion (interlocking) is a contribution to the observed adhesive strength, and "at the very least, London dispersion force interactions between the adhesive and substrate" also exist.

Gent and Lin,[20] using uniformly perforated aluminum plates bonded with a vulcanized rubber adhesive, showed that when an elastic adhesive layer penetrates the pores, extra work, of up to 20% more than with planar aluminum adherends is required to debond joints in a 90^{o}-peel or a T-peel configuration. The extra work is due to the elastic deformation of the adhesive in the pores as adhesive is pulled out. When the perforations were interconnected, extra work by as much as several hundred times was required to fail the joint. In the interconnected situation, the chemical

---

17. G. D. Davis and J. D. Venables, in "*Durability of Structural Adhesives*," A. J. Kinloch, ed., Applied Science Pub., NY (1983) p. 43.
18. D. E. Packham, *Adhes. Aspects Polym. Coat. Proc. Symp.*, ***1***, Plenum Press, New York, NY (1983) 19.
19. D. E. Packham and C. Johnston, *Int. J. Adhes. Adhes.*, **14** (1994) 131.
20. A. N. Gent and C.-W. Lin, *J. Adhes.*, ***32*** (1990) 113.

bonds in the adhesive had to break for the joint to fail; this was manifested in the observed increased joint strength.

2. Diffusion Theory

The diffusion theory of adhesion proposes that adhesion can be attributed to the interdiffusion of polymer molecules at the interface.[7,8,21,22] Since this requires that the adhesive and substrate are mutually soluble and have significant mobility, the mechanism does not directly apply in the case of metal to polymer adhesion.[9] Allen[8] argues that the penetration of polymers into interstices of a metal surface involves a diffusion mechanism, although he admits that this is an extreme interpretation of the original proposals of Voyutskii[21] that deal with the interdiffusion of polymers. Interdiffusion may, however, be operative in the adhesion of the polymer to primers and coupling agents, if a high degree of crosslinking or crystallinity is lacking.[7]

3. Electronic Theory

According to this theory, adhesion occurs due to electrostatic effects arising from contact potential at the adherend / adhesive interface.[7,8,23,24,25,26] Electron transfer is expected to occur between the adhesive and the substrate due to a difference in their electronic band structures. This transfer leads to the formation of an electrostatic double layer at the surface, and subsequently to adhesion due to the attractive forces inherent in the double layer. Although the

---

21. S. S. Voyutskii, *Rubber Chem. Technol.*, ***33*** (1960) 748.
22. R. M. Vasenin, in "*Adhesion Fundamentals and Practice*," McLaren & Sons, Pub., London, England (1969) p. 29.
23. B. V. Derjaguin and V. P. Smilga, *J. Appl. Phys.*, ***38*** (1967) 4609.
24. B. V. Derjaguin and Yu. P. Toporov, *Physiochem. Aspects Polym. Surf. Proc. Int. Symp.*, ***2*** (1983) 605.
25. J. A. Cross, *Surf. Contami. Genesis Detect. Control Proc. Symp.*, ***1*** (1979) 89.
26. W. Possart, *Int. J. Adhes. Adhes.*, ***8*** (1988) 77.

mechanism is likely to occur in metal / polymer systems, researchers have calculated, from charge densities at surfaces, that the electronic contribution to the thermodynamic work of adhesion (W_A) is small compared to the contribution from chemical interactions.[9,27,28]

4. Chemical / Adsorption Theory

Adhesion by this mechanism is attributed to surface chemical forces, and the chemisorption or physisorption of atomic and molecular species.[9] The attractive forces working across two surfaces include weak dispersion forces and stronger forces due to hydrogen, covalent, and ionic bonding.[7,8,9,29,30,31,32] Zisman has shown that van der Waals dispersion and polarization forces are more than adequate to account for the observed strengths of adhesive joints.[33] The types of bonds formed between two surfaces depend upon the chemical constitution of the interface. The criterion for chemisorption / physisorption processes to occur across the interface is that the adsorbate wet the substrate. In general, for spontaneous wetting, the surface energy of the solid must be greater than that of the liquid. Then the thermodynamic work of adhesion between the solid and the liquid can be expressed as: $W_A = \gamma_S + \gamma_L - \gamma_{SL}$, where γ_S is the surface energy of the solid, γ_L is the surface tension of the liquid, and γ_{SL} is the solid / liquid interfacial tension.

Schultz, et al.,[34] proposed that the surface free energy can be generally expressed by two terms corresponding to dispersion forces and to polar forces: $\gamma_S = \gamma_S^D + \gamma_S^P$. For Al_2O_3,

---

27. A. D. Roberts, *J. Phys. D:*, ***10*** (1977) 1801.
28. A. Roberts, *Adhesion (London)*, ***1***, (1977) 207.
29. A. F. Lewis and L. J. Forrestal, *ASTM Spec. Tech. Publ.*, ***360*** (1964) 59.
30. J. E. Rutzler, Jr., *Adhes. Age*, ***2*** (July 1959) 28.
31. R. B. Dean, *Off. Dig. Fed. Soc. Paint Technol.*, ***36***, (June 1964) 664.
32. R. E. Baier, E. G. Shafrin, and W. A. Zisman, *Science*, ***162*** (1968) 1360.
33. W. A. Zisman, *Ind. Eng Chem.*, ***55*** (1963) 18.
34. J. Schultz, K. T. Sutsumi, and J. B. Donnet, *J. Colloid Interface Sci.*, ***59*** (1977) 27.

$\gamma_S^D = 100mJ/m^2$, $\gamma_S^P = 538mJ/m^2$, and $\gamma_S = 638mJ/m^2$.[35,36]

Carré and Schultz,[37] using a two liquid contact angle method developed for high-energy solids, determined the surface energetics of aluminum that had received various pretreatments. By measuring the contact angle of water on the solid, in the presence of a non-polar liquid, they demonstrated that surface pretreatments affect the dispersion and polar components of the surface energy. A sulfuric acid anodized sample had a high dispersive component, and a high polar component of surface energy. This surface exhibited a low resistance to corrosion. A chromate-phosphate conversion coated sample had a high dispersion component, but a lower polar component of surface energy. The chromate-phosphate coated specimen was highly corrosion resistant. Carré and Schultz[37] concluded that for good "dry" adhesive joint strength, and for good durability in the presence of moisture, the surface should have a high dispersive component of surface energy, γ_D^S, and a low polar component, γ_S^P. The contribution of dispersion and polar components can then be used to predict interactions at the interface. It was hypothesized that the work of adhesion, W_A, can be correlated to the measured joint strength.[37]

Ahagon and Gent[38] showed that the observed adhesion of polybutadiene to organosilane treated glass increased by 35 times when the silane was vinylsilane, compared to ethylsilane. This was attributed to the formation of chemical bonds at the interface. However, adhesion to the ethylsilane and the vinylsilane treated glass was 25% greater than predicted by W_A arguments. These higher than predicted values in joint strength were attributed to the energy absorbing, viscoelastic effects associated with polymer deformation, such as chain stressing and sliding.

---

35. A. J. Kinloch, W. A. Dukes, and R. A. Gledhill, in "*Adhesion Science and Technology*," L. H. Lee, ed., Plenum Press, NY (1975) p. 597.
36. M. K. Bernett and W. A. Zisman, *J. Colloid Interface Sci.,* ***28*** (1968) 243.
37. A. Carré and J. Schultz, *J. Adhes.,* ***15***, (1983) 151.
38. A. Ahagon and A. N. Gent, *J. Polym. Sci. Polym. Phys. Ed.,* ***13*** (1975) 1285.

For cohesive failure of aluminum / elastomer joints, Schultz and Carré[39] express the energy of separation of a joint, ω, in three terms: 1) the reversible work of adhesion or cohesion, W_0; 2) a microscopic dissipation factor, $f(R)$, related to the hysteresis of the properties of an elastomer; and 3) a molecular dissipation factor, $g(M_C)$, that deals with the average length of polymer chains crossing the cohesive fracture plane. For cohesive failure, the resulting equation was given as: $\omega = W_0^C g(M_C) f(R)$, where $W_0 g(M_C)$ is the failure energy that would be observed without any viscoelastic dissipation.

The wetting and spreading processes are influenced by the geometric features of the surface, and by the presence of chemical functionalities that can alter the surface energy of the substrate. Lee,[40] using contact angle measurements, determined the wettability of silica surfaces primed with reactive silanes. The wettability was determined by the conformation of the organic portion, R, of the silane molecule: R - $Si(OR')_3$. Lee classified various silanes into three groups based on polarity of the R group. For example, if the R group was vinyl-, the silane treated surface was classified as having low polarity, for amino- groups, the silane treated surface was classified as having medium polarity, and for glycidoxy- groups, the surface was classified as having high polarity.

Baier, et al.,[32] using the concept of critical surface tension, γ_c, have measured γ_c on several structurally homologous series of solids, including unbranched polyethylene, and chlorinated and fluorinated analogues of polyethylene. They correlated these empirical measurements of surface energy "with respect to the most probable exposed atoms." In the same work, Baier, et al.,[32] concluded that in order to get good adhesion, the adherend surface should be kept free from low surface tension organic films. They predicted that substituent groups, such as -OH, -SH, -COOH, and $-NH_2$, at the outermost surface, would increase the "adhesiveness" of the surface by

39. J. Schultz and A. Carré, *J. Appl. Polym. Sci.*, ***39*** (1984) 103.
40. L-H. Lee, *J. Colloid Interface Sci, **27*** (1968) 751.

increasing the surface energy; whereas less polar groups, such as $-CH_3$ or $-CH_2-$ would decrease the bondability of the surface.

Imai and Nishio[41] claim that the number of hydroxyl groups on the surface correlates well with the adhesion of polymers, and determined that the epoxide rings can react with surface hydroxyl groups. They found that the number of hydroxyl groups on pretreated aluminum surfaces varied in the following fashion: phosphoric acid anodization > sulfuric acid anodization >> alkali cleaning = chromate-phosphate conversion coating = degrease only. No data were provided on joint durability.

Recently, it has been suggested that another class of interaction, namely acid-base, is in part responsible for the intrinsic adhesion forces at inorganic / polymer interfaces.[42,43,44] More than seventy years ago, Lewis proposed that bases are electron donors and acids are electron acceptors.[45] Fowkes[42] extended this viewpoint to the understanding of adhesion of polymers on inorganic surfaces, by proposing that the thermodynamic work of adhesion could be separated into components of: London dispersion (d) forces, hydrogen-bond (h) forces, acid-base (ab) forces, dipole-dipole (p) interactions, and induced dipole-dipole (i) interactions. Namely:
$W_A = W_A^d + W_A^h + W_A^{ab} + W_A^p + W^i{}_A$.

Later, Fowkes[46] demonstrated that hydrogen bonding is a subset of the acid-base reactions. Using

---

41. M. Imai and M. Nishio, *Sumitomo Keikinzoku Giho, **30*** (1989) 22.
42. F. M. Fowkes, *J. Adhes., **4*** (1972) 155.
43. S. R. Cain, *J. Adhes. Sci. Technol., **4*** (1990) 333.
44. M. D. Vrbanac and J. C. Berg, *J. Adhes. Sci. Technol., **4*** (1990) 255.
45. secondary reference, G. N Lewis, "Valence and the Structure of Atoms and Molecules," p. 142, Chem. Cat. Co., New York, 1923, cited in F. M. Fowkes, *Physiochem. Aspects Polym. Surf. Proc. Int. Symp., **2***, (1983) p. 583.
46. F. M. Fowkes, *Physiochem. Aspects Polym. Surf. Proc. Int. Symp., **2*** (1983) 583.

the Drago E and C constants and equations,[47] Fowkes calculated the enthalpies of acid-base interaction between various hydrogen bonding liquids, and compared these calculated values with measured enthalpies of interaction. The calculated acid-base enthalpies agreed well with the measured interaction enthalpies, giving rise to Fowkes' claim that hydrogen bonds are a subset of acid-base interactions.

Fowkes[46] also argued that the "polar" dipole-dipole and induced dipole-dipole interactions do not contribute significantly to intermolecular attractions in condensed phases. Fowkes showed that the product of the dipole moment of two molecules does not correlate with the measured enthalpies of interaction. He used the same acid-base equation of Drago to calculate the enthalpies of interaction in polar liquid solutions, and found that the enthalpies of interaction calculated from the acid-base equations correlated with the measured enthalpies of interaction.[46] Fowkes argued that in the gas phase, there are relatively large distances between molecules, which do not allow for acid-base interactions. Furthermore, in the gas phase, interactions generally involve only two molecules, whereas in the condensed phase each molecule may have several different nearest neighbors. Each dipole in the condensed phase provides a conflicting local field to the surrounding molecules, resulting in a minimization of dipole interaction. Since all of the polar and hydrogen-bonding forces could be quantitatively explained by acid-base interactions, Fowkes proposed that the work of adhesion between a polymer and an inorganic substrate could be accounted for by dispersion forces and acid-base interactions,[46] $W_A = W_A^d + W_A^{ab}$.

Fowkes[48] also suggests that one can improve adhesive joint strengths by predictably enhancing the interfacial acid-base interactions through proper surface modifications, including the use of

47. R. S. Drago, G. C. Vogel, and T. E. Needham, *J. Am. Chem. Soc.*, ***93*** (1970) 6014.
48. F. M. Fowkes, *J. Adhes. Sci. Technol.*, ***1*** (1987) 7.

organosilanes. Fowkes[49] provides a review of techniques that can be used to quantitatively characterize the acid-base properties of liquids, polymers, and inorganic surfaces.

In a metal / polymer system, both the polymer and the metal substrate can exhibit amphoteric behavior. Bolger[50,51] claims that the only forces worth considering, in addition to dispersion forces, are hydrogen bonding forces, and used an acid-base mechanism to predict the relative magnitude of the hydrogen bonds. Since under ambient conditions, metal oxide surfaces are generally hydroxylated, the hydroxyl group can act as either an acid or a base. He proposed the following reactions between the polymer and the oxide surface:

1. With an organic acid polymer:

$$\text{-Metal-OH} + \text{HX\sim R} \rightarrow \text{-Metal-O}\cdots\text{HX\sim R} \leftrightarrow \text{-Metal-O}^{+}\text{H}_2\cdots\text{X\sim R}$$

2. With an organic base polymer:

$$\text{-Metal-OH} + \text{X\sim R} \rightarrow \text{-Metal-OH}\cdots\text{X\sim R} \leftrightarrow \text{-Metal-O}^{-}\cdots\text{HX}^{+}\text{\sim R}$$

where: X = O, S, or N; and R = organofunctional group and polymer chain.

Based on assignments of the bands in an infrared spectrum (IR), Sugama, et al.,[52] proposed two mechanisms by which a poly(acrylic acid) polymer interacts with iron surfaces coated with either iron(III) orthophosphate dihydrate or zinc phosphate hydrate (hopeite) crystalline films. One of these was an acid-base reaction between the acidic -COOH group and the hydroxylated oxide surface, and the other a salt bridge formation between the metal ion (Fe^{3+} or Zn^{2+}) and the carboxylate anion. Sugama, et al.,[52] showed that when the poly(acrylic acid) solution was

---

49. F. M. Fowkes, *J. Adhes. Sci. Technol.*, ***4*** (1990) 669.
50. J. C. Bolger, *Adhes. Aspects Polym. Coat. Proc. Symp.*, ***1***, Plenum Press, New York, NY (1983) p. 3.
51. J. C. Bolger, *Ann. Tech Conf. Soc. Plast. Eng.*, ***18*** (1972) 402.
52. T. Sugama, L. E. Kukacka, and N. Carciello, *J. Mater. Sci.*, ***19*** (1984) 4045.

partially neutralized with NaOH, the poly(acrylic acid) molecules formed entangled balls on the surface, did not extensively interact with surface hydroxyl groups and yielded lap shear specimens with significantly decreased strengths. This also occurred when significant amounts of divalent metal ions were on the surface. When the surfaces were fully hydroxylated, and when the poly(acrylic acid) solution was not neutralized, the poly(acrylic acid) molecules wet the surface, and reacted with the surface hydroxyl groups through an acid-base, charge transfer mechanism. Joints prepared with these adherends exhibited significantly higher lap shear strengths.

Lee[53] describes the overall nature of acid-base interactions with solid surfaces in terms of electrostatic, charge transfer, exchange, polarization, and dispersion components. Among these, Lee considers the electrostatic (or ionic) and charge transfer (or covalent) to be the major components. Lee also describes acid-base interactions in terms of density-functional theory, and provides an equation for the number of transferred electrons for solid interactions involving metals or polymers. Jensen[54] provides a thorough review on the current theories of acid-base interactions with relation to surface chemistry and adhesion.

In a review of contemporary theories of adhesion, Allen, et al.,[9] conclude that "there is a steadily growing body of evidence for the existence and significance of primary chemical bonding in addition to the secondary bonding in adhesion." Demonstrated interactions of epoxy resin analogues with aluminum oxide surfaces include the acid-base interaction of amines (curing agents) with Lewis acid sites (coordinatively unsaturated Al) on the oxide surface,[55] and the reaction of surface hydroxyls with hydroxyl groups in the resin to form alkoxide linkages to the surface.[55]

---

53. L.-H. Lee, *J. Adhes. Sci. Technol.*, ***5*** (1991) 71.
54. W. B. Jensen, *J. Adhes. Sci. Technol.*, ***5*** (1991) 1.
55. S. Affrossman, J. M. R. MacAllister, R. A. Pethrick, B. Thomson, N. M. D. Brown, and B. J. Meenan, in "*Polymer Surfaces and Interfaces*," W. J. Feast and H. S. Munro, eds., John Wiley & Sons, New York (1987) p. 99.

Thomas, et al.,[56] used interfacial force microscopy (IFM) to study the force encountered between a functionalized substrate, and a functionalized microscope tip. A gold tip and substrate were functionalized with n-alkanethiols containing specific functional groups. The tip and substrate were coated with thiols containing: 1) methyl groups, to study van der Waals interactions, 2) amines, to study hydrogen bonding, and 3) with an amine-carboxylic acid combination, to study acid-base interactions. The measured force values scaled qualitatively with those expected for van der Waals, hydrogen bonding, and acid-base interactions.[56]

Of the theories of adhesion described in the preceding sections, it is generally agreed that adhesion occurs by a synergistic combination of two or more of mechanisms.[19,57] For example, increasing the adherend roughness may contribute to mechanical forces of adhesion, but because of capillary forces could also result in increased wettability of the substrate by the adhesive. Also, the increased surface area could result in an increased number of total primary or secondary bonds between the adhesive and adherend, per geometric area.

The synergism of adhesion mechanisms is illustrated by the work of Arrowsmith, et al.[58,59] In an attempt to develop a new surface treatment for aluminum, Arrowsmith and Clifford[58] describe the hard anodizing[60] of aluminum alloy NS4 (5152) in sulfuric acid solution, followed by dipping in phosphoric acid solution. The hard anodization was done to provide a dense corrosion resistant oxide, whereas the phosphoric acid dip etched the outer surface of the hard oxide.[58] By citing wedge crack test durability results of acrylic bonded joints, Arrowsmith and Clifford[58]

---

56. R. C. Thomas, J. E. Houston, R. M. Crooks, T. Kim, and T. A. Michalske, *J. Am. Chem. Soc.*, ***117*** (1995) 3830.
57. W. Brockmann, O.-D. Hennemann, and H. Kollek, *Int. J. Adhes. Adhes.*, ***2*** (1982) 33.
58. D. J. Arrowsmith and A. W. Clifford, *Int. J. Adhes. Adhes.*, ***5*** (1985) 40.
59. D. J. Arrowsmith, D. A. Moth, and S. P. Rose, *Int. J. Adhes. Adhes.*, ***12*** (1992) 67.
60. S. Wernick, R. Pinner, and P. G. Sheasby, "*The Surface Treatment and Finishing of Aluminium and its Alloys, Fifth Edition*," Redwood Burn Limited, Trowbridge, Great Britain (1987).

claim that phosphoric acid dipping, after hard anodizing, provides: 1) more surface area for increased chemical bonding of the oxide with the adhesive, 2) better stress distribution due to the roughened surface, 3) reinforcement of the adhesive by mechanical interlocking with the roughened surface, and 4) hydration resistance to the oxide due to the adsorbed phosphate ions. In subsequent work, Arrowsmith, et al.,[59] etched the hard anodic oxide in sodium hydroxide solution to obtain the same surface topography as was obtained with the phosphoric acid dip, but with a different surface chemistry. When bonded with the acrylic adhesive, the phosphoric acid and sodium hydroxide etched surfaces had similar dry lap shear strengths, and did not significantly lose strength after 1500 h room temperature water immersion.[59] Epoxy bonded joints did lose some joint strength after water immersion, and the authors claim that this was due to inadequate wetting of the adhesive during cure, resulting in air gaps in the bond line. Migration of water into the voids led to the loss of adhesion strength.[59] From these observations, Arrowsmith, et al.,[59] state that "The extended surface area, which provides more sites for an increased number of physical and chemical bonds between oxide and adhesive, is therefore considered the main cause of increased joint strength. The reinforcement of the adhesive layer by the conical spikes of alumina may also have contributed to the increased joint strength." Arrowsmith, et al.,[59] did not comment on the expected differences in surface chemistry between the phosphoric acid dipped and sodium hydroxide dipped adherends, and why there was no observed effect from the different adherend surface chemistries on the strength and durability of the adhesive joints.

The literature described in the electronic and diffusion theories sections of this review has shown that these phenomena do not contribute significantly to aluminum / polymer adhesion. The original work, presented in later chapters of this dissertation, uses a systematic approach to determine the contributions of the mechanical and chemical aspects of adhesion to aluminum / epoxy systems.

B. Aluminum Surface Pretreatments

Among the many factors that affect the durability and integrity of adhesively bonded aluminum joints, the choice of a surface pretreatment is crucial in realizing the required bond strength and durability.[61,62] The objective of the pretreatment is to develop a clean, uniform, wettable surface. Increased roughness and intrinsic hydrolytic stability of the surface have also been identified as being important for good bondability.[5] The surface preparation, in general, consists of several steps, among which are: initial cleaning to remove surface contamination; acid or base etching to remove the weak, inhomogeneous oxide formed by thermal exposure of the metal during the fabrication process; and a chemical or electrochemical treatment to stabilize the surface and promote adhesion.[1]

Surface contaminants vary in their chemical make-up, ranging from inorganic salts, non-polar organic compounds, residual mill lubricants, thermal oxides, hydroxides, adsorbed water, and various adsorbed gases. Mittal[63] has published a comprehensive review on the origin, detection, removal, and control of surface contamination. Cleaning of aluminum and aluminum alloys is generally accomplished with alkaline solvents.[1]

The aluminum surface treatments that follow cleaning generally consist of one or more steps consisting of: acid etching, chemical conversion coating, or acid anodizing.[60] The last treatment is a stabilizing step, in which the aluminum oxide and hydroxide layer formed or remaining on the surface after cleaning is chemically modified or replaced by treatments which increase corrosion and hydration resistance and enhance adhesion to organic polymeric adhesives.[64]

---

61. J. A. Bishopp, E. K. Sim, G. E. Thompson, and G. C. Wood, *J. Adhes.*, ***26*** (1988) 237.
62. J. A. Bishopp, E. K. Sim, G. E. Thompson, and G. C. Wood, *Trans. Inst. Met. Finish.*, ***66*** (1988) 127.
63. K. L. Mittal, *Surf. Contami. Genesis Detect. Control Proc. Symp*, ***1***, (1979) 3.
64. J. C. McMillan, *AGARD Lect. Ser.*, ***102*** (1979).

1. Acid Etching of Aluminum

a. Cr(VI)-Based Etchants

For adhesively bonded structural aluminum joints, requiring high strength and long term durability, the cleaned aluminum is typically etched in either a chromic/sulfuric acid etch,[65, 66] or a dichromate/sulfuric acid etch.[61,67] The chromic/sulfuric acid etch is used predominantly in Europe, whereas the dichromate/sulfuric acid etch, known as the FPL (Forest Product Laboratory) etch,[64] or the optimized FPL etch,[68] is used by the North American aerospace industry. Sun, et al.,[69] have shown that the MgO layer produced on the surface of 2024 alloys[70] during thermal treatments is removed during FPL etching. Using Auger electron spectroscopy (AES) data they also suggest that during etching, both dissolution of oxide and formation of new oxide take place. As etching continues, the oxide surface retreats from the solution interface, and eventually a certain mass of the alloy is dissolved. Sun, et al.,[69] claim that a thin oxide is maintained on the surface during the process, thickening of the oxide occurs during the rinsing step that follows the etch. Venables, et al.,[5] propose a model for the surface oxide structure (Figure 2.1) after FPL etching.

---

65. W. Brockmann and O.-D. Hennemann, *Nat. SAMPE Tech. Conf.*, ***11*** (1979) 804.
66. secondary reference, UK DEF STAN 03-2/1, HMSO and German Standard DIN 53 281, cited in D. J. Arrowsmith, D. A. Moth, and C. M. Vickery, *Trans. Inst. Met. Finish.*, ***66*** (1988) 112.
67. secondary reference, H. W. Eickner and N. E. Schowalter, *Forest Product Laboratory Report No. 1813* (1950), cited in J. D. Venables, D. K. McNamara, J. M. Chen, T. S. Sun, and R. L. Hopping, *Appl. Surf. Sci.*, ***3*** (1979) 88.
68. secondary reference, *Boeing Process Specification BAC 5514*, cited in D. J. Arrowsmith, D. A. Moth, and C. M. Vickery, *Trans. Inst. Met. Finish.*, ***66*** (1988) 112.
69. T. S. Sun, J. M. Chen, and J. D. Venables, *Appl. Surf. Sci.*, ***1*** (1978) 202.
70. Please see Appendix 1 for aluminum alloy compositions.

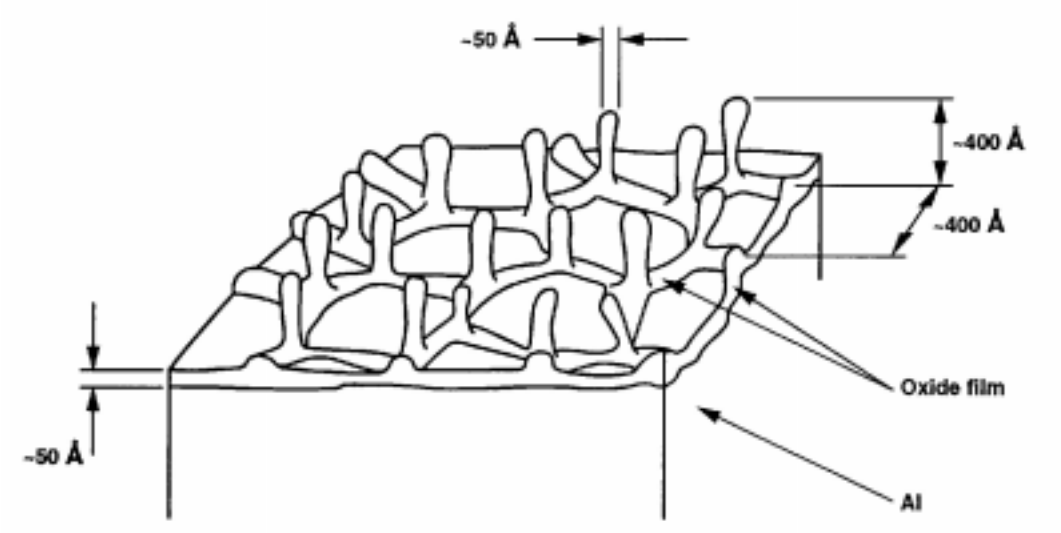

Figure 2.1. Oxide Morphology Produced on Al Alloy by the FPL Process[5]

The FPL etched oxide consists of a cell structure of thin barrier layer oxide with protrusions, or whiskers, of oxide 5 nm thick, sticking out of the surface to about 40 nm, at a concentration of about $10^{10}/cm^2$. The mechanism for growth of the whiskers was not addressed. Venables, et al.,[5] claim that from prior work,[71] the presence of the whiskers, and the mechanism of mechanical interlocking, is crucial for enhancing the environmental durability of joints with FPL etched adherends. For the 2024 and 7075 alloys, AES and X-ray photoelectron spectroscopy (XPS) spectra revealed only Al, O, Cu, C, and Cr on the surface.[69,72]

71. J. M. Chen, T. S. Sun, J. D. Venables, and R. L. Hopping, *Nat. SAMPE Symp. Exhib. Proc.*, ***22*** (1977) 25.
72. N. T. McDevitt, W. L. Baun, and J. S. Solomon, "Surface Analysis of 2024 and 7075 Aluminum Alloys After Conditioning by Chemical Treatments," *Tech. Rep. AFML-TR-75-122* (1975).

Contaminants such as silicates and chlorides interfere with the etching process.[73] The conversion of Cr^{6+} to Cr^{3+} can also be deleterious to oxide stability.[73] Contaminants such as SO_4^{2-} found in tap water are said to be desirable in the rinsing process, since it is believed that such anions retard the formation of a thick, cohesively weak, oxide layer that could form during rinsing.[74]

Due to their practical significance in the aerospace industry, most of the work in the literature on the effect of alloying elements on etching has been directed towards the characterization of oxide properties of commercial 2024 and 7075 alloys. An accumulation of Cu, up to 16% (w/w), at the oxide/metal interface of FPL etched aluminum alloy 2024 was detected by Sun, et al.,[69] using XPS. The nominal bulk value for Cu in 2024 alloy is 4.4% (w/w).[75] McDevitt, et al,[72] reported similar results. As would be expected from the lower oxidation potential of Cu^0 relative to Al^0, the interfacial Cu was present in metallic form,[69] as determined by comparing the experimental results with AES standard line shapes[76] of metallic and oxidic Cu.[69] Sun, et al.,[69] attributed the enrichment Cu^0 at the metal/oxide interface to the slower diffusion of Cu^0, compared to Al^{3+}, through the Al_2O_3 layer at the surface. Sun, et al.,[69] concluded that the Cu^0 did not plate out on the surface from Cu^{2+} in solution, since the amount of copper was the same for a freshly prepared FPL solution (without any Cu species), as for a heavily used bath, containing a large concentration of Cu^{2+} ions. Secondly, the amount of Cu^0 enrichment at the interface was a function of the amount of Cu^0 in the alloy. The nominal Cu concentration in 7075 is 1.6% (w/w),[75] and after FPL etching the amount of Cu^0 at the metal/oxide interface was approximately 3% (w/w).[69] Sun, et al.,[69] argue that during etching, a steady state oxide layer is maintained on

---

73. A. C. Moloney, in "*Surface Analysis and Pretreatment of Plastics and Metals*," Applied Science Pub., Essex, England (1982) p. 175.
74. R. F. Wegman, W. M. Bodnar, M. J. Bodnar, and M. J. Barbarisi, "Effects of Deionized Water Immersion of Prepared Aluminum Surfaces on Adhesive Bondability," *Tech. Rep. Picatinny Arsenal PA-TR-3495* (May 1967).
75. "*Aluminum Standards and Data 1984*," the Aluminum Association, Inc., Washington, D. C. (1984).
76. A. Joshi, L. E. Davis, and P. W. Palmberg, in "*Methods of Surface Analysis*" A. W. Czanderna, ed., Elsevier Scientific Publishing Company, NY (1975) p. 159.

the metal surface. Wefers[77] speculates that the Cu^0 found at the oxide/metal interface is plated out Cu^0, due to the ~2 eV difference in oxidation potentials of Al^0 and Cu^0, and that there is no coherent Al_2O_3 layer on the metal during etching. Furthermore, Wefers[77] suggests that Cu^0 undergoes dissolution and reprecipitation during etching, and that the oxide forms on top of the plated Cu^0 during the rinsing step when the acidic species are removed from the surface.

Smith[78] claims that for pure Al (99.99%) in a Cu^{2+} enriched FPL etch bath, the system becomes "self-anodizing", that is the presence of Cu^{2+} in the solution increases the cathodic current, thus increasing the mixed potential and anodic voltage. Pocius[79] correlated the increase Cu^{2+} concentration in the bath with improved bond durability for 2024-T3 alloys. The increased etching, caused by the presence of Cu^{2+} also resulted in increased oxide thickness, and a change in oxide morphology. From AES and electrochemical potential data, Pocius[79] concluded that the function of Cu^{2+} in solution is to provide a "surface activating" species that catalyzes the growth of surface oxide. Smith[78] also showed that the contact angle of water decreases as the solution Cu^{2+} concentration increases, that is, the oxide becomes more wettable as the solution Cu^{2+} concentration increases. This agrees with the stronger etching of the surface in the presence of Cu^{2+} that was observed by Pocius.[79] Although the oxide becomes more wettable, the author failed to explain the mechanism of increased bond *durability* with increased dissolved Cu^{2+}.

The major alloying element of 7075-T6 aluminum alloy is zinc (Appendix 1). A T6 designation signifies that the alloy was solution heat treated, then artificially aged.[80] McDevitt, et al.,[72] using AES, ion scattering spectroscopy (ISS), and secondary ion mass spectroscopy (SIMS), did not detect any zinc in the solvent degreased 7075-T6 oxide. Using AES, Zn was not detected in the

---

77. K. Wefers, Virginia Polytechnic Institute & State University and Alcoa Technical Center (retired), personal communication.
78. A. W. Smith, *J. Electrochem. Soc.*, ***120*** (1975) 1551.
79. A. V. Pocius, *Adhes. Aspects Polym. Coat. Proc. Symp.*, ***1***, Plenum Press, New York, NY (1983) 281.
80. "*Aluminum Standards and Data, 1986 Metric SI, second edition*" The Aluminum Association, Washington, DC (1986).

aluminum oxide after FPL etching of 7075 alloy.[72,81] Furthermore, the FPL etch did not cause an enrichment of zinc at the metal/oxide interface,[81] as was observed for copper in the 2024 alloy.[69]

Another common alloying element, magnesium, has often been associated with poor bond durability.[69,82,83,84] Mg^{2+} segregates at the surface following a thermal treatment of the alloy.[85] At the surface, Mg^{2+} exists as MgO or $Mg(OH)_2$. Using XPS, Kinloch[83] observed that increased durability could be correlated directly to a decrease in Mg^{2+} concentration at the surface. Sun, et al.,[69] have shown that the MgO can be removed after an FPL etch, but Mg^{2+} can diffuse to the surface again during curing of the adhesive at elevated temperatures. While Al_2O_3 is stable in the pH range from about pH 4-9,[86] MgO is not stable in solutions with a pH < 11.[69] Considering that in-service joints will be exposed to water containing salts and acidic pollutants, the presence of MgO on the Al_2O_3 layer could render the oxide susceptible to attack by moisture.[69]

Although much of the research in the literature suggests that Mg^{2+} is detrimental to adhesive joint durability, Critchlow and Brewis,[87] recently noted little effect of Mg^{2+} on joint durability. Aluminum alloy 5251 (see Appendix 1) was subjected to mechanical grit blasting treatments, which resulted in surface Mg:Al atomic ratios as high as 0.24. When bonded in a single lap shear configuration, with an epoxy adhesive, varying surface Mg:Al ratios (≤ 0.24) had little effect on either joint strength or durability. It was further noted that the degreased-only alloy surfaces had a Mg:Al ratio > 0.5. Bonds formed with the degreased-only adherends had lower initial strengths than the grit blasted adherends, and failed cohesively in the Mg-rich oxide. The joints with grit blasted adherends failed cohesively in the adhesive. Despite the lower joint

---

81. J. S. Solomon and D. E. Hanlin, *Appl. Surf. Sci.*, ***4*** (1980) 307.
82. A. J. Kinloch, H. E. Bishop, and N. R. Smart, *J. Adhes.*, ***14*** (1982) 105.
83. A. J. Kinloch, *Adhesion (London)*, ***6*** (1982) 95.
84. A. J. Kinloch and N. R. Smart, *J. Adhes.*, ***12*** (1981) 23.
85. K. Wefers, *Aluminium (Düsseldorf)*, ***57*** (1981) 722.
86. K. Wefers and C. Misra, "Oxides and Hydroxides of Aluminum," *Tech. Pap. Alcoa Res. Lab.*, ***19*** (1987).
87. G. W. Critchlow and D. M. Brewis, *Int. J. Adhes. Adhes.*, ***15*** (1995) 173.

strengths for the degreased-only adherends, however, these joints did not lose any strength after immersion in deionized water at 60°C for 211 days.[87]

b. Non-Cr(VI) Etchants

For environmental and safety reasons, alternatives to Cr(VI)-containing etchants for the surface preparation of aluminum for adhesive bonding are being researched. Solomon and Hanlin[81] examined anodic oxides formed after etching in a hydrofluoric/nitric acid etch, and a proprietary deoxidizing solution from Oakite,[88] which contained F, N, and S compounds. These authors showed that the chemical composition of the etchant had an effect on the structure and thickness of a phosphoric acid anodic oxide, applied in a subsequent step. Typical concentrations for HF/HNO_3 etchants are found in the review of aluminum surface treatments by Werner, et al.[60]

Arrowsmith, et al.[89] compared the FPL etch with etchants based on phosphoric acid or sodium hydroxide. Using aluminum alloy 5251, they observed that all of the etched surface topographies were scalloped. The caustic etched scallops were larger and more irregular than either those observed on the phosphoric acid or the FPL etched surfaces. The initial single lap shear bond strengths for FPL and phosphoric acid etched aluminum, bonded with an acrylic adhesive, were generally higher than those with caustic etched adherends. The authors speculate that the initial joint strength may be due to both the composition and the morphology of the etched surface. The highest joint strengths were obtained with surfaces that had regularly scalloped etch pits. These etch pits were produced with the FPL etch, the phosphoric acid based solutions, or a caustic solution containing a proprietary strong oxidizing agent.

---

88. Oakite Products of Canada Ltd., Bramlea, Ontario, Canada.
89. D. J. Arrowsmith, D. A. Moth, and C. M. Vickery, *Trans. Inst. Met. Finish.*, ***66*** (1988) 23.

Bijlmer[90] compared non-chromate etchants with dichromate / sulfuric acid etching of 2024-T3 aluminum alloy. By varying the concentration of dichromate and sulfuric acid, Bijlmer noted that the best peel strengths, after bonding with a phenolic adhesive, occurred when the scalloped etch pits were small and uniform. He was able to reproduce this topography, and good peel strength, using a sulfuric acid / hydrogen peroxide etchant. He concluded that in order to achieve the desired topography a sufficient concentration of H^+ ions and a strong oxidizing agent must be present in the etchant. The oxidizing agent was the most important factor, and Bijlmer determined that this could be replaced by applying an anodic current. The desired topography was obtained by applying several hundred millivolts to the work piece immersed in sulfuric acid solution (250 g/L) at 50^{o}C for 30 min.[90]

A mechanical abrasive pretreatment, prior to phosphoric acid anodizing, produced results equivalent to the FPL etch prior to phosphoric acid anodizing.[91] The aluminum alloy surfaces were abraded with Scotch-Brite®[92] brushes. Pocius and Claus[91] concluded that Scotch-Brite® brushing produced a surface that was elementally cleaner than the FPL surface, and was receptive to anodization. The brushed/phosphoric acid anodized aluminum alloys were used to make adhesive joints with equivalent performance to joints with FPL etched/phosphoric acid anodized aluminum adherends.

A non-chromate etch, designated P2, was shown to be as effective as the FPL etch when clad copper containing aluminum alloy BS-L165,[93] was bonded with Redux 312/5,[94] a bisphenol-A epoxy resin film adhesive.[95] The P2 etchant contains sulfuric acid and ferric sulfate. Digby and Packham,[95] using the wedge test, also demonstrated that joints formed with P2 etched, then

---

90. P. F. A. Bijlmer, *Met. Finish.,* ***75*** (August 1977) 22.
91. A. V. Pocius and J. J. Claus, *Nat. SAMPE Tech. Conf.,* ***13*** (1981) 629.
92. 3M Corporation, Minneapolis, MN, USA.
93. British standard alloy consisting of alloy 2014A clad with alloy 1050A (see Appendix 1).
94. Ciba-Geigy.
95. R. P. Digby and D. E. Packham, *Int. J. Adhes. Adhes.,* ***15*** (1995) 61.

phosphoric acid anodized adherends had higher strain energy release rates (G_I), than joints formed from FPL/phosphoric acid anodized adherends.

2. Anodizing

a. Phosphoric Acid Anodizing (PAA)

Anodizing in phosphoric acid is the preferred surface treatment for structural adhesive bonding in the North American aerospace industry.[1] The choice of phosphoric acid over other electrolytes for anodizing is related to the considerably slower hydration rate of the phosphated oxide formed during anodization, which makes this oxide layer environmentally stable.[60,73,96,97] Excellent reviews can be found in the literature describing the anodization process, the properties of the anodic oxide films, pore formation theories, and structural features of the oxide.[60,98,99,100,101] Anodization of aluminum in solutions of certain acid electrolytes, such as sulfuric, chromic, oxalic, and phosphoric acids, produces a "porous" oxide film, due to the solvent action of these acids towards aluminum oxide.[98] The oxide consists of a regular array of hexagonal cells with a cylindrical pore from the top surface to the continuous passivation layer formed at the metal /oxide interface.[98] The dimensions of the pores depend upon the applied potential and the electrolyte.[98] The thickness of the oxide is a function of the current density and anodizing time.[98]

---

96. J. D. Venables, M. E. Tadros, and B. M. Ditchek, *U.S. Pat. 4,308,079* (1981).
97. A. J. Kinloch, L. S. Welch, and H. E. Bishop, *J. Adhes.*, ***16*** (1984) 165.
98. F. Keller, M. S. Hunter, and D. L. Robinson, *J. Electrochem. Soc.*, ***100*** (1953) 411.
99. J. W. Diggle, T. C. Downie, and C. W. Goulding, *Chem. Rev.*, ***69*** (1969) 365.
100. S. Tajima, *Adv. Corros. Sci. Technol.*, ***1*** (1970) 229.
101. Y. Xu, "*The Growth Mechanisms of Anodic Films on Aluminum*," Ph.D. Thesis, The University of Manchester Institute of Science and Technology, England (1983).

Electron microscopy was used to examine the morphology and surface topography of Boeing PAA surfaces that are used for structural adhesive joining.[5,81,102] A model proposed for the structure of these oxide surfaces, is based on the work by Venables, et al.,[5] and is shown in Figure 2.2.

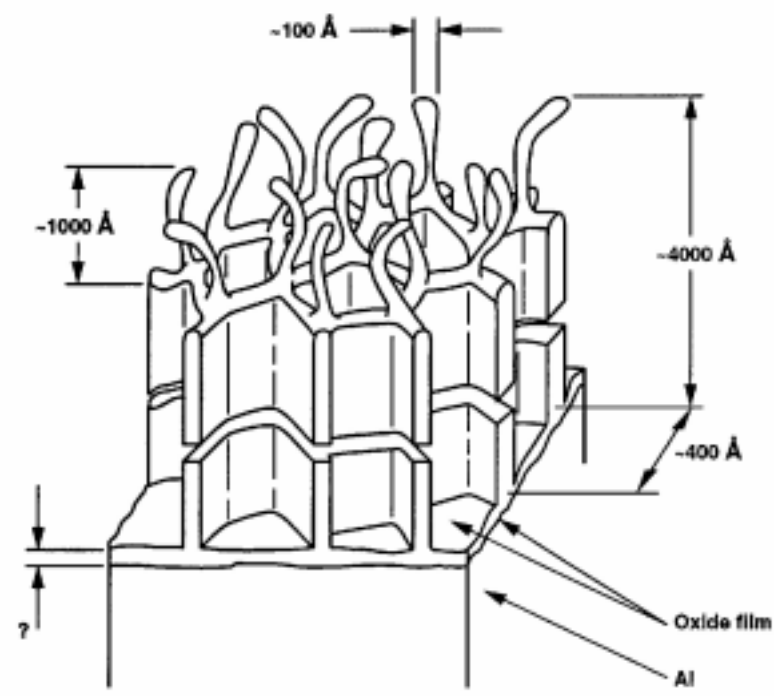

Figure 2.2. Schematic Diagram of Anodic Oxide Formed on Aluminum Alloy Surface by the Phosphoric Acid Anodizing Process[5]

"Whisker"-like protrusions at the cell junctions are noted for the PAA surface as they were for the FPL etched surface.[69] Venables, et al., attributes the presence of whiskers on the PAA

102. G. E. Thompson, R. C. Furneaux, G. C. Wood, J. A. Richardson, and J. S. Goode, *Nature (London), **272*** (1978) 433.

surface to the dissolution of cell walls.[5,103] Using evidence from transmission electron microscopy studies, a similar structure was reported by Thompson, et al.[102]

Using a combination of surface analytical tools, various researchers have determined the elemental composition of these surfaces.[4,81,82,83] Based upon binding energies in the X-ray photoelectron spectra, the chemical states of Al and P were assigned to Al_2O_3 and $AlPO_4$, respectively.[4] By Auger electron spectroscopy depth profiling, Solomon and Hanlin[81] found P throughout the anodic oxide film, with increased concentrations at the surface.

Ginsberg and Wefers,[104] and later, Thompson, et al.,[102] proposed a model of anodic oxide film growth and asserted that the anodic oxide consists of two parts: 1) relatively pure alumina at the cell boundary, and 2) a layer of phosphate incorporated microcrystallites extending from the cell wall towards the pore. A schematic representation, proposed by Thompson, et al.,[102] of the structure and composition of the PAA oxide used in structural adhesive joining is shown in Figure 2.3. Results from scanning transmission electron microscopy (STEM) and energy dispersive spectroscopy (EDS) analyses of the cell walls supported this model.[105] A phosphorus signal in the EDS spectrum was detected only for the region away from the cell boundary wall. Kinloch, et al.,[82] using XPS depth profiling assert that phosphorus is not detected after sputtering 30 nm into the PAA surface. From the studies described above, there appears to be some conflict with respect to the distribution of phosphate within the PAA anodic oxide. Its chemical composition and the distribution of phosphate within the anodized surface should dictate the reactivity of the oxide.[77]

---

103. J. S. Ahearn, T. S. Sun, C. Froede, J. D. Venables, and R. Hopping, *SAMPE Q.*, ***12*** (October 1980) 39.
104. H. Ginsberg and K. Wefers, *Metall (Berlin)*, ***16*** (1962) 173.
105. G. E. Thompson, R. C. Furneaux, and G. C. Wood, *J. Electrochem.Soc.*, ***125*** (1978) 1480.

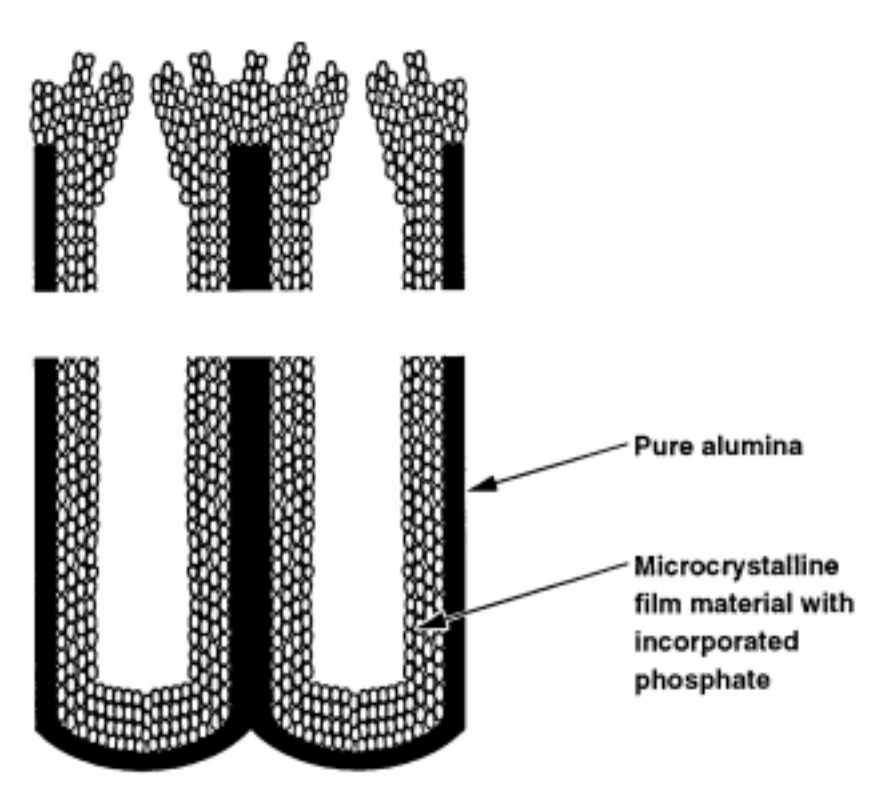

Figure 2.3. Schematic Diagram Representing the Distribution of Phosphate in Porous Anodic Film Formed in H_3PO_4 Solution[102]

The crystallinity and degree of hydration of the PAA oxide used in adhesive joining can be expected to influence bond durability.[77] Bowen[106] reported that the oxide on such surfaces consists of a mixture of bayerite and boehmite. However, Venables, et al.,[107] using electron diffraction, concluded that the oxide films are amorphous in nature. McDevitt and Solomon[108] reported similar results after comparing the thermal stability of the anodic oxide layer to that of boehmite and bayerite standards. They found no direct relationship of the anodic aluminum oxide to either compound. Other researchers claim that the PAA oxide contains a small percent

106. B. Bowen, *Nat. SAMPE Tech. Conf.*, ***7*** (1975) 374.
107. J. D. Venables, D. K. McNamara, T. S. Sun, B. Ditchek, J. M. Chen, and R. L. Hopping, *Struct. Adhes. Bond. Pap. Struct. Adhes. Bonding Conf.*, ***1*** (1979) p. 22.
108. N. T. McDevitt and J. S. Solomon, "Thin Anodic Oxide Films on Aluminum Alloys and Their Role in the Durability of Adhesive Bonds," *Tech. Rep. AFML-TR-79-4216* (1980).

of crystalline γ-Al_2O_3, depending on the applied potential and electrolyte concentration.[60] Infrared spectroscopy data[109] indicate that the oxide layer is composed primarily of a pseudoboehmite structure that contains both electrolyte anions and water. Venables, et al.,[107] used X-ray photoelectron spectroscopy to determine the degree of hydration of the oxide layer. Comparing the oxide film to standards of Al_2O_3 and $Al(OH)_3$, it was concluded that the spectrum compared favorably with Al_2O_3.[107] However, the authors did not argue that some water of hydration could be associated with the oxide.

b. Chromic Acid Anodizing (CAA)

Chromic acid anodizing has been the aluminum pretreatment of choice of the European aerospace manufacturers for over 60 years.[10,77] This process includes a chromic-sulfuric acid etch (German Standard LN 029751) followed by chromic acid anodizing (German Standard DIN 53281).[10] This specification is a modified version of the original process developed by Bengough and Stuart,[60] and is a stepwise process where the voltage is increased form 0 V to 40 V in 40-50 minutes.[110] The process has been modified several times, with the most recent modification being to increase the final voltage to 50 V.[111] Depending upon the alloy, the thickness of the CAA oxide can range from 2-6 μm,[112,113,114] It is postulated that since the

---

109. W. Vedder and D. A. Vermilyea, *Trans. Faraday Soc.*, ***65*** (1969) 561.
110. R. F. Wegman, in "*Surface Preparation Techniques for Adhesive Bonding,*" Noyes Publications, Park Ridge, New Jersey (1989) pp. 9, 33-34.
111. P. F. A. Bijlmer, Jr., in "*Adhesive Bonding of Aluminum Alloys*," E. W. Thrall and R. W. Shannon, ed., Marcel Dekker, Inc., New York (1985) p. 21.
112. G. A. Nitowski, K. Wefers, and N. R. Dando, in "*Haftung Bei Verbundwerkstoffen un Werkstoffverbunden*," W. Brockmann, ed., DGM Informationsgesellschaft mbH, Oberursel, Germany (1989) p. 237.
113. I. Berbezier, M. Romand, J. M. Martin, and J. M. Cuntz, *J. Adhes. Sci. Technol.*, ***6*** (1992) 829.
114. D. J. Arrowsmith and D. A. Moth, *Trans. Inst. Met. Finish.*, ***64*** (1986) 91.

European aerospace manufacturers typically use aluminum alloys clad with a purer aluminum cladding, this relatively thick anodic oxide is necessary to prevent galvanic corrosion of the cladding.[115] The diameter of the pores in these oxides has been reported at 5-10 nm,[112] 40 nm,[113] and 100 nm.[12] The reasons for the discrepant observations are not known. However, since anodic oxide pore sizes are proportional to the anodizing voltage,[98] and since the CAA process starts out at a low initial voltage (5 V),[110] it is reasonable to assume that the pore size on the outer surface of the oxide should be less than that observed for PAA oxide surfaces that are anodized at 10-15 V.[77] Compared to the PAA films, the CAA anodic oxides have little electrolyte anion incorporation, and consist of relatively pure alumina.[60]

Constant voltage variations of CAA, rather than the stepwise voltage process, have been proposed. A constant voltage process, known as the Bell process,[5] was patented.[116] A process similar to the Bell process, in which FPL etched clad 2024-T3 aluminum alloy was anodized at a constant voltage (49 V) for 40 min at 35°C, resulted in an anodic oxide that was approximately 1.5 μm thick.[5] The oxide had a dense structure that was completely solid in some areas.[5] A schematic representation of this CAA film is shown in Figure 2.4.[5] The authors[5] also suggest that the morphology of CAA films is very dependent upon processing parameters, and can show marked variations. There seems to be agreement that the stepwise 40-50 V CAA process, rather than a constant voltage CAA process, is best suited for the adhesive bonding of aluminum.[12,16,111]

---

115. G. D. Davis and D. Kent Shaffer, in "*Handbook of Adhesive Technology*," A. Pizzi and K. L. Mittal, ed., Marcel Dekker, Inc., New York (1994) p. 113.
116. H. L. Rogers, *U. S. Pat. 3,414,489 (1968).*

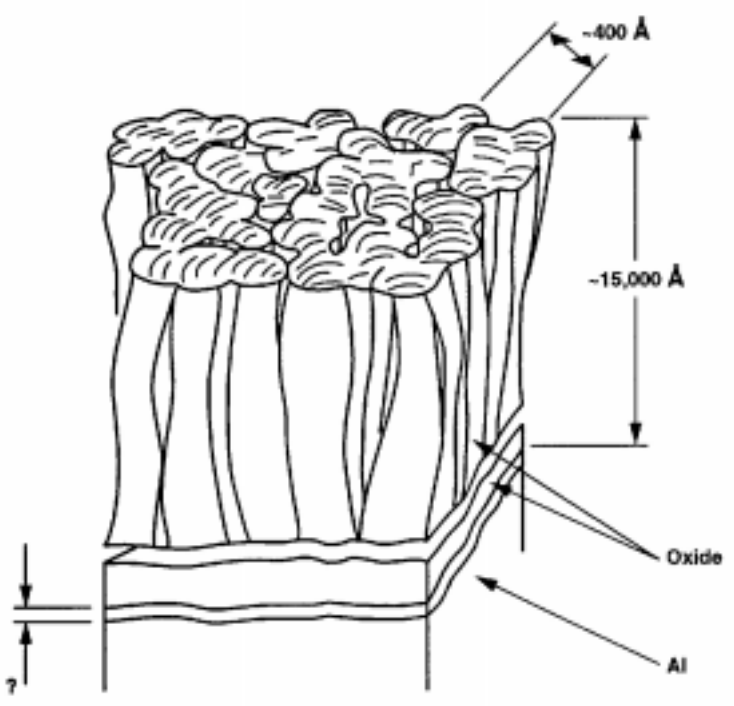

Figure 2.4. Oxide Morphology Produced on Al Alloy by a Constant Voltage CAA Process[5]

3. Chemical Conversion Coating

Anodic oxidation in solutions of chromic or phosphoric acid is the preferred stabilizing treatment for the structural adhesive bonding of high-strength aluminum alloys in critical applications such as aircraft components.[1] However, due to high capital and process costs, and treatment times of at least several minutes, anodic oxidation is not economically feasible for lower cost markets, such as the automotive and packaging industries. For these applications, chemical conversion treatments, particularly those based on chromium-containing solutions have become widely accepted as commercial practice.[1]

a. Cr(VI)-Based Conversion Coatings

Both chromate and chromate-phosphate conversion coatings are good inhibitors of corrosion and hydration of aluminum.[60] The hydration-inhibitor property of chromate-phosphate conversion

coatings can be attributed to the presence of a hydrolytically stable surface film of hydrated chromium(III) phosphate / chromium(III) oxide.[117] The main advantages of chromate-phosphate conversion coatings, over anodizing, are short treatment times, generally less than 10 seconds, and fairly inexpensive chemical components, i.e., chromic acid, phosphoric acid and acid fluorides such as ammonium bifluoride. Disadvantages are the presence of Cr(VI) and F^- ions in the treatment solution, which presents health and waste treatment problems; the precipitation of an unusable aluminum-chromium hydroxide sludge during the coating process;[77] and lower bond strength and durability, compared to anodized aluminum adherends.[1] A brief review of chromate-phosphate-type conversion coatings follows.

Treverton and Davies presented an initial characterization of chromate-phosphate conversion coatings on aluminum.[117] From the results of X-ray photoelectron spectroscopy (XPS) studies, the authors concluded that the bulk of the coating consists of $CrPO_4 \cdot 4H_2O$, plus about 10% (atomic) $Cr_2O_3 \cdot H_2O$ concentrated near the metal interface. A thin layer of less than 20% of the total thickness was assumed to consist of a mixture of Al_2O_3, AlOF and AlF_3. This layer is located at the metal / film interface (Figure 2.5).[117]

117. J. A. Treverton and N. C. Davies, *Met. Technol. (London), **4*** (1977 October) 480.

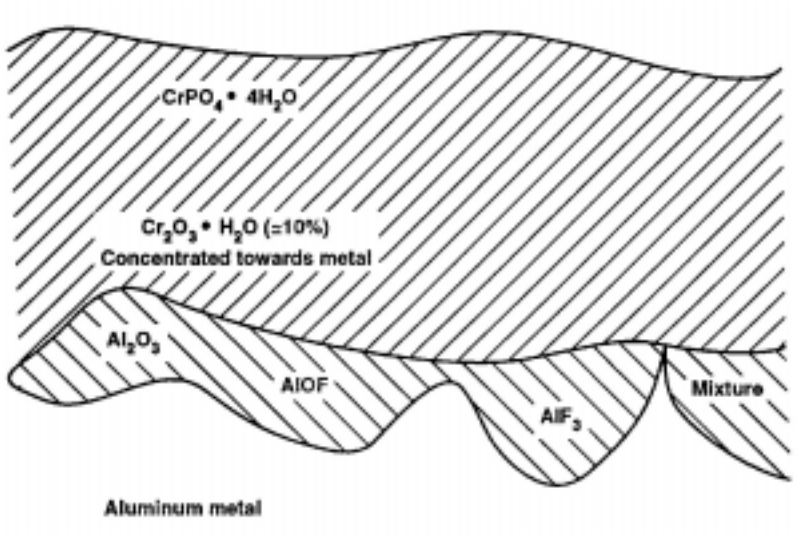

Figure 2.5. Schematic Representation of a Chromate-Phosphate Conversion Coating on Aluminum Alloy[117]

The presence of fluorine at the interface comes as a result of the role of F^- in dissolving the initial oxide and depassivating the aluminum metal. However, considering the oxidation-reduction reaction required for film growth,

$$Al^0 \rightarrow Al^{3+} + 3e^+$$

$$Cr^{6+} + 3e^- \rightarrow Cr^{3+}$$

and since these films can be grown to various thicknesses, one would expect to find Al^{3+} in the bulk of the conversion coating film.[77] This was originally not observed,[117] and suggested a deficiency in their model.[77]

In later studies, Crompton, et al.,[118] reported a composition for chromate-phosphate conversion coatings consisting of Cr, Al and P for a matrix that surrounded particles of a chromium compound, and a second type of Cr, and Al-rich particles near the metal interface. Treverton, et

118. J. S. Crompton, P. R. Andrews, and E. McAlpine, *SIA, Surf. Interface Anal.*, ***13*** (1988) 160.

al.,[119] supported Crompton's results, showing that the films are discontinuous and consist of a network of filaments composed of densely packed spherical particles. XPS analysis showed Al^0, regardless of the thickness of the conversion coating, indicating the coating is non-continuous. AES depth profiling revealed Cr, Al, P, O, and F. Treverton, et al.,[119] related aluminum and fluorine to "circular cathodic areas," but did not further discuss their observation or present a mechanism of film formation.

Arrowsmith, et al.,[120] studied the influence of dissolved metal ions on the conversion coating process. They determined that dissolved aluminum affects the growth and compactness of the conversion coating film. With Al levels of 0.5 g/L, the most compact and corrosion resistant films were formed. Increased magnesium ions in the bath resulted in flaking of the conversion coating film.[120]

Using Fourier transform-infrared spectroscopy (FT-IR) and surface-enhanced Raman spectroscopy (SERS), Ahern, et al.[121] deduced that the main component of these films was a hydrated chromium phosphate, and that the conversion coating was detectable at coverage as low as 9 mg Cr/m^2.

A mechanism of chromate conversion coating formation from Katzman, et al.,[122] and a mechanism for chromate-phosphate conversion coating formation from Asami, et al.[123] are summarized below:

---

119. J. A. Treverton, M. P. Amor, and A. Bosland, *Corros. Sci.*, ***33*** (1992) 1411.
120. D. J. Arrowsmith, J. K. Dennis, and P. R. Sliwinski, *Trans. Inst. Met. Finish.*, ***62*** (1985) 110.
121. A. M. Ahern, P. R. Schwartz, and L. A. Shaffer, *Appl. Spectrosc.*, ***46*** (1992) 1412.
122. H. A. Katzman, G. M. Malouf, R. Bauer, and G. W. Stupian, *Appl. Surf. Sci.*, ***2*** (1979) 416.
123. K. Asami, M. Oki, G. E. Thompson, G. C. Wood, and V. Ashworth, *Electrochim. Acta*, ***22*** (1987) 337.

Depassivation

$$AlOOH + 6F^- + 3H^+ \rightarrow Al_6^{3-} + 2H_2O$$
$$Al^0 + 3H^+ \rightarrow Al^{3+} + 1.5H_2$$

Film Formation

$$2Al^0 + Cr_2O_7^{2-} + 2H^+ + 6HF \rightarrow 2CrOOH\downarrow + 2AlF_{3\,(sol)} + 3H_2O$$
$$2Al^0 + Cr_2O_7^{2-} + 8H^+ + 6HF + 2PO_4^{3-} \rightarrow 2CrPO_4\downarrow + 2AlF_{3\,(sol)} + 7H_2O\,.$$

Haaksma and Weir[124] propose that the local pH increase accompanying the depassivation reaction results in the precipitation of $CrPO_4$. The initial aluminum surface reaction occurs in the areas with the highest electrochemical activity, and that since these are the areas where corrosive attack is most likely, the conversion coating forms where the protection is most needed.[124]

b. Non-Cr(VI) Conversion Coatings

During the past three decades, numerous publications and patents have appeared which deal with chemical conversion coatings that do not employ Cr(VI) compounds.[125,126,127,128,129] These treatments provide corrosion protection for bare aluminum or a base for painting, coating or adhesive bonding.[125]

---

124. R. A. Haaksma and J. R. Weir, *Internat. SAMPE Tech. Conf.*, ***27***, (1995) 1074.
125. G. D. Wilcox, D. R. Gabe, and M. E. Warwick, *Corros. Rev.*, ***6*** (1986) 327.
126. M. S. Vukasovich and J. P. G. Farr, *Mater. Perform.*, ***25*** (1986) 9.
127. G. H. Pimbley, *U.S. Pat. 2,976,193* (1961).
128. H. B. Romans, *U. S. Pat. 3,272,665* (1966).
129. M. S. Boulos, *U. S. Pat. 5,143,562* (1992).

Parker Co.'s Bonderite 1325 and Amchem Co.'s Alodine 4830 and 4831 are examples of commercial non-chromate conversion coating systems. Amchem's patent U. S. 4,148,670 describes a composition consisting of Zr^{4+} and/or Ti^{4+}, phosphate and sufficient fluoride to form a soluble complex with all the Zr^{4+} and Ti^{4+} in the system. U. S. patent 5,296,052 describes a conversion coating bath consisting of niobium, tantalum, zirconium, titanium, fluorine, and phosphate ions, and that aluminum coated using this process exhibited good adhesion of an epoxy-phenolic paint. U. S. patent 4,391,652, assigned to Chemical Systems, Inc., describes a solution made up of potassium zirconium fluoride, nickel nitrate, sodium fluorophosphate, hydrofluoric and nitric acid.

According to Newhard,[130] the zirconium-based conversion coatings have a layered texture with an outer layer composed of Zr, O, and F. Two layers of ZrO_2 and Al_2O_3, respectively, make up about four-fifths of the coating thickness. The coating is assumed to form by the precipitation of zirconium oxide due to an increase in pH of the treatment solution at the metal oxide/liquid interface. Wittel gave a detailed description of the film forming mechanism and XPS analyses of zirconium phosphate layers.[131] According to Wittel,[131] the reaction proceeds in three steps. These are depassivation, complexation, and precipitation, as shown in the following equations:

130. N. J. Newhard, Jr., *Corros. Control Coat. Pap. Meet.* (1979) 225.
131. K. Wittel, *Metalloberf.,* ***42*** (1988) 523.

Depassivation Step

$$AlOOH + 6F^- + 3H^+ \rightarrow AlF_6^{3-} + 2H_2O$$

$$Al + 3H^+ \rightarrow Al^{3+} + 1.5H_2$$

Complexing Step

$$Al^{3+} + ZrF_6^{2-} \rightarrow AlF_6^{3-} + Zr^{4+}$$

Film Formation

$$3Zr^{4+} + 4H_2PO_4^- \rightarrow Zr_3(PO_4)_4 + 8H^+$$

$$Zr^{4+} + 3H_2O \rightarrow ZrO(OH)_2 + 4H^+$$

Wittel[131] measured the thickness of zirconium phosphate films and found 4 nm for a well-developed coating, but only about 1 nm for films formed in solutions containing excess fluoride. Control of compositions and pH obviously is very critical for this coating process. Titanium phosphate films are formed in an analogous reaction sequence.[130]

Schram, et al.,[132] analyzed the composition of a zirconium-based conversion coating, Alodine 4830/4831,[133] which contains a fluorinated zirconium salt and a water-soluble polymer. Schram, et al.,[132] concluded that the thickness of the conversion coating formed on 1050 aluminum alloy was nearly independent of the time that the metal spent in the conversion coating bath. The authors also describe the film as a two layered structure with the bottom layer containing only Al and O, and the top layer containing the fluorinated zirconium compound and the polymer.

4. Boehmite Coatings

In the system Al-O-H_2O, aluminum trihydroxide $Al(OH)_3$ is the thermodynamically stable phase between room temperature and 100°C.[86] However, gelatinous hydroxides of the composition

132. T. Schram, G. Goeminne, H. Terryn, W Vanhoolst, and P. Van Espen, *Trans. Inst. Met. Finish.*, ***73*** (1995) 91.

AlO(OH, H_2O) are often kinetically favored, especially under the conditions of metal oxidation in ambient environments.[86,134] A simple approach for slowing the rate of the aluminum surface reaction with atmospheric moisture at ambient temperatures is to treat the metal with water or steam at 100°C or higher to form a stable oxide-hydroxide film.[77]

Strålin and Hjertberg[135] recently reported on the hydration, in boiling water, of aluminum alloy surfaces containing varying amounts of magnesium. Their work shows that there is an induction period before hydration that is due to the presence of the protective natural oxide film.[135] The length of the induction period correlates with the magnesium content of the alloy, there being an optimal concentration of Mg for increased hydration rate. Previous work by Wefers[85] on the thermal oxidation of Al-Mg alloys had shown that during typical heat treating temperatures, crystallites of γ-Al_2O_3 form. The rate of diffusion of Mg to the surface increases, since it is then possible for diffusion to occur at the interfaces between the crystalline and amorphous Al_2O_3 phases. Strålin and Hjertberg[135] propose a similar mechanism for the increased hydration rate of Al-Mg alloys. These authors noted that the original MgO layer on the heat-treated alloys was not dissolved in the boiling water, and that the aluminum hydroxide formed on top of the original Al - Mg oxide surface. During hydration, it was speculated that "channels" between amorphous and crystalline Al_2O_3 phases, which were formed during heat treatment, facilitated the initial rate of Al diffusion to the surface. Diffusion of Al in the channels was thought to take place at the interface boundaries between MgO and Al_2O_3 phases.[135] They further speculate that these boundaries increase the number of nucleation sites, and hence the nucleation rate. For alloys with higher Mg content, a secondary crystalline Mg-containing oxide forms, during heat treatment, and fills the channels between the amorphous and crystalline Al_2O_3 phases, thereby slowing down the metal/oxygen reaction.[85] The presence of the crystalline MgO phase on the outer surface of these alloys was also used to explain the longer hydration induction period that was observed for aluminum alloys containing the higher concentration of magnesium.[135]

---

133. Henkel (formerly Parker Amchem)
134. B. R. Baker and J. D. Balser, *Aluminium (Düsseldorf), **52*** (1976) 197.

The process of forming a boehmite film on aluminum surfaces has been known for more than 40 years.[136,137,138] Minford[139] has shown that boehmite surface films provide a favorable surface condition for adhesive bonding, but generally require treatment times on the order of a minute, and thus are limited to batch processing. Except for Minford's study,[139] there is little information in the literature on bond strength and durability of joints formed with hydroxylated aluminum alloy surfaces. The recent publications of Strålin and Hjertberg[135,140,141,142] report improved adhesion of low density polyethylene, and ethylene-butyl acrylate copolymer laminates on hydrated Al-Mg alloys. The hydrated adherends resulted in laminates that failed cohesively in the polymer. The authors concluded that the pseudoboehmite layer was strong enough, "at least for coating and painting applications."[135]

Although numerous patents describe methods and solution compositions for improving properties and rate of formation of boehmite films, there are no reports on major commercial use for coated or painted products.[60] The rate of film formation is generally increased by the use of alkaline solutions, e.g., aqueous solutions of alkanol amines.[60] Activators such as organic fluorides may be added to the solution, as taught by a patent issued to Showa Light Metals Co.[143] Post-treatment with silicate solutions improves corrosion resistance and adhesion.[144] Addition of glycerol to the water improves the properties of boehmite films.[145]

---

135. A. Strålin and T. Hjertberg, *Appl. Surf. Sci.*, ***74*** (1994) 263.
136. D. G. Altenpohl, *Corrosion (Houston)*, ***18*** (1962) 143.
137. D. G. Altenpohl, *Aluminium (Düsseldorf)*, ***29*** (1953) 361.
138. H. G. Ginsberg and K. Wefers, *Aluminium (Düsseldorf)*, ***37*** (1961) 19.
139. J. D. Minford, *Adhes. Joints: Form. Charact. Test. Proc. Conf.*, ***1***, Plenum Press, New York, NY (1984) 503.
140. A. Strålin and T. Hjertberg, *J. Appl. Polym. Sci.*, ***49*** (1993) 511.
141. A. Strålin and T. Hjertberg, *J. Adhes.*, ***41*** (1993) 51.
142. A. Strålin and T. Hjertberg, *J. Adhes. Sci. Technol.*, ***6*** (1992) 1233.
143. *Jap. Pat. JAJ 80141572* (1979).
144. *Jap. Pat. JP 87124282A* (1985).

5. Organosilanes

Historically, organosilanes have been used to improve the performance of glass/polymer composites.[146] It is proposed that organosilanes act as coupling agents between a glass fiber and a polymer matrix. In theory, the silane hydrolyses to form a silanol, which chemically reacts with the hydroxyl groups on the surface of the glass. The organic functional group of the hydrolyzed silane reacts with other silane molecules and with functional groups of the polymer, thus forming a hydrolytically stable, polymerized (polysiloxane), chemical couple between the polymer and the glass. This is schematically depicted in Figure 2.6.[147]

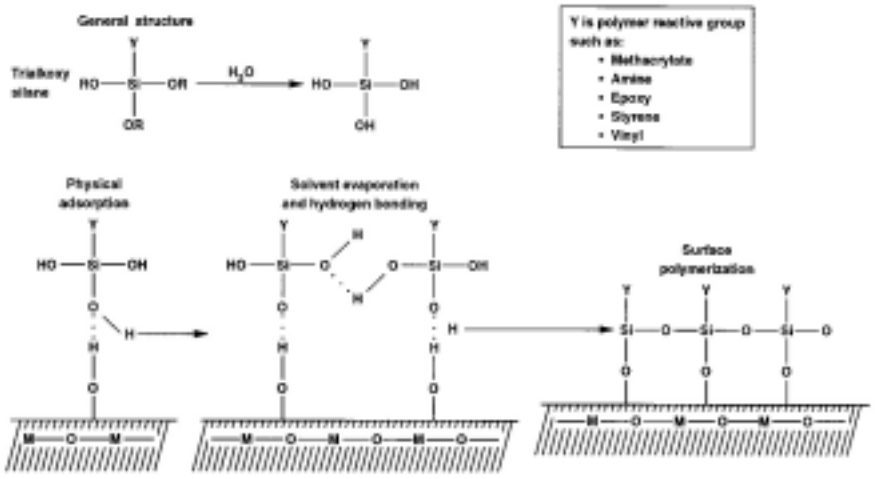

Figure 2.6. A Representation of the Bonding of Silane Coupling Agents to Mineral Surfaces[147]

Silane pretreatments of aluminum alloys for structural adhesive bonding are attractive in that they have the potential of requiring short pretreatment times, and obviously, do not require the use of toxic chromates. The use of silanes has several disadvantages, including: high cost, hydrolytic instability of the treatment baths,[77] and poorer performance on non-siliceous

---

145. *Jap. Pat. J 78005256* (1971).
146. E. P. Plueddemann, "*Silane Coupling Agents*," Plenum Press, New York (1982).
147. M. K. Chaudhury, T. M. Gentle, and E. P. Plueddemann, *J. Adhes. Sci. Technol.,* ***1*** (1987) 29.

substrates.[148] Therefore, only a brief survey of the silane literature, related to aluminum will be presented.

Literature describing the use of organosilane pretreatments for structural adhesive bonding of aluminum is extensive.[149,150,151,152,153,154,155,156,157,158,159,160] Much of the literature on aluminum describes the use of dilute aqueous solutions of γ-aminopropyltriethoxysilane (γ-APS) to improve aluminum epoxy adhesive joint performance.[150-155,158-160] It was reported that epoxy/aluminum joint performance is dependent upon the pH of the organosilane solution,[149,153,160] upon the length of treatment,[153] and upon the solvent used for deposition.[149]

On the basis of Inelastic Electron Tunneling Spectroscopy (IETS), it was suggested that γ-glycidoxypropyltrimethoxysilane applied to an aluminum reacts to form carbon-carbon and carbon-oxygen double bonds.[150,151] It was also demonstrated that vinyltrimethoxysilane reacts with the aluminum oxide surface via the methoxy groups, leaving the vinyl- group intact and

---

148. L. B. Cohen, *J. Adhes. Sci. Technol.*, ***5*** (1991) 439.
149. F. J. Boerio and J. Williams, *Appl. Surf. Sci.*, ***7*** (1981) 19.
150. D. M. Brewis, J. Comyn, D. P. Oxley, R. G. Pritchard, S. Reynolds, C. R. Werret, and A. J. Kinloch, *SIA, Surf. Interface Anal.*, ***6*** (1984) 40.
151. J. Comyn, A. J. Kinloch, C. C. Horley, R. R. Mallik, D. P. Oxley, R. G. Pritchard, S. Reynolds, and C. W. Werrett, *Int. J. Adhes. Adhes.*, ***5*** (1985) 59.
152. F. J. Boerio, R. G. Dillingham, and R. C. Bozian, *Proc. Annu. Conf. Reinf. Plast. Compos. Inst. Soc. Plast. Ind.*, ***39*** (1984) 1.
153. F. J. Boerio, C. A. Gosselin, R. G. Dillingham, and H. W. Liu, *J. Adhes.*, ***13*** (1981) 159.
154. C. S. Paik Sung, S. H. Lee, and N. H. Sung, *Adhes. Adsorp. Polym. Proc. Int. Conf.*, ***1***, American Chemical Society, Washington, DC (1979) 757.
155. P. N. Henriksen, A. N. Gent, R. D. Ramsier, and J. D. Alexander, *SIA, Surf. Interface Anal.*, ***11*** (1988) 283.
156. J. D. Alexander, A. N. Gent, and P. N. Henriksen, *J. Chem. Phys.*, ***83*** (1985) 5981.
157. D. J. Ondrus, F. J. Boerio, and K. J. Grannen, *J. Adhes.*, ***29*** (1989) 27.
158. F. J. Boerio and C. H. Ho, *J. Adhes.*, ***21*** (1987) 25.
159. A. Kaul, N. H. Sung, I. Chin, and C. P. Sung, *Proc. Annu. Conf. Reinf. Plast. Compos. Inst. Soc. Plast. Ind.*, ***37*** (1982) 1.
160. F. J. Boerio, C. A. Gosselin, R. J. Dillingham, and J. M. Burkstrand, *Nat. SAMPE Tech. Conf.*, ***15*** (1983) 212.

oriented away from the surface.[155,156] Vibrational spectroscopic studies of γ-APS adsorbed onto aluminum indicate that the surface amino groups are either associated with each other through hydrogen bonding, or are back bonded to the underlying polysiloxane network.[150,151,154]

Enhancement of adhesion when using silanes with reactive functionalities has been reported, and a chemical coupling mechanism has been proposed. However, data demonstrating a chemical reaction of an organosilane adsorbed on aluminum oxide and a polymer has only recently been reported.[157] The amine of an aminosilane primer preferentially reacted with an anhydride curing agent, and not with the epoxy resin.

It has also been suggested that good adhesion is possible when silanes with non-reactive functionalities are used as primers.[161] Good peel strength retention after exposure to liquid water, or to humidity, was observed when silanes were used with (non-reactive) thermoplastics, such as polyethylene.[159]

The various observations listed above indicate that enhanced adhesion of systems with substrates primed with silanes cannot be attributed entirely to the formation of chemical bonds between the aluminum oxide, silane, and adhesive. Accordingly, other mechanisms for the observed silane adhesion promotion have been proposed. Good adhesion of silane primed epoxy bonded aluminum joints has been ascribed solely to the corrosion protection offered by a cured polysiloxane film on the aluminum oxide.[151,158] This was attributed to the formation of a highly cross linked polysiloxane network which slows the diffusion of water to the aluminum oxide,

161. Personal communication with E. P. Plueddemann, formerly of Dow Corning Corp.

thus inhibiting the hydration of the oxide and resulting joint failure.

As previously mentioned, it was suggested that adhesive joint performance can be improved by using silanes which do not contain a reactive functional group.[161] Thick layers of silane (up to 1 μm) can be deposited, from alcoholic solution, onto the adherend. During curing of the joint, it is postulated that the silane and the adhesive interdiffuse to form an interpenetrating network (IPN).[147,159] This is shown schematically in Figure 2.7.[147]

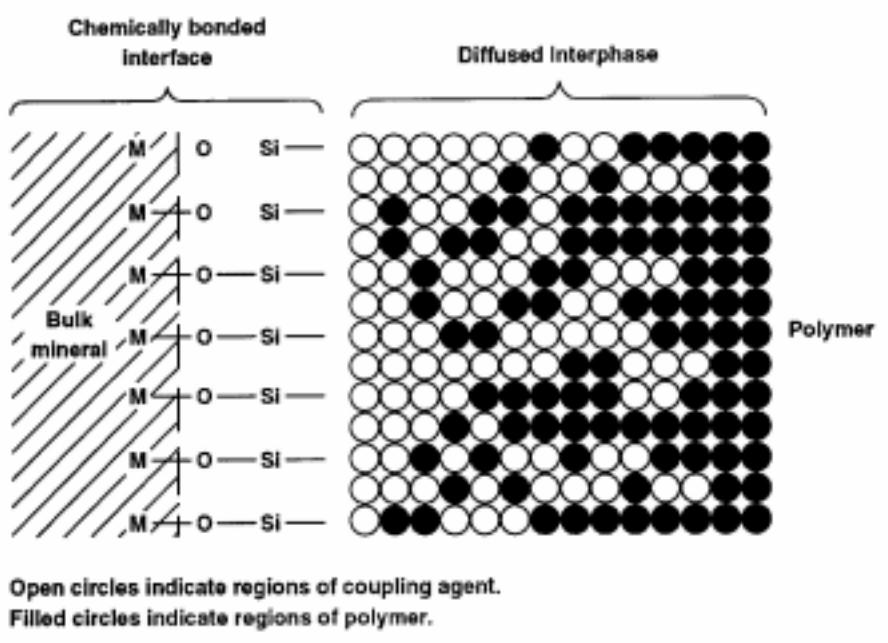

Figure 2.7. Interdiffusion Model for a Silane-Primed Mineral/Polymer Bonding System, Interpenetrating Network - IPN[147]

Furthermore, it is reported[162] that incorporation of a hydrophobic silane in the polysiloxane film will limit diffusion of water to the aluminum oxide interface, and, hence, inhibit hydration of the aluminum oxide and failure of the bond by mechanical weakening.

---

162. E. P. Plueddemann and P. G. Pape, *Mod. Plast.*, ***62*** (July 1985) 78.

Woo, et al.,[163] used cathodic electrodeposition to deposit organosilane films on aluminum alloy 2024-T3, and suggested that the films are more uniform than films formed by dipping without an applied potential. The electrodeposited films provided epoxy bonded joints with durability performance that was "at least similar or, in some cases, better" than joints formed with the immersion-only process.[163]

A patent was recently awarded to Betz Laboratories,[164] Inc. in which organosilanes are used in conjunction with cationic polymers and aqueous alkaline silicate for conversion coating aluminum, steel, and zinc. Several patents[165] were awarded to Armco Steel Company, that describe the pretreatment of steels with solutions containing inorganic silicates, organosilanes, and a silane crosslinking agent.

Recently, a two-step metal treatment process involving silanes has been proposed.[166] It is suggested that a nonfunctional silane, bis-1,2-(triethoxysilyl)ethane (BTSE), is a stronger acid than organofunctional silanes, and therefore can instantaneously form covalent, hydrolysis-resistant bonds with basic hydroxyl groups on oxidized metal surfaces. Since there are six silanol groups on hydrolyzed BTSE molecule it is proposed that some of the silanol groups of the molecule form covalent bonds with the surface, while others on the molecule remain for interaction with silanol groups from the second step of the process. The second step is to treat the surface with an organosilane that contains a functional group, which is specified for optimum interaction with the top coating or adhesive.[166]

---

163. H. Woo, P. J. Reucroft, and R. J. Jacob, *J. Adhes. Sci. Technol., **7*** (1993) 681.
164. D. L. Purnell, B. S. Morris, and D. W. Reichgott, *U.S. Pat. 5,389,405* (1995).
165. W. J van Ooij, *U. S. Pat. 5,455,080* (1995); A. Sabata and W. J. van Ooij, *U. S. Pat. 5,326,594* (1994); W. J. van Ooij and A. Sabata, *U. S. Pat. 5,322,713* (1994); W. J. van Ooij, R. A. Edwards, and A. Sabata, *U. S. Pat. 5,292,549* (1994); W. J. van Ooij and A. Sabata, *U. S. Pat. 5,200,275* (1993); W. J. van Ooij and A. Sabata, *U. S. Pat. 5,108,793* (1992).
166. W. J. van Ooij and T. Child, *Chemtech, **28*** (February 1998) 26.

6. Nitrilotris(methylene)triphosphonic Acid --- (NTMP)

The adsorption of amino phosphonic acids onto etched aluminum alloy surfaces improved the subsequent environmental durability of adhesively bonded joints.[167,168,169,170,171] These investigators show that etching 2024-T3 and 2219-T87 with the FPL etch, followed by the adsorption of nitrilotris(methylene)triphosphonic acid (NTMP), yields epoxy resin bonded joints with environmental durability equivalent to those formed from phosphoric acid anodized adherends.[172] The structure of the NTMP molecule is shown in Figure 2.8.a.[173]

NTMP adsorbed onto the aluminum oxide surface inhibits hydration of aluminum oxide to aluminum hydroxide, in the presence of water, and thus, improves the durability of the adhesive joint.[173] Hardwick, et al.,[173] also showed that the durability of joints formed with phosphoric acid anodized adherends can be improved when the phosphoric acid anodic oxide is treated with 10-300 ppm NTMP aqueous solutions prior to bonding. The optimum NTMP surface coverage was one monolayer. When surface coverage was more than one monolayer, the subsequent

---

167. G. D. Davis, J. S. Ahearn, L. J. Matienzo, and J. D. Venables, *J. Mater. Sci.*, ***20*** (1985) 975.
168. J. S. Ahearn, G. D. Davis, T. S. Sun, and J. D. Venables, *Adhes. Aspects Polym. Coat. Proc. Symp.*, ***1***, Plenum Press, New York, NY (1983) 281.
169. D. A. Hardwick, J. S. Ahearn, A. Desai, and J. D. Venables, *J. Mater. Sci.*, ***21*** (1986) 179.
170. G. D. Davis, J. S. Ahearn, and J. D. Venables, "Environmental Durability of Aluminum Adhesive Joints Protected with Hydration Inhibitors, Third Year Report," *Tech. Rep. MML TR 83-34c* (1983).
171. G. D. Davis, J. S. Ahearn, L. J. Matienzo, and J. D. Venables, "Mechanical Properties of Adhesively Bonded Aluminum Structures Protedted with Hydration Inhibitors," *Tech. Rep. MML TR 84-54c* (1984).
172. J. D. Venables, M. E. Tadros, and B. M. Ditchek, *U.S. Pat. 4,308,079* (1981).
173. D. A. Hardwick, J. S. Ahearn, and J. D. Venables, "Mechanical Properties of Adhesively Bonded Aluminum Structures Protected with Hydration Inhibitors, Second Year Report)," *Tech. Rep. MML TR-23c* (1982).

fracture path, in the wedge crack test, was through the physisorbed NTMP layer, since P was detected by XPS on both failure surfaces.[173]

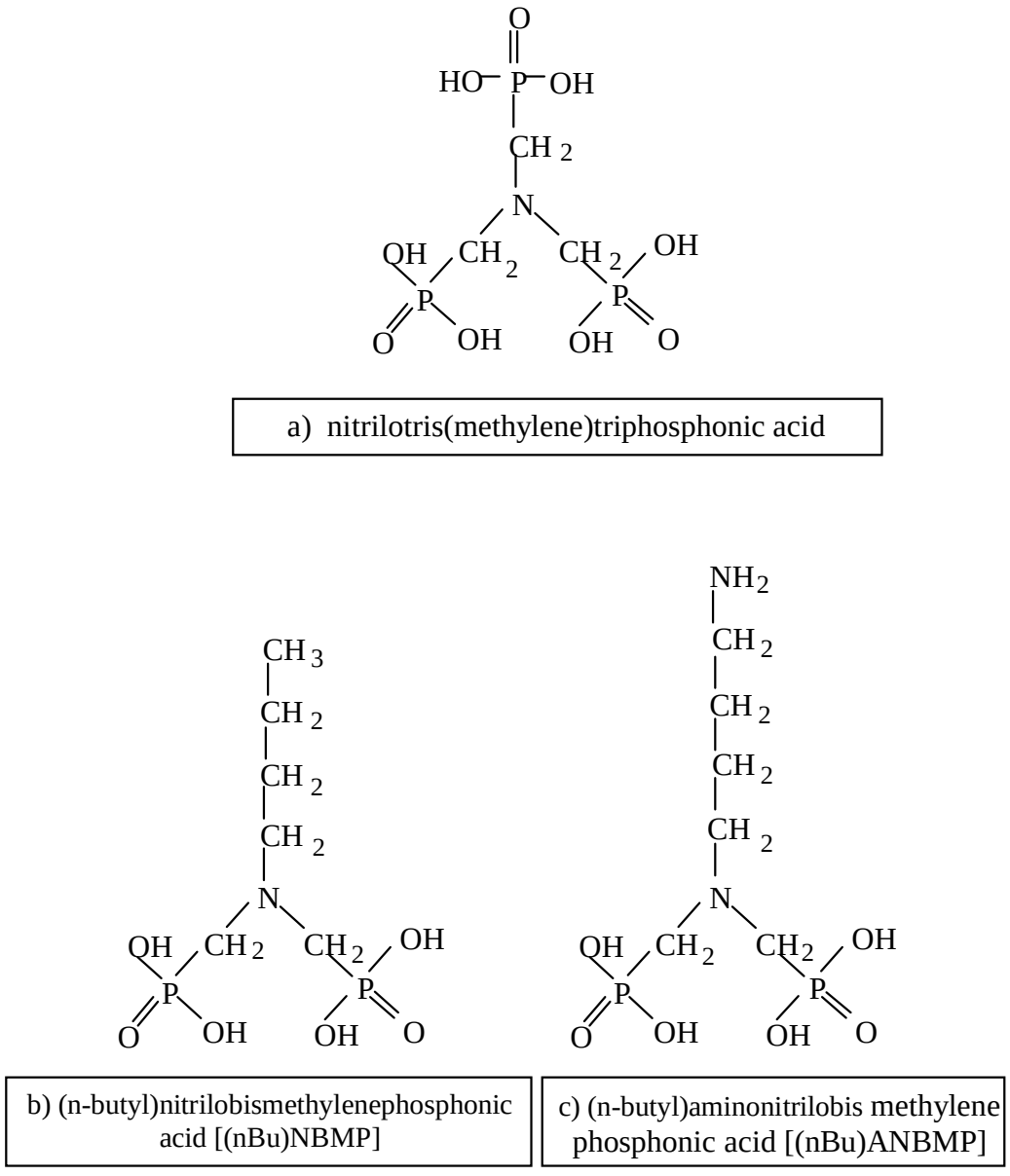

Figure 2.8. Aminophosphonic Acid Hydration Inhibitors for Aluminum Oxide: a) NTMP, b) (n Bu) NBMP, c) (n Bu) ANBMP

Davis, et al.,[170] identified four properties of the ideal hydration inhibitor for adhesively bonding aluminum. These are: 1) all of the active sites on the surface should be occupied by the inhibitor molecules, 2) the inhibitor molecules should strongly interact with the surface, 3) the inhibitor-oxide complex should be insoluble in water, and 4) the inhibitor molecules should be compatible with the primer or adhesive. Davis, et al.,[170] also indicate that NTMP interferes with the near-surface curing of the nitrile phenolic adhesive, used in their investigations.

In a later investigation, Davis, et al.,[174] modified the NTMP molecule to include a hydrocarbon chain that would allow for molecular mechanical interlocking. This inhibitor is (n-butyl) nitrilobis methylene phosphonic acid (*n*BU-NBMP), and the molecular structure is shown in Figure 2.8.b. Davis, et al., suggest that the hydrocarbon chain (n-butyl) can interlock with the polymer chains of the adhesive.[174] Furthermore, Davis, et al.,[174] assert that adding an amino group to the n-butyl portion of the molecule, to form (n-butyl) aminonitrilobis methylene phosphonic acid (Figure 2.8.c), provides an opportunity for the adhesive to chemically couple with the treated oxide. Davis, et al.,[174] did not see any superior results when using the n-butyl inhibitors, compared with NTMP, and suggested that the reason for this was that the n-butyl molecules had only two phosphonic acid groups to occupy the active sites on the surface, whereas the NTMP molecule has three phosphonic groups. Therefore, NTMP provided superior hydration resistance to the oxide surface.[174]

Arrowsmith, et al.,[59] bonded 5251 alloy adherends that were hard anodized in sulfuric acid solution, dipped in sodium hydroxide solution to enhance surface roughness, dipped in 10 ppm NTMP, and bonded with an acrylic and an epoxy adhesive. After 1500 hr immersion in room temperature water, Arrowsmith, et al.,[59] report that joints formed with adherends that were treated with the NTMP solutions showed a 3-13% loss of joint strength compared with joints

---

174. G. D. Davis, J. S. Ahearn, and J. D. Venables, "Mechanical Properties of Adhesively Bonded Aluminum Structures Protected with Hydration Inhibitors, Final Report," *Tech. Rep. MML TR85-7c* (1985).

with adherends that did not receive the NTMP treatment.

Rider and Arnott[175] exposed aluminum alloy 2024-T3 to 300 ppm aqueous solutions of NTMP, *n*Bu-NBMP (see Figure 2.8), and (3-hydroxypropyl)nitrilobismethylene phosphonic acid. The solutions were adjusted to pH 3.5 with dilute nitric acid, and the samples soaked for 15 min. Thorough distilled water rinsing, and drying with nitrogen followed the surface treatment. Metal was also treated with γ-glycidoxypropyl trimethoxysilane (γ-GPS), for comparison with the organophosphonate treated metal. Some treated metal was exposed to condensing humidity at 50°C, and the rate of oxide growth was monitored using XPS. Other treated samples were bonded with FM-73 modified epoxy film adhesive and wedge tested according to ASTM D3762-79. The results showed that NTMP inhibited oxide/hydroxide formation when exposed to humidity, and was more effective than γ-GPS. However, none of the organophosphonates improved bond durability, as compared with FPL-etched surfaces, and all of the organophosphonates reduced the durability of manually abraded surfaces. γ-GPS did improve joint durability. This improvement was attributed to the formation of a multilayer, cross-linked siloxane film on the surface, and effective coupling with the epoxy adhesive. These authors[175] concluded that the even though the organophosphonates inhibited hydration, they poorly coupled with the adhesive. Failure analysis showed that the bonds with organophosphonate treated adherends failed in the organophosphonate layer, indicating multilayer adsorption. The multilayer served as a weak boundary layer in the joint. It is suggested that phosphonate performance could be improved by more thorough rinsing and modifying the ligand interacting with the adhesive.

---

175. A. N. Rider and D. R. Arnott, *SIA, Surf. Interface Anal.*, ***24*** (1996) 583.

7. Inorganic Primers

Pike formed amorphous aluminum oxide coatings on phosphoric acid anodized 2024-T3 alloy by solvent casting solutions of aluminum alkoxides in toluene.[176] The cast coatings were converted to amorphous alumina by heating at 325°C. Pike found that the joints with the inorganic primer had wet and dry lap shear and T-peel strengths that were equivalent to joints containing standard organic primers. Furthermore, the amorphous alumina primer filled the surface porosity produced in the phosphoric acid anodizing step. Thus, Pike concluded that the mechanism of mechanical interlocking does not play a significant role in determining the adhesive durability of bonds formed with inorganic primed surfaces. He suggested that some type of chemical interaction could be responsible for the improved adhesion, or that the morphology of the primed surface minimized the formation of weak boundary layers in the adhesive interphase.

Pike later demonstrated that the initial aluminum alkoxide on the surface could be converted to amorphous alumina at room temperature.[177] In his investigation it was also determined that a four- to ten-fold improvement in joint durability, as measured by crack propagation in the wedge test, was obtained with inorganic primers, when compared with organic primer controls. Furthermore, joints with the inorganic primer on either FPL etched or phosphoric acid anodized adherends showed no difference in joint durability. The effective thickness of the inorganic primer on FPL etched aluminum was approximately 300 nm.[178] The effective thickness appeared to be a function of the depth of the oxide porosity.[179] In the same publication,[179] it was related that the shelf life of the inorganic primed adherends was at least one year. No difference in wedge test performance was observed when the inorganic primed adherends were bonded immediately after priming, or when the primed adherends were bonded one year after priming.

---

176. R. A. Pike, *Int. J. Adhes. Adhes.*, ***5*** (1985) 3.
177. R. A. Pike, *Int. J. Adhes. Adhes.*, ***6*** (1986) 21.
178. R. A. Pike and F. P. Lamm, *Polym. Mater. Sci. Eng.*,***56*** (1987) 299.
179. R. A. Pike and F. P. Lamm, *J. Adhes.*, ***26*** (1988) 171.

Pike and Golden[180] described a water based inorganic primer, based on a solution of "hydrated, polymeric aluminum oxide," which provided acceptable adhesively bonded 2024 aluminum joint strengths and wedge crack test durability, when using certain, but not all, epoxy adhesives. Pike and DeCrescente[181] showed that the adherends prepared with the water-based inorganic primers had to be dried sufficiently, presumably to remove the waters of hydration of the alumina deposited onto the adherend surface; control of pH was also critical. Pike and DeCrescente,[181] also demonstrated that the addition of an aminosilane to the water based alumina system resulted in a more versatile primer system, with respect to different epoxy adhesive formulations. Pike and DeCrescente[181] did not determine the precise structure of the inorganic primer in aqueous solution, but from spectroscopic data, concluded that it is not the same as an acid hydrolyzed aluminum alkoxide sol.

8. Treatment of Surfaces with Polymers

Sugama, et al.,[182] used aqueous solutions of poly(acrylic acid) to prime FPL-etched, aluminum alloy 2024-T3 surfaces, which were then laminated with polyurethane. Sugama, et al.,[182] exposed these laminates to 0.1 M NaOH at 80°C for 5 h, and observed that the poly(acrylic acid) primed laminates retained as much as 70% of the initial strength in a 180° peel test. The strength retention of the poly(acrylic acid) primed systems was a three-fold improvement over laminates with etched-only aluminum.[182] When the reaction product of poly(acrylic acid) with a hydrated aluminum surface was examined using XPS, a shift (from bulk values) in the component of the XPS C 1s band assigned to -C(O)O- carbon led Sugama, et al., [182] to the conclusion that the poly(acrylic acid) forms hydrogen bonds with the surface through proton donor/acceptor mechanism as follows:

---

180. R. A. Pike and G. S. Golden, *J. Adhes.*, ***29*** (1989) 111.
181. R. A. Pike and M. A. DeCrescente, *Int. J. Adhes. Adhes.*, ***11*** (1991) 154.
182. T. Sugama, L. E. Kukacka, C. R. Clayton, and H. C. Hua, *J. Adhes. Sci. Technol.*, ***1*** (1987) 265.

-COOH (proton donor) + HO-Al (proton acceptor) $\rightarrow$ -$COO^{-\cdots\cdots\cdots+}H_2O$-Al.

Sugama, et al.,[182] also give infrared spectroscopic evidence that the following chemical reaction takes place between the -N=C=O groups of the polyurethane resin and -COOH groups of the poly(acrylic acid) primer at the prime/resin interface:

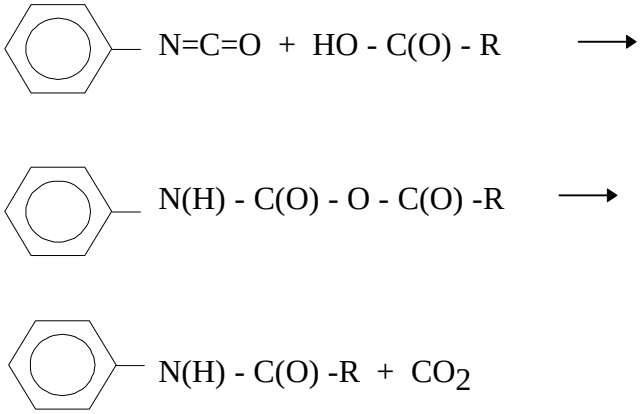

Later, Sugama, et al.,[183] used poly(itaconic acid) as primer for adhesive bonding, and found increased durability, compared to poly(acrylic acid). This molecule differs from poly(acrylic acid) by having two, instead of one, pendent carboxylic acid groups on the same backbone carbon. Sugama, et al.,[183] found that when exposed to hot alkali solution, the primed joints failed by hydrolysis of polyurethane-primer mixed layer. Sugama, et al.,[183] also studied three other water soluble polymers, as primers, including: poly(styrenesulphonic acid), polyacrylamide, and polyvinylpyrrolidone, but none of these polymers performed as well as the poly(itaconic acid). Schmidt, et al.,[184] have shown that poly(ethylene mercaptoester) (EME) treatments of steel improved that adhesion of a polyamide coating, and Bell, et al.,[185] showed that the EME treatment also improves the durability of epoxy-bonded steel.

---

183. T. Sugama, L. E. Kukacka, and N. Carciello, *Int. J. Adhes. Adhes.*, ***8*** (1988) 101.
184. R. G. Schmidt, J. P. Bell and A. Garton, *J. Adhes.*, ***27*** (1989) 135.
185. J. P. Bell, R. G. Schmidt, A. Malofsky, and D. Mancini, *J. Adhes. Sci. Technol.*, ***5*** (1991) 927.

Nesbitt, Bell, and Nikles[186] presented data regarding two proposed coupling agents for aluminum and polymers. These were low molecular weight β-diketones, and polymeric quinone-amines. Modified torsional shear butt joints were prepared with adherends that were methanol wiped, and with adherends that were wiped and soaked in 0.2% (w/w) of the coupling agents for ten minutes at room temperature, then air dried. Adherends with both coupling agents provided increased strength retention, after a 4-day water soak, compared to the methanol wiped-only adherends.

9. Other Non-Chromate Surface Treatments

Patents[187] were recently issued to The Boeing Company on cobalt-based conversion coatings. In their patent, a cobalt(III) hexacoordinated complex, along with acetic acid is reacted with the aluminum surface. The preferred hexacoordinated complex is $[Co(NH_3)_6]X_3$, where X is a suitable counter ion. The largest volume percent of the conversion coating is Al_2O_3. In addition, the cobalt oxides, CoO, Co_3O_4, and Co_2O_3 are present.

Brockmann[188] has shown that the adsorption of aromatic and heterocyclic organic compounds onto FPL treated and chromic acid anodized aluminum surfaces can increase the retention of peel strength in phenolic resin bonded joints, after exposure to high pressure and temperature (0.2-2 atm and 105^{o}-133^{o}C). Brockmann[16] speculates that one compound, 5,7,2,4-tetrahydroxyflavonene, can bond to both the oxide and to the phenolic adhesive through hydroxyl groups on opposite ends of the aromatic molecule.

A coupling agent based on a chromium(III) fumarato coordination compound was patented and assigned to the E. I. duPont de Nemours and Company.[189] When aluminum is treated with the

---

186. S. L. Nesbitt, J. P. Bell, and D. E. Nikles, *Proc. Annu. Meet. Adhes. Soc.*, ***18*** (1995) 191.
187. M. P. Schriever, *U.S. Pat: 5,298,092* (1994) and *5,378,293* (1995).
188. W. Brockmann, *Adhes. Age*, ***20*** (June 1977) 30.
189. A. J. Deyrup, *U. S. Pat. 3,787,326* (1974).

coordination compound (commercially known as Volan 82),[190] the adhesion of polyethylene to the treated aluminum remains strong in the presence of water. Yang and Zhou[191] have shown that when aluminum foil was coated with Volan 82 and then extrusion coated with low density polyethylene, the laminates showed high peel strengths, and good retention of strength even after soaking for three years in solutions of sodium hydroxide, acetic acid, and sea water.

Zircoaluminates (ZA), are bifunctional molecules, that when added to adhesives or coatings, exhibit a substantial increase in the corrosion resistance and adhesive bond strength of coated or bonded metal.[148] The structure of a zircoaluminate is shown in Figure 2.9.[148]

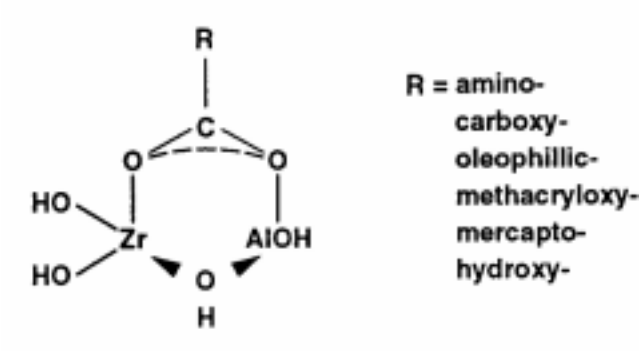

Figure 2.9. Molecular Structure of a Zircoaluminate Coupling Agent[148]

Cohen[148] envisions that when zircoaluminates are added to a polymer in contact with a high energy metallic surface, the ZA migrates to the metal interface and hydroxyl bridging linkages are formed between the ZA and hydroxyl groups on the metal surface. Furthermore, when the polymer is cured, a functional group on the ZA, for example a carboxyl group, can chemically react with functional groups in the polymer. Cohen[148] refers to this coupling of the metal with the polymer as a "zircoaluminate chemical bridge."

---

190. C. Q. Yang, T. W. Rusch, S. P. Clough, and W. G. Fateley, *Polym. Mater. Sci. Eng.*, ***56*** (1987) 304.
191. C. Q. Yang and Q. Zhou, *Appl. Surf. Sci.*, ***23*** (1985) 213.

A method to prepare highly corrosion resistant aluminum alloys is described by Mansfeld and Wang.[192,193] Their approach is to incorporate rare earth elements, particularly cerium compounds, into the surface film. This is accomplished by boiling the metal in $Ce(NO_3)_3$ solution. In addition, molybdenum is incorporated into this surface by a subsequent anodization in Na_2MoO_4 solution. This is then followed by another boiling step in $CeCl_3$ solutions. While Mansfeld observes that the treatments provide highly corrosion resistant metal, there appear to be no published data on polymer adhesion. A patent[194] was assigned to the Lockheed Corporation that teaches the formation of a corrosion resistant conversion coating that involves a three-step process using cerrous and strontium chloride solutions, molybdate, nitrate and silicate solutions, and organosilanes. Again, there is no mention of polymer adhesion.

Walker[195] provides a review of the use of zirconium and titanium coupling agents for improved adhesion of various materials. Yang, et al.,[190] using AES conclude that a titanium coupling agent, KR 238[196] bonds to the aluminum oxide through a hydrolytically stable Al-O-Ti linkage. Moles[197] concludes that there is not a large amount of work published on zirconium coupling agents, but demonstrated that the adhesion of aluminum-polymethylmethacrylate laminates is markedly increased when zirconium coupling agents are used.

Pike, et al.,[198] used plasma sprayed coatings to improve the adhesion of 2024-T3 aluminum to a glass/epoxy composite, and to sheet molding compound. Alumina coatings were plasma sprayed

---

192. Mansfeld and Wang, *Br. Corros. J.*, ***29*** (1994) 194.
193. F. Mansfield and Y. Wang, *Mater. Sci. Eng.* ***A198*** (1995) 51.
194. R. N. Miller, *U. S. Pat.* 5,221,371.
195. P. Walker, in "*Surface Coatings*, ***1***," A. D. Wilson, J. W. Nicholson and H. J. Prosser, eds., Applied Science Publishers, NY (1988) p. 189.
196. Kenrich Petrochemicals, Inc.
197. P. J. Moles, *J. Adhes. Sci. Technol.*, ***6*** (1992) 61.
198. R. A. Pike, V. M. Patarini, R. Zatorski, and F. P. Lamm, *Int. J. Adhes. Adhes.*, ***12*** (1992) 227.

onto the 2024-T3 aluminum alloy. Compressive shear strengths measured after exposure to elevated temperature and humidity allowed Pike, et al.,[198] to conclude "that a thin, microporous, plasma-sprayed alumina primer is a viable approach to achieve acceptable adhesively bonded structures consisting of metal/composite adherends."

Kester[199] used a pulsed Nd:YAG laser to modify 2024-T3 aluminum alloy surfaces. The laser treated surfaces were then primed with a phenolic primer, BR 127[200], and bonded with an epoxy film adhesive, AF-163-2.[201] These joints exhibited good initial strength and wedge test durability. The laser pulse melts the surface region of the metal, which rapidly solidifies at the end of the pulse, resulting in a dendritic topography on the surface. Kester,[199] also shows, using XPS, that the laser pulse removes hydrocarbon contamination and MgO from the surface. Kester[199] claims that the laser increases the basicity of the surface (determined by a change in the ratio of O/Al in XPS spectra), most likely by changing the coordination of aluminum in the oxide. This increase in basicity could result in durable bonds with adhesives that contain carboxylic or phenolic groups.[199]

10. Pretreatment Summary

In summary, the type of pretreatment selected for an aluminum piece is dependent upon the end use. For structural adhesive joining, particularly in the aerospace industry, anodization is the preferred treatment.[1] However, for less critical applications, and for the adhesion of paints and coatings, where high bond strength is not a requirement, less expensive conversion coatings can be used.[1]

---

199. J. J. Kester, in "*Chemically Modified Surfaces in Science and Industry*," D. E. Leyden and W. T. Collins, eds., Gordon and Breach Science Publishers, NY (1988) p. 455.
200. American Cyanamid (now Cytec).
201. 3M Corporation.

As mentioned previously, due to the toxic nature of Cr(VI) ions, chromate-free pretreatments of aluminum for adhesive bonding or coating need to be developed. An evaluation of state-of-the-art, non-chromate pretreatments, supplied by various vendors, was coordinated by the National Center for Manufacturing Sciences (NCMS).[202] Several of the proprietary conversion coatings performed as well as the chromate conversion coating for corrosion resistance and paint adhesion; only minimal information is provided on processing steps.[202] Cohen[203] reviews current efforts in non-chromate conversion coatings, anodization, anodic spark coatings, rare-earth oxide additives, pyroltic tin oxide coatings, ion beam and vapor deposited coatings, and organic and polymeric coatings. Cohen[203] observed that the development of non-chromate treatments "is still in its infancy." However, an increasing number of choices are found in the literature, ranging from simple conversion coatings to coatings requiring extensive equipment. Cohen[203] concludes that the mechanism of protection offered by chromium remains controversial, and that once a better understanding of this mechanism is gained, the replacement of chromate coatings should proceed more rapidly. Hinton[204] provides an additional review of current efforts into non-chromate conversion coatings.

C. Durability and Failure of Structural Adhesive Joints

One of the limitations in the use of structural adhesives is the failure of these systems in a moist environment.[1] Although much is known about the deleterious effect of moisture on various adhesive systems, the fundamental mechanisms involved in environmental failure of a joint are still not clearly understood. In order to alleviate failure problems due to attack by moisture, it is important to acquire an understanding of these mechanisms so that appropriate measures can be taken to render the joint stable to the environment. Failure mechanisms that have been reported in the literature follow.

---

202. National Center for Manufacturing Sciences, "Alternatives to Chromium for Metal Finishing," *Final Report NCMS 0273RE95*, NCMS, Ann Arbor, MI (October 1995).
203. S. M. Cohen, *Corrosion (NACE), **51*** (1995) 71.
204. B. R. W. Hinton, *Met. Finish., **89*** (1991) 55.

Comyn[205] discussed the various mechanisms by which water may enter the joint, and the means by which the joint can be weakened. The presence of moisture at the interface can cause plasticization of the adhesive, swelling stresses, hydrolysis and cracking or crazing of the adhesive, and hydration of the metal or metal oxide.[205]

One failure mechanism considers the effect of moisture on the adhesive, and the adhesive layer adjacent to the metal oxide.[115,206,207,208] The presence of moisture leads to changes and weakening of the polymer in the interphase region, with subsequent joint failure in this region.[16] There can be reversible changes in the adhesive, such as plasticization or swelling of the adhesive that result in internal stresses in the bonded system, which increase the possibility of joint failure.[115] At high service temperatures the changes could be an irreversible hydrolysis of the adhesive, resulting in a lowering in the cross-linking density and strength of the bulk adhesive.[209]

Gledhill, et al.,[210] propose that there is a critical concentration of water in the adhesive, at which point weakening of the joint will occur. Gledhill, et al.,[210] state that at the outer edges of the joint the critical water concentration can be exceeded, and that when this occurs, this region can be treated as a virtual crack in the bondline, which can be modeled using fracture mechanics. Using this approach with an amine cured epoxy adhesive, Gledhill, et al.,[210] showed that the observed

---

205. J. Comyn, in "*Durability of Structural Adhesives*," A. J. Kinloch, ed., Applied Science Publ., NY (1983) p. 85.
206. R. A. Gledhill and A. J. Kinloch, *J. Adhes.*, ***6*** (1974) 315.
207. A. J. Kinloch, W. A. Dukes, and R. A. Gledhill, *Amer. Chem. Soc. Preprints*, ***135*** (1975) 546.
208. M. Gettings, F. S. Baker, and A. J. Kinloch, *J. Appl. Poly. Sci.*, ***21*** (1977) 2375.
209. A. J. Kinloch, "*Adhesion and Adhesives: Science and Technology*," Chapman and Hall, New York (1987).
210. R. A. Gledhill, A. J. Kinloch, and S. J. Shaw, *J. Adhes.*, ***11*** (1980) 3.

weakening of joint strengths could be correlated to a critical water concentration of 1.35% (w/w).

Brewis, et al.,[211] extended this view, by using a similar adhesive formulation, to show that there also exists a critical relative humidity. Above the critical relative humidity, joint strength declines more readily. For an adhesive consisting of an epoxide based on the diglycidylether of bisphenol-A (DGEBA), cured with 1,3-diaminobenzene, the value for the critical relative humidity was 65%.

Bowditch, et al.,[212] attempted to evaluate the concept of critical water concentration, using fillers as model "finely divided adherends," and exposing these to equilibrium water contents (EWCs). Various metal salts and oxides were dispersed into a epoxy matrices. The concentration of filler was picked to develop as high a modulus as possible while maintaining an elastic material. By doing so, any changes in modulus caused by even small amounts of water would be significant. Bowditch, et al.,[212] could not confirm the existence of a limiting EWC (or critical water concentration). Even low concentrations of water in the system caused reductions in modulus. The authors[212] attributed this to water disrupting the adhesion between the adhesive and adherend (fillers).

Rider and Arnott[175] propose that the rate of water diffusion ahead of the crack tip is dependent upon the density of adhesive/adherend bonds. The density of bonds influences the number of "micro-cavities" formed between the adhesive and adherend in the stressed joint, which ultimately determines the rate and mechanism of joint failure.

The effect of moisture on the adhesive is confounded by the following observations, which show that the structure of the interphase adhesive may be different from that of the bulk adhesive.

---

211. D. M. Brewis, J. Comyn, A. K. Raval, and A. J. Kinloch, *Int. J. Adhes. Adhes.*, ***10*** (1990) 247.
212. M. R. Bowditch, D. Hiscock, and D. A. Moth, *Int. J. Adhes. Adhes.*, ***11*** (1991) 163.

Therefore, the effect of water on the "interphase polymer" must also be considered, particularly when the locus of failure is within the adhesive, but close to the oxide/adhesive interface.

Brockmann,[213] as suggested by Kollek,[214] modeled the curing reactions of an adhesive joint by utilizing wooden toy balls with Velcro attached to represent reactive sites on monomers. Brockmann demonstrated that the formation of voids and orientation of the polymer in the interphase should be possible.[213] Brockmann, et al.,[16] studied the interphases of pretreated (PAA and CAA) aluminum that was coated with a polymeric primer system. Using transmission electron microscopy of ultramicrotomed cross-sections, Brockmann, et al., [16] observed "bright zones" in polymer adjacent to the pretreated aluminum. Providing arguments that discount the formation of artifacts from ultramicrotoming, Brockmann, et al.,[16] offered an explanation that selective adsorption of different chemical species (with different chemical reactivity towards the oxide surface) in the primer could account for the bright zones in the interphase. Alternately, these regions could be due to the inability of larger size molecules to penetrate the porosity of the anodized surfaces.[16]

Kötting,[215] using ion milling combined with scanning electron microscopy, has demonstrated that a region of lamellar polymer microstructure (epoxy or phenolic resins), which has a lower density than the bulk polymer, develops near aluminum adherend interfaces. In some cases, this microstructure extends up to 8 μm into the bulk adhesive away from the adherend surface. Kötting, in offering a simplified explanation of the observation, claimed that the microstructure was due to the presence of the adherend surface, and the chemical reaction of bifunctional resin molecules with the adherend surface.[215] This surface "anchoring" provides the basis for

---

213. W. Brockmann, *J. Adhes.*, ***37*** (1992) 173.
214. secondary reference, W. Kollek, personal communication, in W. Brockmann, *J. Adhes.*, ***37*** (1992) 173.
215. G. Kötting, "*Investigation of Adhesive Layer Morphology and Stress-Related Deformation and Failure Mechanisms in Adhesive Joints (translation),*" Ph.D. Dissertation, University of Paderborn, Paderborn, Germany (1984).

continued orientation of the microstructure during curing of the adhesive. Kötting also continued to show that the chemical state of the surface had an effect on the polymer microstructure near the surface.[215] When the surface was covered with a grease prior to bonding, no vertical orientation of the polymer microstructure in the interphase was observed; on the greased adherend, only the microstructure typical of the bulk adhesive was observed after ion milling.[215] Kötting attributed this to the lack of formation of a chemical bond between the adhesive and the grease covered adherend.[215]

Crompton,[216] while studying ultramicrotomed sections of aluminum epoxy joints, also noted a "transitional" layer of polymer near the surface, but did not notice any variation in this transitional region when the adherend surface was either acid etched or conversion coated.

In addition to the transitional layer of polymer near the oxide surface, Berbezier, et al.,[113] using electron microscopy of cross-sectioned joints, detected a "true" interphase between an epoxy-novolac-based primer (BR 127[217]), and an epoxy adhesive (FM 73[217]). Berbezier, et al.,[113] argue that this interphase is created by a diffusion process between the primer and the adhesive.

Bikerman[218] proposed that although failure often visually appears to be interfacial, the actual break occurs cohesively in the adhesive in a weak boundary layer (WBL). He considered several classes of WBLs, some of which include air pockets from incomplete wetting of the adhesive, impurities in the adherend and adhesive, and low molecular weight components in the adhesive.

Nitschké[219] studied PAA and CAA aluminum adherends primed with an epoxy primer, EC 3924, and bonded with an epoxy adhesive, AF-126-2. Both the primer and the adhesive are from the 3M Company. In this work, Nitschké, using various techniques to study the morphology and

---

216. J. S. Crompton, *J. Mater. Sci.*, ***24*** (1989) 1575.
217. American Cyanamid (now Cytec).
218. J. J. Bikerman, *Ind. Eng. Chem.*, ***59*** (1967) 40.
219. F. Nitschké, *J. Adhes. Sci. Technol.*, ***4*** (1990) 41.

composition of the interphase region, showed that the primer in the pores of the anodic oxides contained more nitrogen compounds than the bulk primer. Nitschké attributed this to the migration of the reactive components of the primer into the pores of the oxide and the segregation and adsorption of low molecular weight components of the primer at the oxide/primer interface.[219]

Patrick, et al.,[220] observed the preferential adsorption of amine curing agents at metal oxide/epoxy adhesive interfaces as early as 1971. Bascom and Patrick[221] state that the enrichment of the interface with amine could cause the epoxy in this region to cure differently than the bulk polymer, and that unreacted excess amine at the interface could play a role in stress-corrosion.

Dillingham and Boerio[222] prepared aluminum/epoxy joints in a geometry that allowed joint failure to occur close to the adhesive/adherend interface. Using X-ray photoelectron spectroscopy, they determined that amine curing agents were protonated by acidic hydroxyl groups on the aluminum oxide surface. The authors also suggest that the hydroxyls on the aluminum oxide surface catalyzed the epoxy adhesive curing reaction, resulting in a highly cross-linked epoxy structure in the interphase, which is different from the bulk epoxy.

A second mechanism of failure[223] attributes failure to environmental attack at the adhesive/oxide interface, and subsequent joint degradation by failure of polymer/oxide bonds. Fowkes[42,46] used an acid-base approach to explain bond degradation in the presence of moisture. H_2O, being amphoteric, can diffuse to the interface, and displace weakly interacting acid-base functional groups. A similar argument was used by Bolger,[50,51] who noted that H_2O at the interface can displace hydrogen bonds.

---

220. R. L. Patrick, W. G. Gehman, L. Dunbar, and J. A. Brown, *J. Adhes., **3*** (1971) 165.
221. W. D. Bascom and R. L. Patrick, *Adhes. Age, **17*** (October, 1974) 25.
222. R. G. Dillingham and F. J. Boerio, *J. Adhes., **24*** (1987) 315.
223. C. Kerr, N. C. MacDonald, and S. Orman, *J. Appl. Chem., **17*** (1967) 62.

Comyn, et al.,[224] suggest that the observed decrease of aluminum/epoxy and aluminum/phenolic joints that were exposed to water could be modeled by the weakening effect of water on ion pairs at the interface. Using an equation to define the attractive forces between ion pairs,

$$F = \frac{q_1 q_2}{4\pi\kappa\varepsilon_0 r^2},$$

where q_1 and q_2 are the ionic charges, r is the inter-ionic distance, ε_0 is the permittivity of vacuum, and κ is the relative permittivity (dielectric constant) of the medium, Comyn, et al.,[224] show that the decrease in strength can be correlated to the increase in the dielectric constant of the adhesive when water diffuses to the interface. Comyn, et al.,[224] claim that epoxy and phenolic adhesives have low dielectric constants ($\kappa \approx 4$-5), whereas the value for water is high ($\kappa \approx 80$). A small amount of water at the interface would increase κ, and thus decrease the force (F) across the interface. Removal of the water would restore the value of F to the original value. Comyn, et al., [224] used these values of κ to predict the reduction of joint strength when exposed to moisture, and predicted values in close agreement with actual observations. Comyn, et al.,[224] further observed that the joints regained joint strength when water was removed from the joint.

Although the failure path in a joint is often complex, for most cases, in the absence of moisture, crack growth propagates, cohesively, in the adhesive layer; however, in a moist environment, the crack can propagate at or near the metal oxide / adhesive interface.[77] Based upon theoretical considerations, Gledhill and Kinloch[206] show that W_A goes from a positive value in a dry environment to a negative value in the presence of moisture, and provides a driving force for the displacement of the adhesive, by water, at the interface. For an epoxide / Al_2O_3 joint, Kinloch[225] determined the values of W_A in air and water, W_{AL}, to be 232 and -137 mJ/m^2, respectively. Although the joint is thermodynamically unstable to moisture, the kinetics of water penetration into the interface can be a key factor in the actual joint durability.[206] From kinetic data, these

224. J. Comyn, D. M. Brewis, and S. T. Tredwell, *J. Adhes.*, ***21*** (1987) 59.
225. A. J. Kinloch, *Adhesion (London),* ***10*** (1979) 193.

authors[206] assert that the debondment process is governed by the rate of water diffusion through the adhesive. The rate of water migrating through the adhesive can be enhanced at high temperatures, particularly at temperatures above the glass transition temperature, T_g, of the polymer.[206]

A third joint failure mechanism suggests that the oxide converts into a hydroxide that is mechanically weak, and joint failure occurs in this weak hydroxide layer.[226,227] It is not universally accepted,[228] however, that the observed change in phase from oxide to hydroxide is the cause of debondment, or is a post-failure phenomenon resulting from continued exposure of the fracture surface to the accelerated test environment.

For an etched Al specimen and FM123 adhesive, Venables, et al.,[229] demonstrated that the failure, in a wedge test, occurs along the adhesive/oxide interface upon exposure to moisture. The oxide layer was completely converted to hydroxide, and the thickness increased. Based upon these results, the authors proposed the model shown schematically in Figure 2.10.[229] The hydroxide formed adheres weakly to the Al substrate, and mechanical failure in the weak hydroxide, leaves the hydroxide sticking to the adhesive.

Other researchers[15,216] argue that the gross transformation of oxide to hydroxide is a post-failure phenomenon, and that this transformation would require a condensed water phase.[77] Since water diffuses through the adhesive in a molecularly dispersed fashion,[77] condensed water would only form in flawed areas of the joint, where the adhesive did not wet the adherend, or in areas where

---

226. J. D. Venables, *Adhes. Joints Form. Charact. Test. Proc. Conf.*, ***1,*** Plenum Press, New York, NY (1984).
227. A. J. Kinloch, L. S. Welch, and H. E. Bishop, *J. Adhes.*, ***16*** (1984) 165.
228. J. S. Crompton, *J. Adhes.*, ***28*** (1989) 135.
229. J. D. Venables, D. K. McNamara, J. M. Chen, B. M. Ditchek, T. I. Morgenthaler, T. S. Sun, and R. L. Hopping, *Nat. SAMPE Tech. Conf.*, ***12*** (1980) 909.

the adhesive bonds were displaced or hydrolyzed by the diffusing water.[77]

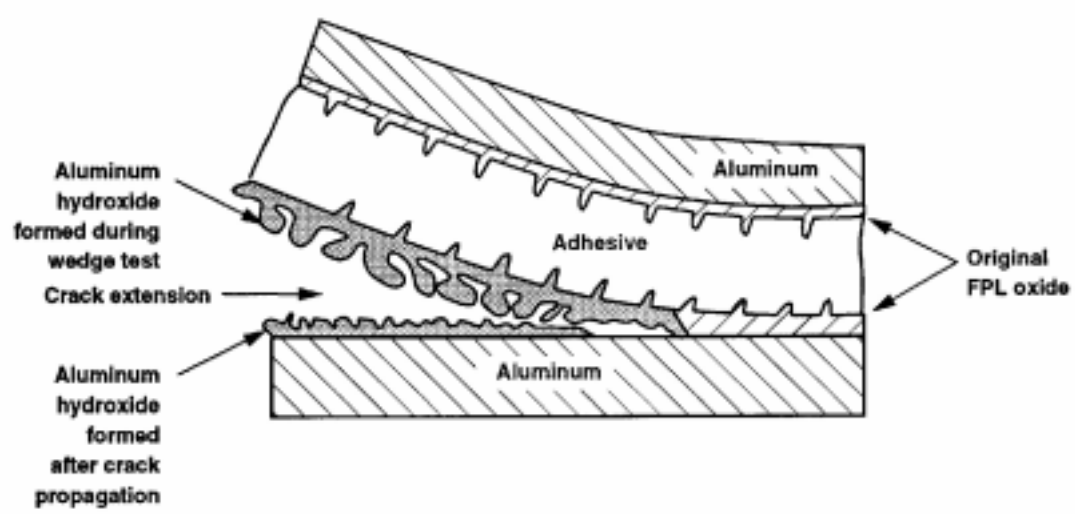

Figure 2.10. Schematic Diagram of a Debondment Mechanism in the Presence of Moisture[229]

In the study of Venables, et al.,[229] the PAA surface was superior to the FPL surface in terms of resistance to moisture attack. The stronger resistance to hydration of the PAA surface has been attributed to the more difficult displacement, relative to other electrolytes, of phosphate by hydroxyl ions.[230,231] A change in morphology and crystallinity of the oxide was noted after exposure.[229] Electron diffraction and electron microscopic investigations of this surface film indicated that the hydrated oxide was crystalline with a structure resembling boehmite {AlOOH}. The amorphous oxide was transformed to crystalline boehmite with a "corn flake"-type morphology, which upon exposure to further moisture, transforms to bayerite $\{Al(OH)_3\}$.[229] Venables, et al.,[229] also noted that certain inclusions, such as $CuAl_2$, at the alloy surface could act as nucleation sites for hydration. Islands of thick hydrated oxide could grow around the

230. W. M. Scardino and J. A. Marceau, *J. Appl. Polym. Sci., Appl. Polym Symp.*, ***32*** (1977) 51.
231. J. F. Murphy, *Plating*, ***54*** (1967) 1241.

intermetallic center. Such inclusions are cathodic to the aluminum matrix, and when exposed to liquid water, produce the hydroxyl groups necessary for the formation of aluminum hydroxides.[77]

For an epoxy/Al joint in a moist environment, Kinloch, et al.,[97] using XPS, showed that the locus of failure was largely within the CAA oxide layer, but with occasional divergence of the crack into the adhesive layer. In the absence of water, crack growth occurred exclusively in the adhesive layer.[97] Improved durability, and a decrease in oxide failure was observed for a joint with PAA adherends.[97]

Davis, et al.,[232] used a novel approach of Surface Behavior Diagrams to study the reaction of the PAA oxide with water, by tracing the surface composition during the entire process. The model proposed for the hydration reaction is as follows:

a) adsorption of water to form $AlPO_4 \bullet H_2O$;
b) nucleation and growth of a hydrated phase ($Al_2O_3 \bullet nH_2O$) which overlays the $AlPO_4 \bullet nH_2O$ layer;
c) dissolution of the $AlPO_4 \bullet H_2O$ without hydration of underlying Al_2O_3;
d) dissolution of the $AlPO_4 \bullet nH_2O$ followed by hydration of the exposed Al_2O_3.[232]

Additional evidence for the hydration reaction was provided by Noland,[233] who reported a shift in the Al 2p peak in an XPS spectrum after exposure of an Al substrate to H_2O. Noland[233] attributed this to the conversion of the oxide to a weak "gelatinous boehmite"-type oxide.

Recently, Davis, et al.,[234] used electrochemical impedance spectroscopy (EIS) to study the changes in the interphase of an FPL etched, aluminum disk laminated with a 70 μm thick layer of

---

232. G. D. Davis, T. S. Sun, J. S. Ahearn, and J. D. Venables, *J. Mater. Sci.*, ***17*** (1982) 1807.
233. J. S. Noland, *Polym. Sci. Technol. (Plenum)*, ***9A*** (1975) 413.
234. G. D. Davis, P. L. Whisnant, and J. D. Venables, *J. Adhes. Sci. Technol.*, ***9*** (1995) 433.

a Cytec (formerly American Cyanamid) adhesive, FM-123. No description was provided about the purity of the aluminum or the formulation of the adhesive. The laminated aluminum was placed in an EIS holder, and immersed in a 0.05 M Na_2SO_4 solution at 58°C. The edges and back of the laminated aluminum were isolated from the solution by the sample holder. The impedance and phase angle were measured as a function of frequency and exposure time for 186 days. At the end of the experiment, white spots were observed in the exposed adhesive, near (~1 mm away from) the edges of the sample holder. Using XPS, these were determined to be aluminum hydroxide protruding through the adhesive. From the EIS data, Davis, et al.,[234] concluded that moisture affects the "open-faced adhesive joint," proceeding in four stages:

1) the adhesive absorbs moisture, and a thin layer of water may form at the adhesive-oxide interface,
2) there is an incubation time for hydration of the oxide,
3) hydration of the oxide occurs,
4) followed by direct contact of the external electrolyte with the hydration products and the metal.

According to Davis, et al.,[234] these data prove that hydration of the oxide can occur under an adhesive, by water diffusing through the bulk of the adhesive, and that hydration of the oxide can lead to crack initiation and propagation.

Kollek, et al.,[235] showed for high temperature cured epoxy resins, such as those cured with dicyandiamide, that the curing agent can be hydrolyzed to ammonia or amines, and that this can have an effect on the oxide structure and joint durability. In cross-sections of intact adhesive joints, exposed to 95% RH and 40°C for one year, it was noted that the "oxide whiskers"

---

235. H. Kollek, W. Brockmann, and O. D. Hennemann, in "*Progress in Advanced Materials and Processes: Durability, Reliability and Quality Control,*" G. Bartelds and R. J. Schliekelmann, ed., Elsevier Science Publishers B. V., Amsterdam (1985) p. 83.

produced by the chromic-sulfuric acid etching process were not present when the cross-section was taken from near the edge of an unsealed joint. The whiskers were observed when the cross-section was from the center of the joint, away from the unsealed edges. Furthermore, using electron energy loss spectroscopy (EELS), Al was detected in the primer, in the cross-section taken near the edge of the joint. It was presumed that the hydrolysis of dicyandiamide, into ammonia and carbon dioxide, and the presence of moisture, resulted in: a localized region of high pH, the subsequent dissolution of the oxide, and diffusion of the oxide into the primer. This was anticipated to result in a lowering of joint strength. For CAA adherends, the dissolution of oxide was not observed until after 3 years of exposure. Furthermore, for CAA adherends primed with a corrosion resistant primer, and bonded with a phenolic adhesive, the first changes in the oxide structure were not observed until after 18 years of exposure. The authors suggest that maintaining the condition of the original pretreatment oxide throughout the service life of the joint is important for durability.[235]

The phase transformation of $Al_2O_3 + 2OH^- \rightarrow 2Al(OH)_4^-$, (sic) caused by amine curing agents, a so called *alkaline failure mechanism*, is reiterated by Brockmann, et al.[12] Brockmann, et al.,[12] also claim that there exists the possibility of an *acid failure mechanism*, that is brought about by the corrosion of aluminum metal, and diffusion of H^+ ions into the polymer, with the subsequent dissolution of the adjacent oxide :

$$2Al + 3H_2O \rightarrow Al_3O_3 + 6H^+ + 6e^-$$
$$Al_2O_3 + 6H^+ \rightarrow 2Al^{3+} + 3H_2O$$

In summary, water can affect joint durability in a complex fashion, perhaps with several mechanisms operating in a synergistic fashion. As reviewed, the durability of adhesively bonded aluminum joints may be dependent on the chemical state of the adherend, both with regard to hydration resistance, and to the degree of (chemical) interaction with the adhesive. Water

uptake, and therefore the bulk properties of the adhesive, can influence joint durability. Finally, the effect of the oxide on the structure and properties of the adhesive adjacent to the oxide (the polymer interphase) can affect joint durability.

D. Thesis Statement

While the composition, structure, and mechanical properties of an interphase are difficult to evaluate, the effects of changing the chemistry or the morphology of the interphase, on the lifetime and failure modes of adhesively bonded systems are readily determined. It is the scope of this work to elucidate the fundamental mechanisms of adhesion that are responsible for durable bonds of epoxy adhesive resins to phosphorus oxo acid treated aluminum alloy adherends. By systematically altering the adherend surface chemistry, surface topography, and the adhesive formulation, combined with accelerated adhesive joint durability tests, the contributions of chemical and mechanical factors that influence the properties of adhesively bonded joints are isolated and assessed.

It is postulated that the chemical state of the aluminum surface film, and the resulting interaction with the adhesive resin, are the dominant factors in determining the environmental durability of epoxy-bonded aluminum joints. It is not denied that surface topography has an effect on the initial “dry” joint strengths. However, in the presence of moisture and stress, epoxy-bonded aluminum requires a chemically coupled, hydrolytically stable interphase to maintain “wet” joint strengths that are comparable to initial dry strengths.

A chemically coupled, hydrolytically stable interphase can be attained when hydrolytically stable primary bonds are formed between the aluminum oxide and the organic adhesive, and when the aluminum oxide is chemically converted to increase the hydration resistance of the oxide. The second requirement is necessary to prevent chemical and physical changes of the substrate surface in the event that water, molecularly diffusing through the polymeric adhesive, would be able to form a liquid phase by capillary condensation in areas of the adherend not wet by the

adhesive, that is, in capillary gaps. Condensed water could change the oxide into a hydroxide, with a concomitant increase in volume, a decrease in the mechanical strength, and subsequent joint rupture.

Morphological changes of the aluminum oxide surface require water in liquid form, while the aluminum oxide - organic adhesive bonds (Al-O-R) can be attacked by molecularly dispersed water. Therefore, the more resistant the Al-O-R bond is to hydrolysis, and the higher density of bonding sites per unit area, the better is bond durability. The durability enhancement observed with certain, but not all, porous anodic aluminum oxides is explained by the increase in total chemical bonds per unit geometric area between the adhesive and the oxide. Also, because there are few capillary gaps in the interphase of a properly prepared joint, even if the substrate oxide is not hydrolytically stable, a high density of hydrolytically stable aluminum oxide - adhesive bonds limits the sites where liquid water can form, and change the composition, morphology, and consequently, the strength of the adherend oxide and the bonded joint.

These conclusions can be drawn from the analysis of the test results for the aluminum alloy / epoxy systems under investigation. It is likely that the conclusions drawn here could be applicable to other metal / adhesive systems.

Chapter 3. EXPERIMENTAL PROCEDURES

A. Materials

Aluminum alloys 2024-T3 and 6061-T6 (Aluminum Co. of America) were bonded with two different epoxy adhesives. Composition limits for the aluminum alloys are found in Appendix A. The adhesives were obtained from the 3M Corporation. A dicyandiamide cured paste adhesive, XA-3498, and a 3M-epoxy film adhesive, AF163-2K were used to bond the aluminum alloy substrates. According to the Materials Safety Data Sheet for the AF163-2K adhesive[236] the material contains 3 nitrogen-containing compounds that could conceivably participate in the curing of the adhesive. These include: dicyandiamide; N,N′-(methyl-1,3-phenylene)bis(N′,N′-dimethylurea); and a proprietary non-volatile amide. The film adhesive came in a weight of 0.3 Kg/m^2, and contained a 0.13 mm thick nylon scrim cloth. Nominal thickness of the AF163-2K adhesive film was 0.23 mm. Aluminum alloy 2024-T3 bonded with AF163-2K epoxy film adhesive represents an adhesively bonded system that one may encounter in the aerospace industry. Alloy 6061-T6 bonded with the epoxy paste adhesive XA-3498 is representative of a bonded system that could find use on ground transportation platforms.

A listing of the organophosphonic acids used in this investigation, their purity, and the suppliers are provided in Appendix B. Inorganic acids were obtained from Fisher Scientific Company. All solutions were prepared using deionized water, with chemicals as-received from the vendors without any further purification. A representative analysis of technical grade vinylphosphonic acid solution is found in Appendix C.

---

236. *Scotch-Weld AF-163*-2K .06 WT. Structural Adhesive Film (1993) 3M Corporation, 3M Center, St. Paul, MN 55144-1000.

B. Surface Preparation

1. Initial Metal Preparation and Degreasing

The aluminum alloys were machined to appropriate dimensions for each set of experiments. Caution was taken to minimize contamination of the metal surfaces, throughout the treatment and bonding operations. Any ink on the metal was removed with a methanol wipe. The alloys were either vapor degreased for 5 min with trichloroethylene, or wiped with toluene soaked cheese cloth to remove any residual oil from the surface.

2. Acid Etching

The 6061-T6 alloy was etched in an hydrofluoric/nitric acid solution, whereas the 2024-T3 alloy was etched in a chromic/sulfuric acid solution. All solutions used in this experiment were freshly prepared for each series of treatments. Relatively large volumes (~4 liters) of etchant were prepared for series of tests, to minimize effects of bath depletion on the results.

The nitric/hydrofluoric acid bath consisted of 13% (v/v) of concentrated HF (49% (w/w), 35% (v/v) of concentrated {70% (w/w)} HNO_3, and 52% (v/v) deionized H_2O. Alloy 6061 was etched for 1.5 min at 23°C, rinsed in flowing deionized water, and dried at 50°C in an oven for approximately 5-10 min.

The chromic/sulfuric acid bath consisted of 50 g/L CrO_3 and 250 g/L of concentrated H_2SO_4 diluted with deionized H_2O. Alloy 2024-T3 was etched for 14 min at 63°C, rinsed in flowing deionized water, dried in an oven at 50°C for 5-10 min.

In certain cases high purity (AA1199) aluminum (Appendix A) samples were prepared for surface analysis by first wiping with toluene-soaked cheesecloth, and then etching in 50 g/L NaOH for 5 min at 66°C. These were rinsed in flowing deionized water, blown dry with filtered dry air, wrapped in laboratory tissue and stored in a desiccator until used. Samples

prepared in this fashion were subsequently dipped in 10% (w/w) aqueous solutions of the phosphorus oxo acid chosen to be studied, rinsed in flowing deionized water, dried with filtered air, and stored in a desiccator prior to analysis.

3. Durability Treatments

a. Anodizing

Aluminum alloys were anodized in a stainless steel tank, which served as the cathode during anodization. Bath temperatures were maintained with a constant temperature circulator connected to a stainless steel cooling coil that was immersed in the bath. In most instances, the bath temperature was $23^{o}C \pm 3^{o}C$, except for chromic acid anodizing, in which the bath temperature was $38^{o}C \pm 3^{o}C$. The electrolyte solutions were vigorously stirred using a magnetic stirrer and a Teflon-coated stir bar. All solutions were prepared with deionized water. Since a variety of different bath concentrations of the phosphorus oxo acid electrolytes were used, the concentrations used for each experiment are specified in the subsequent chapters. Anodizing times and voltages were also varied; therefore these are also specified in the subsequent chapters, along with the test results. After anodization, all metal was thoroughly rinsed in deionized water, dried in an oven at $50^{o}C$ for approximately 5-10 min. Treated metal was wrapped in laboratory tissue and stored in a desiccator containing Drierite®.[237] Surface analysis and adhesive bonding were done within 24 h after treatment. There was no visual transfer of the laboratory tissue to the treated metal, nor was there any perceived effect of contamination from the laboratory tissue in the subsequent analyses and tests.

The chromic acid electrolyte was an aqueous 0.5 M solution of CrO_3. For CAA, the aluminum was anodized by a step-voltage process. The cell potential was held at 4 V for 2 min, then increased by 4 V/min up to 40 V. It was held at 40 V for 20 min, increased to 42 V, which was

---

237. Anhydrous $CaSO_4$, W. A. Hammond Drierite Company, Xenia, OH.

maintained for 2 min, and then increased to 50 V at a rate of 2 V/min. The potential was held at 50 V for 5 min. Post-anodization processing and handling of the CAA metal was the same as described above.

Barrier anodic aluminum oxides were used to calibrate the Auger depth profiling, and for comparison of the structure of anodic oxides formed in organophosphonic acid solutions. A neutral solution of boric acid and anhydrous sodium borate was used as the electrolyte for the formation of these barrier oxides. The solution was prepared by titrating 2500 ml of a 0.39 M boric acid solution with a 0.12 M sodium borate solution to a end point of pH 7.0. The resulting solution was then diluted with distilled water to a final volume of 3000 ml. Barrier anodic oxides were formed under potentiostatic conditions, and the thicknesses of the oxides formed in this solution are self-limiting.[86] The voltages used are specified in the text, and were varied to obtain the desired anodic oxide thickness for each experiment. Unless otherwise specified, the neutral borate-formed anodic oxides were anodized at 23°C for 30 s, at which point current ceased to flow, and anodic oxide film formation was complete.

In addition to the porous anodic oxides formed in certain phosphorous oxo acid electrolytes, porous anodic oxides were also formed in oxalic acid solution. Oxalic acid-formed porous oxides were prepared galvanostatically in 2% (w/w) oxalic acid for 250 s and 1 A/dm^2 at 23°C. Using these conditions a ~1 μm thick porous oxide was formed on 6061-T6 alloy, as confirmed by examination of a cross-sectioned sample with scanning electron microscopy. These anodic oxides were lightly hydroxylated by exposing the anodized metal to a pH 9 triethylamine solution for 10 s at 50°C. In some cases, hydroxylation was followed with a 10 s dip in 0.1 M aqueous solutions of various organophosphonic acids.

b. Hydrothermal Coatings

Aluminum hydroxide (pseudoboehmite) films were formed on the surfaces of aluminum alloys by boiling the metal in a pH 9 solution of triethylamine in deionized water, contained in a

stainless steel beaker. The choice of beaker material was important in that silicon-containing ions, in general,[60] and specifically silicon-containing ions from Pyrex beakers initially used in this investigation inhibited the surface hydroxylation reaction. The boiling solutions were prepared by adding triethylamine to water, until the pH was ~9.0 at boiling temperature. The pH was measured and adjusted at boiling temperature using an Accumet® 950 pH/Ion Meter[238] equipped with an auto-temperature compensation probe. The pH meter was initially calibrated using a two-point calibration with Fisher Scientific pH Standards of 2.00 and 9.00. Additional triethylamine was added drop-wise during boiling to maintain the pH at ~9. The metal was typically boiled for 30 s, however boiling times were varied as specified in the following text. The samples were removed, rinsed with flowing deionized water and dried with filtered compressed air. Hydroxide surface films that were to be functionalized with phosphorus oxo acids were dipped in aqueous solutions of the acids. The concentration of these solutions varied, and is specified in the text. Dipping times were generally 30 s. The functionalized metal was rinsed in flowing deionized water, dried with compressed air, wrapped in laboratory tissue, and stored overnight in a desiccator (as above).

An experiment to determine the role of aluminum surface hydroxylation for the adsorption of organophosphonic acids was undertaken. This included etching 99.99% aluminum (1199 alloy) in 33% (w/w) NaOH at 50°C for 1 min, rinsing with deionized water, boiling the caustic etched metal in a pH 9 solution of NH_4OH for 15 s, rinsing with deionized water, dipping the boiled metal in a 0.1 M solution of phenylphosphonic acid (ϕPA) or 10% (w/w) vinylphosphonic acid (VPA) for 10 s at room temperature, followed by deionized water rinsing. Metal after each rinse step was dried and examined using reflection-absorption infrared spectroscopy (RAIRS). A high purity aluminum mirror served as the reference.

238. Fisher Scientific.

4. Adhesive Bond Evaluation

a. Lap Shear Testing

6061-T6 coupons for lap shear testing were machined to 2.54 x 10.16 x 0.203 cm. 2024-T3 coupons were machined to 2.54 x 10.16 x 0.160 cm. The coupons were treated as described above. A 1.27 cm overlap (3.226 cm^2 overlap area) was used and the glue line thickness was maintained at 0.051 cm using fixtures specially machined for this purpose.[239] Excess XA-3498 paste adhesive, or four plies of AF163-2K film adhesive, were applied to the overlap area to achieve the 0.51 mm glue line thickness, and to form the required fillets as described in ASTM standard D-1002. The XA-3498 adhesively bonded lap joints were cured in air at 149°C for 30 min. AF163-2K adhesively bonded joints were cured in air at 121°C for 1 hr. Breaking strength (load at failure/overlap area) was determined on an Instron Model 1127. The Instron was equipped with a 222.4 KN load cell. The cross-head speed was 1.27 cm/min. Measurements were made at ambient laboratory conditions. Stress-strain curves were recorded on a strip-chart recorder with 22.24 KN full-scale. Each reported breaking strength is an average from at least five equivalent joints.

b. Wedge Testing

Panels of 6061-T6 and 2024-T3 were machined to 15.24 x 22.86 x 0.318 cm, and pretreated as described above. Panels of 6061-T6 bonded with XA-3498 epoxy paste adhesive were cured at 149^{o}C for 30 min in a platen press with 310 KPa applied pressure. The epoxy paste thickness was maintained at 0.38 mm using stainless steel shims. Wedge test assemblies were also fabricated with the AF163-2K epoxy film adhesive. Two plies of AF163-2K adhesive were used per assembly. The AF163-2K wedge assemblies were cured in a platen press for 1 h at 121^{o}C

239. Details of the fixture have not been published. The fixture was machined to precise tolerances to obtain the desired glue line thickness and overlap alignment.

with 310 KPa applied pressure.

The bonded assemblies were machined to 2.54 x 15.24 cm according to ASTM specification D3762-79 (1983). Degreased 6061-T6 aluminum alloy wedges (0.318 cm thick) were slowly inserted into the bond line using a hand hydraulic press. The specimens were examined with a 30X microscope, and the initial crack length was marked, as measured from the tip of the wedge. The specimens were placed in a humidity chamber at 50^{o}C with 100% relative humidity, and periodically removed to measure the progression (if any) of the crack. At the end of exposure, the samples were removed, the final crack tips were marked, and the marks were measured with the aid of a vernier caliper and a 30X binocular microscope. The reported data are the averages of the crack extension for at least ten joints (2 repetitions). For VPA treated samples, 20-25 joints (4-5 repetitions) were tested for each condition. The crack length on each side of each joint was measured and averaged for each exposure time. The wedge specimens were opened after crack measurement, and the failure mode, in the region of the crack tip, was assessed visually, or with X-ray photoelectron spectroscopy.

c. Surface Oxide Hydration Rate

To examine the relative hydrolytic stability of oxide surfaces, hydration rates were determined. Freshly treated metal was exposed to 98% R.H. at 50^{o}C for 1 to 23 h. Relative degrees of hydration were determined using FT-IR and measuring the area of the hydroxyl stretching band near 3500 cm^{-1} in the FT-IR spectra. The increase in total absorbance units was obtained by subtracting the spectrum of the as-prepared sample from the spectra of the samples exposed to humidity.

5. Bulk Reaction Product Preparation

Bulk chemical reaction products were prepared in an attempt to simulate reactions that could occur between the vinyl-group of surface vinylphosphonic acid (VPA) and components of the

epoxy resin. These samples were prepared by reacting dimethylvinylphosphonate (DMVP) and either propylene oxide (PPO) or dicyandiamide (DICY) in various stoichiometric ratios in Teflon-lined stainless steel pressure reactors. The reactors were sealed and heated for 24 h at 150°C (to simulate a typical curing temperature). The ester DMVP was used in lieu of VPA to eliminate the possibility of the other reactants forming a salt with acidic protons on VPA, while still allowing the possibility of reaction with the C=C bond. In addition, a listing of the stoichiometric ratios used, along with the amount of material included in each bomb is found in Table 3.1.

Table 3.1. Stoichiometry and Amount of Reactants for Bulk Reaction Product Simulation of Adhesive Resin and Surface Vinylphosphonic Acid Interaction

Dimethylvinylphosphonate (DMVP), Dicyandiamide (DICY), Propylene Oxide (PPO)			
mole DMVP : mole DICY	DMVP (g)	DICY (g)	PPO (g)
0:1	0.000	5.001	0.000
1:2	3.021	4.010	0.000
1:1	4.541	3.019	0.000
3:1	4.536	0.998	0.000
6:1	4.532	0.504	0.000
1:0	5.005	0.000	0.000
1 mole DMVP : 1mole PPO	2.997	0.000	1.610

C. Electron Microscopy

1. Scanning Electron Microscopy (SEM)

The surface films were examined both with scanning electron microscopy (SEM) and transmission electron microscopy (TEM). For the SEM analyses the treated coupons were coated with a 21 nm layer of evaporated gold to minimize charging in the electron beam. An ISI-40

SEM was used in the secondary electron mode with an accelerating voltage of 15 KV and a sample tilt of 30^{o}.

2. Transmission Electron Microscopy (TEM)

In most cases, anodic oxides were examined directly in the TEM by separating the oxide films from the metal by amalgamating the metal in a saturated aqueous solution of $HgCl_2$. Squares, big enough to fit a TEM sample grid, were scribed through the anodic oxide on the metal surface. The scribed metal was placed in saturated aqueous $HgCl_2$ until the anodic oxides separated from the base metal. These oxides were transferred to a dish containing distilled water, and were immersed in the water for approximately 30 min. The films were transferred to fresh distilled water and immersed for another 30 min. The rinsing step was repeated a third time. Hydrothermally treated samples were anodized at 20 V in neutral borate solution prior to amalgamation. This provides a featureless barrier oxide film that facilitates handling, and does not contribute to the image of the as-etched oxide or conversion coating.[77] For the thick CAA oxides, carbon replicas were prepared, in which C was evaporated onto the oxide surface, followed with a short evaporation of Pt onto the C film to provide shadowing in the subsequent TEM image. The C films were floated off the surface and inserted onto TEM sample grids. A Phillips EM 420 microscope was used with an accelerating voltage of 120 KV.

D. Spectroscopy

1. Auger Electron Spectroscopy (AES)

A Kratos XSAM 800 Auger Electron Spectrometer was used to determine elemental depth profiles through the oxide films. The instrument uses a hemispherical analyzer, which was operated in the fixed retarding ratio mode at high magnification. The electron gun potential was 10 KeV with a spot size diameter of approximately 3 μm. Elemental depth profiles were determined by ion sputtering the surface films and subsequent AES analysis. Ar, at a pressures

between 2×10^{-8} and 7×10^{-8} Torr, was used for sputtering. Barrier anodic aluminum oxides, formed in neutral borate solution, with known thicknesses of 20 nm and 50 nm (corresponding to 1.4 nm/V of anodizing potential) were used to determine the ion sputtering rate. The ion gun was operated at 2.5 KeV with a 3 x 5 mm raster. Under these conditions, the sputtering rate was ~1.2 nm/min. For thicker anodic oxides, the ion gun accelerating voltage was increased (for example to 4 KeV) in order to achieve a higher sputtering rate (~1.9 nm/min at 4 KeV). Other sputtering rates used in this investigation are specified in the text.

2. X-ray Photoelectron Spectroscopy (XPS)

XPS spectra were obtained using the same Kratos XSAM 800 Spectrometer. Mg K_α radiation (1253.6 eV) was used to produce the photoelectron spectra. The anode was operated at 15 KV and 10 mA. Both high resolution and medium resolution spectra were recorded. All binding energies were referenced to the main C 1s photoelectron peak at a binding energy of 285.0 eV. Dr. Alfred C. Miller calculated elemental sensitivity factors for quantitative analysis.[240] These were not checked experimentally, but have been shown to be accurate when analyzing materials of known composition and stoichiometry.[241]

Metal samples were analyzed by cutting or punching out the sample and mounting these on the sample stubs using two-sided adhesive tape. Powder samples were analyzed by placing the two-sided tape on a sample stub and sprinkling the powder on the tape. The stubs were gently bumped against the counter top to remove any loose powder. The reported data are representative of two or more repetitive measurements.

---

240. Dr. Miller, formerly of Alcoa Technical Center, and currently with Lehigh University, used the theoretical Scofield cross-sections, along with the transmission function for the Kratos XSAM800 spectrometer, to calculate the elemental sensitivity factors.
241. B. R. Strohmeier, PPG Industries, personal communication.

3. Inelastic Electron Tunneling Spectroscopy (IETS)

Inelastic electron tunneling spectroscopy is a vibrational spectroscopy, in which electrons tunneling from an aluminum electrode to a superconducting lead electrode (liquid He temperature) excite the vibrational states of adsorbates on the aluminum oxide surface.[242] A thorough review of application of the technique, and the physics of the tunneling phenomenon can be found in a book by Hansma.[242]

IETS samples were prepared by evaporating 99.999% aluminum from a tungsten filament onto clean glass substrates inside a vacuum chamber with a base pressure of ~10^{-6} Torr. The aluminum samples were then oxidized in a DC glow discharge of O_2 at < 1 x 10^{-2} Torr. The samples were removed from the vacuum chamber and spin coated with aqueous (or ethanolic) solution of 0.1 g/L of the organophosphonic acid to be studied. All organophosphonic acids used for IETS were purchased from Aldrich Chemical Company as 98% (w/w) pure reagents, and were not further purified. The organophosphonic acid coated sample was returned to the vacuum chamber, and the tunnel junction was completed with the evaporation of a lead counter electrode. The completed device was submerged in liquid helium to obtain a spectrum using a spectrometer similar to the one described by Wang, et al.[243]

4. Nuclear Magnetic Resonance (NMR)

Oxide films for solid state magic angle spinning, nuclear magnetic resonance (MAS-NMR) analysis were obtained by dissolving the underlying aluminum metal in a 10% (w/w) solution of Br_2 in dry methanol. The anodized samples were abraded on one side and placed in the bromine solution. Additional bromine solution was added as needed to maintain the dissolution. After all the metal was dissolved, the mixture was filtered. The remaining oxide was washed generously

---

242. P. K. Hansma, in "*Tunneling Spectroscopy*," P. K. Hansma, ed., Plenum Press, New York (1982) pp.1,17-20.
243. Y. Wang, R. R. Mallik, and P. N. Henriksen, *Rev. Sci. Instrum.*, ***64*** (1993) 890.

with deionized water, and allowed to air dry. Due to safety and environmental concerns associated with bromine, this procedure was only attempted once each for topographically identical aluminum anodic oxides that were formed in H_3PO_4 and H_3PO_3 solutions (see Chapter 4).

Solid state MAS-NMR ^{27}Al and ^{31}P single pulse, ^{1}H-decoupled (50 KHz decoupling) and cross polarization (CP) spectra were acquired to determine the degree of tetrahedral and octahedral Al bonding in certain anodic oxides. The data were acquired by Dr. Neal R. Dando, of the Alcoa Technical Center, Alcoa Center, PA using a GE-GN300 wide-bore spectrometer equipped with a Chemagnetics solids accessory and a 7.05 T cryomagnet operating at a proton frequency of 300.1 MHz. Samples were packed in ceramic rotors with Kel-F endcaps and spun at sample rates of 4-9 KHz. The magic angle was adjusted using the ^{79}Br resonance of KBr.[244] Chemical shifts for ^{27}Al and ^{31}P were externally referenced to aqueous $Al(H_2O)_6^{3+}$, and aqueous phosphoric acid, respectively. Single pulse ^{27}Al MAS-NMR spectra were acquired at 78.2 MHz using 1.5 ms observe pulses and 2s recycle time. ^{27}Al CPMAS data were acquired using 0.5 ms contact times for efficient proton polarization transfer. ^{31}P CPMAS-NMR spectra were acquired at 121 MHz, at CP contact times of 1-2 ms.

Bulk reaction products were analyzed using NMR by Mr. Geno Iannaccone, Director Analytical Services, Department of Chemistry, Virginia Polytechnic Institute and State University. Neat DICY is a solid, whereas neat DMVP and PPO are liquids. All of the reaction products, except samples 1:1 and 1:2 / DMVP : DICY were liquids. All of the materials except the 1:2 solid were dissolved in d_6-DMSO (dimethylsulfoxide). The 1:2 solid was insoluble. 300 or 600 mg of each soluble sample was dissolved in the DMSO. ^{13}C NMR spectra were obtained for all of the DMSO solutions. All solution spectra were obtained in 5 mm tubes on a Bruker/IBM WP270SY spectrometer with an Oxford 6.34 T, 54 mm bore magnet operating at 270 MHz for ^{1}H and

244. J. Frye and G. Maciel, *J. Magn. Reson.*, ***48*** (1982) 125.

67 MHz for ^{13}C. Carbon was proton decoupled using the WALTZ16 pulse decoupling sequence. All ^{13}C NMR data are non-quantitative.

The insoluble 1:2 sample was analyzed using MAS-NMR. 400 mg of the 1:2 sample was placed in a 7 mm solid state rotor and a ^{13}C CPMAS-NMR spectrum was acquired on a 7.05 T, 89 mm bore magnet operating at 300 MHz for ^{1}H and 75.47 MHz for ^{13}C. No effort was made to quantify the data.

5. Fourier Transform-Infrared Spectroscopy (FT-IR)

Infrared spectra were obtained with an IBM IR-98 Fourier transform-infrared spectrometer. The source was a helical glow-bar, and the detector was a narrow band mercury cadmium-mercury telluride (MCT) detector. Spectral resolution was 4 cm^{-1} and 128 scans were recorded for each spectrum. Specular reflectance spectra were obtained using a Harrick, Inc. accessory with a 45^{o} angle of incidence. Attempts to determine surface species were done using the reflection adsorption infrared spectroscopy (RAIRS) technique.[245] A Harrick, Inc. accessory was used with an angle of incidence of 77^{o}. A KRS-5 polarizer was placed between the source and the sample, so that the beam was polarized parallel to the sample surface. During analyses, the optics bench vacuum was maintained at < 15 Torr, while the reflection accessories were purged with N_2. Sample spectra were referenced to the spectra of high purity (99.99%) aluminum mirrors. Band areas were determined using the ATS software that came with the IBM 98 FT-IR spectrometer. The software constructs a baseline for the desired band of the spectrum, integrates the area under the band, and provides the total absorbance units, or area, under the band.

For transmission FT-IR analysis, approximately 15 mg of the material of interest was mixed with ~300 mg dry KBr powder, and ground using a mortar and pestle. These mixtures were

245. P. R. Griffiths and J. A. de Haseth, "*Fourier Transform Infrared Spectrometry*," John Wiley & Sons, New York (1986).

hydraulically pressed into pellets, placed into a sample holder, and immediately placed into the N_2 purge box of the spectrometer. Instrument settings were comparable to those used for reflectance FT-IR, described above; no polarizer was used in the transmission mode.

Grazing angle RAIR spectra were also collected by Dr. Angela M. Ahern, at the Alcoa Technical Center, using a Digilab FTS-15/90 spectrometer equipped with a MCT detector and a Digilab grazing angle accessory. All spectra were obtained with 8 cm^{-1} resolution and averaged over 512 scans. These spectra did not provide any valuable information, and are mentioned, but not presented, in this dissertation.

6. Raman and Surface Enhanced Raman (SERS) Spectroscopies

Samples for surface enhanced Raman spectroscopy (SERS) were coated with a layer of Ag by Dr. Richard A. Hoffman and Mr. Norman J. Panseri, of the Alcoa Technical Center. Silver overlayers were deposited by electron beam evaporation in an oil-free, cryopumped vacuum system having a base pressure of 2×10^{-7} Torr. The film thickness (5 nm) and the deposition rate (0.05 nm/s) were controlled using a quartz microbalance.

All Raman and SER spectra were obtained by Dr. Angela M. Ahern with a Spex model 1403 double monochromator equipped with a Hamamastu R928 PMT detector, a DM1B computer and 100 mW (measured at the source) of 514.5 nm radiation using a Coherent Innova 70 argon ion laser. Samples were irradiated at an incident angle of 60°. The scattered light was collected at 90°. All spectra are single scans obtained at a scan rate of 2 cm^{-1}/5 s. Slit settings were 200-300-300-200 μm for all scans.

7. Ion Scattering Spectroscopy (ISS) / Secondary Ion Mass Spectrometry (SIMS)

ISS and SIMS spectra were obtained with a 3M Model 525/610 ISS/SIMS spectrometer. ISS spectra were obtained using $^{4}He^{+}$ ions for the primary beam. Primary beam energy was 2 KeV. The specimen current was 75 μA, and the primary beam was rastered over a 0.5 mm^2 area.

For SIMS analysis, a mixture of $^{4}He^{+}$ and $^{20}Ne^{+}$ was used as the primary ion beam. The primary beam energy was 2 kV, with the beam rastered over a 0.5 mm^2 area. The analysis chamber was first back-filled with ^{20}Ne until a specimen current of 25 μA was obtained. The chamber was then back-filled with ^{4}He until a total specimen current of 125 μA was obtained. Under these conditions, the pressure in the analysis chamber was approximately 4×10^{-5} Torr. Before analysis, typical base pressures of 5×10^{-9} Torr were achieved. The analysis conditions that were used correspond to a sputtering rate of approximately 40 nm/min. The sputtering rate was determined from barrier aluminum oxides of known thickness (as with Auger).

Chapter 4. POROUS ANODIC OXIDES

A. Introductory Comments

The survey of the literature, presented in Chapter 2, clearly indicates that for adhesively bonded aluminum to meet strict requirements of bond strength and durability, anodic oxidation is the preferred treatment. The primary mechanism for achieving durable adhesively bonded aluminum, when using certain porous anodic oxides however is not widely agreed upon. Debate is ongoing as to whether durable adhesion is due to mechanical forces, from the penetration and interlocking of the adhesive into the pores of the anodic oxide, or to the increased surface area available for the formation of primary and secondary bonds between the oxide and the adhesive.

The review of the literature failed to reveal any methodical investigation that distinguished the effects of adherend topography and chemistry on the durability of adhesively bonded aluminum. Therefore, the debate surrounding the role of chemical forces and mechanical forces in the adhesion of polymeric resins to porous anodic oxides continues.

The investigation presented in this chapter, firstly examines the anodic oxides produced by PAA and CAA processes, and then introduces a new anodizing process for adhesive bonding: phosphorous acid anodizing (HPAA[246]).[247,248] The significance of pore texture and increased surface area for chemical interaction between the adhesive and the substrate oxide for adhesive bond strength and durability is assessed by varying the anodization times in phosphoric and phosphorous acid electrolytes, and correlating cell structure and total surface area with adhesive bond durability. As will be demonstrated, by using the new HPAA process together with a PAA

---

246. Phosphorous acid anodizing has been given the acronym HPAA, to distinguish it from phosphoric acid anodizing (PAA). The phosphorous acid molecule differs structurally from the phosphoric acid molecule by the substitution of a proton in place of a hydroxyl group bound to the phosphorus atom --- hence, HPAA.
247. G. A. Nitowski, K. Wefers, and L. F. Wieserman, *U. S. Pat. 5,131,987* (1992).
248. G. A. Nitowski, K. Wefers, and L. F. Wieserman, *U. S. Pat. 5,325,587* (1994).

process, it was possible to form anodic oxides with similar topographies and thicknesses, but different solid state, short-range clustering of ions in the bulk anodic oxide. Accelerated durability testing (wedge tests) of epoxy-bonded joints formed with adherends with topographically identical porous oxides formed with the two phosphorus oxo acids failed cohesively in the adhesive, but with different crack lengths. It is suggested that the difference in crack lengths could be attributed to different acid-base character of the anodic oxide surfaces, which could result in different types and/or density of bonds formed at the oxide/adhesive interface.

Lastly, it is shown that functionalizing porous anodic oxides with different organic moieties, results in differing adhesive bond durability. By functionalizing porous anodic oxides formed in oxalic acid solution with two different organophosphonic acids, it was possible to improve or degrade the adhesive bond durability of joints, compared with joints formed from anodized-only adherends. It is proposed that when the surface is functionalized with organophosphonic acids, which can form primary chemical bonds with the oxide surface and with components of the adhesive resin, durable adhesion is achieved. The precise nature of the chemical interaction and the structure of the reaction product of the organophosphonic acids and the oxidized aluminum surfaces are the subjects of subsequent chapters.

B. Significance of Porosity

A complicating factor in distinguishing the effects of adherend chemistry versus topography is that the anodic cell structure and oxide chemical composition produced by two commercially used processes, phosphoric acid anodizing (PAA)[249] and chromic acid anodizing (CAA),[110] are markedly different. TEM of the detached PAA oxide film from alloy 2024 (Figure 4.1) shows cell diameters between 50-60 nm in diameter, with a pore diameter of about 40 nm.

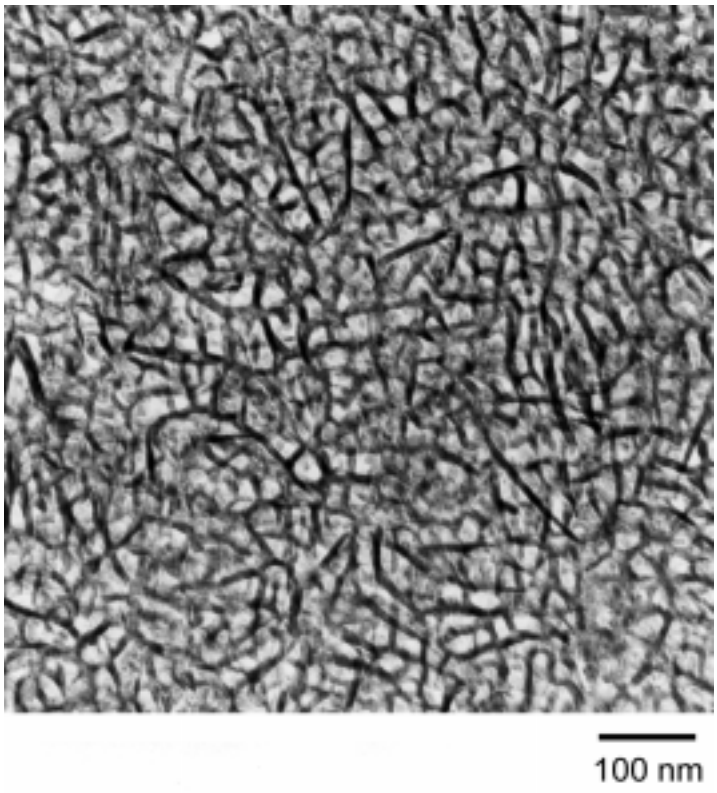

Figure 4.1. Transmission Electron Micrograph of PAA Oxide Film Formed on Alloy 2024-T3

249. Boeing Aerospace Corporation Specification *BAC5555*; *U.S. Pat. 4,085,012* (1978).

The oxide thickness of the phosphoric acid anodic oxide formed at 10 V for 20 min in 10% (w/w) H_3PO_4 was 400 nm.[5]

In contrast, the TEM of a carbon replica of the surface of anodic oxide produce by the CAA process[110] (Figure 4.2), shows that the pores on the outer surface of the oxide are generally smaller than 5-10 nm. The oxide thickness is between 2-3 μm.[113]

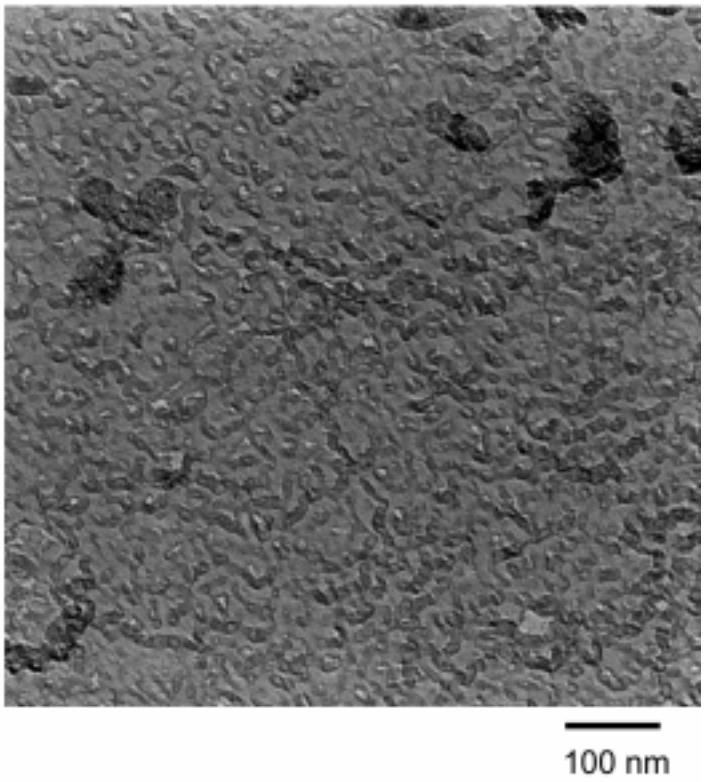

Figure 4.2. TEM of CAA Oxide Film Formed on Alloy 2024-T3

Not all porous oxides yield durable adhesively bonded aluminum.[58] The initial strength and durability of joints with adherends containing porous anodic oxides formed in sulfuric acid were improved significantly by etching the anodized adherends in “dilute” phosphoric acid solution prior to bonding.[58] While this prior investigation[58] did not definitively distinguish between the

effects of chemistry and surface topography on bond durability, it did show that simply providing a porous anodic oxide on an aluminum adherend is not a sufficient prerequisite for acceptable bond durability. It is observed that the porous anodic oxides used commercially for adhesive bonding differ in topography and in composition. It is also observed that these oxides, despite the differences, have in common a well-defined cell structure with cell walls and cylindrical pores, as originally modeled by Keller, et al.,[98] and subsequently modified and schematically presented by Wefers and Misra[86] (Figure 4.3).

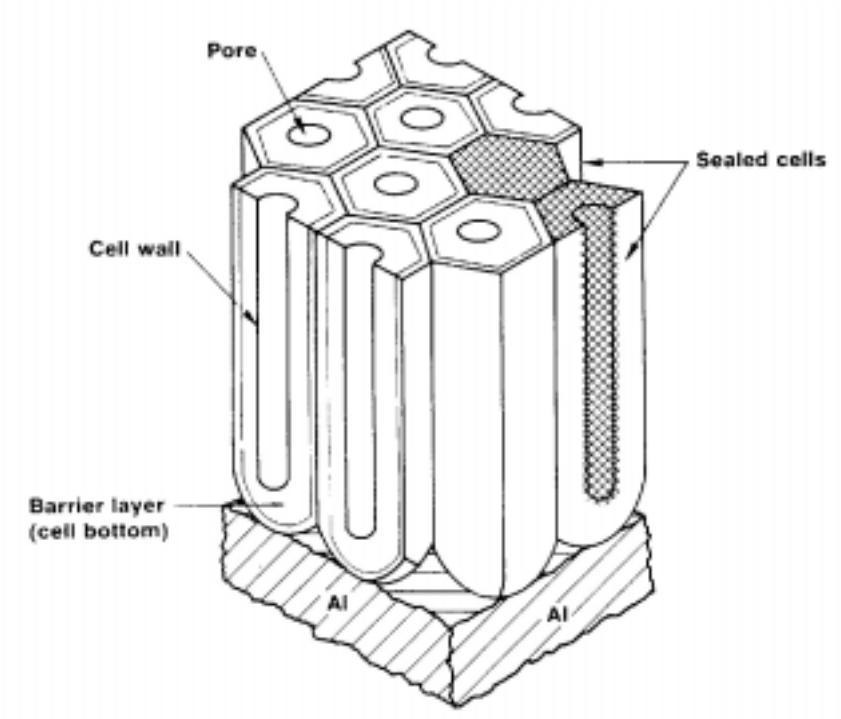

Figure 4.3. Schematic Representation of the Cell and Pore Structure of Porous Anodic Oxides on Aluminum[86]

O'Sullivan and Wood[250,251] studied the pore initiation mechanism for PAA and sulfuric acid anodized aluminum using TEM. O'Sullivan and Wood[250,251] noted that localized thick regions

250. J. P. O'Sullivan and G. C. Wood, *Proc. Roy. Soc. Lond. A, **317*** (1970) 511.
251. J. P. O'Sullivan and G. C. Wood, *Electrochim. Acta, **15*** (1970) 1865.

form in the film after 40 s of anodization, and that after 120 s these thicker regions merge resulting in adjacent thin regions of incipient pores. Localized thick regions of anodic oxide are evident on the TEM of an anodic oxide formed on 6061-T6 alloy after 60 s at 0.65 A/dm^2 in 10% (w/w) phosphoric acid solution (Figure 4.4.b), as compared with the sample anodized for 30 s (Figure 4.4.a). After 120 s of anodization, incipient porosity is observed (Figure 4.4.c). Incipient pores are localized reaction sites in which a thinner (< 1.4 nm/V) oxide advances into the metal.[86] The incipient pores appear lighter in the electron micrographs, since they are thinner than the surrounding regions and absorb fewer electrons. The emerging cell walls appear dark, since in these regions the oxide is thicker, the electron path is longer, and thus more electrons are absorbed. As anodization continues, the number of incipient pores decreases as the incipient pores coalesce into true pores.[250,251] The remaining true pores increase in size until steady state pore and cell dimensions are reached.[250,251] This condition is depicted in the electron micrograph of Figure 4.4.d, which shows the PAA oxide after 10 min of anodization. In this dissertation, it is the point during anodization when the true pores and cell walls form that is referred to as "steady state cell structure."

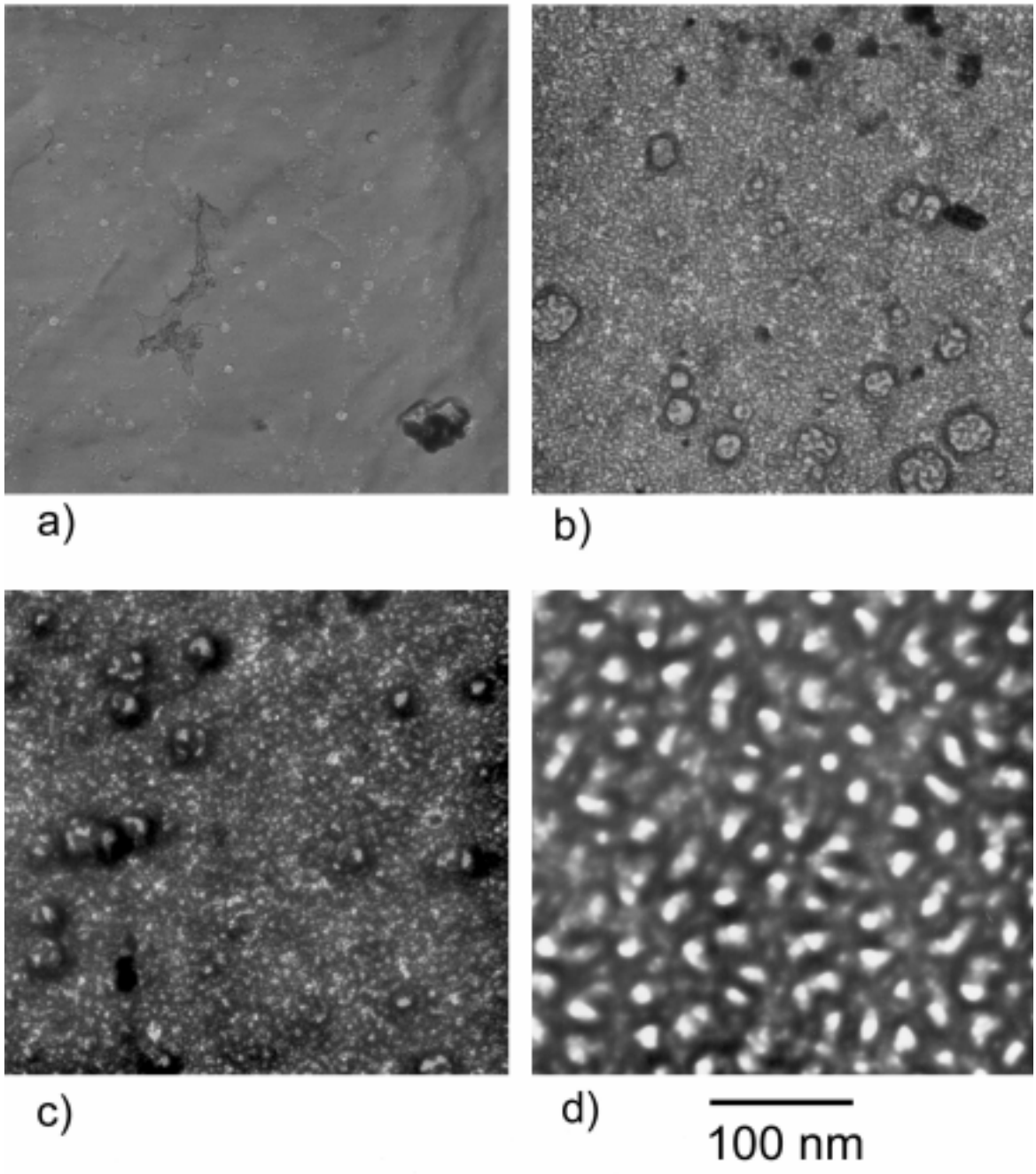

Figure 4.4. Transmission Electron Micrographs of Anodic Oxide Formed on Aluminum Alloy 6061-T6 in 10% (w/w) Phosphoric Acid at 0.65 A/dm^2 for: a) 30 s, b) 60 s c) 120 s, and d) 10 min

To ascertain the significance of the steady state cell structure for adhesive bond strength and durability, 2024-T3 samples were anodized in 10% (w/w) phosphoric acid solutions for varying times to determine the minimum time when the steady state cell structure developed. To more precisely measure total current consumption, the alloy was galvanostatically anodized at 0.65 A/dm^2 at 23^oC. Under these laboratory conditions, the time required to develop a cell and pore structure (Figure 4.5) that was similar to that formed in commercially used potentiostatic PAA process[249] (Figure 4.1) was approximately two minutes. Note that for 6061-T6 alloy anodized under the same conditions, after two min, only incipient porosity was observed (Figure 4.4c).

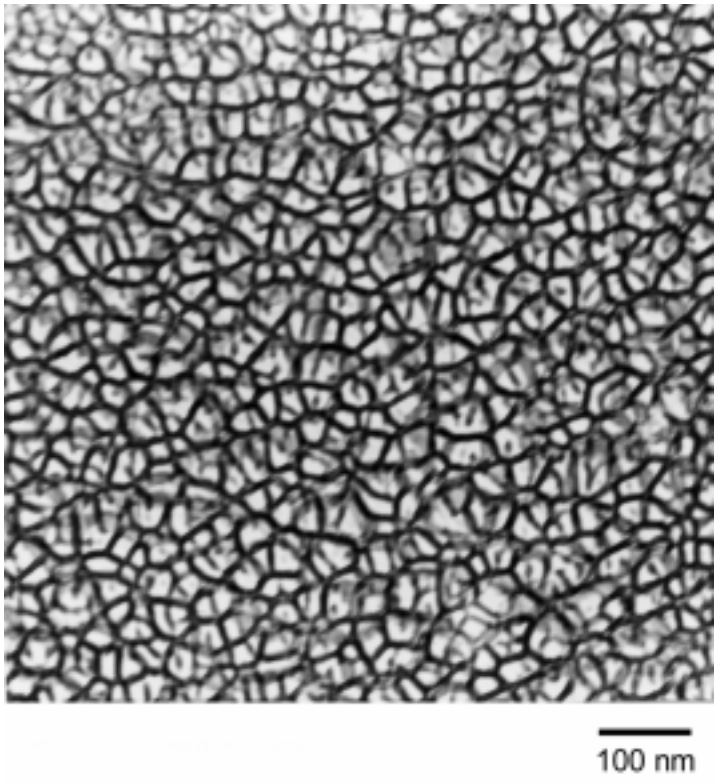

Figure 4.5. Transmission Electron Micrograph of Anodic Oxide Film Formed on Aluminum Alloy 2024-T3 in 10% (w/w) Phosphoric Acid at 0.65 A/dm^2 for 2 min

Faster formation of pores on 2024-T3 is due to the presence of about 4% (w/w) Cu in the base alloy 2024-T3, compared with about 0.2% (w/w) Cu in 6061-T6. Alloy 2024 has large Cu-bearing constituent particles, such as Al_2Cu and Al_2CuMg,[252] which do not form an anodic oxide. These constituents provide pathways for electronic current, thus lowering ionic current, which controls oxide formation. This "short circuiting" by increased electrical current, lowers the resistance and cell potential at a given current, thus decreasing barrier layer thickness. Less oxide is formed in a given time on 2024 compared to 6061, and there is faster formation of pores on the thinner oxide at a given dissolution rate.[77]

The PAA film formed galvanostatically in two minutes on 2024-T3 alloy (Figure 4.5) had an oxide thickness of 26 nm, as measured by Auger electron spectroscopy (AES) depth profiling. This anodized aluminum was bonded in the lap shear and wedge test configurations with AF163-2K film adhesive. Adherends treated with the 10-volt/20 min PAA process[84] and the step-voltage CAA process[30] were tested for reference. The measured lap shear strengths are presented in Table 4.1.

Table 4.1. Lap Shear Strengths of Adhesively Bonded Aluminum as a Function of Type of Porous Anodic Oxide (3.226 cm^2 overlap area)

Anodic Oxide	Film Thickness (nm)	Breaking Strength (MPa)	Standard Deviation (MPa)
2 min PAA	26	40.1	2.1
20 min PAA	400	42.2	0.7
40 min CAA	3000	40.4	1.6

252. J. E. Hatch, ed., "*Aluminum Properties and Physical Metallurgy*," American Society for Metals, Metals Park, Ohio (1984) p. 144.

All of the lap shear specimens failed cohesively in the adhesive, and had equivalent average breaking strengths. This indicates that the thin oxide film (26 nm for the 2 min PAA) provides a threshold interfacial bond strength that exceeds the cohesive strength of the adhesive, and that it is adequate for "dry" adhesion.

Durability testing shows, however, that steady state cell structure is apparently not a sufficient prerequisite for durable wedge test response. This is indicated by the wedge test results presented in Figure 4.6.

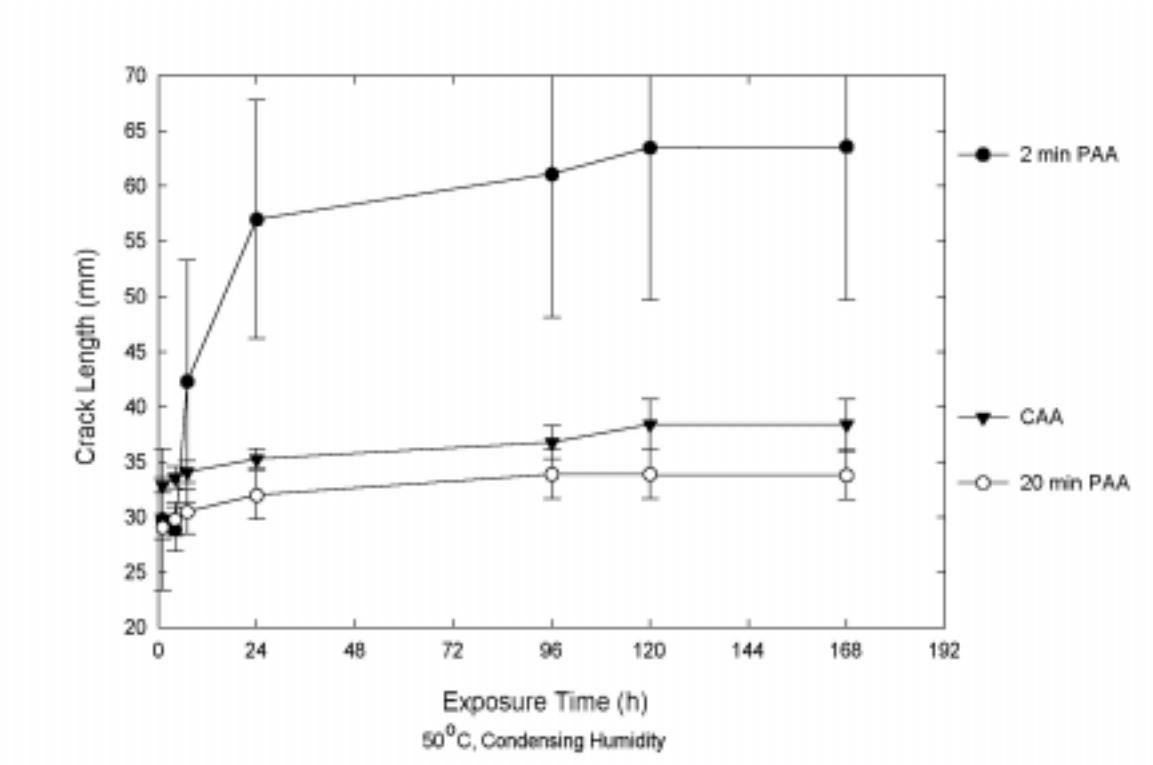

Figure 4.6. Significance of Pore Texture on the Durability of Adhesively Bonded Aluminum, Wedge Test - 2024-T3 Alloy, AF163 Epoxy

The 2 min PAA sample had a final crack length greater than 60 mm, or almost twice that of the 20 min PAA and the 40 min CAA samples. In addition, from visual inspection, the 2 min PAA samples failed interfacially, whereas the other samples failed cohesively in the adhesive nearer to

the interface of one adherend, than to the other adherend. This latter type of failure will be referred to as thin cohesive failure.

The significance of steady state cell structure and increased surface area were also evaluated for phosphorous acid anodic oxides (HPAA), formed in aqueous solutions of 10% (w/w) phosphorous acid (H_3PO_3). Phosphorous acid is also referred to as phosphonic acid.[253] Phosphorous acid is a stronger acid than phosphoric acid; the pK values are 1.8 and 2.2, respectively.[253] A higher degree of dissociation results in a higher ionic current at a given potential, thus increasing the rate of film growth. A series of HPAA samples was prepared from 0.5 min to 10 min at 10 V and 23°C. TEM revealed that a steady state cell structure was present at 30 s of phosphorus acid anodization (Figure 4.7). TEM micrographs of HPAA films produced in times between 2 and 20 minutes did not look different.

The average lap shear breaking strength for bonds with 2 min HPAA adherends was 40.4 ± 0.9 MPa. This is equivalent to strengths of bonds prepared with adherends that were treated using industry standard anodizations (see Table 4.1). All lap joints failed cohesively.

The wedge test crack lengths (Figure 4.8) for the specimens with adherends anodized in H_3PO_3 for 1 min and 2 min were comparable to those of the PAA and CAA standards, whereas the 0.5 min HPAA films yielded large wedge crack growths. The wedge test failure modes were: interfacial for the wedge specimens with 0.5 min anodized adherends, approximately 50% interfacial and 50% thin cohesive for joints with 1 minute anodized adherends, and thin cohesive failure for those specimens with adherends anodized for 2 min or longer.

---

253. F. A. Cotton and G. Wilkinson, "*Advanced Inorganic Chemistry, 4th Ed.*," John Wiley & Sons, Inc., New York (1980) pp. 473-474.

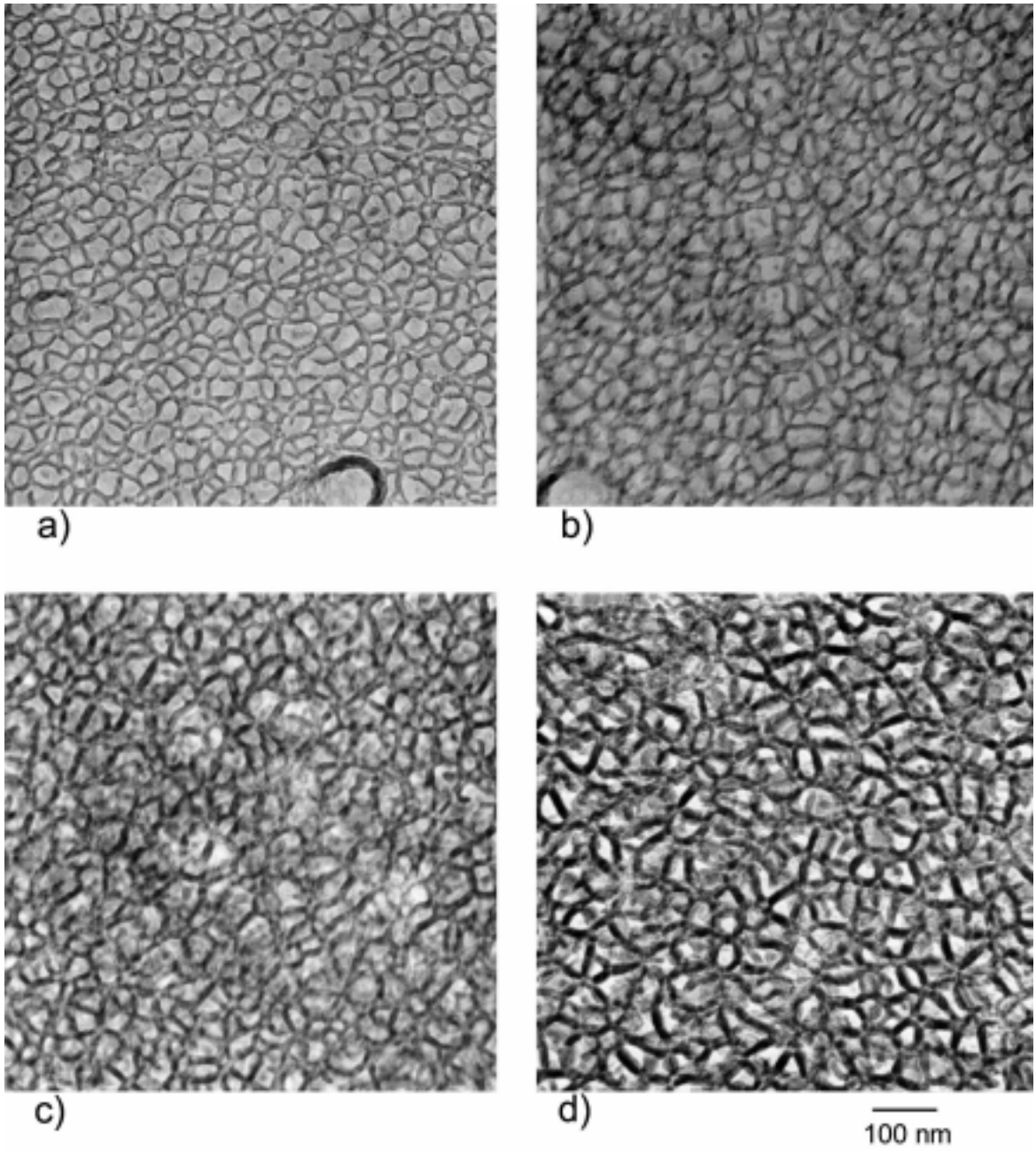

Figure 4.7. Transmission Electron Micrographs of Anodic Oxide Formed on Aluminum Alloy 2024-T3 in 10% (w/w) Phosphorous Acid at 10 V for: a) 30 s, b) 60 s, c) 120 s, and d) 5 min

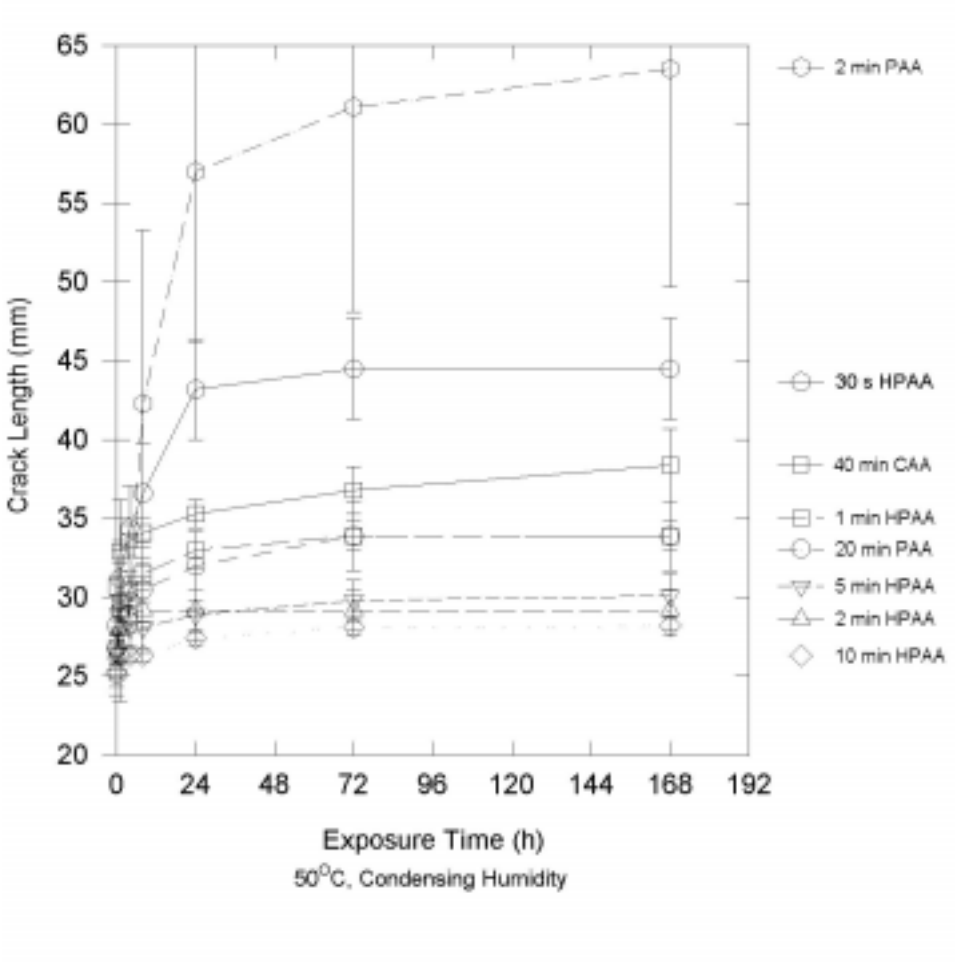

Figure 4.8. Effect of Phosphorous Acid Anodizing Time on the Durability of Adhesively Bonded Aluminum - Wedge Test: 2024-T3 Alloy, AF163 Epoxy

While the wedge test crack lengths were comparable for joints with the 1 min HPAA oxide and the standard controls, the mode of failure for the 1 min HPAA specimen was mixed, with areas of apparent interfacial failure and areas of thin cohesive failure. Since the failure mode of bonds with 1 min HPAA adherends was not 100% cohesive, these results would not satisfy the Boeing

BAC5555 specification.[254] The 1 min HPAA treatment provides some improvement to adhesive bond durability, as determined by the crack growth data of Figure 4.8. However, the improvement is not sufficient, since mixed mode locus of failure was observed as opposed to the required cohesive failure mode. After 2 min of phosphorous acid anodization, both the crack length *and* failure mode are equivalent to, or better, than what were observed using industry standard (20 min PAA and 40 min CAA) anodizations.

The crack lengths for the bonded specimens with adherends anodized for 2 min or longer in phosphorous acid, but not phosphoric acid, solution were comparable to the CAA and 20 min PAA results (Figure 4.8). The thickness of the HPAA oxide grown in 2 min of anodization at 10 V was 120 nm. This is less than half of the thickness of the oxide formed in the 20 min PAA process. Since cell and pore diameters of the anodic oxide on the 2 min HPAA adherend (Figure 4.7) are the same as those on the 20 min PAA adherend (Figure 4.1), the pore volume and bonded surface area of the 20 min-PAA oxide are at least twice as large as those of the 2 min-HPAA oxide films, assuming complete adhesive penetration. Consequently, if the crack propagation rate in the wedge test is influenced by the chemical state of the surface, the effect of HPAA oxides on the environmental durability of the adhesive bond must be significantly greater than that of the PAA oxide. A summary of wedge test results and oxide thicknesses is presented in Table 4.2.

---

254. Boeing specification BAC5555 states that acceptable crack *growth* in the wedge test is approximately 7.5 mm, and the acceptable failure mode is cohesive. All evaluations in this work were judged relative to the performance of standard PAA and CAA control samples tested in this laboratory.

Table 4.2. Comparison of Oxide Topography and Wedge Test Results for Adhesive Bonds Prepared with Adherends with Varying Anodic Oxide Films

Anodization (Time/Acid)	Oxide Thickness (nm)	Approx. Avg. Pore Diameter (nm)	Final Wedge Test Crack Length (mm)	Apparent Failure Mode
2 min PAA	26	40	63	interfacial
20 min PAA	400	40	33	thin cohesive
40 min CAA	3000	3	37	thin cohesive
0.5 min HPAA	not determined	40	44	interfacial
1 min HPAA	not determined	40	34	mixed mode
2 min HPAA	120	40	29	thin cohesive

To test the assumption regarding the influence of the chemical state on the durability of the adhesive bond, topographically identical anodic oxide layers were formed on alloy 2024-T3 in solutions of H_3PO_4 and H_3PO_3. A 10% (w/w) solution of phosphorous acid had a measured conductivity of 103 mS. A phosphoric acid solution having this conductivity was prepared by increasing the concentration from 10% to about 12% (w/w). By galvanostatically anodizing the 2024 alloy in these solutions of equivalent ionic strength, topographically identical surface films were produced. Anodic oxidation was performed at a constant current density of 0.7 A/dm^2 for 5 min, for a total of 210 coulombs. The oxides formed under these conditions in H_3PO_4 and H_3PO_3 solutions were practically identical, having pore diameters in the range of 20-30 nm (Figures 4.9a and 4.9b, respectively), with oxide thicknesses of 75 nm and 95 nm, respectively.

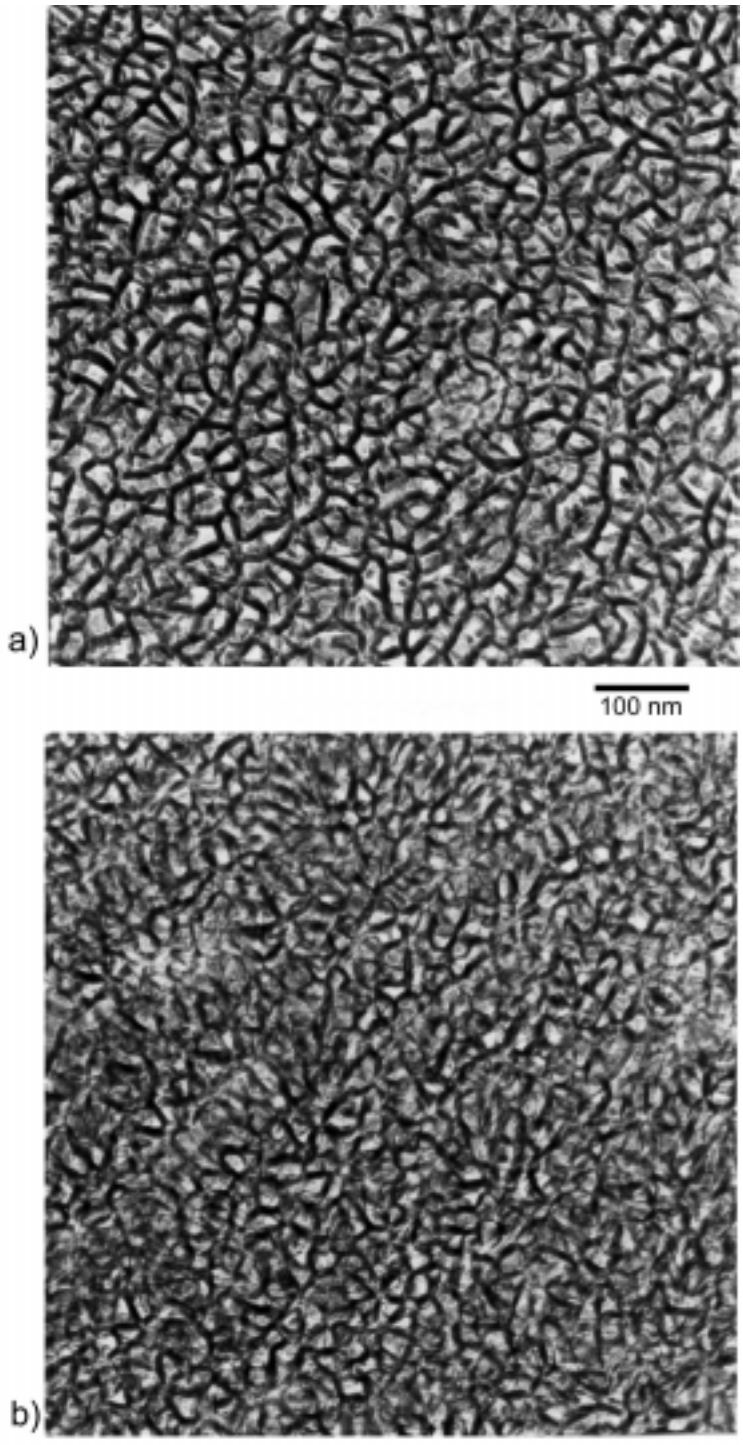

Figure 4.9. Transmission Electron Micrographs of Anodic Oxides Formed with 210 Coulombs in Solutions of 103 mS: a) H_3PO_4 and b) H_3PO_3

As the anodic oxides formed in phosphorous and phosphoric acids of equivalent ionic strength were practically identical in topography, any mechanical contributions to the durability of adhesive bonding would be effectively equal for the HPAA and PAA adherends. With equivalent pore dimensions, the total surface area available for interaction of the oxide with the adhesive is similar for the two anodic oxides. Further, since both anodic oxides are presumed to be high energy surfaces, and since during the time between anodization and bonding (< 24 hr), the anodized samples were kept in a desiccator, it is reasonable to assume the adhesive wets both of the inorganic oxide surfaces equally. That is, even if the surface energies of the two systems are different, they are each sufficiently high to assume that the adhesive adequately wet both surfaces. While this was not checked directly, the assumption is corroborated by thin cohesive failure modes that were observed for both systems after wedge testing (the wedge test crack lengths will be presented shortly). When an adhesive does not properly wet an adherend, one would predict interfacial, or at least mixed mode, failure. Since the wedge test failure mode results indicate that the adhesive wet each anodized surface equally well, and since similar topographies would indicate similar mechanical contributions to adhesion durability for both adherends, any differences in bond durability in systems incorporating these adherends are attributed to differing surface chemistries and the to chemical interactions occurring between the modified surface and the adhesive resin, and not to differences in mechanical interlocking or wettability.

Wedge tests results of joints bonded with the AF163-2K epoxy film adhesive are displayed in Figure 4.10. There is a significant difference in the durability of the two bonded systems. The bonded specimen with HPAA adherends had significantly lower crack lengths than the bonded PAA aluminum. The topographies of the anodic oxides are comparable. Therefore, the mechanical contributions to adhesion should be equivalent. Thus, it is reasonable to infer that the chemical state of the HPAA adherend surfaces had a greater positive effect on bond durability than did the chemical state of the PAA adherends.

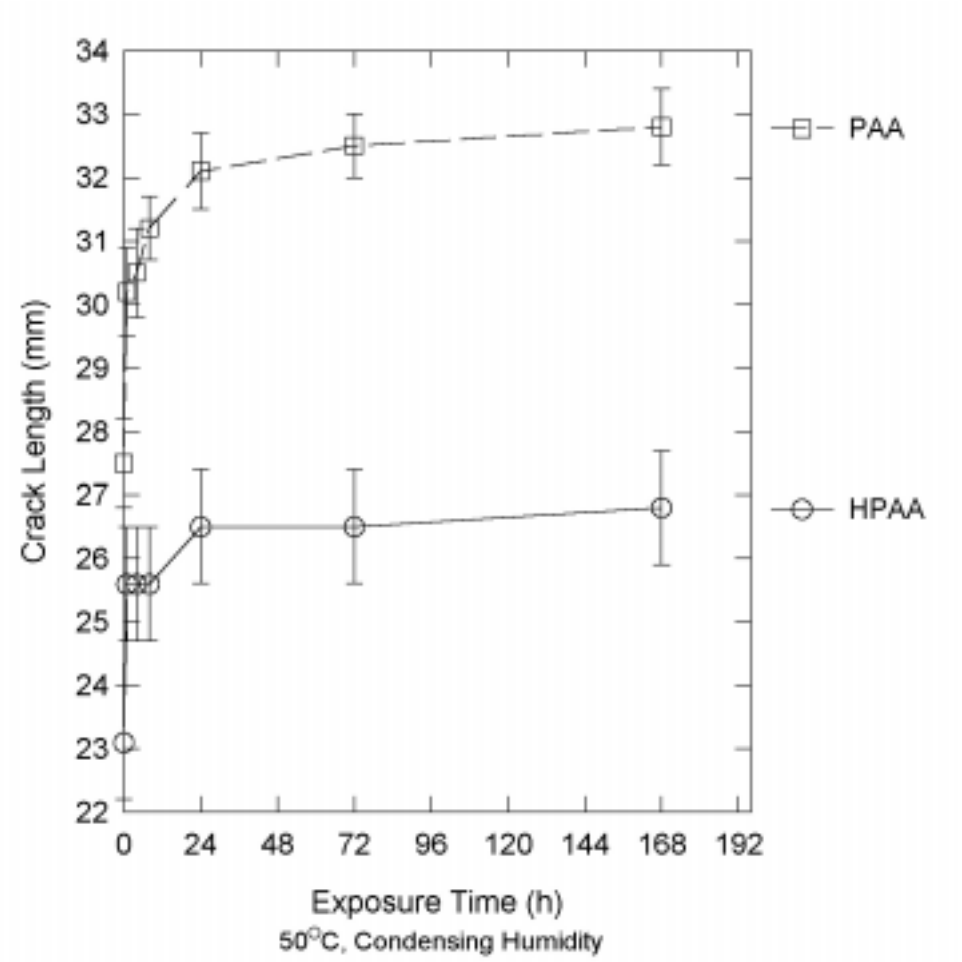

Figure 4.10. Wedge Test Durability of Aluminum Adherends with Topographically Identical Anodic Oxides Formed in Phosphoric and Phosphorous Acid Electrolytes

While the data indicate empirically that the surface chemistries of the PAA and HPAA adherends were responsible for the observed differences in performance, Fourier transform-infrared spectroscopy (FT-IR) and X-ray photoelectron spectroscopy (XPS) did not reveal a difference in composition between the two films. The FT-IR spectra (45° specular reflectance) were qualitatively similar (Figure 4.11).

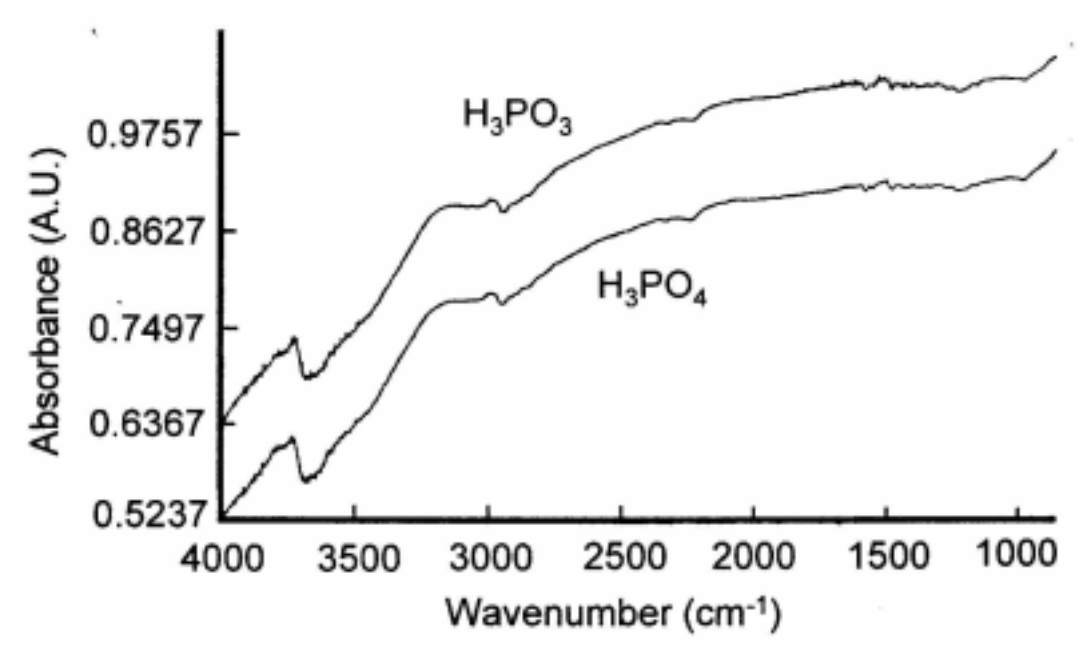

Figure 4.11. Fourier Transform-Infrared Spectra of Topographically Identical Anodic Oxides Formed in Phosphoric and Phosphorous Acid Electrolytes

The only feature observed in these spectra is a broad OH stretching band between 3000 and 3500 cm^{-1}. The increase in the absorbance *below* 1000 cm^{-1}, on both spectra, is most likely attributed to Al-O stretching modes, but these values are near the end of the range for the MCT detector that was used to acquire the spectra, so that the entire band is not shown. Anticipated P-O bands, in the region between 1050 and 1150 cm^{-1}, are not present. The concentrations of these groups in the thin anodic oxides must be below the detection limit of the MCT detector. XPS, however,

revealed that the films contained approximately 3.4 % (at) P with a P 2p binding energy of approximately 134.3 eV. The results from XPS and AES analyses are summarized in Table 4.3.

Table 4.3. Summary of Elemental Composition (at % by XPS), P 2p Binding Energy (by XPS), and Oxide Thicknesses (by AES) of Anodic Oxides Formed in H_3PO_4 and H_3PO_3 Solutions of the Same Conductivity with 210 Coulombs

Acid	C	N	O	F	Al	P	P 2p Binding Energy (eV)	Oxide Thickness (nm)
H_3PO_3	26.8	0.3	41.0	1.4	27.1	3.4	134.4	95
H_3PO_4	26.6	1.0	42.6	1.5	24.9	3.5	134.1	75

While there are small differences in P surface concentration (Table 4.3) these are within the error of the measurement, and indicate that phosphorus is present at similar concentrations in both anodic oxide films. Carbon is present as adventitious hydrocarbon contaminant, that is found on high energy surfaces that are exposed to the atmosphere. Fluorine is present on many aluminum surfaces, and could result from chemicals used to condition alloy heat treatment furnace atmospheres.[77] The source of nitrogen is undetermined, but is also occasionally found on oxidized aluminum surfaces, and could be from adsorbed atmospheric NO_x pollutants.[255]

The similar P 2p binding energies for P in both anodic oxide films needs to be explained, since one would expect different XPS binding energies for P(III) and P(V), which are found in H_3PO_3 and H_3PO_4, respectively. A general range for the P 2p binding energy of phosphate species is given as slightly above 132.0 eV to slightly below 133.0 eV.[256] The binding energy for $AlPO_4$ is

255. B. R. Strohmeier, PPG Industries, personal communication.
256. "*Handbook of Photoelectron Spectroscopy*," Perkin Elmer Corporation, Physical Electronics Division, Eden Prairie, MN (1992).

given as 132.9 eV (referenced to C 1s at 285.0 eV).[256] Also, for the series of sodium phosphate salts, from tribasic to dibasic to monobasic, the P 2p binding energies increase as 132.4 to 133.1 to 134.2 eV, respectively.[256] The P 2p binding energy increases as the salt becomes more acidic. It might be assumed that aluminum acid anion salts on the surface of the anodic oxide, and those incorporated in the anodic oxide, could account for the P 2p binding energy being similar and around 134 eV for both anodic oxide films. Wefers has shown that in a closed system, a hydrolysis reaction with sulfuric acid anodic oxide films that were separated from the metal resulted in the formation of H_2SO_4, indicating that acid anions are present in the anodic oxide.[257] Therefore, it is a reasonable analogy to extend this to PAA oxides. This concept alone would not however, account for the observed differences in bond durability, particularly since only phosphorus in the P(V) oxidation state was detected by solid-state NMR for both the PAA and HPAA oxides. These NMR data are presented and described later in this chapter.

An alternative explanation is that the spectrometer could not resolve a shift in binding energy of the P 2p peak between P(V) as in H_3PO_4, and P(III) in H_3PO_3. Since H_3PO_4 is available as an aqueous solution, and H_3PO_3 as an extremely hygroscopic solid, direct analysis of these compounds is difficult or impossible using XPS in ultrahigh vacuum (UHV). Therefore, to test this alternative explanation, neat powdered samples of phenylphosphonic acid --- C_6H_5-P(O)$(OH)_2$ --- and phenylphosphoric acid --- C_6H_5-O-P(O)$(OH)_2$ --- were analyzed by high resolution XPS. Phenylphosphoric acid contains P(V) phosphorus surrounded by 4 oxygen atoms, the same as H_3PO_4. Phenylphosphonic acid has P(III) phosphorus surrounded by 3 oxygen atoms and a carbon, similar electronically to H_3PO_3, which is surrounded by three oxygen atoms and a proton. The binding energies and concentrations of the elements in these compounds (average of 3 analyses each) are found in Table 4.4.

257. K. Wefers, *Aluminium (Düsseldorf),* ***49*** (1973) 2.

Table 4.4. High Resolution XPS Analysis of Phenylphosphonic Acid and Phenylphosphoric Acid Powders: Binding Energy (eV) and Concentration (at%)

Acid	Binding Energy (eV)			Concentration (atomic %)		
	C 1s	O 1s	P 2p	C	O	P
Phenylphosphonic	285.0	533.0	134.1	62.1	27.5	10.4
Phenylphosphoric	285.0	533.7	135.1	57.7	32.7	9.7

The data in Table 4.4 reveal that the P 2p binding energy for P(V) in phenylphosphoric acid is 1.0 eV higher than that for P(III) in phenylphosphonic acid, 135.1 eV versus 134.1 eV, respectively. Since P in the P(V) compound has four electronegative oxygen nearest neighbors, compared to three in the P(III) compound, a higher P 2p binding energy for phenylphosphoric acid {P(V)} is to be expected.

There is the possibility that the powders could decompose under the X-ray beam providing false results for XPS chemical shifts. To check this, one can look at the atomic ratios of elements in the compounds to the detected ratios. For example, C/P = 6 is the theoretical value for both compounds. The measured values for C/P are 6.0 and 5.9 for phenylphosphonic acid and phenylphosphoric acid, respectively (Table 4.4). There is excellent agreement for the theoretical and measured values of C/P. One can state that the P 2p binding energies of neat phosphoric acid and derivatives of this acid can be detected 1 eV higher than the P 2p binding energies of neat phosphonic acid and its derivatives.

A simple adsorption experiment was conducted to determine if aluminum oxide -phosphorus oxo acid *reaction products* could be distinguished using chemical shifts in XPS. Caustic etched 1199 alloy (99.99% Al) was reacted with 10% (w/w) aqueous solutions of H_3PO_3 or H_3PO_4. These samples were analyzed using high resolution XPS, and the results are displayed in Table 4.5.

Table 4.5. Elemental Composition (at. %) and Binding Energies (eV) of Etched High Purity Aluminum Dipped in 10% (w/w) Solutions of Phosphorus Oxo Acids

Acid Dip		C 1s	O 1s	Al 2p	P 2p	P 2s
H_3PO_4	(atomic %)	24.3	34.3	40.5	---	0.9
	(eV)	285.0	531.6	74.6	~133.7	191.5
H_3PO_3	(atomic %)	30.1	34.5	34.9	---	0.6
	(eV)	285.0	531.6	74.6	~133.9	191.5

The phosphorus XPS binding energies for H_3PO_4 and H_3PO_3 reacted with aluminum oxide are equivalent (Table 4.5). The P 2p binding energies are given as approximate values since there was uncertainty of these values due to the overlap of an aluminum metal plasmon signal in this region. This plasmon was detected because of the thin oxide (< 5 nm) formed on the aluminum metal after caustic etching.[241] The Al-O-P surface bonds that are formed in the reaction product of H_3PO_4 or H_3PO_3 with aluminum oxide result in an electronic environment for P that is similar for either P(V) or P(III) species on the aluminum oxide surfaces.

The results above suggest that either XPS chemical shifts cannot be used to distinguish between oxidation states for aluminum oxide - phosphorus oxo acid reaction products. However, one could still argue that H_3PO_3 is oxidized as soon as it reacts with aluminum oxide. The work of Ramsier, et al.,[258] demonstrates that H_3PO_3 is *not* oxidized as it adsorbs onto and reacts with an oxidized aluminum surface. Using inelastic electron tunneling spectroscopy (IETS), Ramsier, et al.,[258] showed that H_3PO_3 reacts with the oxidized aluminum surface in a tridentate fashion through the three oxygen atoms on the H_3PO_3 molecule with hydroxyl groups on the oxidized aluminum surface to form a hybrid $(Al\text{-}O)_3$-P-H structure . In this configuration, the P-H bond is

258. R. D. Ramsier, P. N. Henriksen, and A. N. Gent, *Surf. Sci.*, ***203*** (1988) 72.

extended away from the surface. Strong P-H vibrations were detected when phosphorous acid was reacted with surface oxides indicating that there was no oxidation of the phosphorus.[258] Since P binding energies were equivalent for both phosphorous oxo acid anodic oxides and for both acids adsorbed onto oxidized aluminum, and since NMR did not detect P(III) anodic oxides, together with the work of Ramsier, et al.,[258] it is concluded that during anodization in H_3PO_3 solutions the P species are oxidized to P(V) as they are incorporated into the forming anodic oxide. This occurs in combination with the reduction of water that always takes place during anodizing. Oxidation of phosphorous acid does not occur to the molecules and anions remaining in solution, since the solutions can be reused and yield the same anodizing response. These results also show that it is not possible to use XPS chemical shifts to distinguish between the reaction products of aluminum oxide and phosphoric acid and aluminum oxide and phosphorous acid.

Since the PAA and HPAA adherends had similar topographies and any mechanical contributions to durable adhesion should be equivalent, the analytical results presented so far cannot be used to explain the observed differences in wedge test performance (Figure 4.10). ^{27}Al solid state-magic angle spinning-nuclear magnetic resonance (MAS-NMR) spectra of the detached oxide films did reveal a distinct difference in the two anodic oxides. Al-O-P and Al-O-Al clusters of tetrahedral symmetry (T_d, four-fold coordination) and of octahedral symmetry (O_h, six-fold coordination) were detected in both films, but the oxides formed in phosphorous acid had more than twice the number of tetrahedral Al-O-Al and Al-O-P clusters than did the oxides formed in phosphoric acid. The MAS-NMR spectra are shown in Figure 4.12. The peaks were fitted using Gaussian line shapes; fitted peak areas are found in Table 4.6. The differences in short-range clusters in the amorphous anodic oxides may arise due to the oxidation of P(III) $\rightarrow$ P(V) that occurs during film formation.

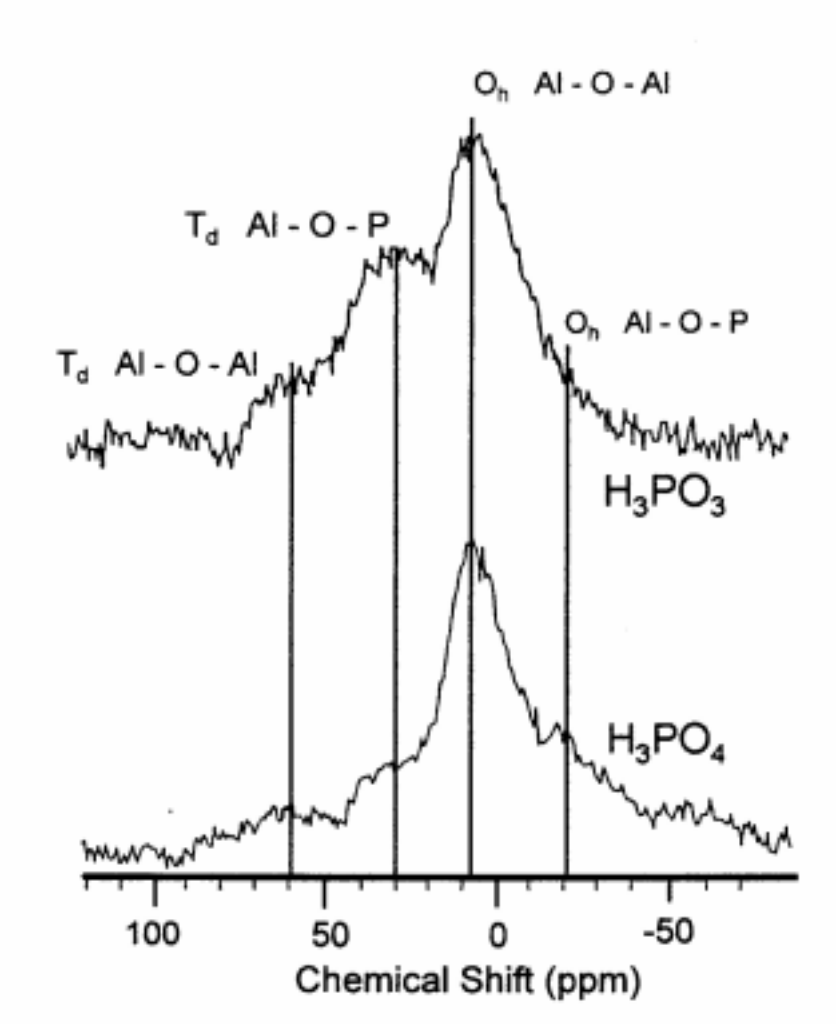

Figure 4.12. ^{27}Al Magic Angle Spinning-Nuclear Magnetic Resonance Spectra of Topographically Identical Anodic Oxide Films Formed in Phosphoric and Phosphorous Acid Electrolytes

Table 4.6. ^{27}Al Solid State Magic Angle Spinning-Nuclear Magnetic Resonance (MAS-NMR) Normalized Peak Areas for Topographically Identical Aluminum Anodic Oxides Formed in Phosphoric and Phosphorous Acid Solutions

Anodizing Electrolyte	Chemical Shift / Species			
	60 ppm T_d Al-O-Al (4-fold)	32 ppm T_d Al-O-P (4-fold)	8 ppm O_h Al-O-Al (6-fold)	-20 ppm O_h Al-O-P (6-fold)
Phosphorous Acid	6	28	53	13
Phosphoric Acid	2	13	74	11

There was no evidence of differing elemental surface compositions for the HPAA and PAA anodic oxides. Also, the topographies were virtually identical. The use of ^{27}Al NMR found differences in short-range clustering of Al-O-P in the anodic oxides. However, NMR is a bulk analytical technique, for which the detected signal is derived from the whole of the oxide. It is considered, however, that differences in the bulk anodic oxides may translate into different chemical structures at the surface. The HPAA film could have a higher surface reactivity due to coordinatively unsaturated (tetrahedrally coordinated) aluminum ions at or near the oxide surface, much like the catalytic activity that is observed in γ-alumina, which has considerable tetrahedral Al-O bonding.[86] The precise nature of differences of the surface structures of the anodic oxides was not determined.

While it is very likely that a difference in the surface reactivity of the PAA and HPAA, topographically identical, oxides contributed to the observed distinct wedge test crack growths, there still is the possibility, as suggested by Davis, et al.,[232] that the inherent hydration resistance

of the surfaces determined the test performance.[226,227,229] An experiment was conducted with topographically equivalent anodic oxides formed in H_3PO_3 or H_3PO_4 to determine their surface hydration resistance. PAA and HPAA substrates with topographically identical oxides were exposed to 50°C and 98 % R.H. for various times. The FT-IR spectra of the anodized surfaces that were exposed to humidity for 23 hr are displayed in Figure 4.13. These should be compared with the spectra of the unexposed anodic oxides (Figure 4.11). Hydration resistance was determined by the relative increase of the hydroxyl stretching band (around 3300 cm^{-1}) as a function of exposure time.

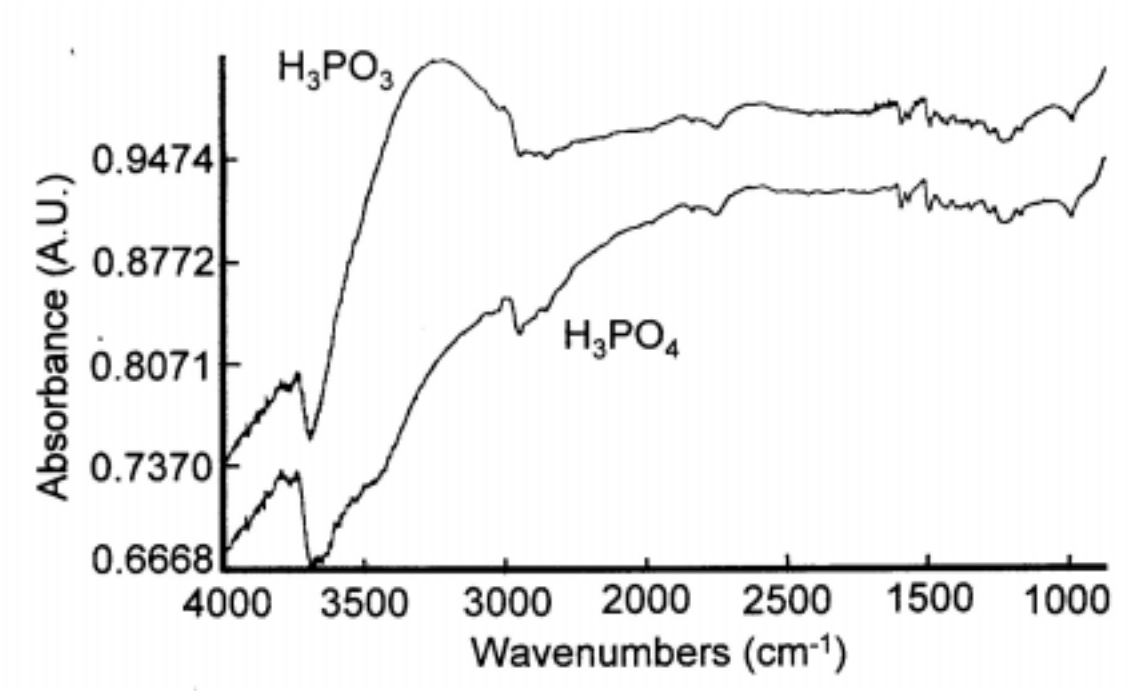

Figure 4.13. Fourier Transform-Infrared Spectra of Topographically Identical Anodic Oxides Formed In Phosphoric and Phosphorous Acid Electrolytes Exposed to 50°C and 98% R.H. for 23 h

The results of humidity exposure are summarized and displayed in Figure 4.14. The "Increase in Total Absorbance Units" plotted on the y-axis of Figure 4.14 was calculated by taking the total absorbance units at each exposure interval and subtracting the total absorbance of the as-prepared sample (no humidity exposure).

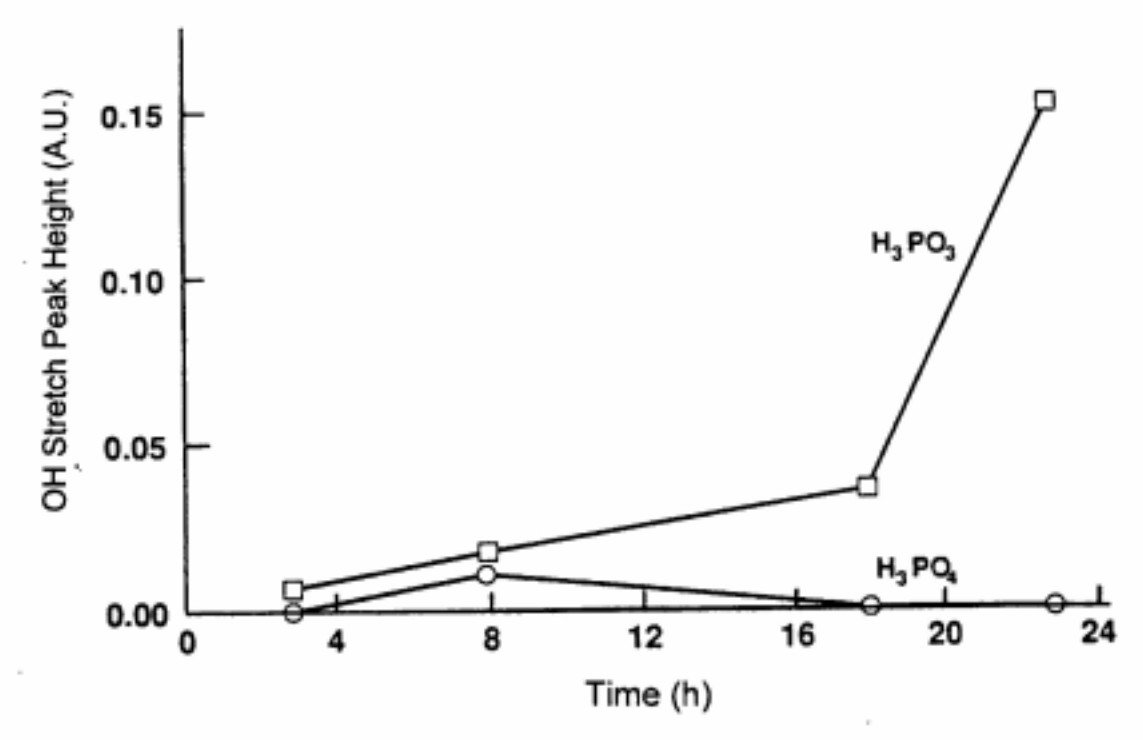

Figure 4.14. Summary of FT-IR Analysis of OH Stretch Intensities of PAA and HPAA Topographically Identical Oxides Exposed to 50°C and 98% R.H. - Referenced to Unexposed Surface

There is a progressive increase in hydration between 1 and 23 hr of exposure for the phosphorous acid-produced oxide. Visual examination of the HPAA samples that were exposed for various times to humidity revealed a uniform surface discoloration with interference colors that changed with the length of exposure. XPS analysis of the HPAA sample exposed for 23 hr showed an absence of phosphorus (~ 0.2 at. % P detection limit for XPS),[241] indicating that the P species in the HPAA surface oxide had most likely been covered with aluminum hydroxide from the reaction of water with the HPAA oxide, and that the thickness of the hydroxide layer was greater than the sampling depth of XPS.

The samples with PAA anodic oxides did not change appearance within the first eight hours of humidity exposure. After this time, a few widely scattered, millimeter-sized spots of interference colors (stains) appeared on the PAA samples, indicating sites of localized hydroxylation. Despite the visual evidence of localized hydroxylation on the PAA oxides, FT-IR analysis, which analyzes a lateral spot size that is an order of magnitude greater than XPS (cm^2 versus mm^2, respectively) did not detect a measurable increase in surface hydroxylation (Figures 4.13 and 4.14). XPS analysis of areas between the widely scattered small stain spots on the PAA oxide revealed the presence of phosphorus, signifying that hydroxylation was limited to the few small stained spots. The FT-IR/humidity study, combined with XPS and visual inspection, indicate a faster reaction of the phosphorous acid-formed anodic oxide with water than that for the phosphoric acid-formed anodic oxide. These findings, along with the wedge test data of Figure 4.10, demonstrate that inherent hydration resistance of the substrate is not an absolute requirement for durable adhesion.

None of the above findings can conclusively explain the observed lower wedge test crack growths for joints bonded with HPAA adherends. The possibility remains that a higher degree of tetrahedral aluminum (coordinatively unsaturated), which was detected in the bulk oxides, affects the acid-base characteristics of the HPAA surface, which in turn influences the interactions of the adhesive with the surface (density and type of bonds) and the subsequent crack growths. This suggests that chemical bonding at the resin-oxide interface should have an influence on adhesive bond durability.

To further evaluate the effect of interfacial chemical bonding on joint durability, porous anodic oxides were separately functionalized with two different organic functional groups. One of these groups was intentionally chosen to form chemical bonds with adhesive resin components, whereas the other was chosen so that chemical bonds would not be formed with the adhesive. Since it was previously demonstrated that organophosphonic acids form strong ionic bonds with hydroxyl groups on oxidized aluminum,[155,258,167-174] organophosphonic acids were selected for use in surface functionalization. Porous anodic oxides were prepared on alloy 6061-T6, using an

oxalic acid electrolyte. Oxalic acid porous anodic oxides were chosen since they can easily be hydroxylated.[77] Hydroxylation of the surface facilitates reaction of the organophosphonic acids with the porous anodic oxide. The oxalic acid anodic oxides were lightly hydroxylated by immersing the samples in a pH 9 solution of triethylamine at 50°C for 10 s.

The general molecular formula for an organophosphonic acid is written as:
R - $[P(O)(OH)_2]$, where R is an organic radical in which a C atom is directly bonded to the P atom. R can be any of a number of organic functional groups. It was anticipated that bonding of this entire class of molecules to aluminum oxide surface film would be through the $P(O)(OH)_2$ groups reacting with surface hydroxyl groups as Ramsier, et al.,[258] have demonstrated for phosphorous acid. This configuration leaves the organic moiety extended away from the surface. By varying the organic moiety, it should then be possible to alter surface chemistry, without affecting surface topography.

Vinylphosphonic acid (VPA) - Figure 4.15 - and nitrilotris(methylene)triphosphonic acid (NTMP) (see Figure 2.8.a) were chosen for the experiments.

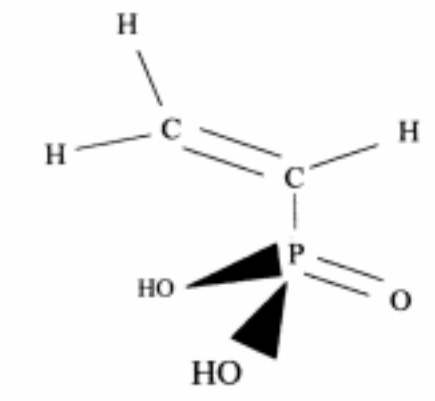

Figure 4.15. Molecular Structure of Vinylphosphonic Acid - VPA

A survey of the literature did not reveal any information on the reaction of epoxides with carbon double bonds. However, the reaction of amines with double bonds occurs,[259] when electron withdrawing groups such as -C=O, -COOH, -COOR, and -CN are attached to the vinyl group.[260] Patai and Rappoport[261] provide a review of nucleophilic attack on carbon-carbon double bonds. For the current investigation, it was postulated that VPA surface vinyl-groups, activated by the electronegative PO_3^{2-}-group, may form chemical bonds with the primary amine of the dicyandiamide curing agent (Michael Addition[259]). Dicyandiamide is present as a latent curing agent in the AF163-2k epoxy resin. The proposed addition of dicyandiamide to surface VPA is presented schematically in Figure 4.16.

For NTMP-functionalized adherends, it was anticipated that there would be no primary chemical bond formation between the substrate and components of the adhesive. Davis and Venables et al.,[167-174] show that NTMP acts as a hydration inhibitor for aluminum, but make no claim of surface NTMP forming chemical bonds with the adhesive. It is known that tertiary amines, such as NTMP, will cause curing of an epoxy resin.[262] This is catalytic curing, in that the tertiary amine does not chemically react with epoxide groups, but catalytically causes the reaction of epoxide groups with each other.[262] Therefore, NTMP at an epoxy adhesive/aluminum adherend interface would accelerate the curing of the adhesive, but would not result in the formation of chemical bonds *across* the interface that would chemically couple the adherend with the adhesive.

---

259. J. March, "*Advanced Organic Chemistry, 2nd Ed.*," McGraw-Hill Book Company, New York (1977) pp. 734-735.
260. R. T. Morrison and R. N. Boyd, "*Organic Chemistry, Third Edition*," Allyn and Bacon, Inc., Boston, MA (1973) p. 868.
261. S. Patai and Z. Rappoport, in "*The Chemistry of Alkenes*," S. Patai, ed., Wiley Interscience, Chichester, England (1994) pp. 469-584.
262. N. J. DeLollis, "*Adhesives, Adherends, Adhesion*," Robert E. Krieger Publishing Co., Inc., Huntington, NY (1980) p. 111.

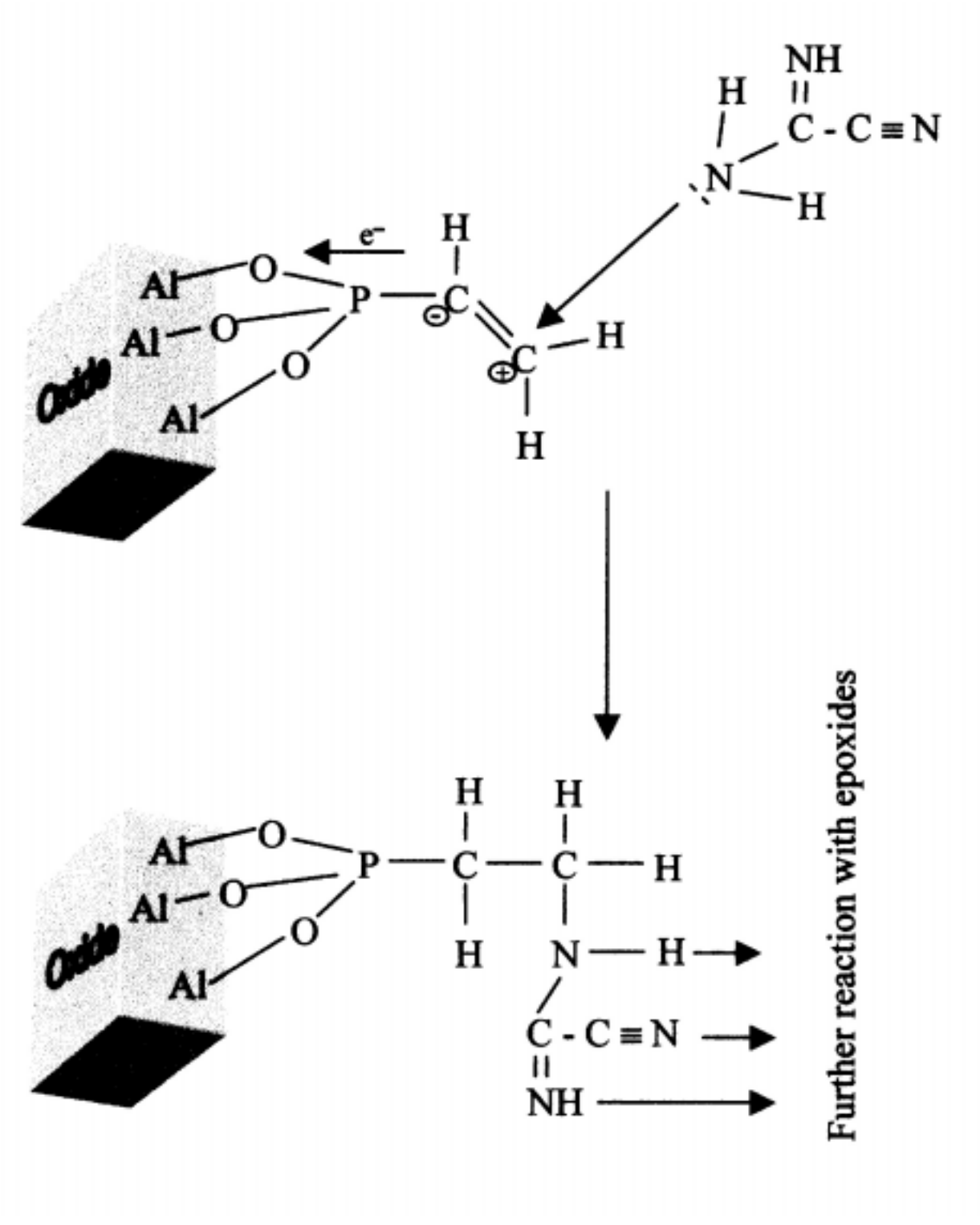

Figure 4.16. Nucleophillic Addition of Dicyandiamide to Vinyl-Group on Vinylphosphonic Acid Treated Oxide Surface

Assuming a current efficiency for oxalic acid anodizing of 70%,[60] the oxalic acid anodizing conditions were chosen to produce a ~1 μm thick porous oxide. This approximate thickness was verified with SEM cross-section analysis of a fractured anodic oxide. The oxide was hydroxylated as previously indicated. Anodized-hydroxylated-only metal was used as a control. The anodized-hydroxylated-organophosphonic acid dipped aluminum alloy specimens were bonded with the AF163-2K epoxy film adhesive and wedge tested. The results of wedge testing are found in Figure 4.17.

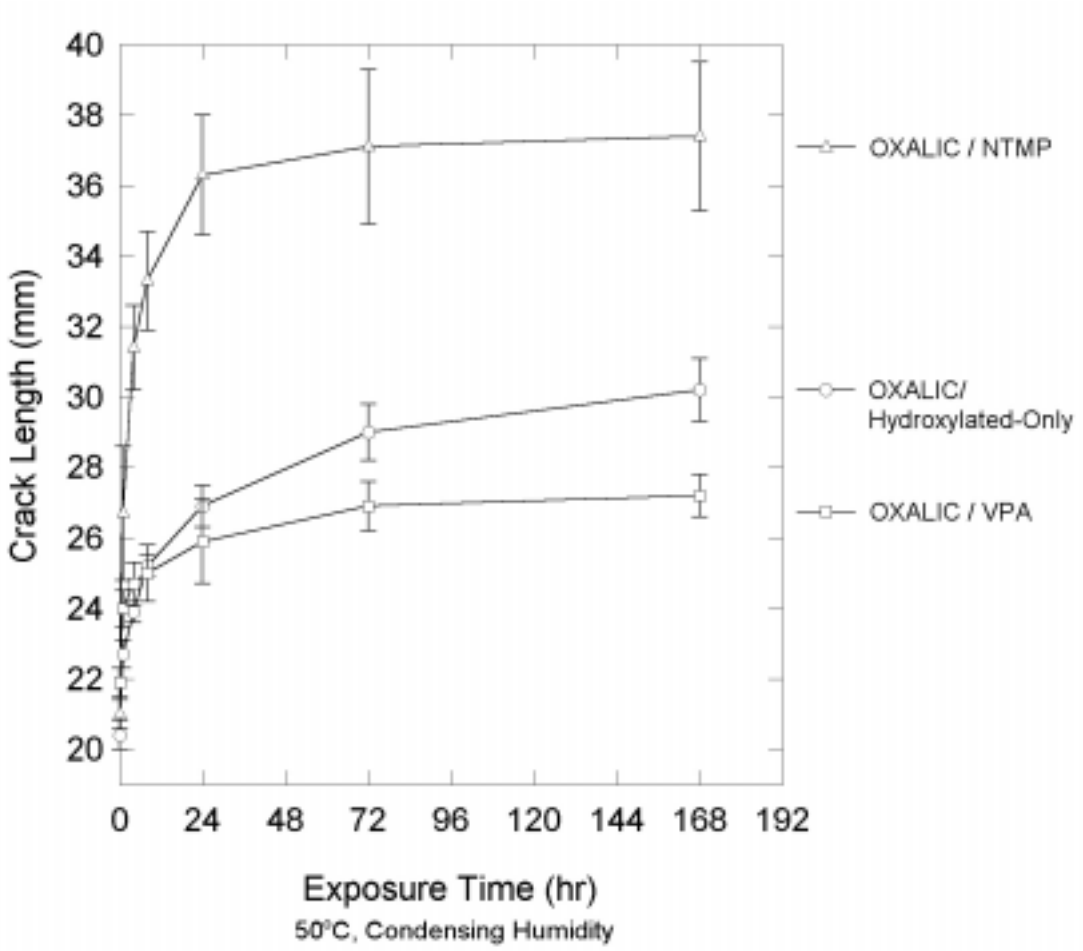

Figure 4.17. Effect of Organophosphonic Acid Functionalization of Porous Oxalic Acid Anodic Oxides on Adhesive Bond Durability, Wedge Test: 6061-T6 Alloy, AF163 Epoxy

The data for organophosphonic acid functionalized, oxalic acid-formed, porous anodic oxides provide more empirical evidence that suggests that chemical bond formation between the adhesive and the oxide surface has an effect on adhesive bond durability. Oxalic acid anodizing, by itself, provided some degree of durability to the joints. However, the crack growth was not arrested by the end of the test; i.e., the residual strength and stresses at the crack tip were not balanced suggesting continued loss of strength with continued exposure. Functionalization with VPA provided statistically lower crack growth that was arrested at the end of exposure to high humidity conditions. Both VPA and anodized-only joints failed in the adhesive near an interface. The wedge data also show that joints with NTMP-treated porous oxides are inferior to those with anodized-only adherends. The NTMP treated joints exhibited a mixed mode failure that showed areas of interfacial and thin cohesive failure.

The results of this investigation on porous oxides and durability empirically suggest that interfacial chemical interactions, or the lack thereof, affect joint durability. They do not support the hypothesis that the intrinsic hydrolytic stability of the surface oxide is a major factor controlling bond failure in the presence of water. The observations and arguments, also, do not conclusively negate a minor role for mechanical interlocking in joint durability, since all of the substrates investigated had porous surfaces, and most of the failures were, at least partially cohesive.

The following chapters will describe empirical investigations to separate the effect of interfacial chemistry from mechanical interlocking in bond durability. This was accomplished by adhesively joining oxide and hydroxide surfaces with topographies that have progressively minimized surface micro-roughness, while varying surface chemistry with organophosphonic acids. Spectroscopic results from experiments that were designed to determine bonding mechanisms of organophosphonic acids on oxidized aluminum and of VPA with adhesive resin components are also presented.

Chapter 5. Gelatinous Boehmite Surface Films

Gelatinous boehmite surface films, generally known as "boehmite" films, on aluminum have been used to enhance adhesion of polymers to aluminum subsrates.[135,139] These films provide an alternative topography to porous anodic oxides for the systematic evaluation of adhesive bond durability mechanisms. Organophosphonic acids are used to functionalize gelatinous boehmite films of similar surface topographies. Accelerated durability testing is used to discern effects of interfacial chemistry on adhesive joint durability.

A. Gelatinous Hydroxide Surface Film Topography

Gelatinous boehmite is a non-stoichiometric hydroxide, which can be given the general formula, AlO(OH, H_2O).[86] For this investigation gelatinous surface hydroxide films were formed by boiling metal in slightly basic (pH 9) aqueous solutions. However, it should be recognized that gelatinous films are formed on aluminum surfaces after most etching or anodizing processes. The notable exceptions to this are aqueous systems incorporating phosphates and silicates, which inhibit hydroxylation of aluminum oxide. [60,263] It is also recognized that similar gels are formed by the hydrolysis of aluminum alkoxides.[86] Pike[176-181] utilizes the hydrolysis of aluminum alkoxides to form an inorganic primer layer (gelatinous boehmite) on phosphoric acid anodic oxides, with resulting improvement in adhesion durability. The chemical reactivity of the gelatinous boehmite with the adhesive is most likely the mechanism of durability enhancement for Pike's work,[176-181] since the gelatinous boehmite completely seals the pores, preventing penetration of the adhesive and mechanical interlocking.

Aluminum hydroxides are amphoteric. The aluminum hydroxides are soluble in acidic and basic

263. D. A. Vermilyea and W. Vedder, *Trans. Farad. Soc.*, ***66*** (1970) 2644.

solutions. This is evident in the solubility curve presented in Figure 5.1.

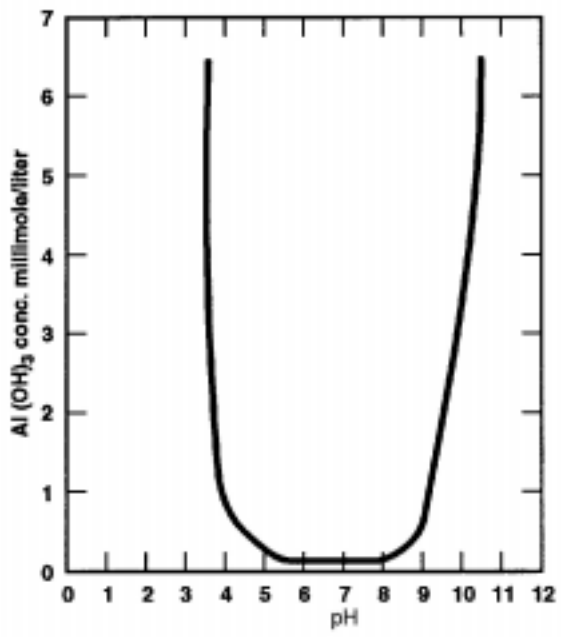

Figure 5.1. Schematic Representation of Solubility of Aluminum Hydroxide as a Function of pH[86]

During boiling at pH 9, aluminum becomes slightly soluble. However, because of the steep slopes of the solubility curve, slight changes of localized pH result in reprecipitation of the solvated aluminum ions as gelatinous boehmite. Above about 75°C, the solvated aluminum ions reprecipitate topochemically in the form of fibrils and sheets of gelatinous aluminum hydroxide.[86] A transmission electron micrograph of a gelatinous hydroxide film that formed on the surface of 2024-T3 after boiling is presented in Figure 5.2. The films have a sheet-like topography that resembles "wrinkled tissue paper"[86] in TEM images. The AES-determined film thickness for the 30 s boil sample was approximately 80 nm; the thickness increased to about 180 nm after 210 s of boiling.

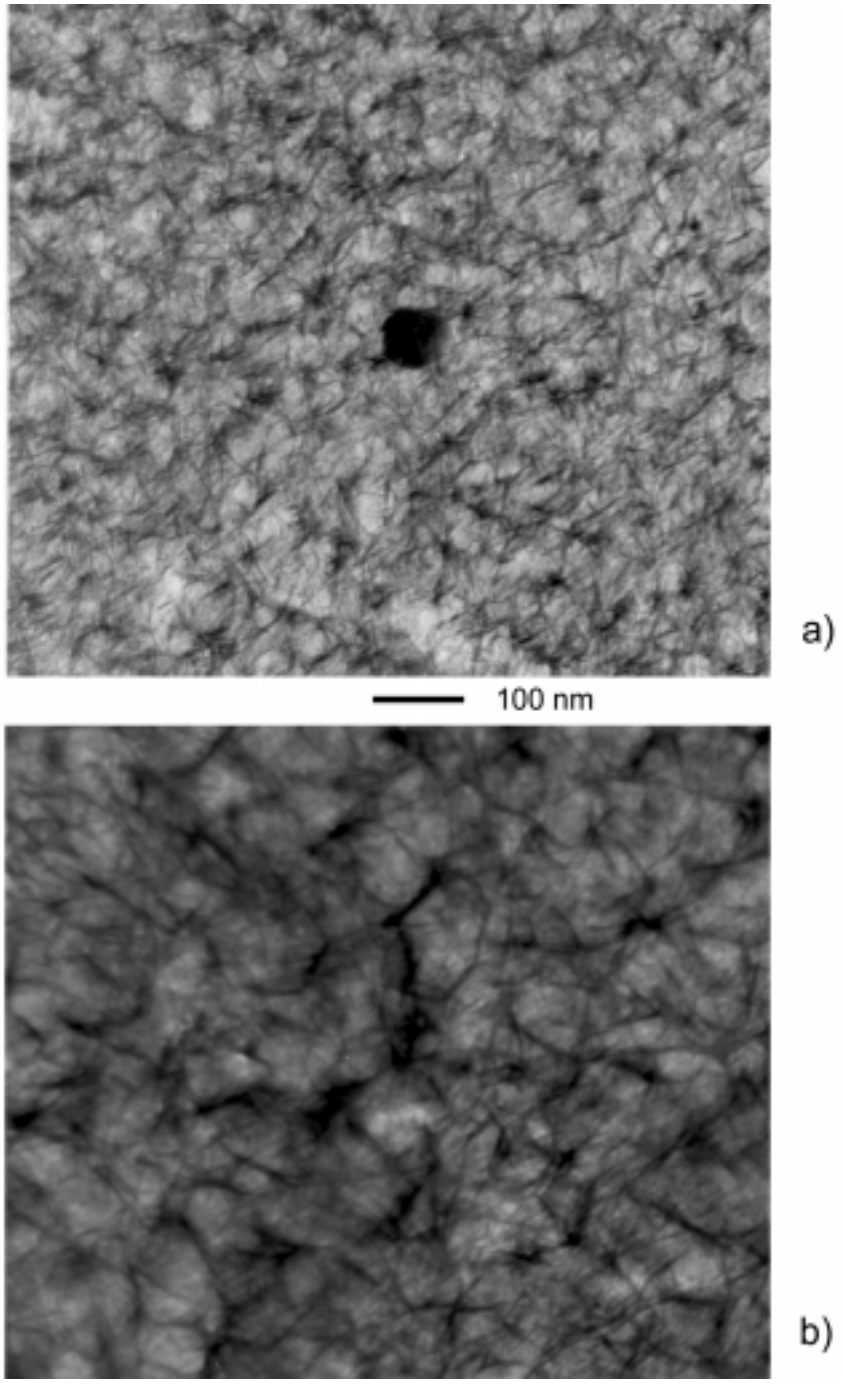

Figure 5.2. Transmission Electron Micrographs of Gelatinous Boehmite Film on 2024-T3: a) 30 s boil, b) 210 s boil

B. Inorganic Phosphorus Oxo Acid Modified Gelatinous Hydroxide Films

1. Film Structure Determination

To further investigate the contribution of surface chemistry to adhesive bond strength and durability, phosphorous acid and phosphoric acid were reacted with gelatinous boehmite surface films by an acid-base reaction. Aluminum hydroxide films were first formed on the 2024-T3 alloy by boiling in pH 9 triethylamine solution for 30 s. These surface films were reacted with the phosphorus oxo acids by dipping for 30 s in 5% (w/w) solutions of H_3PO_3 or H_3PO_4. The resulting acid-modified surface films had thicknesses of about 70 nm for both acid treatments. While the acids thinned the original gelatinous boehmite surface film (from approximately 80 nm to 70 nm), the acid treatments did not affect the topography of the films, as is evident in the transmission electron micrographs of Figure 5.3. The acid-functionalized films exhibited comparable morphologies, and thicknesses.

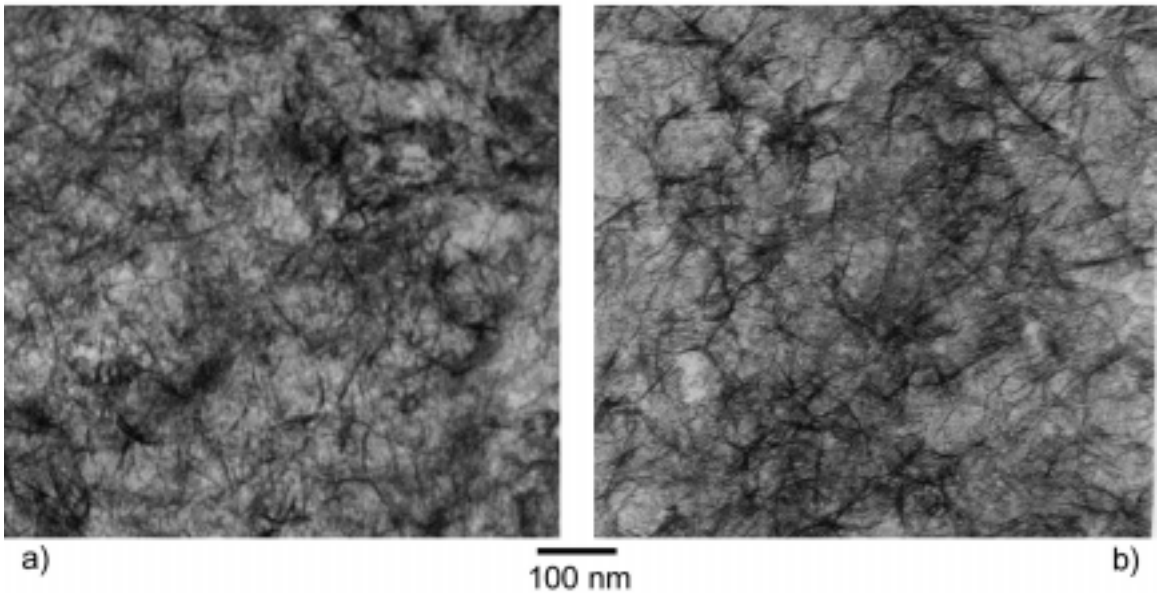

Figure 5.3. Transmission Electron Micrographs of Acid Functionalized Gelatinous Boehmite Films: a) H_3PO_4 and b) H_3PO_3

The elemental compositions of the acid-modified films were similar. Each had approximately 2.5% P (atomic). XPS data for the boiled-only, and acid modified 2024-T3 hydroxide films are presented in Table 5.1.

Table 5.1. Elemental Surface Compositions (at. %) and Binding Energies (eV) of Gelatinous Boehmite and Acid-Modified Gelatinous Boehmite Films on Aluminum Alloy 2024-T3 as Determined by XPS

Sample	XPS	C 1s	N 1s	O 1s	Al 2p	P 2p
Boiled-Only	%	38.4	<0.2*	36.2	25.5	<0.2*
	B.E. (eV)	285.0	not determined	532.1	74.5	not determined
Boil/H_3PO_3	%	26.6	<0.2*	45.1	25.9	2.5
	B.E. (eV)	285.0	not determined	531.7	74.4	133.8
Boil/H_3PO_4	%	24.6	0.5	46.6	25.7	2.5
	B.E. (eV)	285.0	not determined	531.8	74.2	134.0

* 0.2% detection limit

The presence of high C signal in the spectra is most likely from hydrocarbon contamination from the laboratory atmosphere, and not due to incorporation of triethylamine, since no N signal was observed in the boiled-only hydroxide. There was no observable difference in P 2p binding energies between the hydroxides after dipping in a solution of a P(V) compound {H_3PO_4}, and a P(III) compound {H_3PO_3}, and also no observable difference in O 1s peak shapes. This result is identical to that for porous anodic oxides (Table 4.3) and for simple adsorption onto aluminum oxide (Table 4.5). The reaction products of aluminum oxide/hydroxide with the two phosphorus oxo acids were not distinguishable using XPS binding energies.

2. Adhesive Bonding

The wedge test data for joints with aluminum hydroxide surface films (30 s boil, pH 9), and for

films functionalized with H_3PO_3 and H_3PO_4 (30 s dip, 5% wt. acid), are presented in Figure 5.4.

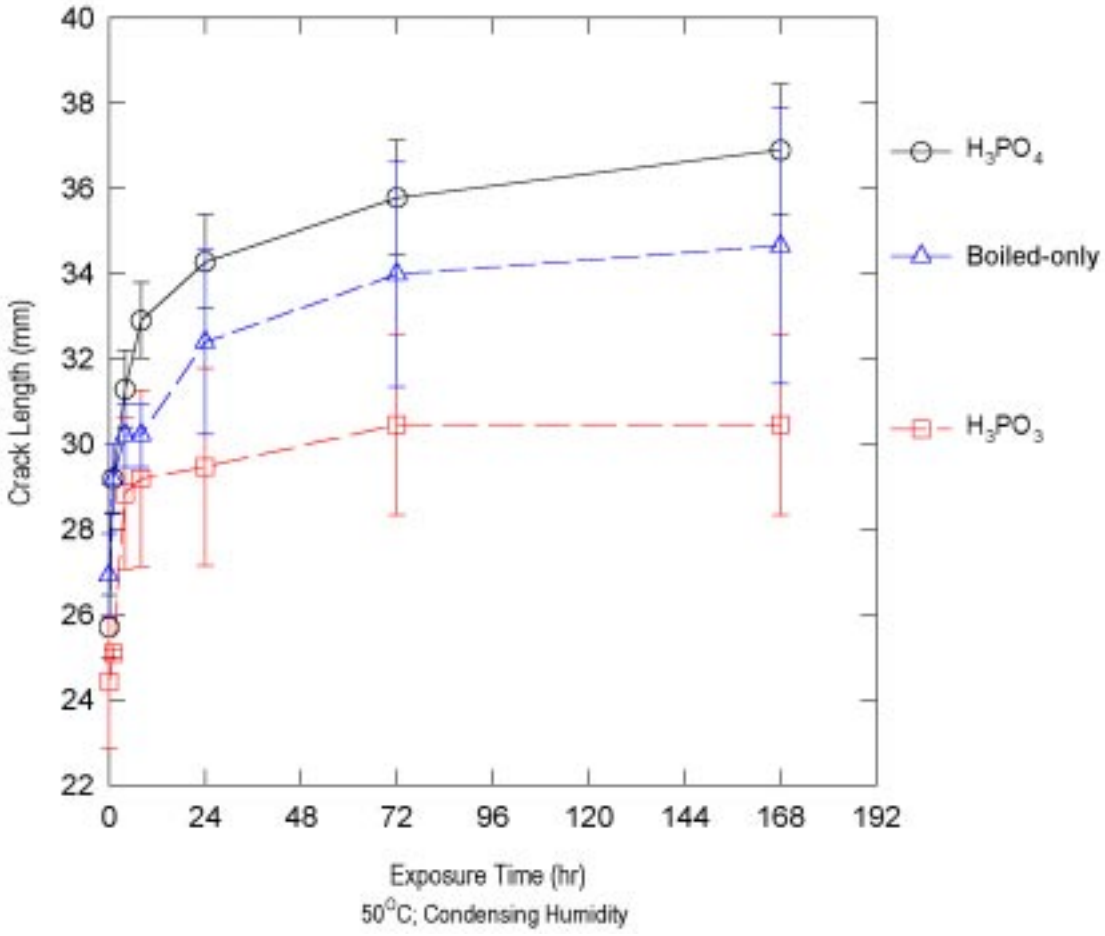

Figure 5.4. Wedge Test Results for 30 s Gelatinous Boehmite and Acid Modified-Gelatinous Boehmite Films on Alloy 2024-T3 Bonded with AF163 Epoxy

Bonds with H_3PO_3-functionalized adherends were significantly more durable than those with H_3PO_4-functionalized adherends. The error bars represent one standard deviation. Upon comparison with the boiled-only crack growth data (Figure 5.4), there appears to be a trend that the phosphoric acid treatment resulted in deteriorated durability, and that the phosphorous acid treatment improved the durability. However, since the error bars of each acid treated sample overlap those of the boiled-only sample, it cannot be stated with a high degree of confidence that

the phosphoric acid dip had any effect on durability beyond that which was imparted by the aluminum hydroxide surface film. The error bars for bonded specimens with the phosphoric acid-modified adherends nonetheless are separated from those with phosphorous acid-modified adherends. The failure loci for *all* of the wedge test specimens with gelatinous boehmite surface films visually appeared to partially occur at the oxide/adhesive interface and partially in the adhesive.

Since the surface topography of the adherends with gelatinous boehmite films is similar, it is speculated, as with the porous anodic oxides, that varying density and type of chemical interactions with the adhesive result in different wedge test failure rates. In order to empirically test this assumption, aluminum adherends with gelatinous boehmite surface films were functionalized with organic groups that have the potential of forming chemical bonds with components of the adhesive, and with groups that are chemically unreactive.

C. Organophosphonic Acids

1. Determination of Surface Film Structure and Composition

Prior to presenting the adhesive bonding data, bonding mechanisms of the organophosphonic acids with aluminum oxide/hydroxide were verified. The role of aluminum surface hydroxylation in the adsorption of organophosphonic acid was determined by examining the surface of aluminum, after each step in processing, using MRAIRS. Phenylphosphonic acid (ϕPA) was reacted with an aluminum hydroxide surface film. The molecular structure of phenylphosphonic acid is presented in Figure 5.5.

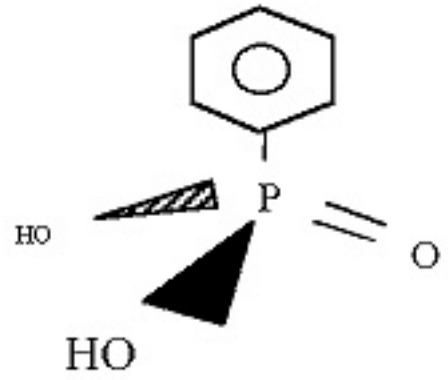

Figure 5.5. Molecular Structure of Phenylphosphonic Acid - ϕPA

The region of the RAIRS spectra (4000 cm^{-1} to 3000 cm^{-1}) containing the hydroxyl stretching band for the metal after each rinse step is provided in Figure 5.6.

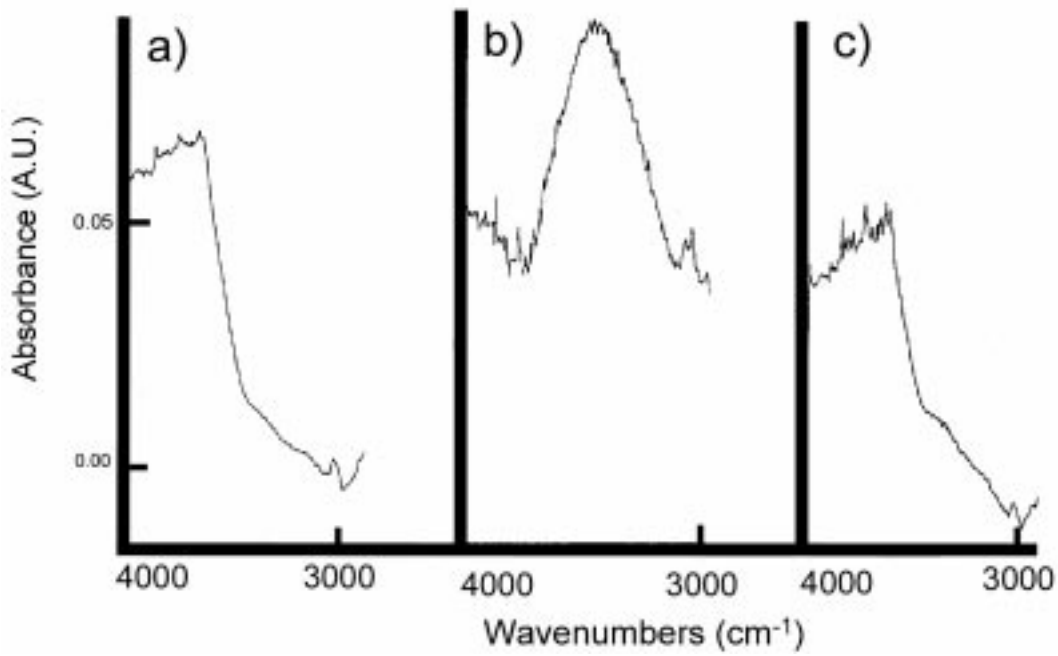

Figure 5.6. Reflection Absorption Infrared Spectra of Hydroxyl Stretching Region: a) Etched, b) Etched and Boiled, and c) Etched, Boiled, and Dipped in ϕPA

Figure 5.6.a shows the hydroxyl band region for the metal after caustic etching. There is little indication of a substantial surface hydroxylation relative to the aluminum mirror. However, after the boiling step (Figure 5.6.b) there is a large and broad hydroxyl band indicating an aluminum hydroxide surface film. When the hydroxylated surface is dipped in ϕPA, the hydroxyl band is no longer present in the RAIRS spectrum (Figure 5.6.c). This is a clear indication that the ϕPA reacted with the hydroxyl groups on the aluminum surface. Due to a low signal to noise ratio for the ϕPA RAIRS spectrum, other regions of the spectrum were not useful for determining the specific reaction of ϕPA with the hydroxylated surface. No features for the phenyl- group or P-O bonds were observed in the spectrum for ϕPA adsorbed on the aluminum hydroxide film.[264]

The organophosphonic acid most studied in this investigation was vinylphosphonic acid - VPA (Figure 4.15). A FT-IR transmission spectrum of ~15 mg of neat VPA between KBr plates is found in Figure 5.7. A RAIRS experiment, similar to the one for ϕPA, was carried out with VPA. The RAIRS spectrum in Figure 5.8 is a difference spectrum of 2024-T3 aluminum boiled for 30 s in a pH 9 aqueous triethylamine solution and dipped in 18% (w/w) VPA solution for 30 s, referenced to a spectrum of a boiled-only sample. Bands for molecular water due to an inadequate nitrogen purge are noted above 3500 cm^{-1}, and around 1500 cm^{-1}. Also, due to the inadequate purge, a negative doublet band for CO_2 was found around 2350 cm^{-1}, and electronically removed from this spectrum. The valuable feature in this spectrum is the broad negative band at 3300 cm^{-1}, which indicates that the VPA molecules react with surface hydroxyl groups, as did the ϕPA molecules (Figure 5.6). The practically featureless spectrum of Figure 5.8 demonstrates the RAIRS is not an adequate technique for studying the reaction of most organophosphonic acids with oxidized aluminum. A listing of band assignments for neat VPA

---

264. The presence of P on the ϕPA dipped sample was not detected by FT-IR, and no other surface analysis technique was used on this sample. It is still argued that the disappearance of the bands due to hydroxyl groups was from reaction of these groups with ϕPA, and that the surface reaction product was not detected by FT-IR. As will be shown, FT-IR was not highly useful for detecting the vibrations of the small organophosphonic acid molecules adsorbed onto aluminum oxide/hydroxide surfaces.

and for VPA adsorbed on high purity oxidized aluminum (IETS experiment) is found in Table 5.2.

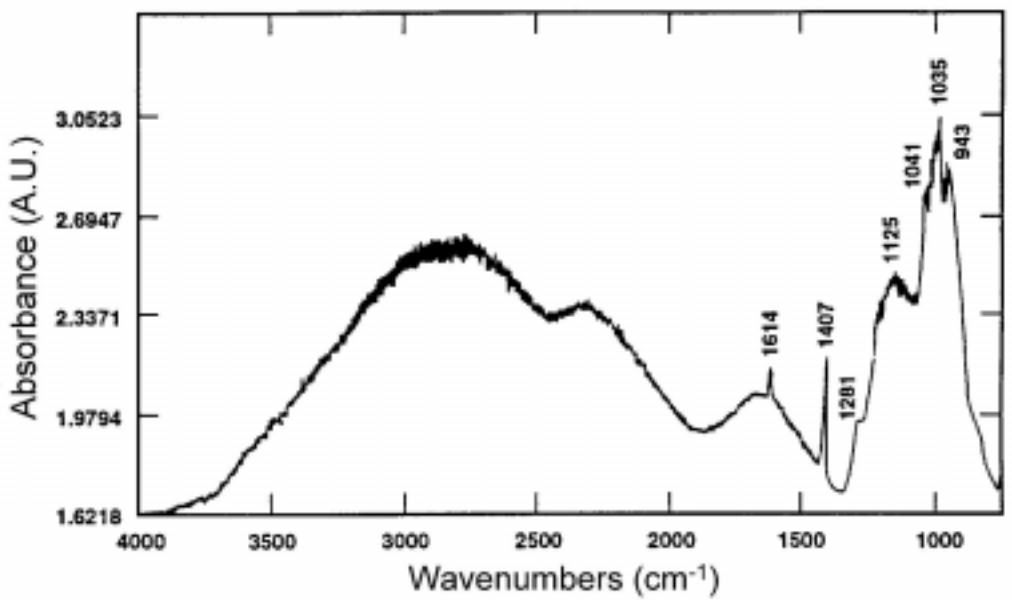

Figure 5.7. FT-IR Transmission Spectrum of ~15 mg VPA between KBr

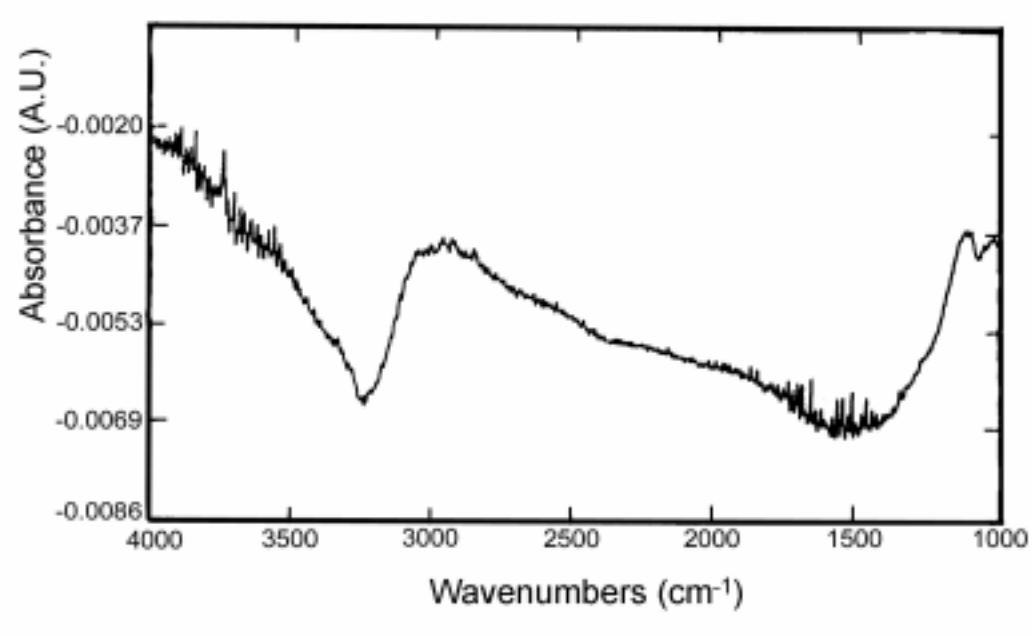

Figure 5.8. Reflection-Absorption Infrared Spectrum (RAIRS) of 2024-T3 Aluminum Alloy Boiled for 30 s in pH 9 Aqueous Triethylamine then Dipped in 18% (w/w) Vinylphosphonic Acid Solution - Referenced to Boiled-Only Metal

Table 5.2. Assignment of Bands for VPA Vibrational Spectra

Neat VPA (IR) (Figure 5.7)		VPA on Al_2O_3 (IETS) (Figure 5.9)		
Band (cm^{-1})	Assignment	Band (cm^{-1})	Assignment	Reference
		573	$\delta(PO_3^{2-})$	265
		774	ν(P-C)	266
943	ν_s(O-P-O)			267
		976	$\omega(CH_2)$	268
1035	ν_a(O-P-O)			267
1041	ω_{trans}(CH)	1024	ω_{trans}(CH)	268
1125	ν(P=O);$\delta_a(CH_2)$			267;268
1281	δ(CH)	1266	δ(CH)	268
1407	$\delta_s(CH_2)$	1395	$\delta_s(CH_2)$	268
		1449	$\delta(CH_2)$ scissor	268
1614	ν(C=C)	1613	ν(C=C)	269
		2960	$\nu_s(CH_2)$	269
		3073	$\nu_{asym}(CH_2)$	269
		3610	ν(AlO-H)	258

For compounds containing -P(O)$(OH)_2$ groups, Thomas[267] reports that phosphoryl stretching is shifted downward from a range above 1200 cm^{-1}. Therefore, the broad band at 1125 cm^{-1}, in the spectrum of Figure 5.7, is assigned to P=O stretching. Thomas[267] also assigns five other characteristic bands to the -P(O)$(OH)_2$ group. The O-P-O symmetric stretching frequency is found near 943 cm^{-1}.[267] This is found at 943 cm^{-1} in the spectrum of neat VPA (Figure 5.7). An asymmetric O-P-O stretching frequency may also be found near 1020 cm^{-1}.[267] The band at

---

265. M. Tsuboi, *J. Am. Chem. Soc.*, ***79*** (1957) 1351.
266. M. K. Templeton and H. W. Weinberg, *J. Am. Chem. Soc.*, ***108*** (1985) 97.
267. L. C. Thomas, "*Interpretation of the Infrared Spectra of Organophosphorus Compounds*," Heyden & Son Ltd., New York (1974) Chapters 3-5, 15.
268. D. Lin-Vien, N. B. Colthup, W. G. Fately, and J. G. Graselli, "*Infrared and Raman Characteristic Frequencies of Organic Molecules*," Academic Press, Inc., San Diego, California (1991) pp. 73-80.

1035 cm^{-1} may arise from this vibration, or could have some contribution from a CH wagging vibration. A broad band near 2300 cm^{-1} may be a combination of POH bending and the asymmetric stretch of O-P-O.[267] The other two bands assigned to $-P(O)(OH)_2$ groups by Thomas[267] are not evident on the spectrum of neat VPA but for completeness are: near 1650 cm^{-1} (combination of phosphoryl bending and stretching), and near 2800 cm^{-1} (PO-H stretch). A striking feature of this spectrum is the absence of distinct C-H stretching mode bands above 3000 cm^{-1}, which were anticipated due to the vinyl- group. The band at 1614 cm^{-1} is assigned to C=C stretching.[269] It should be noted that the C=C stretching frequency for an isolated vinyl- group, such as that in ethene, is in the range of 1645-1640 cm^{-1}.[269] Attached electronegative groups, such as the $-P(O)(OH)_2$ group, withdraw electrons from the C double bond and lower C=C stretching vibration frequency.[269] Other vibrational bands in the spectrum of neat VPA include: trans CH out of plane bending (1041 cm^{-1}), CH in plane bend (1281 cm^{-1}), and CH_2 scissoring (1407 cm^{-1}).[268] A vinylic CH_2 may also contribute to the broad band at 1125 cm^{-1}, making the determination of the exact position of the P=O stretching frequency unattainable.

An important observation from the VPA and ϕPA RAIRS experiments is that RAIRS is not a useful technique for determining the precise mechanism of the bonding of VPA, and other organophosphonic acids to hydroxylated aluminum surfaces, but does demonstrate the consumption of surface hydroxyl groups in the formation of the surface reaction product. The sensitivity of RAIRS, as employed, is not sufficient to study the reaction of organophosphonic acids on aluminum.

In order to determine the molecular structure of organophosphonic acids reacted on hydroxylated aluminum surfaces, inelastic electron tunneling spectroscopy (IETS) was used. In this case it was not possible to study engineering alloys, with thick aluminum hydroxide surface films. This

---

269. G. Socrates, "*Infrared Characteristic Group Frequencies*," John Wiley & Sons, New York (1980) pp. 32-33.

is because electron tunneling will occur only when there is approximately a monolayer of adsorbate on a thin (~3 nm) surface oxide film; thicker surface films prevent electron tunneling. Therefore, IETS samples were prepared by evaporating high purity aluminum onto a glass slide, oxidizing in a glow discharge, hydroxylating by exposure to atmospheric moisture, then adsorbing VPA from a dilute solution in ethanol. The IETS spectrum of clean, oxidized aluminum is presented in Figure 5.9.a.

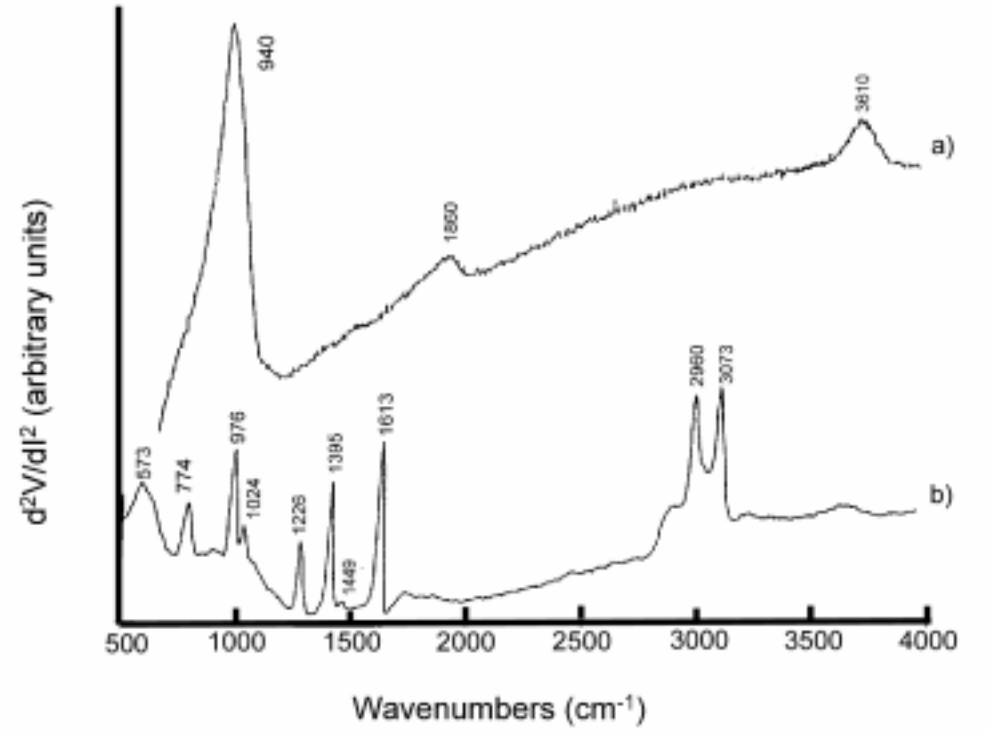

Figure 5.9. Inelastic Electron Tunneling Spectra of: a) Hydroxylated Oxide Film on 99.999% Al and b) Hydroxylated Oxide Film Reacted with VPA

Three bands are present: the Al-O-Al phonon mode at 940 cm^{-1},[258] a band at 1860 cm^{-1} that is attributed to valence vibrations of aluminum hydride that is formed during the IETS tunnel junction fabrication,[270] and the band at 3610 cm^{-1} attributed to stretching vibrations of surface

270. J. Igalson and J. G. Alder, *Phys. Rev. B, **28*** (1983) 4970.

O-H groups.[258] The presence of the hydroxyl groups on the surface indicates that the same reaction mechanism for adsorption is possible on the evaporated aluminum films as was observed for the engineering alloys previously studied using RAIRS; namely, the adsorption reaction involving consumption of surface hydroxyl groups.

The IETS spectrum of VPA reacted on a hydroxylated aluminum oxide surface film is presented in Figure 5.9.b. The band at 573 cm^{-1} is attributed to PO_3^{2-} group.[265] The IETS spectrum of VPA reacted on aluminum oxide contains a band attributed to the P-C stretching mode at 774 cm^{-1}.[266] While there are no strong selection rules for tunneling spectroscopy, there is an orientational preference, in that tunneling electrons interact more strongly with vibrations that involve oscillating dipoles that are parallel to the direction of the tunneling electrons (or perpendicular to the surface).[242] The relatively strong intensity of the P-C stretching band (774 cm^{-1}) suggests that this bond is oriented perpendicular to the surface. The IETS spectrum of VPA on oxidized aluminum also exhibits a C=C stretching vibration at 1613 cm^{-1}, and a band that is attributed to the asymmetric CH_2 at 3073 cm^{-1},[271] indicating that the vinyl- group does not participate in bonding to the aluminum oxide surface. As mentioned earlier, one would expect isolated vinyl- groups to exhibit the C=C stretching mode around 1640 cm^{-1}.[269] The value of the C=C stretch is shifted lower for both neat VPA (1614 cm^{-1}) and for VPA reacted on the evaporated aluminum surface (1613 cm^{-1}). The electron withdrawing effect by the electronegative PO_3^{2-} group attached to the vinyl-group is maintained after the reaction of VPA with the aluminum surface. It is noted that this electron withdrawing effect is necessary for the proposed nucleophilic addition of the surface VPA vinyl group with amines derived from the adhesive curing agent (Michael Addition, Figure 4.16). Distortion of the electron cloud towards the electronegative $(Al\text{-}O)_3$-P groups would lower the C=C stretching frequency, and possibly have an effect on the C-H stretching modes, as well. A band at 2960 cm^{-1} is assigned to the symmetric CH_2 stretching mode, which falls about 20 cm^{-1} below the anticipated range,[271]

---

271. N. B. Colthup, L. H. Daly, and S. E. Wilberly, "*Introduction to Infrared and Raman Spectroscopy, 2nd ed.,*" Academic Press, New York (1975) pp. 220, 246, 257.

whereas the high wavenumber shoulder of this band may be due to the anticipated vinylic C-H stretch.[271] The remainder of the bands in the IETS spectrum arise from various vibrations of the atoms in the vinyl- group and from the aluminum oxide substrate and are assigned in Table 5.2. There is a small absorbance in the hydroxyl stretch region (3600 cm^{-1}) of the IETS spectrum of surface reacted VPA, suggesting that under the experimental conditions, VPA is reacted in submonolayer coverage with some unreacted hydroxyl groups remaining on the surface. The observation of CH stretch and deformation bands in the IETS spectrum, and not in previous infrared spectra, show that IETS provides more structural information about the organophosphonic acids reacted on aluminum oxide surfaces than does infrared spectroscopy.

The presence of a band assigned to the PO_3^{2-} deformation mode (573 cm^{-1}) and the absence of P=O stretching band (1125 cm^{-1}) in the IETS spectrum of VPA reacted with hydroxylated aluminum oxide (Figure 5.9) indicate that VPA reacts with the oxide in a tridentate fashion, depicted here as $(Al\text{-}O)_3$-P. It was previously demonstrated by IETS analysis that the reaction of inorganic phosphorous acid and various different organophosphonic acids with oxidized aluminum surfaces results in the formation of resonance stabilized symmetric PO_3^{2-} groups.[258] The other organophosphonic acids previously studied were: methylphosphonic acid, hydroxymethylphosphonic acid, and aminomethylphosphonic acid.[258] The proposed adsorption reaction is an acid-base (condensation) reaction in which deprotonated hydroxylic oxygen atoms on the organophosphonates form a resonance stabilized structure with the phosphoryl oxygen.[258] It was also previously shown that the lattice spacing of alumina can permit bridging of the resonance stabilized tridentate anion to three Al^+ sites.[266] The proposed bonding mechanism of organophosphonic acid with oxidized aluminum surfaces is presented in Figure 5.10.

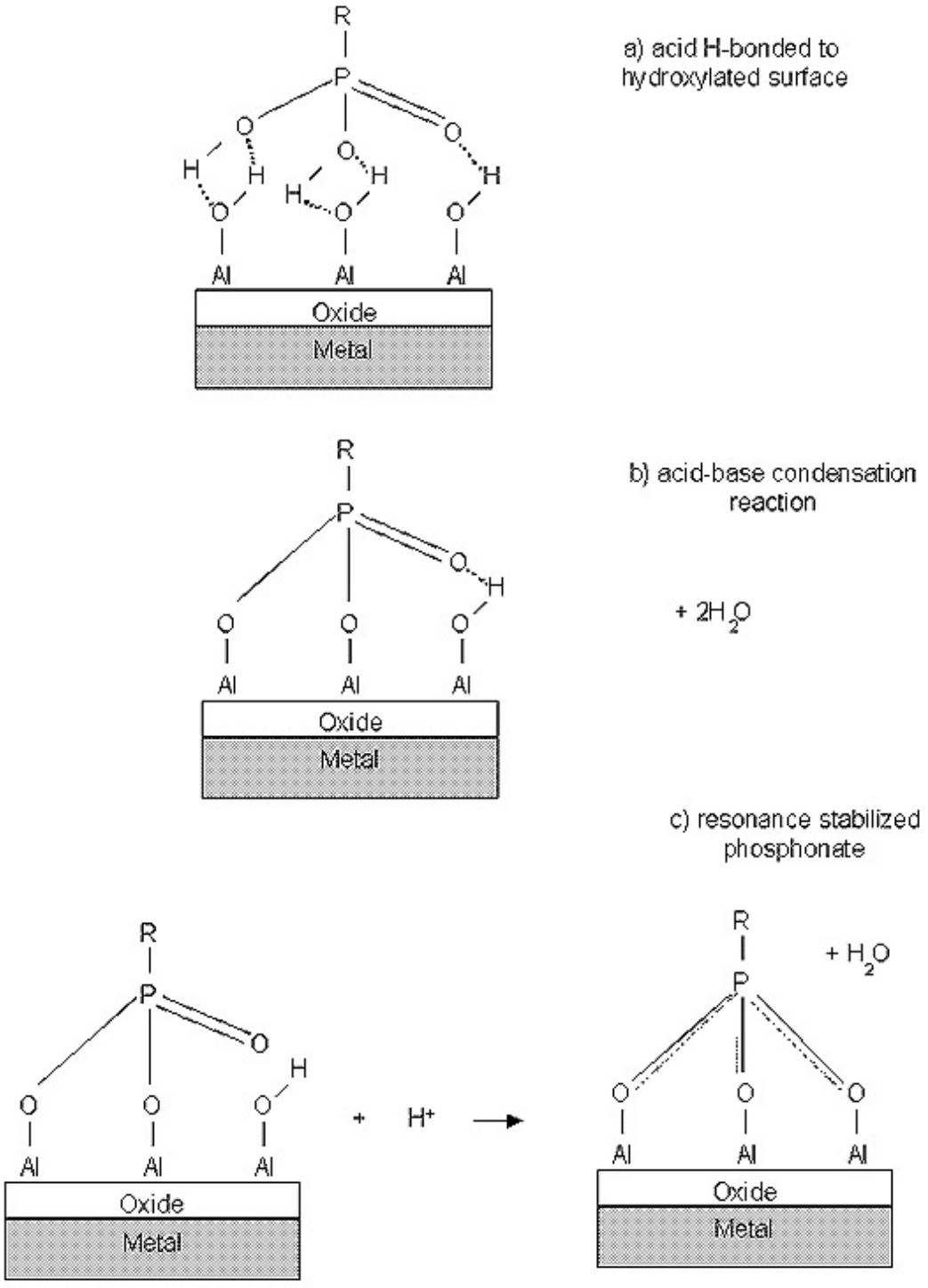

Figure 5.10. Adsorption of Organophosphonic Acid onto Hydroxylated Aluminum Oxide

Based upon: 1) the cited literature results;[258,266] 2) the absence of P=O stretch band in the IETS spectrum of surface reacted VPA (Figure 5.9);[258] and 3) the presence, in the same spectrum, of the deformation mode of the PO_3^{2-} band at 573 cm^{-1}, it is concluded that the VPA molecule reacts with the hydroxylated aluminum oxide/hydroxide surface by an acid-base (condensation) reaction (Figure 5.10.b), and the formation of a resonance stabilized symmetric PO_3^{2-} group (Figure 5.10.c). A schematic representation of the proposed structure of a single layer of VPA on a thin hydroxylated surface is provided in Figure 5.11.

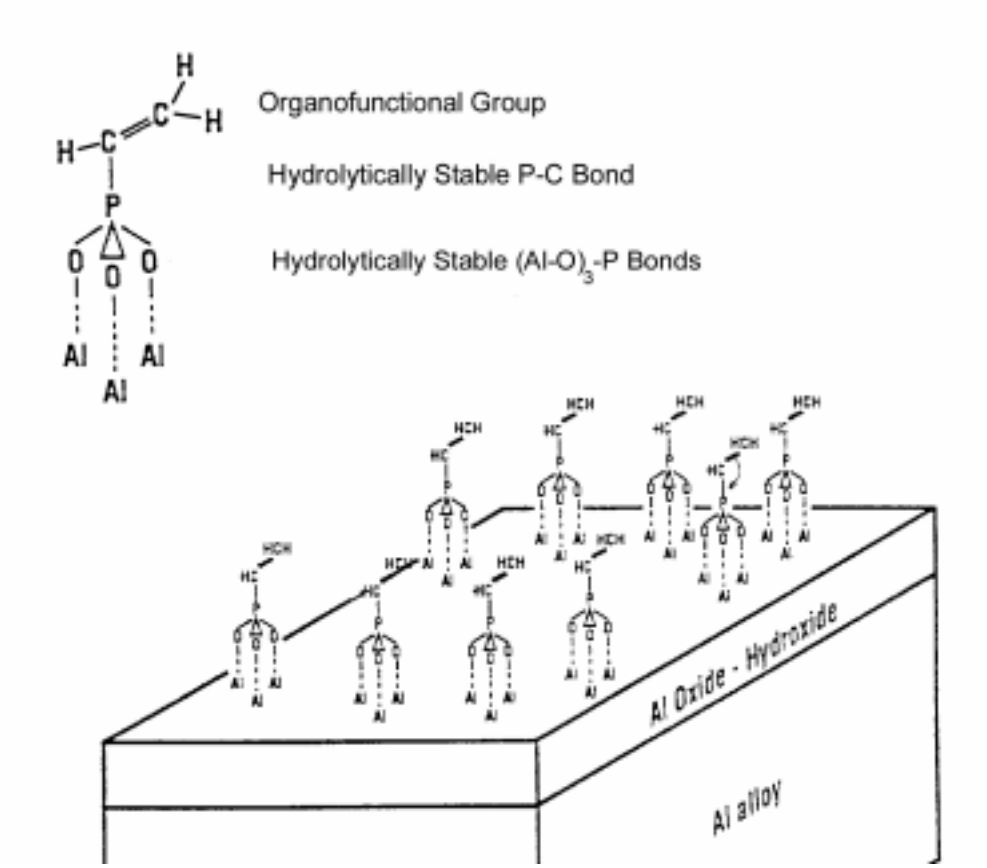

Figure 5.11. Schematic Representation of VPA Functionalized Aluminum Oxide/Hydroxide Surface

In an adhesive joint, chemically anchoring the vinyl- group to the aluminum surface (through the aluminum phosphonate bonds) provides the potential for a specific chemical reaction of the surface vinyl- groups with functional groups of an overlaid adhesive or primer.

The distribution of VPA throughout the thickness of a VPA functionalized hydroxide surface film was measured by dynamic secondary ion mass spectrometry (SIMS). Figure 5.12 shows the results of positive ion SIMS for a 2024-T3 alloy boiled for 30 s in pH 9 aqueous triethylamine, rinsed, and then dipped for 30 s in 18% (w/w) VPA. The AlO^+ and the PO^+ peaks were selected from the positive SIMS spectrum, and the intensity of these peaks is plotted as a function of sputtering depth in Figure 5.12. The SIMS profile of boiled 2024 that was dipped in 9% (w/w) VPA (not shown) was equivalent to that of 18% VPA.

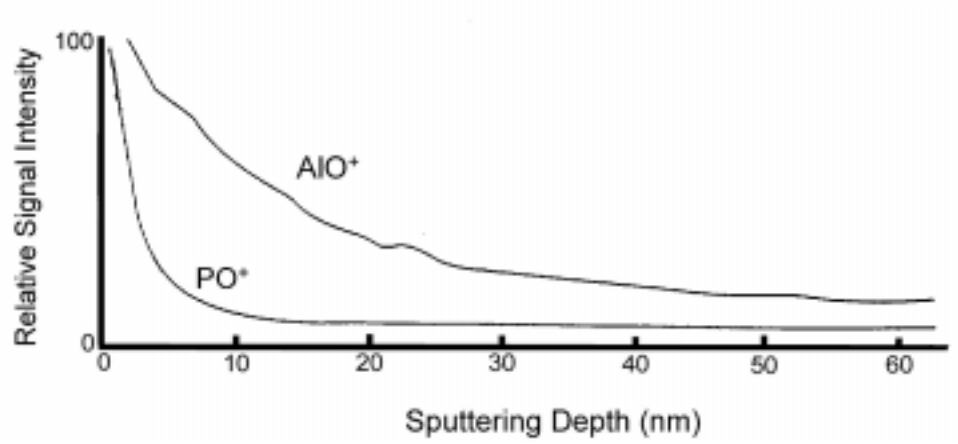

Figure 5.12. Secondary Ion Mass Depth Profile Showing Intensity of AlO^+ and PO^+ Peaks for 2024-T3 Alloy, 30 s Boil, 30 s Dip in 18% (w/w) VPA Solution

The hydroxide was sputtered to a depth of approximately 65 nm. The depths are approximate since barrier anodic oxides were used to calibrate the sputtering rate, and the sputtering rates of aluminum oxide and aluminum hydroxide are not necessarily the same. It was previously established using AES depth profiling that for this alloy, these boiling conditions produced a hydroxide film with a thickness of approximately 70-80 nm. The AlO^+ signal leveled out at a

low value at the end of SIMS sputtering indicating that the oxide/metal interface was reached at around 60 nm. The small differences in the measured thickness between AES and SIMS could be accounted for by the somewhat arbitrary definition of when the interface is reached for both techniques, and should not be considered significant. It is observed in Figure 5.12 that the PO^+ fragment exhibits the highest intensity in the outer 10 nm of the film and drops off to low levels upon continued sputtering. This suggests that VPA is predominantly on the outer surfaces of the hydroxide surface film, and does not become incorporated into the bulk of the hydroxide film during dipping.

2. Adhesive Bonding

Lap shear breaking strengths were determined for joints bonded with AF163-2K epoxy adhesive, having hydroxide films on 2024-T3 alloy, and those with hydroxide films functionalized by dipping in VPA solution. These were compared to the breaking strengths of joints with phosphoric acid anodized (PAA) adherends prepared according to the Boeing process.[249] The results are presented in Table 5.3.

Table 5.3. Average Lap Shear Breaking Strengths of Joints with Hydroxide Films and VPA Functionalized Hydroxide Films on 2024-T3 Alloy and Compared with Joints with Phosphoric Acid Anodized Adherends (AF163-2K Epoxy Adhesive)

Treatment	Average Strength (MPa)	Standard Deviation (MPa)
30 s, pH 9 Boiled-Only	43.0	3.3
30 s, pH 9 Boil 30 s, 18% (w/w) VPA Dip	41.7	0.8
PAA	42.2	0.7

The data in Table 5.3 indicate that joints with the hydrothermally formed films exhibit similar dry lap shear strength to those with the PAA films, and that VPA functionalization does not provide an advantage in initial strengths when compared with boiled-only substrates. All failures occurred in the adhesive layer (cohesive failure).

Wedge tests were conducted to determine the effect of organophosphonic functionalized gelatinous boehmite films on adhesive bond durability. The wedge test results for specimens prepared from aluminum alloy 2024-T3 boiled for 30 s in a pH 9 aqueous solution of triethylamine, and a boiled film dipped in 18% (w/w) VPA are shown in Figure 5.13.

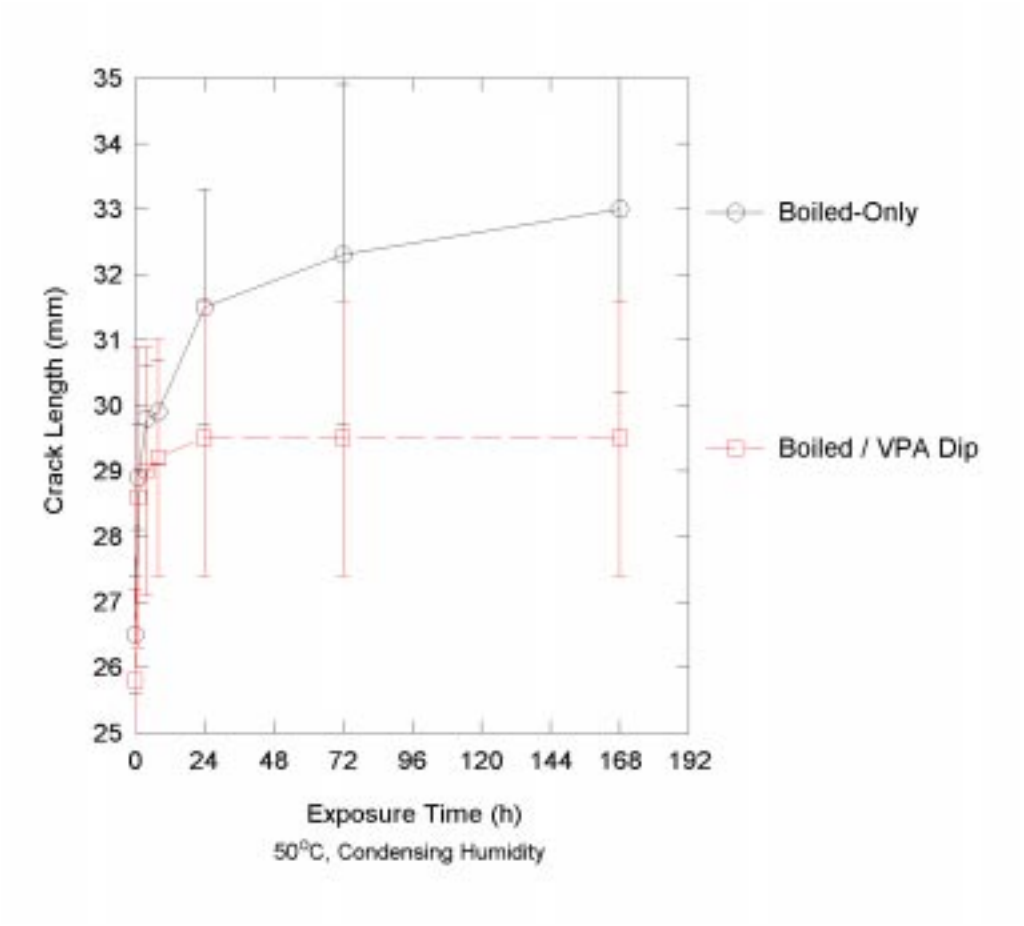

Figure 5.13. Effect of VPA Functionalization on Hydrothermal Stability of Joints with Gelatinous Boehmite Films, 2024-T3, AF163 Epoxy Adhesive

While the error bars (representing 10 joints each and one standard deviation) overlap, there is a trend indicating improvement of durability for the VPA functionalized film. At the end of the exposure period, the adhesive bonds with VPA treated adherends had a lower crack length, and crack growth had arrested after 24 h of exposure. The boiled only specimens, however, did not exhibit arrested crack growth, and presumably the crack would continue for some distance if humidity exposure were continued. The wedge specimens with boiled-only and VPA treated adherends were visually judged to have failed in a mixed mode fashion, as was the case for the inorganic phosphorus oxo acid treated hydrothermal films. The precise nature of this mixed mode failure will be presented shortly.

To gauge the performance of the joints with VPA treated hydroxide adherends, the wedge test results were compared with those obtained from wedge specimens with PAA[249] adherends. These results are found in Figure 5.14. These data indicate that there is no significant difference in the wedge test crack lengths for bonds formed with adherends treated by the industry standard PAA process[249] and with those formed with adherends containing VPA modified hydroxide surface films. A difference in failure mode was noticed, in that the PAA failed surfaces were completely thin cohesive, whereas the VPA modified hydroxide failed surfaces were mixed mode failure.

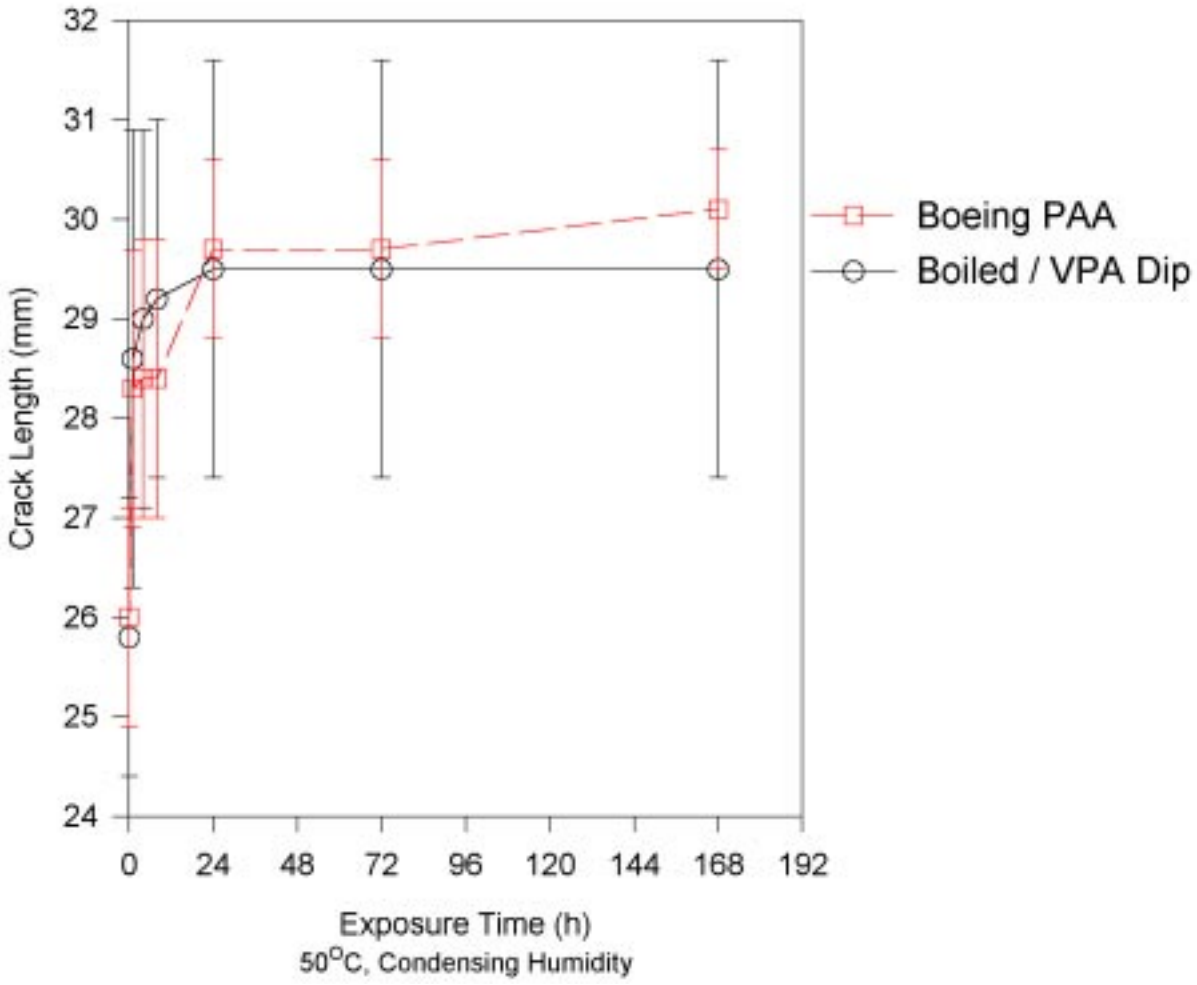

Figure 5.14. Comparison of Standard Phosphoric Acid Anodizing with VPA Functionalized Gelatinous Boehmite Film, 2024-T3, AF163 Epoxy Adhesive

Scanning electron microscopy (Figure 5.15) of failure surfaces form joints with gelatinous boehmite films showed that bayerite particles, $Al(OH)_3$, were present on the adhesive, corresponding to areas on the opposing adherend that appeared to have failed interfacially. Since bayerite could have only grown by the reaction of water with the gelatinous aluminum oxide hydroxide of the original surface film, the fracture that was visually judged to be interfacial was actually crack propagation in the surface oxide hydroxide layer. Therefore, the mixed mode failures had areas that failed in the interphase of the adhesive (thin cohesive) and areas that failed

in the hydroxide layer of one or the other adherend. The bayerite particles have dimensions of micrometers, whereas the original hydroxide layer had a thickness on the order of 100 nm. Reaction of water with gelatinous film that was adhered to the adhesive during cracking is most likely the origin of the bayerite particles.

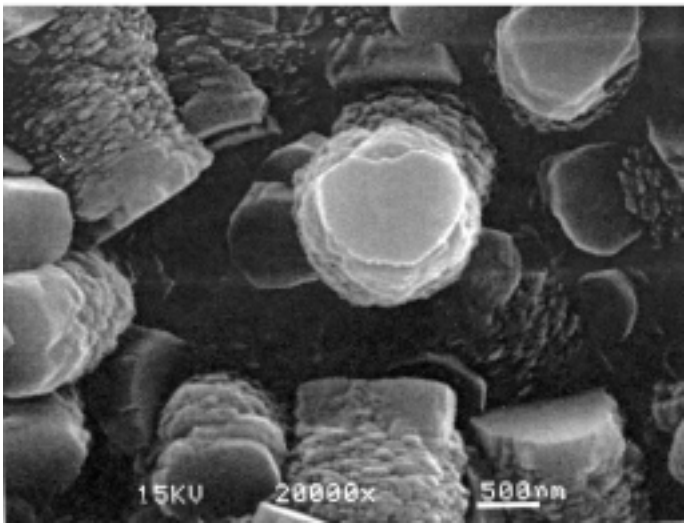

Figure 5.15. Bayerite, $Al(OH)_3$, Crystals on Adhesive Side of Cracked Wedge Test Specimen, 2024-T3, AF163 Epoxy Adhesive

In most cases, for surface pretreatments that provide good "dry" strength, the failure mode upon insertion of the wedge is cohesive in the adhesive. After exposure to moisture, the locus of failure shifts towards an adhesive/oxide interface. It has been the observation in these studies that if the chemical composition of the interphase is stable to hydrolysis, then the ultimate failure mode will be thin cohesive in the adhesive. When the interfacial bonds are not resistant to moisture, the resulting failure mode is observed closer to the interface and is classified as apparent interfacial failure. It is *apparent* interfacial failure since the failure surfaces were only characterized visually, and since other researchers have shown that in many cases a microscopic layer of adhesive remains on the metal failure side for joints that macroscopically appear to fail interfacially.[16,206-208]

In the case of the hydrothermally grown hydroxide films, however, the hydroxide film is not as strong as the interfacial bond in some areas, thus giving rise to mixed mode failure that occurs in the hydroxide layer in some areas and thin cohesive in the adhesive in other areas. While not documented here, it was observed during the course of this work that thick hydroxide films fail entirely in the hydroxide layer, in both lap shear and wedge tests. Therefore, to use these films in a commercial joining operation, one would need to ensure that the acid functionalized hydroxide film is thin (<100 nm).

In wedge testing, once crack growth has arrested, the residual strength of the bond and the stresses experienced at the crack tip are balanced. Therefore, unless irreversible changes in the substrate or adhesive occur, such as hydroxylation of the oxide in front of the crack tip, or hydrolysis of bonds in the adhesive, the locus of failure or crack length will not change with continued exposure. Unarrested crack growth was observed for joints with boiled-only adherends (see Figure 5.13), whereas for the duration of exposures used for wedge testing, crack growth arrested in bonds that had adherends with the phosphorus oxo acid functionalized hydroxide films. The crack growth data suggest that proper acid functionalization of the surface, and the subsequent chemical interaction of functional groups on the adherend with functional groups in the adhesive results in interfacial bonds that have a higher degree of hydrolytic stability than those formed on boiled-only adherends.

An advantage of functionalizing aluminum oxide hydroxide surfaces with organophosphonic acids is that it is possible to change the organic functional group on the surface, without changing the surface topography. This provides an effective tool for distinguishing the effects of chemistry and topography on bond durability. The vinyl- group on the VPA modified surface film has potential for chemically reacting with components of the adhesive, as would other

organophosphonic acids such as aminophosphonic acids and phosphonocarboxylic acids.[272] However, by reacting the gelatinous boehmite surface film with an organophosphonic acid that does not contain a reactive organic functional group, such as ethylphosphonic acid (EPA), the effect of chemical bond formation (or lack thereof) between the adherend and the adhesive could be evaluated. The EPA coated surface does not have reactive functional groups for interaction with the adhesive (Figure 5.16). Only dispersion forces (secondary bonding) are available for adhesion to EPA treated adherends. If the hypothesis that hydrolytically stable chemical (primary) bonds between the adhesive and adherend are necessary for durable adhesion, epoxy-bonded joints with EPA treated adherends should not be durable.

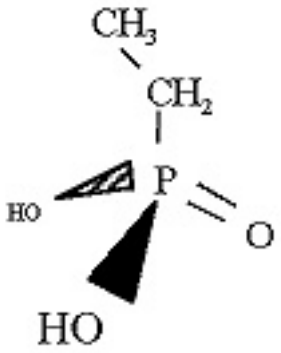

Figure 5.16. Molecular Structure of Ethylphosphonic Acid

An FT-IR transmission spectrum of EPA in a KBr pellet is presented in Figure 5.17. An IETS spectrum of EPA adsorbed onto an aluminum surface is presented in Figure 5.18.

---

272. Most of these other bifunctional organophosphonic acids, however, are Zwitter ions, and because of this the nature the reactions of these Zwitter ions with the aluminum oxide surface are less defined and more complicated to control. Thus, this dissertation concentrated on VPA functionalized films.

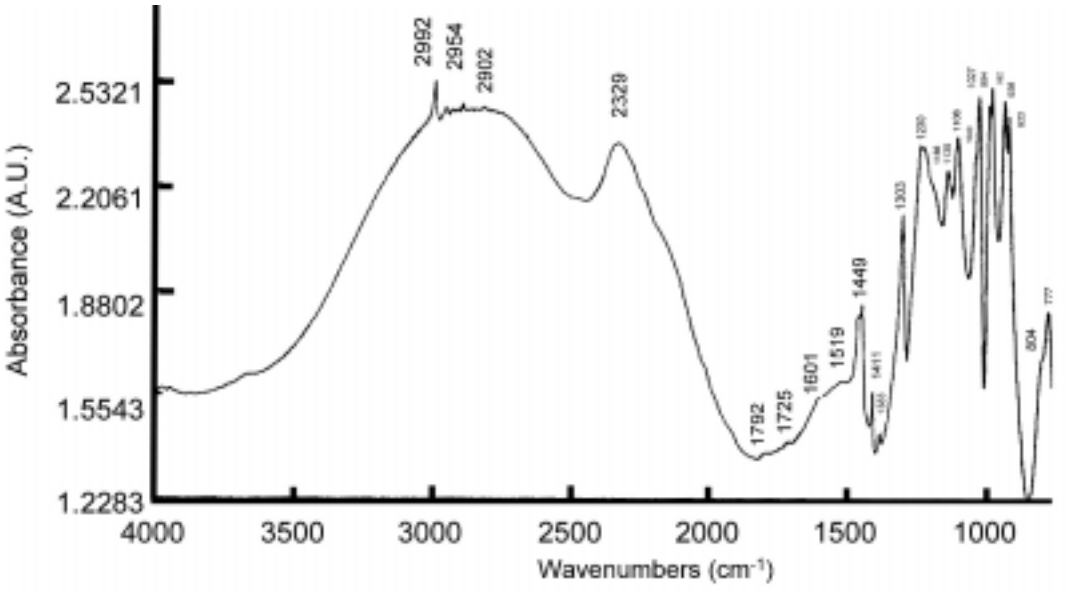

Figure 5.17. Fourier Transform-Infrared Transmission Spectrum of Neat Ethylphosphonic Acid in a KBr Pellet

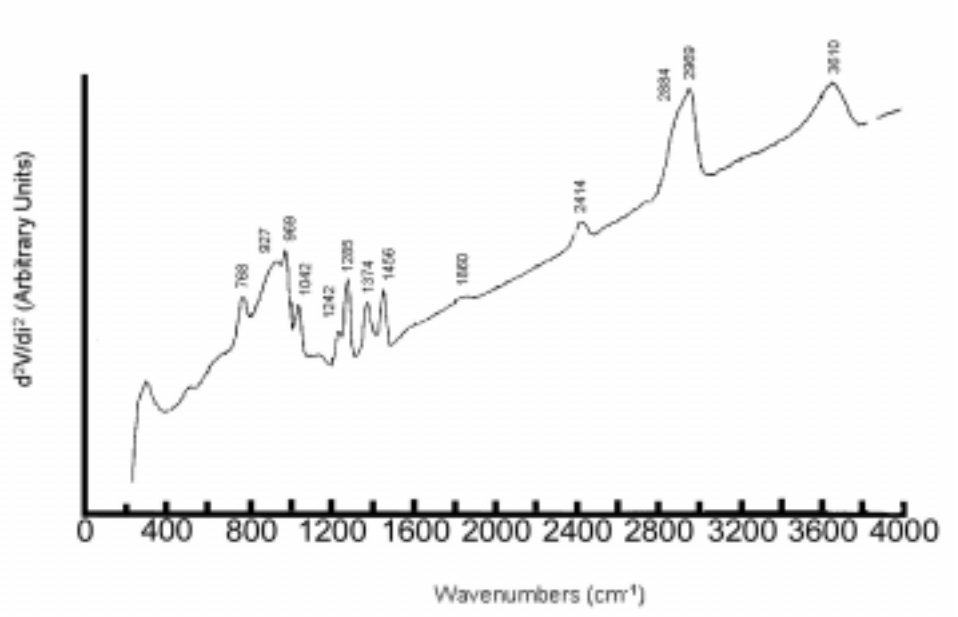

Figure 5.18. Inelastic Electron Tunneling Spectrum of Ethylphosphonic Acid (EPA) Adsorbed onto Oxidized 99.999% Aluminum

As expected, the EPA spectra show the absence of any band in the 1605-1650 cm^{-1} region that was attributed the C=C stretching frequency for the VPA spectra. Aliphatic C-H stretches are observed from 2884-2969 cm^{-1} on both EPA spectra, although the bands are unresolved on the IETS spectrum. These are further identified in Table 5.4. Other bands in the EPA spectrum are also identified in Table 5.4. Bands from impurities are found around 1040 cm^{-1} in both the spectra of neat and adsorbed EPA, along with a band in the IETS spectrum at 2414 cm^{-1}. These are assigned to P-H deformation and P-H stretching modes.[258] This is obviously from a contaminant, most likely phosphorous acid in the EPA material. Since the purity of the EPA was cited as 98% (w/w) by the vendor, one would not expect to see bands from impurities, since the surfaces were treated with dilute solutions (0.1 g/L). However, it was previously shown[258] that the P-H vibrational modes resulted in intense bands in the IETS spectrum of phosphorous acid reacted with oxidized aluminum. Therefore, the anomalous bands at 1042 cm^{-1} and 2414 cm^{-1} in the IETS spectrum of adsorbed EPA are assigned to the presence of a small amount of impurity, most likely phosphorous acid, in the EPA reagent.

Table 5.4. Vibrational Band Assignments for Neat Ethylphosphonic Acid (EPA) and EPA Adsorbed onto Oxidized 99.999% Aluminum

Neat EPA (FT-IR cm^{-1})	Adsorbed EPA (IETS cm^{-1})	Band Assignment
777	768	ν(P-C)[266]
923	927	? and ν(Al-O) [258]
936		δ_s(HO-P-OH) [267]
	969	$\omega(CH_2)$[268]
982		ν(P-OH) [267]
1027		ν_a(HO-P-OH) [267]
1040	1042	δ(P-H) [258] (contaminant)
1106		?
1138		?
1230		ν(P=O)[273]
	1242	?
1303	1285	$\delta(CH_2)$ wag [268]
1383	1374	$\delta_s(CH_3)$ [269]
1411		$\delta_a(CH_3)$ [269]
1449	1456	$\delta(CH_2)$scissor[269]
1519-1601		δ(P-OH)[273]
	1860	ν(Al-H) [258]
2329		2x sumband ν(P-OH) [273]
	2414	ν(P-H) [258] (contaminant)
	2884	$\nu_s(CH_2)$ [269]
2902		$\nu_s(CH_3)$ [269]
2954		$\nu_a(CH_2)$ [269]
2992	2969	$\nu_a(CH_3)$ [269]
	3610	ν(OH) [269]

273. R. R. Shagidullin, A. V. Chernova, V. S. Vinogradova, and F. S. Mukhameiov, "*Atlas of IR Spectra of Organophosphorus Compounds (Interpreted Spectrograms),*" Kluwer Academic Publishers, Boston, MA (1990).

Wedge test results for EPA functionalized adherends, which were prepared analogously to the VPA functionalized adherends, are compared with VPA results and presented in Figure 5.19.

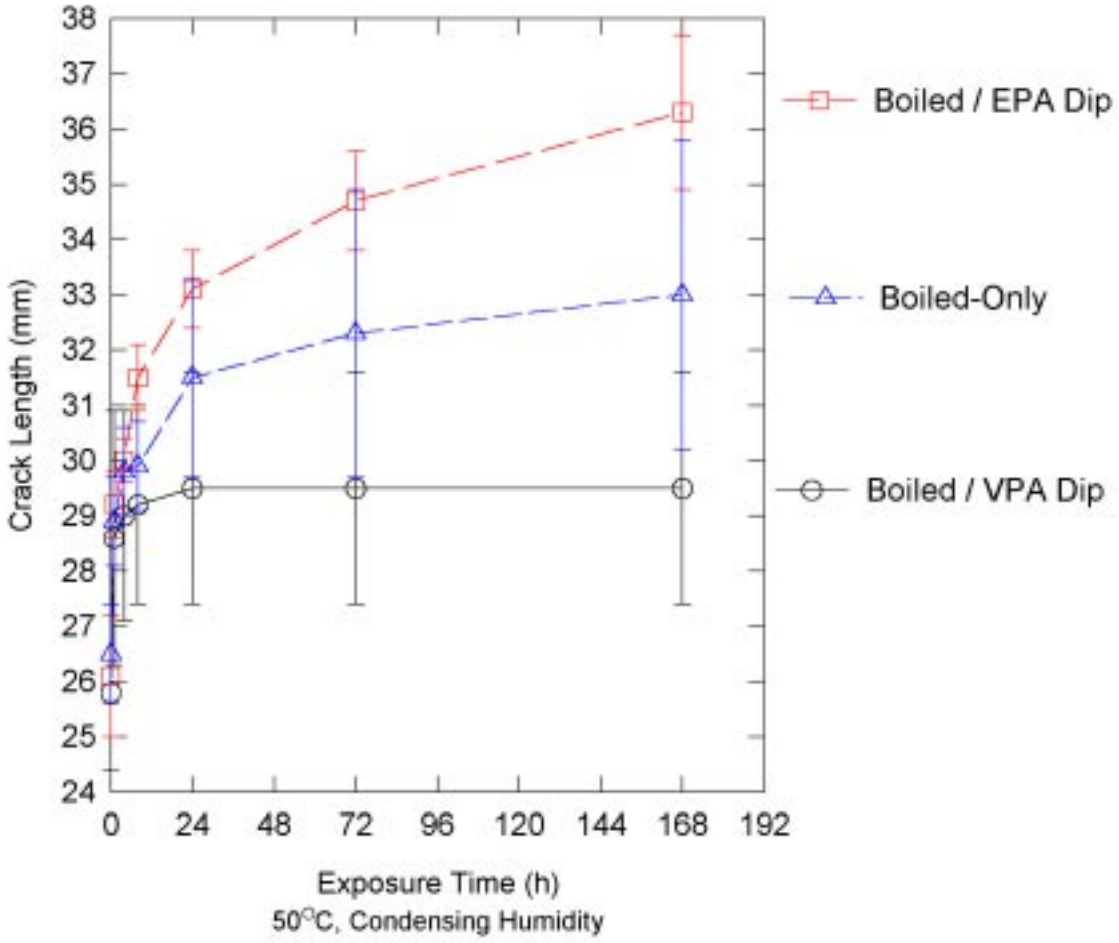

Figure 5.19. Effect of Possible Primary Interfacial Interactions (Surface VPA) versus Secondary van der Waals Dispersion Interactions (Surface EPA) in Adhesive Bond Durability, 2024-T3, AF163 Epoxy Adhesive

The data in Figure 5.19 empirically suggest the importance of interfacial chemistry for the production of durable structural adhesive joints. The average crack length of the specimens with EPA treated adherends was significantly larger than the crack lengths for specimens containing VPA treated adherends (approximately 36 mm and 29 mm, respectively). Also, the apparent failure mode for the EPA specimens was interfacial, whereas the failure mode for the VPA treated adherends was mixed mode, as described above.

In the following chapter, it was determined that by anodizing in aqueous organophosphonic electrolytes, it was possible to prepare almost microscopically smooth surface topographies. At the same time these flat surfaces were functionalized with a surface layer of the reaction product of the organophosphonic acid and the underlying aluminum oxide. By employing reactive and non-reactive organofunctional groups on the flat oxides, a clear distinction between the contributions of chemical and mechanical forces in adhesive bond durability was possible.

Chapter 6. Organophosphonic Acid Barrier Anodic Oxides

This chapter describes the anodization of aluminum alloys in aqueous solutions of organophosphonic acids. The solutions used in this investigation generally had a pH of around 1, or less. It is known that the solubility of aluminum oxide (hydroxide) is low between pH values of 4 and 9, and increases exponentially as the solution becomes more acidic or basic (Figure 5.1).[86] It is precisely due to the solvating ability of acidic solutions that porous anodic oxides are formed in certain inorganic acid solutions, such as phosphoric, sulfuric, oxalic, and chromic acids.[100] This is also the reason for the current finding that porous anodic oxides are formed in phosphorous acid solutions. When anodizing in solutions of organophosphonic acids of pH of 1 or less, one would expect either porous anodic oxide formation, similar to the oxides formed in the inorganic acids mentioned, or burning (localized areas of dielectric breakdown of the oxide), as occurs for example, in solutions of nitric or hydrochloric acid.[77] However, as will be demonstrated, anodic polarization of aluminum alloys in solutions of most organophosphonic acids, resulted in a duplex barrier layer film consisting of a dense, non-porous, barrier aluminum oxide adjacent to the metal, with an outer layer consisting of the reaction product of the organophosphonic acid electrolyte and the anodic barrier aluminum oxide. Evidence for this film structure follows in the next section. A plausible explanation for anodic barrier oxide formation in highly acidic solutions will also be given.

The unexpected result of a functionalized, non-porous, barrier layer film formed in acidic electrolytes allowed for a systematic investigation of the role of chemical bond formation between the substrate and the adhesive in determining bond durability, while minimizing any effect on durability that could be attributed to mechanical interlocking. It was possible to vary the organophosphonic acid functionality on the surface, while not significantly roughening the surface. Using the wedge test, the effect of interfacial chemistry on adhesive joint durability was evaluated.

A. Barrier Anodic Oxides formed in Aqueous Organophosphonic Acid Solutions

Evidence for the formation of a duplex barrier layer during anodization in VPA solutions follows. First however, it is noted that due to the difficulty in forming barrier oxides on high Cu^0 alloyed aluminum,[77] such as 2024 alloy, a less alloyed aluminum, 6061-T6 (containing Mg_2Si as the major alloying constituent - Appendix 1) was used in this portion of the investigation. The difficulty in forming a barrier anodic oxide on 2024-T3 alloy is a result of high electronic leakage current during anodization and is further elaborated upon later in this section.

The scanning electron micrographs (SEM) of 6061-T6 surfaces that were etched in HF/HNO_3 solution, then anodized at 40 V in 18% (w/w) VPA solution (Figure 6.1) show no evidence of porosity in the vinylphosphonic acid anodized (VPAA) film, but do show the characteristics of acid etched surfaces: etch pits and preferential etching at grain boundaries.[90]

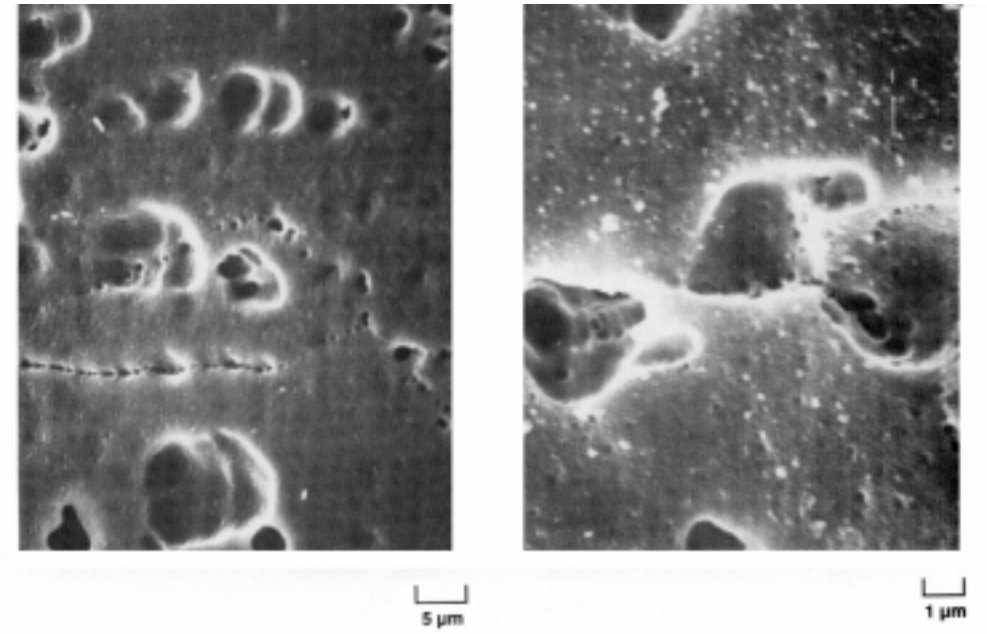

Figure 6.1. Scanning Electron Micrographs of Vinylphosphonic Acid Anodized 6061-T6, 18% (w/w) VPA, 40 V, 30s, 23°C

When the detached film is examined at higher magnification by TEM (Figure 6.2), the anodic

oxide formed in VPA solutions is conclusively determined to be microscopically non-porous.

Figure 6.2. Transmission Electron Micrograph of Anodic Film Formed on 6061-T6, 18% (w/w) VPA, 40 V, 30 s, 23°C

The small circular areas of lighter contrast, in the TEM micrograph of Figure 6.2, are most likely areas where dissolution of oxide begins in the acidic electrolyte during the initial stages of anodization (incipient porosity). However, dissolution of the oxide stops after the formation of these incipient pores, and with further anodization, the oxide grows as a compact, non-porous barrier film. This indicates that the reaction product of the organophosphonic acid with the aluminum oxide on the outer surface prevents the acidic medium from dissolving the underlying oxide, but allows the field-driven ingress of OH^- and O^{2-} ions into the forming anodic oxide. Thus, without further dissolution, the incipient pores cease to grow and anodization continues in a barrier-type fashion.

In order to compare the structure of and composition of anodic oxides formed in aqueous organophosphonic acid solutions with those formed in aqueous solutions such as neutral borate or tartrate,[60] a description of the composition of the films formed in these neutral pH electrolytes is provided here. A characteristic feature of barrier anodic oxide formation is that, at constant voltage, the anodizing current decays exponentially to a low value. This is due to the self-limiting characteristics of anodic barrier oxides formed on valve metals, such as aluminum.[100] During anodization in a barrier oxide forming electrolyte there is no chemical dissolution of the oxide, as occurs in electrolytes that form porous anodic oxides. Therefore, a dense, non-porous layer of Al_2O_3 forms. Formation of this barrier layer, by way of ionic diffusion, occurs as long as the minimum field strength for ionic diffusion (7.1×10^6 V/cm) is supplied.[86] The field strength corresponds to 1.37 nm of oxide thickness per V of applied potential;[100] this is generally rounded to 1.4 nm/V.[77] Because the thickness of the barrier anodic oxides can be precisely controlled, and because these films have significant electrostatic capacity, these films are widely used on capacitor foils.[100]

A neutral solution of sodium borate and boric acid is an electrolyte used to form barrier oxides.[86] When anodizing pure aluminum in such an electrolyte, a current efficiency close to 100% of the theoretical Faraday equivalent is achieved.[86] This indicates that the barrier anodic oxide is almost pure Al_2O_3. Up to 2% (w/w) water has been observed in the anodic oxide film,[274] and the water exists in a molecular state.[104] The incorporation of a low level of anions from the electrolyte into the barrier anodic aluminum oxide has also been observed.[275] Konno et al.,[276] give the composition of the outer surface of a film formed in neutral borate solution as $AlO_{1.36}\bullet(OH)_{0.28}\bullet(B_2O_3)_{0.07}$. Using AES, Strohmeier[277] did not detect B on the surface of neutral

---

274. secondary reference, A Güntherschulze and H. Betz, "*Die Elektrolyt Kondensatoren*," Verlag M. Krain, Berlin (1937) in S. Tajima, *Adv. Corros. Sci. Technol.*, ***1*** (1970) 229.
275. M. M. Lohrengel, *Mater. Sci. Eng.*, ***R11*** (1993) 243.
276. H. Konno, S. Kobayashi, H. Takahashi, and M. Nagayama, *Electrochim. Acta.*, ***25*** (1980) 1667.
277. B. R. Strohmeier, *Aluminium (Düsseldorf)*, ***67*** (1991) 1209.

borate-formed anodic oxides on 99.99 % (w/w) aluminum. XPS was used in the current investigation to determine incorporation of borate in the outer surface of barrier aluminum anodic oxides formed in neutral borate solution. These data are found in Table 6.1.

Table 6.1. Surface Composition of Barrier Aluminum Anodic Oxide Formed in Neutral Borate Solution as Determined by XPS (atomic %)

Sample	B	C	O	Al
50 nm barrier anodic oxide on 1199 alloy (sputtering rate calibration standard)	0.1	41.9	36.2	21.8

Boron was detected on the 99.99% pure aluminum (1199 alloy) surface at a barely detectable level of 0.1% (atomic). The C signal is attributed to atmospheric hydrocarbon contamination. Assuming that 0.3% of the O signal comes from the incorporated borate (BO_3^{3-}), 35.9% of the O signal can be attributed to the oxide. This yields an Al/O ratio of 1.8/3. This ratio indicates that the barrier oxide has the approximate stoichiometry of pure Al_2O_3.

A plot of current density versus time for high purity metal (99.99%) anodized in neutral borate solution is presented in Figure 6.3. The current surges, then falls rapidly to a value near zero. The step-wise changes in current density on the plot of Figure 6.3, and subsequent plots of current density, are artifacts from the electronic circuitry used to acquire the data.[278] The initial current surge represents ionic conduction through the forming anodic oxide.[100] Once the self limiting thickness is reached, the field is no longer high enough to drive ionic diffusion, the film stops growing, and the current decays to a finite value near zero, which represents electronic leakage current.[100]

278. This was demonstrated in this laboratory, after the investigations described in this dissertation, when the power supply used to generate these data was replaced with one that had a smaller amperage range.

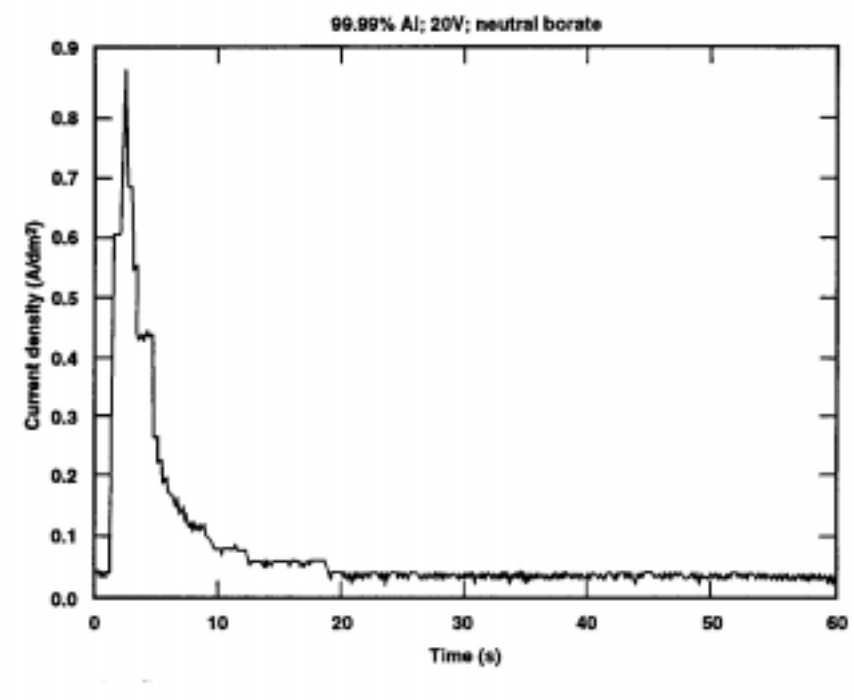

Figure 6.3. Current Transient for Anodization of 1199 Aluminum Alloy in Neutral Borate Solution

Evidence that VPA is a barrier-forming electrolyte is provided in the current density transients provided in Figures 6.4 and 6.5. Figure 6.4 represents the potentiostatic anodizing behavior of 99.99% (w/w) aluminum in VPA solution, whereas Figure 6.5 represents the anodizing behavior of alloy 6061-T6. The anodizing current surges, then drops to near zero in 10 s, for both materials.

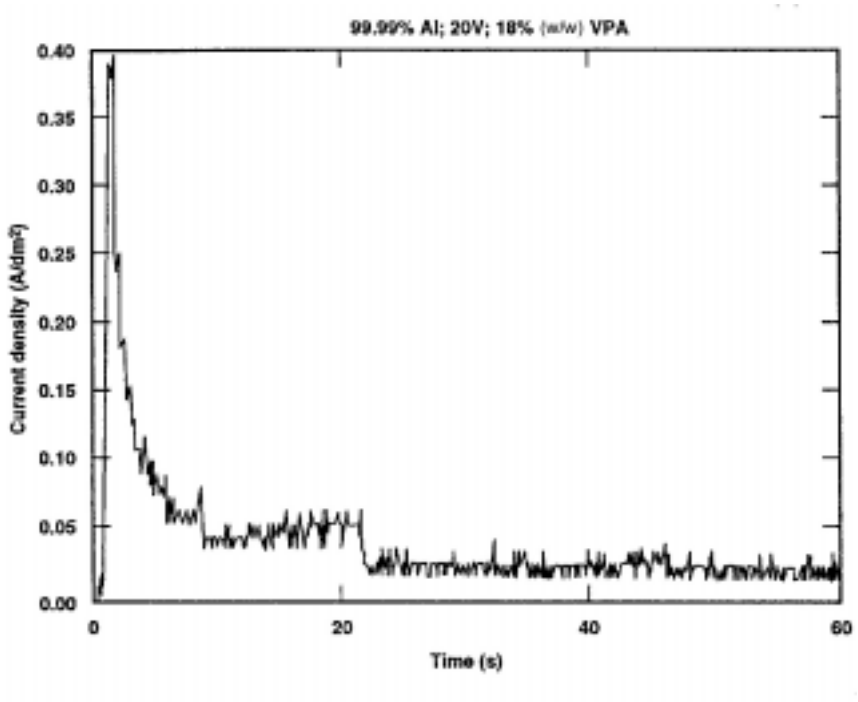

Figure 6.4. Current Transient for 1199 Aluminum Alloy Anodized at Constant Voltage in Vinylphosphonic Acid Solution

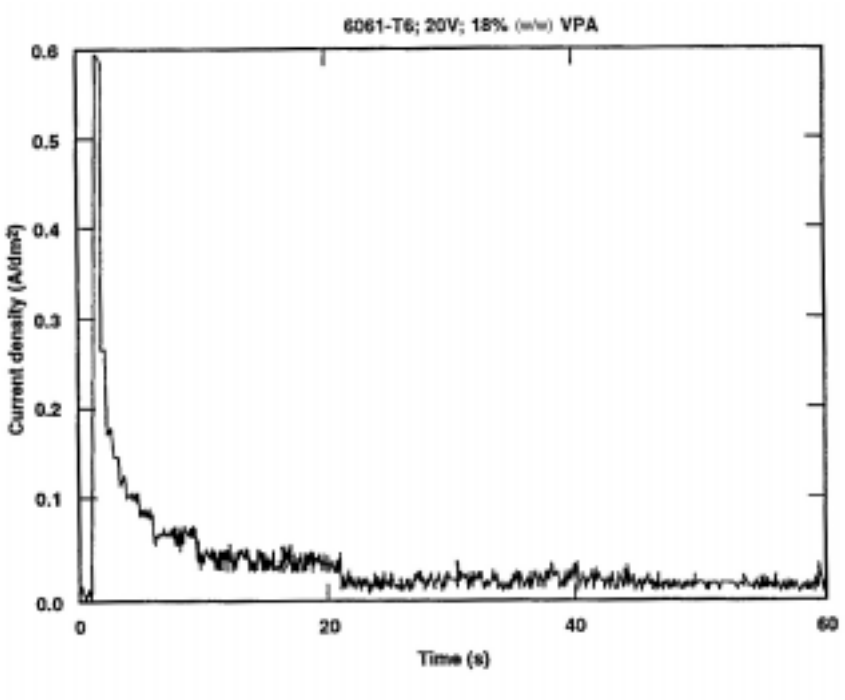

Figure 6.5. Current Transient for 6061 Aluminum Alloy Anodized at Constant Voltage in Vinylphosphonic Acid Solution

Early in the investigation of organophosphonic acid anodizing it was determined from leakage current values that the 2024-T3 alloy studied in the preceding chapters did not passivate during anodization in organophosphonic acid solutions. Optical microscopic investigation of 2024-T3 anodized for 10-30 s in VPA solutions revealed intermetallic particles protruding through the surface of the oxide. The high concentration of alloying elements, particularly copper in this aerospace alloy,[75] results in intermetallic phases such as S phase (Al_2CuMg),[252] which do not anodically oxidize and therefore serve as pathways for high electronic leakage currents.[77] The values for the leakage currents for coupons of high purity aluminum (99.99% - 1199 alloy) and alloy 2024-T3 anodized in a 10% (w/w) VPA solution are presented in Figure 6.6.

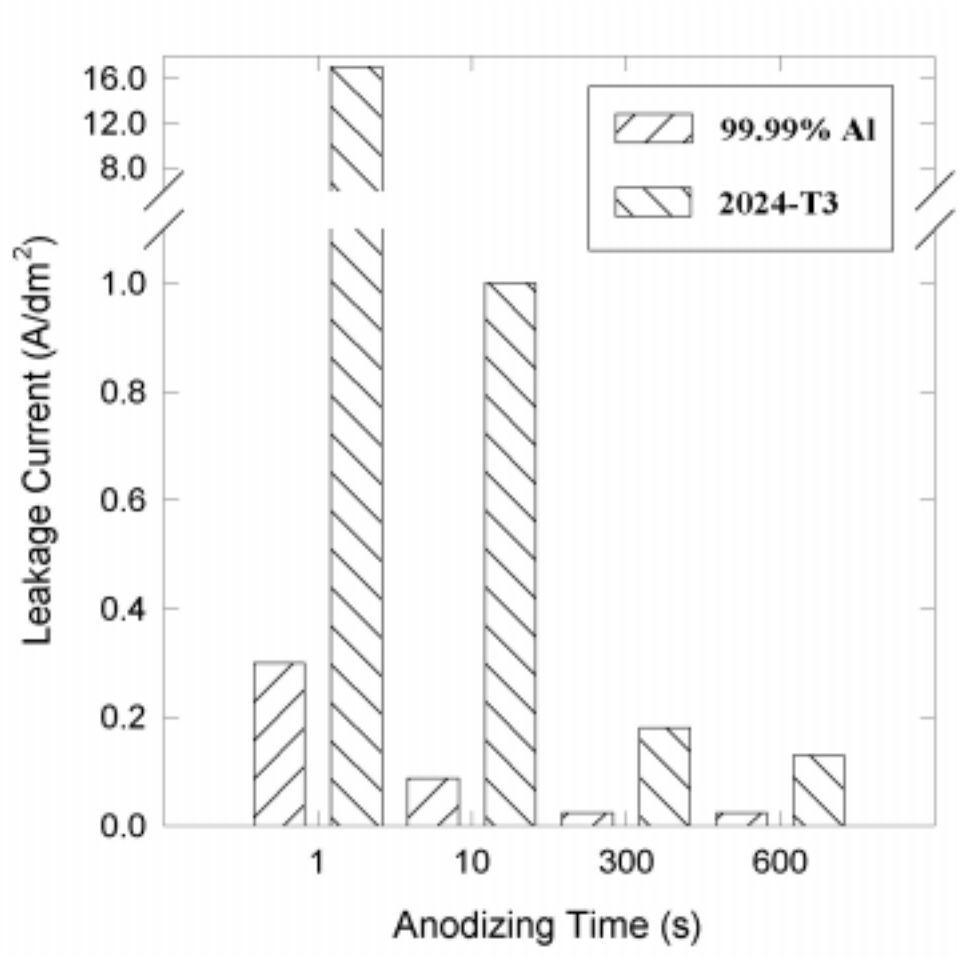

Figure 6.6. Anodizing Current as a Function of Alloy and Anodizing Time, 18% (w/w) VPA, 40 V, 23°C

After 10 s of anodization the 2024-T3 alloy was still drawing about 1 A/dm^2 of current, whereas the leakage current for the high purity aluminum was approaching zero. Even after 5 min, the 2024-T3 alloy still had a significant leakage current. Due to the inability of the barrier oxide forming organophosphonic acid electrolytes to passivate the 2024-T3 alloy surface, and since it was shown that 6061-T6 did passivate during anodic oxidation in organophosphonic acid (VPA) solutions (see Figure 6.5), 6061-T6 was chosen for all further work, including characterization and bond testing. Furthermore, since this 6061 alloy is not widely used in the aerospace industry, and since it is similar to alloys that would be used in less demanding applications, such as in the

automotive industry, a dicyandiamide-cured, DGEBA epoxy paste adhesive, XA-3498, was chosen to bond the 6061-T6 aluminum alloy. This adhesive was an experimental adhesive being evaluated by the 3M Corporation for automotive applications.

Further evidence that a barrier oxide is formed by anodization in VPA solution is given by the AES depth profile of Figure 6.7.

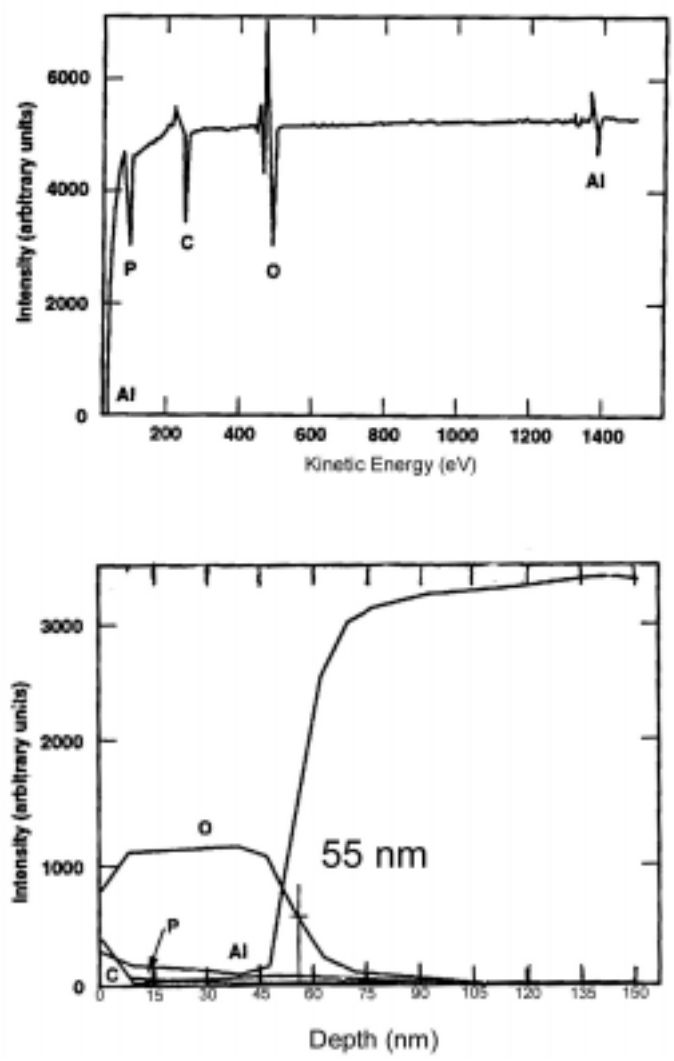

Figure 6.7. Auger Electron Spectroscopy Analysis of 6061-T6 Surface Anodized at 40 V in 18% (w/w) Vinylphosphonic Acid Solution

The top portion of Figure 6.7 is an AES surface scan of the VPA anodized metal. The spectrum has peaks for Al, O, C, and P. These surface elements can be attributed to anodic aluminum oxide, and to the reaction product of VPA and the surface of the anodic oxide. The bottom portion of Figure 6.7 is an AES depth profile of the same material. The oxide/metal interface is arbitrarily assigned at the point where the oxygen signal reaches one-half of its maximum value. For the metal anodized at 40 V in 18% (w/w) VPA solution, this is observed at approximately 55 nm, which is close to the expected value of 56 nm of a typical barrier oxide film (40 V x 1.37 nm/V = 54.8 nm). Therefore, within the error of the measurement, AES depth profiling supports the premise that the anodic oxide formed in VPA solution is of the barrier type.

Ion scattering spectroscopy (ISS) depth profiling confirms that the measured oxide thickness corresponds to the calculated value that indicates the formation of a barrier anodic oxide in solutions of VPA. This is evident in the depth profile of Figure 6.8.

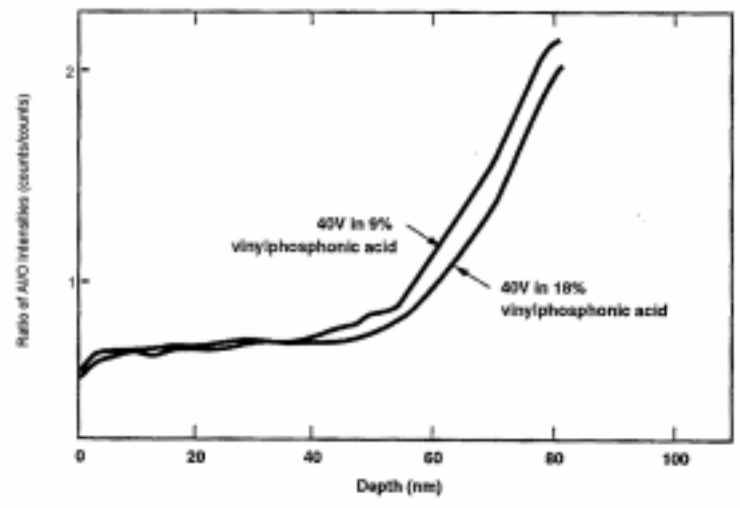

Figure 6.8. Ion Scattering Spectroscopy Depth Profile of 6061-T6 Anodized for 30 s at 23°C in Vinylphosphonic Acid Solution - Ratio of Al/O Intensities

For the purposes of oxide thickness determination, only the Al/O ratio is plotted in Figure 6.8 as a function of sputtering depth. For aluminum alloy 6061-T6 anodized at 40 V in either 9% or

18% (w/w) VPA, the metal/oxide interface, identified by the rise of the Al/O signal ratio, is detected near the expected value of 56 nm. The reaction product of VPA anodization is found only on the outermost surface of the barrier anodic oxide. In the AES depth profile of Figure 6.7, the P signal is zero in the second scan, or considering the sputtering rate, after about 7 nm is sputtered off of the surface. The thickness of the VPA reaction product layer is, therefore, at least less than 7 nm.

As long as the surface is thoroughly rinsed after anodization, intuitively, one would expect only one layer of chemisorbed VPA species on the surface. Due to the sputtering and sampling rates chosen for AES analysis, the AES depth profile of Figure 6.7 only shows that the VPA layer is less than 7 nm, which still allows for the possibility of a layer of physisorbed VPA on top of the chemisorbed (surface reacted) VPA. The notion that VPA is present as a single layer reaction product of the VPA and the anodic oxide was confirmed empirically during wedge testing, when rinsed and unrinsed VPA anodized adherends were bonded and exposed to humidity. As will be seen shortly, rinsed and dried VPA adherends provide adhesive bonds with excellent durability. However, when the VPA anodized adherends were not rinsed prior to bonding, wedge test specimens totally delaminated within 24 h, with apparent interfacial failure. The failure surfaces of the bonds with unrinsed adherends were not analyzed, nor was the sputtering rate decreased to improve the depth resolution of the AES depth profile. For unrinsed anodized VPA adherends, it is proposed that there was multilayer adsorption of the VPA, including a chemisorbed layer adjacent to the oxide, and physisorbed layers on top of the chemisorbed layer. After placing a bonded sample into humidity, water diffusing to the physisorbed VPA is able to solubilize this weak boundary layer resulting in quick delamination of the adhesive bond. Therefore, after anodizing, and with thorough rinsing, VPA is present on the surface in approximately one layer that is chemically reacted with the underlying aluminum oxide.

XPS confirms the presence of surface P after anodization of 6061-T6 in different concentrations of VPA solutions. These data are summarized in Table 6.2.

Table 6.2. XPS Analysis of 6061-T6 Surfaces Anodized in Vinylphosphonic Acid Solution (w/w) at 40 V and 23°C for 30 s (elemental composition in atomic % and binding energy (B.E.) in eV)

VPA Conc.	XPS	C 1s	N 1s	O 1s	F 1s	Al 2p	P 2p
9%	at. %	22.1	0.1	48.9	0.3	25.2	3.4
	B.E.	285.0	not measured	531.9	not measured	74.5	134.1
18%	at. %	22.8	0.1	47.5	< 0.2*	26.8	2.8
	B.E.	285.0	not measured	532.0	not measured	74.7	134.0

* not detected

The entire P signal is attributed to the adsorbed VPA. If the entire C signal was from VPA the C/P ratio would be 2. Since it is on the order of 7, the excess carbon is attributed to atmospheric hydrocarbon contamination. Al is from the barrier anodic oxide, and O is from the anodic oxide and from the reacted VPA. The O 1s peak shape was symmetrical, and there was no evidence of -OH. The O/P ratio for reacted VPA would be 3. For the surface with 3.4% P, the percent of the O signal due to reacted VPA would be 10.2%. This leaves 38.7% of the O signal for the anodic oxide. The Al/O ratio then is given by 25.2/38.7, which is equivalent to approximately 2/3. Therefore, the oxide has the expected stoichiometry of Al_2O_3. N and F may be residuals from the HF/HNO_3 pre-etch, or may be from atmospheric pollutants, and aluminum heat treating chemicals, respectively.[241]

Angle resolved XPS (ARXPS) analyses on 6061-T6 surfaces anodized in VPA solution (0.1 M) were conducted by Dr. A. C. Miller of Lehigh University. As the sample is tilted with respect to the analyzer, the sampling depth of XPS is varied.[279] At lower electron take off angles relative to the sample surface, XPS becomes more surface sensitive. Briggs gives the sampling depth (95%

279. W. M. Riggs and M. J. Parker, in "*Methods of Surface Analysis,*" Elsevier Scientific Publishing Company, New York (1975) p. 103.

of the peak signal) of XPS as 3λ, where λ is the inelastic mean free path.[280] The effect of tilting the sample with respect to the photoelectron analyzer in an X-ray photoelectron spectrometer is illustrated in Figure 6.9.[281] In Figure 6.9 the sampling depth (d) is given as $d = \lambda\sin\theta$. However, according to Briggs[280] this should more accurately be given as $d = 3\lambda\sin\theta$. By inserting values of 10° and 90° for θ, it is calculated that at 10°, the sampling depth is approximately 17% of that at 90°. The inelastic mean free paths (λ) for electrons in Al_2O_3 were presented by Tanuma, et al,[282] as a function of electron kinetic energy. Mg K_α radiation ($h\nu$ = 1253.6 eV) was used to acquire the XPS spectra. The kinetic energy of photoelectrons is given by: K.E. = $h\nu$ - B.E., where B.E. is the binding energy. For the Al 2p peak, with an observed binding energy of 74.7 eV (Table 6.2), the kinetic energy of these electrons is 1178.8 eV. Similarly, the kinetic energies for P 2p (B.E. = 135.0) and O 1s electrons (B.E. = 532.0) are 1118.6 eV and 721.6 eV, respectively. Using the data of Tanuma et al.,[282] the sampling depth (3λ) at 90° sample tilt for Al 2p, P 2p and O 1s is approximately 7.5 nm, 6.9 nm, and 4.8 nm, respectively. For a 10° sample tilt, the sampling depths for the same three signals (Al 2p, P 2p, and O 1s) are approximately 1.3 nm, 1.2 nm, and 0.8 nm, respectively. Therefore, true surface species will have larger peaks at low electron take off angles, compared to angles approaching normal to the sample surface; surface species will have a larger photoelectron peak intensity at 10° than at 90°.

---

280. D. Briggs, *X-ray Photoelectron Spectroscopy as an Analytical Technique*, in "*Handbook of X-ray Photoelectron Spectroscopy*," D. Briggs, ed., Heyden Publishers, Philadelphia, PA (1977) pp.153-181.
281. *Physical Electronics Division Applications Note No. 8401*, Perkin-Elmer, Eden Prairie, MN (1984).
282. S. Tanuma, C. J. Powell, and D. R. Penn, *SIA, Surf. Interface Anal.,* ***11*** (1988) 577.

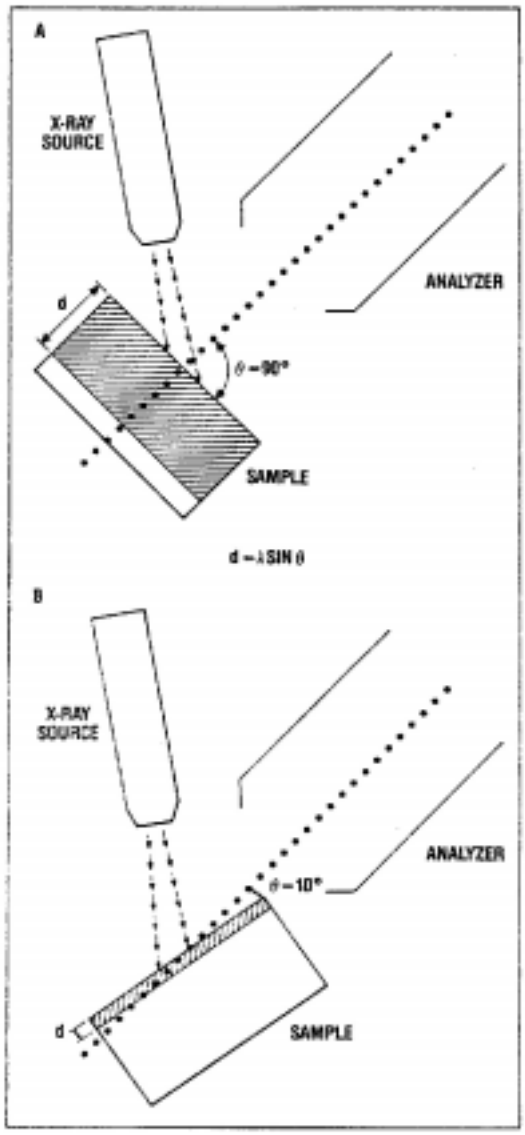

Figure 6.9. Schematic Drawing Illustrating the Effect of Sample Tilt on the Sampling Depth of X-ray Photoelectron Spectroscopy[281]

While the actual angle resolved spectra obtained by Dr. Miller are not provided, a summary of various peak height ratios at high and low take off angles for VPA anodized 6061-T6 alloy are presented in Table 6.3.

Table 6.3. ARXPS Analysis of 6061-T6 Surfaces Anodized at 40 V and 23°C for 30 s in 0.1 M Solution of Vinylphosphonic Acid (VPA) --- [ratio of peak heights]

Take Off Angle	P/Al	C/Al	O/Al
90^{O}	0.6	4.9	13.7
10^{O}	2.1	16.0	15.7

Since peak heights, and not peak areas, were reported by Dr. Miller, one cannot use these numbers to determine exact stoichiometry. However, these values can be used in a qualitative way to determine surface versus bulk species. The ratio of peak heights of P/Al photoelectron peaks increases as the electron take off angle decreases. The C/Al ratio also increases at lower take off angles. However, analysis of the table shows that at 10° take off angle, the C/P peak height ratio is approximately 8. If the C signal was due solely to VPA the expected peak height ratio would be closer to 2. Therefore, there is an outermost layer of hydrocarbon contamination on the sample surface. In combination with AES depth profiling (Figure 6.7), the ARXPS data (Table 6.3) confirm that the reaction product of vinylphosphonic acid and the anodic oxide is a surface species, and is not found in the bulk anodic oxide.

It was shown in Chapter 5 that RAIRS provided rather featureless spectra, and only indicated that hydroxyl groups on the aluminum surface were consumed when the surface hydroxide film was functionalized with organophosphonic acids. IETS results, also presented in Chapter 5, showed further that the organic portion of the organophosphonic acids did not participate in bonding to the surface hydroxide film, and it was determined that these groups were oriented away form the surface, in a position to interact with the adhesive. IETS cannot be used to analyze anodic films formed in organophosphonic acid solutions, since the electrical resistance of the barrier anodic aluminum oxide prevents tunneling of the electrons.

Grazing angle RAIRS, Raman spectroscopy, and surface enhanced Raman spectroscopy (SERS) were conducted by Dr. Angela M. Ahern (formerly of Alcoa Technical Center) on 1199

aluminum alloy anodized at 20 V and 23°C for 30 s in 0.1 M solutions of VPA[283] and ϕPA. The RAIRS spectra and the Raman spectra of these anodic films were generally featureless, and it is concluded that these vibrational spectroscopic techniques are not sensitive enough to characterize the surface layer of the reacted organophosphonate layer. However, the SERS spectra did provide information on the reacted organophosphonate layer. SERS is a sensitive technique for characterizing the structure of adsorbed species on rough metals, particularly on silver. The mechanisms for surface enhancement are reviewed elsewhere.[284,285] The intensity of Raman bands in SERS may be enhanced up to six-fold for small molecules adsorbed on (or near) certain rough metal surfaces.[286] The drawback of the technique is that the enhancement only occurs with certain metal substrates, such as silver, gold, and copper.[286] To obtain the enhancement in the present work, islands of silver were deposited onto the duplex barrier layer anodic films formed in the organophosphonic acid electrolytes.

The Raman and SERS spectra for the duplex barrier films formed in organophosphonic acid electrolytes are presented in Figures 6.10 and 6.11. The Raman spectra (spectra labeled "a" in Figures 6.10 and 6.11) exhibit only weak, low frequency modes below about 400 cm^{-1}. These modes are most likely attributed to Al phonon and Al-O modes.[287] The Raman spectra contain no information regarding the structure of the reacted organophosphonates. The SERS spectra (spectra labeled "b" in Figures 6.10 and 6.11) exhibit many vibrational bands (see Table 6.4).

---

283. 0.1 M VPA ~1% w/w VPA. During anodization in organophosphonic acid solutions ranging in concentration from 0.1 M (~1% w/w) to ~1.7 M (18% w/w) the duplex barrier film always formed on the surface; in these acidic solutions anodizing currents fell to near-zero within 10-30 s. Based on these results, it is concluded that changing electrolyte concentrations within these limits had no effect on the final structure of the surface film, including organophosphonate coverage. This will become more clear in subsequent discussions.
284. M. Moskovits, *Rev. Mod. Phys., **57*** (1985) 783.
285. R. L. Garrell, *Anal. Chem., **61*** (1989) 401A.
286. Personal communication with Dr. A. M. Ahern, formerly of Alcoa Technical Center.
287. P. V. Thomas, V. Ramakrishnan, and V. K. Vaidyan, *Thin Solid Films, **170*** (1989) 35.

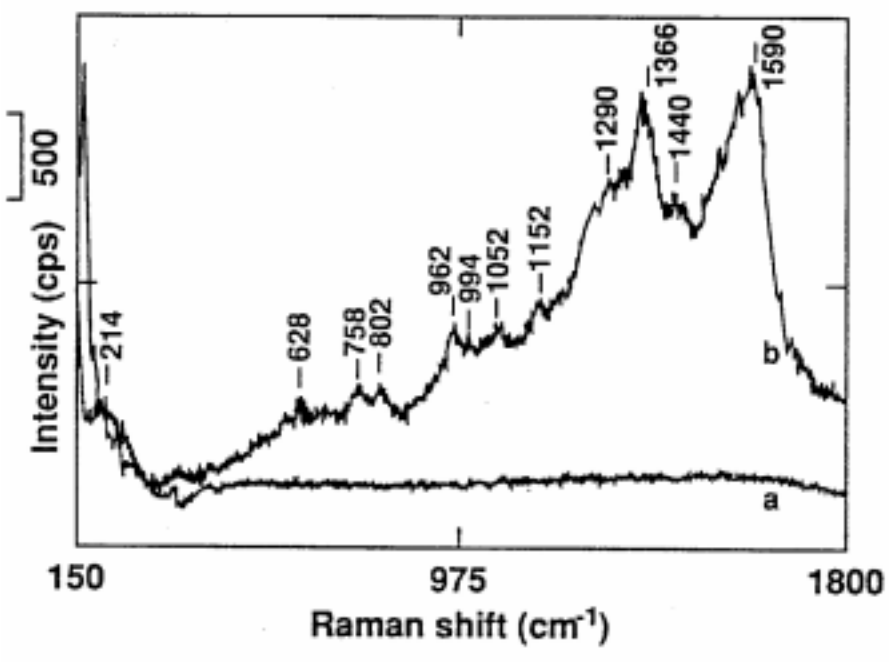

Figure 6.10. The a) Raman and b) SERS Spectra of Phenylphosphonic Acid Anodized Aluminum

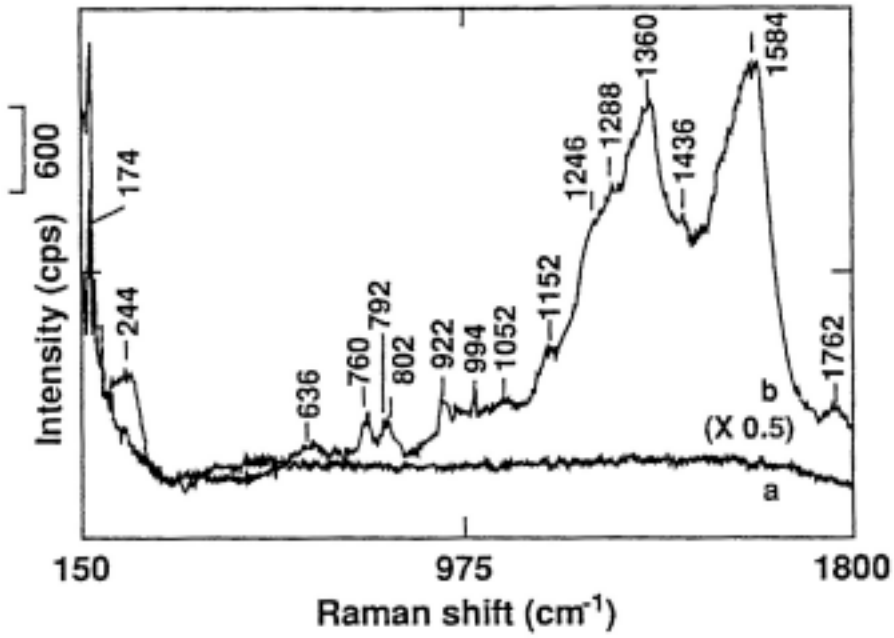

Figure 6.11. The a) Raman and b) SERS Spectra of Vinylphosphonic Acid Anodized Aluminum

Table 6.4. SER Spectral Frequencies and Assignments for ϕPA- and VPA- Anodized Aluminum Alloy 6061-T6 (0.1M, 40 V, 23°C, 30 s)

Frequencies (cm^{-1})		
ϕPA	VPA	Assignments
	174	Al phonon mode
214	244	ν Ag-organophosphonic acid[288]
628	636	δ (PO_3)[258]
758	760	Al-O-P[167]
	792	?
802	802	ν (P-C) [266]
	922	ν (Al-O) [258]
962		?
994	994	ring breathing mode (ϕPA)[271] and ν (P-C)[269]
1052	1052	ν_s (PO_3) [258]
1152	1152	ν_a (PO_3) [258]
	1246	?
1290	1288	ν_{7a} ring mode (ϕPA)[289] and δ (CH_2) [258]
1366	1360	graphitic carbon[290]
1440	1436	Aromatic ring in-plane stretch (ϕPA) [269] and δ (CH_2) [258]
1590	1584	Aromatic ring in-plane stretch (ϕPA) [269] and graphitic carbon[290]
	1762	irreproducible bands
2855	2855	ν_s (CH_2/CH_3) degradation products [271]
2929	2929	ν_a (CH_2/CH_3) degradation products [271]
3069		ν_s (CH) [271]
	3073	ν_a $(=CH_2)$ [271]

Assignments: ν = stretch, δ = deformation, s = symmetric. a = asymmetric

288. K. D. Beer, W. Tanner, and R. L. Garrell, *J. Electroanal. Chem., **258*** (1989) 313.
289. A. M. Ahern, formerly of Alcoa Technical Center, personal communication.
290. R. P. Cooney, M. W. Howard, M. R. Mahoney, and T. P. Mernaugh, *Chem. Phys. Lett, **79*** (1981) 459.

In general, comparison of the SERS spectra shows that they contain many similarities. This suggests that the organic group of the organophosphonates on the oxide surfaces do not contribute much to these spectra. An obvious similarity is the increase in the background that dominates the 1000-1700 cm^{-1} region. Two broad bands at about 1360 and 1590 cm^{-1} are observed in this region and are assigned to graphitic carbon,[290] most likely from laser induced degradation of the organophosphonic acids.[286] Figure 6.12 presents the intensity of the band at 1360 cm^{-1} for VPA anodized 1199 aluminum, as a function of the time of laser irradiation.

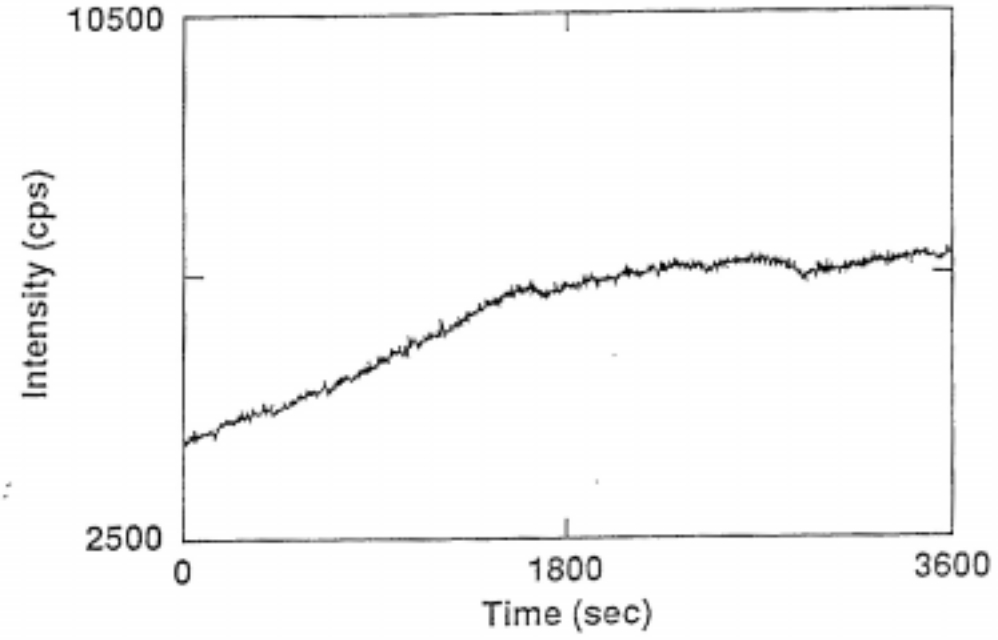

Figure 6.12. Intensity of the 1360 cm^{-1} Graphitic Carbon SERS Band for VPA Anodized Aluminum as a Function of Time of Exposure to Laser Radiation

The intensity of this graphitic carbon band increases from approximately 4000 counts/s to about 6500 counts/s, or by more than 50%, after 1 hr of irradiation. Typical spectra acquisition times were slightly greater than 1 h. It is concluded that degradation of the reacted organophosphonates occurs during laser irradiation of the samples during analysis, and is not a result of evaporation of the silver overlayer required for signal enhancement. Efforts by Dr. Ahern to reduce the graphitic carbon background, while retaining the desired surface

information, by reducing laser power or acquisition time were not successful.

In the spectrum of ϕPA (see Figure 6.10 and Table 6.4), bands assigned to the phenyl ring appear at 994, 1290, and 1440 cm^{-1}, with a possible contribution to the graphitic carbon band at 1590 cm^{-1}. An aliphatic C-H stretching mode was also observed at 3069 cm^{-1}.[286] All other bands are due to the phosphonate group or to laser-induced degradation of the ϕPA.

The presence of the bands associated with the phenyl group indicates that in spite of the large background due to the degradation of the organophosphonate into graphitic carbon, some useful information regarding the organic portion of these surface species is obtained. As exhibited in Figure 6.12, the degradation takes place over time, suggesting that portions of the intact surface organophosphonates are present throughout the duration of the scan.

A band at 214 cm^{-1} is assigned to a silver-phosphonic interaction.[288] Bands at 628 , 1052, and 1152 cm^{-1} are assigned to vibrations of the PO_3^{2-} group.[258] No bands are observed at 946 and 1026 cm^{-1}. These would be attributed to vibrations of the $P(OH)_2$ group. [258] While it is conceivable that the laser irradiation dehydrated this material so that no $P(OH)_2$ would be observed, the absence of bands in the 420-460 cm^{-1} region and at 1179 cm^{-1}, which are indicative of the phosphoryl group, leads to the conclusion that during anodization ϕPA reacts with the aluminum surface through an acid-base reaction to form a resonance stabilized, tridentate PO_3^{2-} anion that is bonded to Al^+ sites on the anodic aluminum oxide. This is analogous to the structure for the reaction of organophosphonic acids with hydroxylated aluminum surfaces, presented in the preceding chapter (see Figure 5.10).

SERS selection rules state that modes oriented perpendicular to the silver overlayer, or surface of interest, will provide the most intense bands, and those parallel to the surface will exhibit the least intense bands. Intermediate orientations will yield intermediate intensities.[291] The P-C

---

291. K. Ohta and R. Iwamoto, *Appl. Spec.*, ***39*** (1985) 418.

stretching mode assigned to the band at 802 cm^{-1}, the PO_3^{2-} stretching modes at 1052 and 1152 cm^{-1}, and the Al-O-P mode at 758 cm^{-1} are relatively intense, in spite of the large background of the graphitic degradation product. This indicates that these bonds are perpendicular, or slightly off normal with respect to the surface.[286]

The SERS bands attributed to the vinyl group (Figure 6.11, Table 6.4) are mostly obscured by the background due to the graphitic degradation product. Specifically, the C=C stretching band, anticipated near 1614 cm^{-1} is apparently obscured by the intense and broad graphitic carbon band at 1584 cm^{-1}. The only evidence for the presence of vinyl groups on the surface was the observation of a band, by Dr. Ahern, at 3073 cm^{-1} that is attributed to the asymmetric $=CH_2$ stretching mode.[286] As with ϕPA (Figure 6.10) no bands are observed for $P(OH)_2$ and P=O vibrations. Bands at 636, 1052, and 1152 cm^{-1} are due to the tridentate PO_3^{2-} resonance structure. An Al-O-P band at 760 cm^{-1} indicates that the VPA is chemically bonded to the underlying anodic aluminum oxide. Following SERS selection rule arguments used for the ϕPA anodized aluminum, it is likely that the P-C, PO_3^{2-}, and Al-O-P bonds are perpendicular or slightly off normal with respect to the surface. Based on the SERS results, and other analytical results previously presented, the structure of the duplex barrier film formed on aluminum as a result of anodizing in aqueous solutions of VPA is similar to that for adsorption onto a hydroxylated surface (Figure 5.11) except that the oxide beneath the VPA/oxide reaction product layer, has a precise thickness corresponding to 1.37 nm/V of applied potential. It is recognized, particularly with the SERS data presented for ϕPA (Figure 6.10) that anodization in aqueous solutions of most organophosphonic acids will result in a similar surface film in which the phosphonate is chemically bonded to the underlying oxide, with the organic portion of the molecule oriented away from the surface, positioned for interaction with the applied adhesive or primer (see Figures 5.10 and 5.11).

In another experiment, 1 M solutions of various organophosphonic acid solutions were prepared, HF/HNO_3-etched metal was anodized at 10 V and 23°C for 5 min, and the oxide film was

detached from the metal and examined by TEM. A transmission electron micrograph of the oxide formed in 1 M VPA is presented in Figure 6.13. This image is similar to that of the oxide formed in 18% (w/w) VPA (~1.7 M VPA) shown in Figure 6.2.

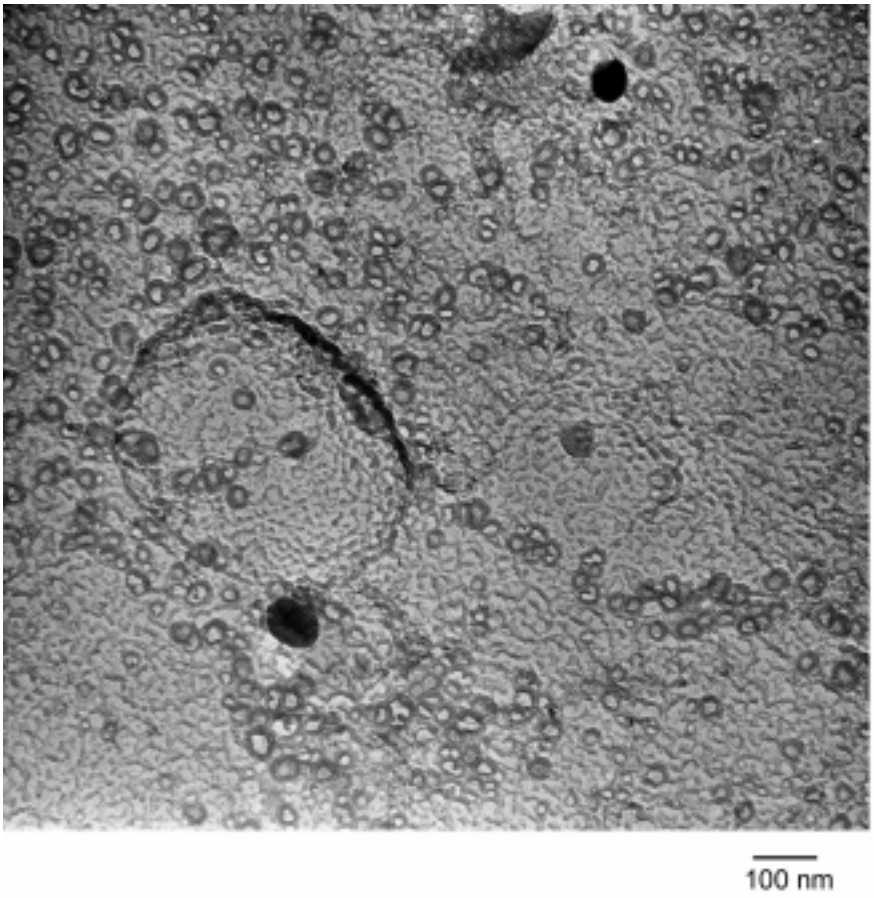

Figure 6.13. Transmission Electron Micrograph of Anodic Film Formed on 6061-T6 in 1 M Vinylphosphonic Acid - 10 V, 5 min, 23°C

Allylphosphonic acid (APA) electrolyte was also used to anodize aluminum. The molecular structure of APA is found in Figure 6.14. Figure 6.15 contains the TEM of the oxide formed in 1 M allylphosphonic acid.

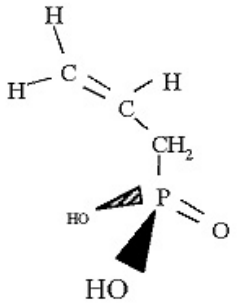

Figure 6.14. Molecular Structure of Allylphosphonic Acid - APA

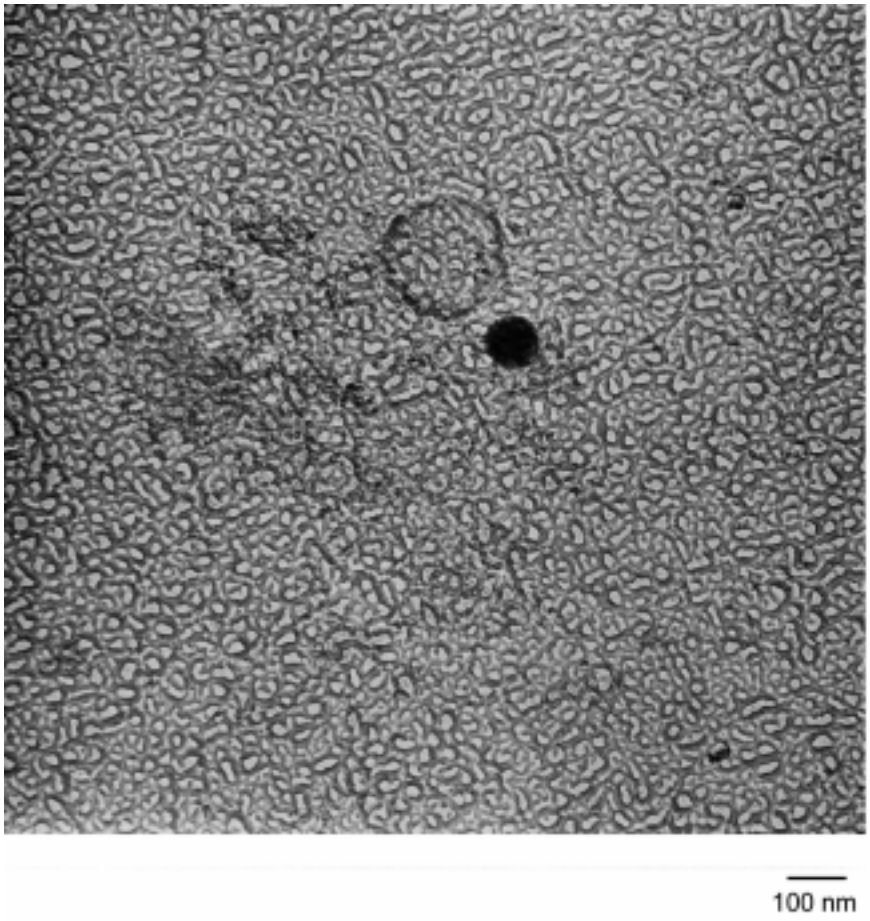

Figure 6.15. Transmission Electron Micrograph of Anodic Film Formed on 6061-T6 in 1 M Allylphosphonic Acid - 10 V, 5 min, 23°C

Incipient porosity, as observed on VPA anodized surfaces, is observed to a greater degree with the APA anodized oxide. The formation of porous cell structure is initiated, but stops early in the process and anodization continues to form a barrier oxide. The acidic solution apparently attacks the forming aluminum oxide surface, resulting in the initiation of porosity. However, as soon as the surface is covered with the organophosphonate reaction product, the dissolution stops, and a barrier oxide is formed.

The oxide formed in 1 M ϕPA (Figure 6.16) is relatively featureless, as is the anodic oxide formed in 0.1 M NTMP Figure 6.17).[292] The darker ovoid-shapes are intermetallic particles lodged in the anodic oxide, and the lighter objects are artifacts introduced by the amalgamation step used to remove the oxide film from the metal. The bulky hydrophobic phenyl- groups of ϕPA (or bonding of the triphosphonate[171] for NTMP) must instantaneously inhibit any oxide dissolution, and prevent the formation of incipient pores.

292. Anodization in 1.0 M NTMP left a white powder residue on the alloy surface. For this reason, anodizing was accomplished using 0.1 M NTMP.

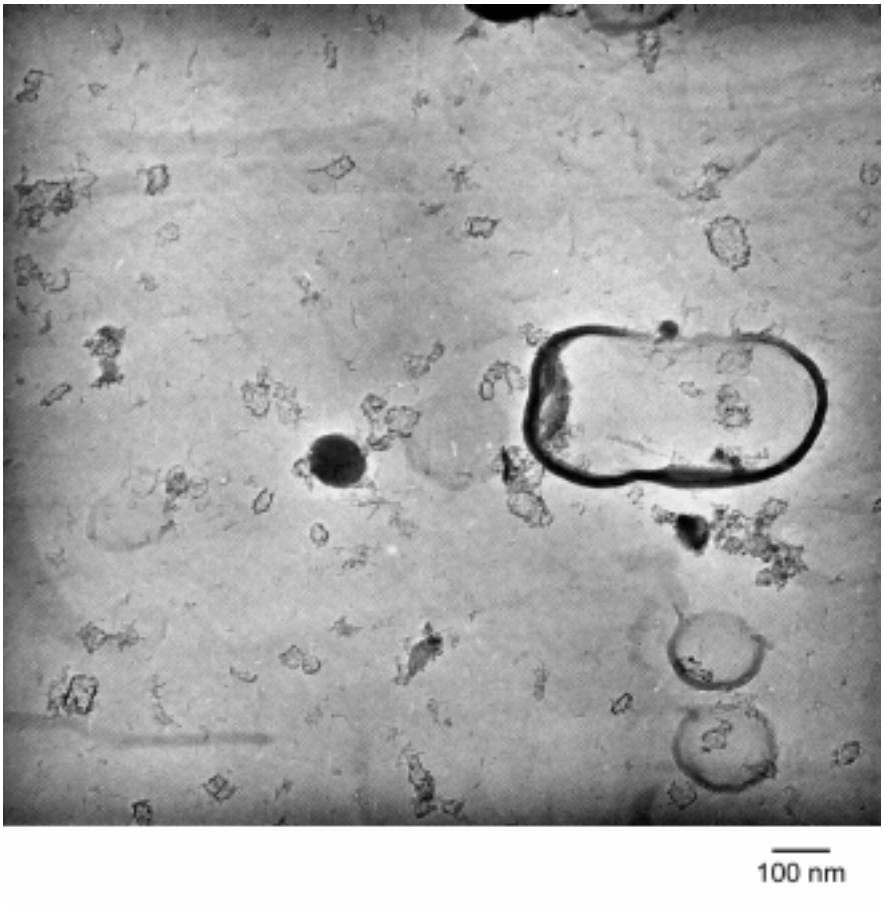

Figure 6.16. Transmission Electron Micrograph of Anodic Film Formed on 6061-T6 in 1 M Phenylphosphonic Acid - 10 V, 5 min, 23°C

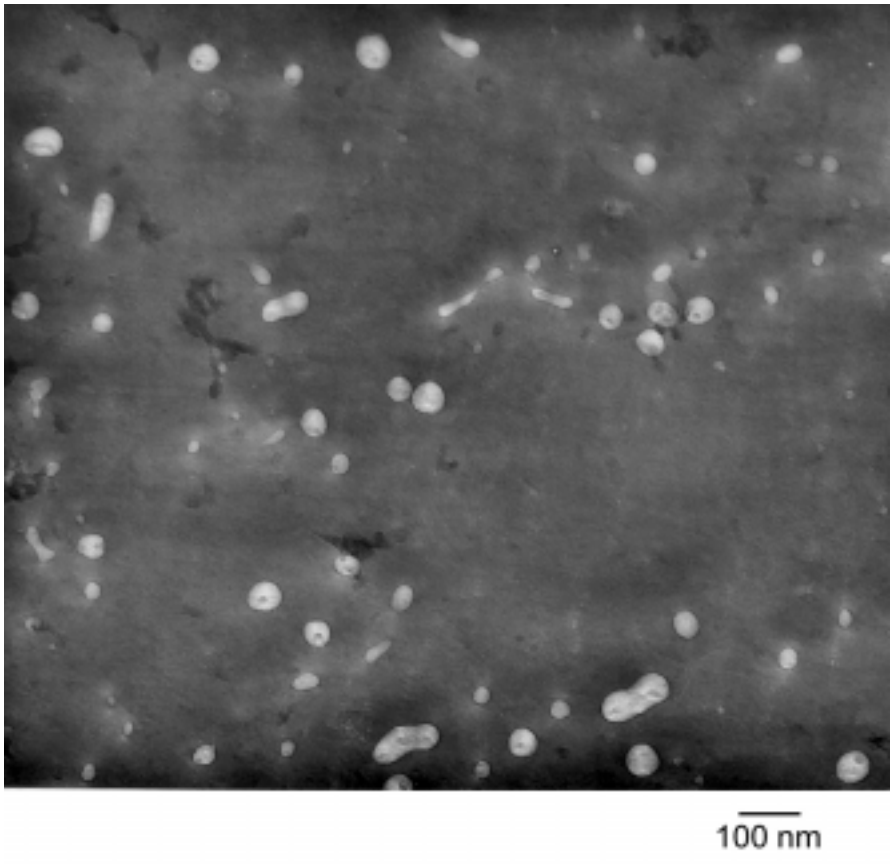

Figure 6.17. Transmission Electron Micrograph of Anodic Oxide Formed on 6061-T6 in 0.1 M NTMP - 10 V, 5 min, 23°C

An AES depth profile of the film formed on 6061-T6 in 1 M ϕPA at 60 V and 23°C for 5 min is presented in Figure 6.18. The surface reacted with the organophosphonate, as demonstrated by signals arising from P and C atoms. As the surface is sputtered, the P and C signals disappear, indicating that the organophosphonate is only present on the outer surface of the film. Furthermore, SERS demonstrated that the phenyl- group survives the anodization and is present on the surface of the film (Table 6.4). The oxide/metal interface is reached after sputtering ~80 nm into the surface. This measured oxide thickness is within the experimental error of the predicted value of 84 nm (obtained from ~1.4 nm/V). Therefore, it is sufficiently proved that anodization of aluminum in solutions of ϕPA results in the formation of a duplex barrier layer, analogous to VPA anodizations.

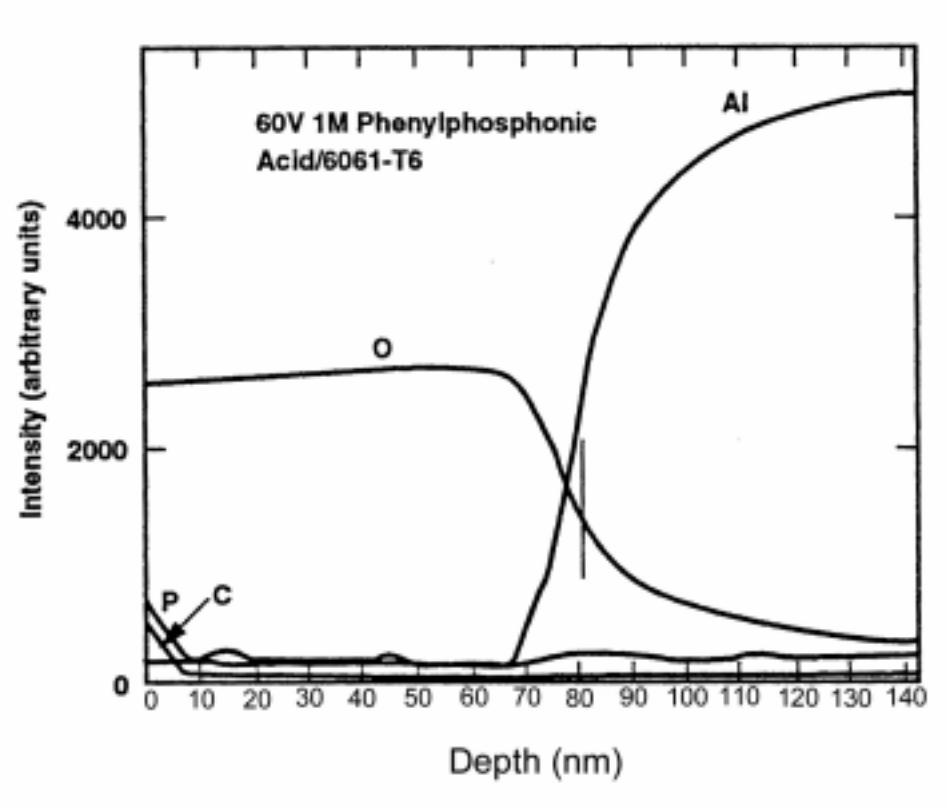

Figure 6.18. Auger Electron Spectroscopy Depth Profile of 6061-T6 Anodized in Phenylphosphonic Acid Solution

The samples anodized in 1 M organophosphonic acid solutions were analyzed using XPS, to determine elemental surface composition. The results of these analyses are presented in Table 6.5.

Table 6.5. XPS Analysis of 6061-T6 Anodized at 10 V and 23°C for 5 min in 1 M Organophosphonic Acid Solutions (concentration {at. %}/binding energies {eV})

Electrolyte	C Conc.	C 1s B. E.	O Conc.	O 1s B. E.	Al Conc.	Al 2p B. E.	P Conc.	P 2p B. E.
VPA	38.4	285.0	37.8	532.1	21.2	74.7	2.7	134.1
APA	27.6	285.0	44.1	532.0	26.0	74.6	2.4	134.2
ϕPA	20.2	285.0	46.4	531.3	32.2	74.6	1.3	134.3

The anodized surfaces are comprised of Al, O, C, and P species. The level of P ranges from 1-3% (at.). There are no significant chemical shifts in P 2p binding energies, relative to each other, or relative to binding energies observed for phosphoric acid or phosphorous acid anodized adherends (see Table 4.3).

During the course of this investigation, aluminum was anodized in solutions of various organophosphonic acids that have not been mentioned in this dissertation. Except for ethylphosphonic acid (EPA), it was observed that all of the organophosphonic acids studied with 2 or more carbon atoms were barrier forming electrolytes at room temperature and at modest voltages. This was determined by the observation of a fast decay of the current to near zero during potentiostatic anodization of aluminum in these electrolytes. While the surface composition of metal anodized in each barrier oxide forming electrolyte was not determined, the anodized surfaces certainly consist of the reaction product of the organophosphonic acid and the aluminum oxide. Otherwise, anodization in acidic solutions would result in a non-zero anodization current, accompanied with the formation of porous oxides or localized oxide breakdown known as burning. Neither porous anodic oxide formation nor burning were observed for any organophosphonic acid electrolyte studied that contained more than 2 C atoms. As previously demonstrated, porous anodic oxides are also not formed in vinylphosphonic acid (2 C atoms) electrolyte.

Potentiostatic anodization in solutions of two of the organophosphonic acids studied resulted in porous anodic oxides. These were methylphosphonic acid (MPA) --- $(CH_3)P(O)(OH)_2$, and ethylphosphonic acid (EPA) --- $(CH_3)(CH_2)P(O)(OH)_2$. Anodic films formed on 6061-T6 at 10 V and 23°C for 5 min in 1 M MPA and EPA electrolytes were examined by TEM. The film formed in 1 M MPA is shown in Figure 6.19.

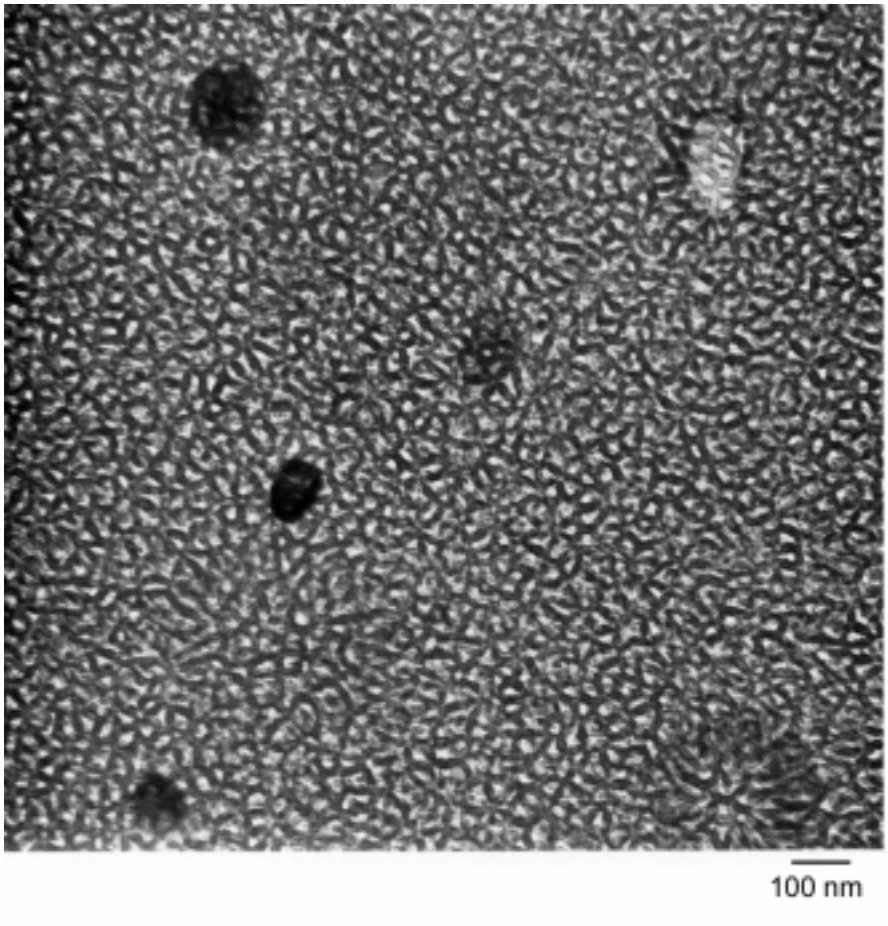

Figure 6.19. Transmission Electron Micrograph of Anodic Film Formed on 6061-T6 in 1 M Methylphosphonic acid - 10 V, 5 min, 23°C

The anodic oxide formed in MPA solution has a classical porous cell structure, with thick cell walls and open pores. This oxide is very similar to those formed with the standard PAA process[249] (see Figure 4.1). The image is that of an array of cells (dark contrast) with a pore in the center of each cell (light contrast). Cells formed in H_3PO_4 solution at 10 V have an average diameter of 40 nm, whereas those formed at 10 V in MPA solution have an average diameter of ~30 nm. Likewise, the pores in the MPA oxide are also smaller than pores in the H_3PO_4 anodic oxide. Control of bath temperature was especially critical for MPA anodizing, since it was noted that there was a tendency for burning to occur if the bath temperature increased above 25°C.

The anodic oxide formed in EPA solution was also a porous-type oxide. This is evident from the micrograph in Figure 6.20 that shows a cell structure similar, but not identical, to that of the MPA anodic oxide. The EPA anodic oxide structure appears to be intermediate between a porous anodic oxide formed in MPA and the barrier anodic oxide formed in VPA solutions. The cells are not uniform in size or array.

Figure 6.20. Transmission Electron Micrograph of Anodic Film Formed on 6061-T6 in 1 M Ethylphosphonic Acid - 10 V, 5 min, 23°C

For methyl- and ethylphosphonic acids, the organic groups are apparently not bulky enough to prevent the acidic medium from dissolving the anodic oxide, resulting in porous anodic oxides. The vinyl group of the VPA molecule is expected to be smaller than the ethyl group of the

ethylphosphonic acid molecule, yet barrier oxides are formed in VPA electrolyte and porous oxides are formed in EPA electrolyte. This is contradictory to the above-proposed mechanism of barrier oxide formation in most organophosphonic acid electrolytes. The reasons for this discrepancy are not apparent. A speculative explanation for this is that delocalization of the electrons away from the vinyl group in VPA results in a longer C=C bond length than would be observed normally, and because of this, the oxide is protected from dissolution by the aqueous acid, or alternatively perhaps there is a small degree of VPA polymerization on the surface.

B. Adhesive Bonding

Single lap shear tests were used to evaluate the initial strength of joints with VPA anodic surface films, and to compare these values with joints prepared with etched-only and phosphoric acid anodized adherends. Unless otherwise specified, all organophosphonic acid anodizations for structural adhesive bonding were done for 30 s at 40 V and 23°C. All organophosphonic acid anodized 6061-T6 adherends were bonded with the XA-3498 paste adhesive, so that the bonded system would be representative of joints used in the automotive industry. The lap shear breaking strengths are presented in Table 6.6.

Table 6.6. Average Lap Shear Breaking Strengths of Joints with VPA Anodized Adherends and Joints with Industry Standard Pretreatments

Pretreatment	Average Breaking Strength (MPa)	Standard Deviation (MPa)	Failure Mode
9% (w/w) VPA anodization	21.4	1.2	cohesive
18% (w/w) VPA anodization	22.0	2.1	cohesive
BAC5555 PAA	21.9	1.3	cohesive
HF/HNO_3 acid etch	22.0	1.3	cohesive

There is no significant difference in the average lap shear breaking strengths for any of the

surface pretreatments; each average is within one standard deviation of all of the other averages. Furthermore, the apparent failure mode for all of the joints was cohesive within the adhesive. The weakest link in the joint in the dry condition is the adhesive, and all of the surface treatments evaluated provided adequate dry strength to the adhesive/substrate interface.

Wedge tests were used to compare the hydrothermal stability of adhesively bonded aluminum with varying adherend surface pretreatments. Figure 6.21 contains the wedge test results comparing the hydrothermal stability of joints with adherends anodized in 9% and 18% (w/w) VPA to joints with etched-only (HF/HNO_3) adherends.

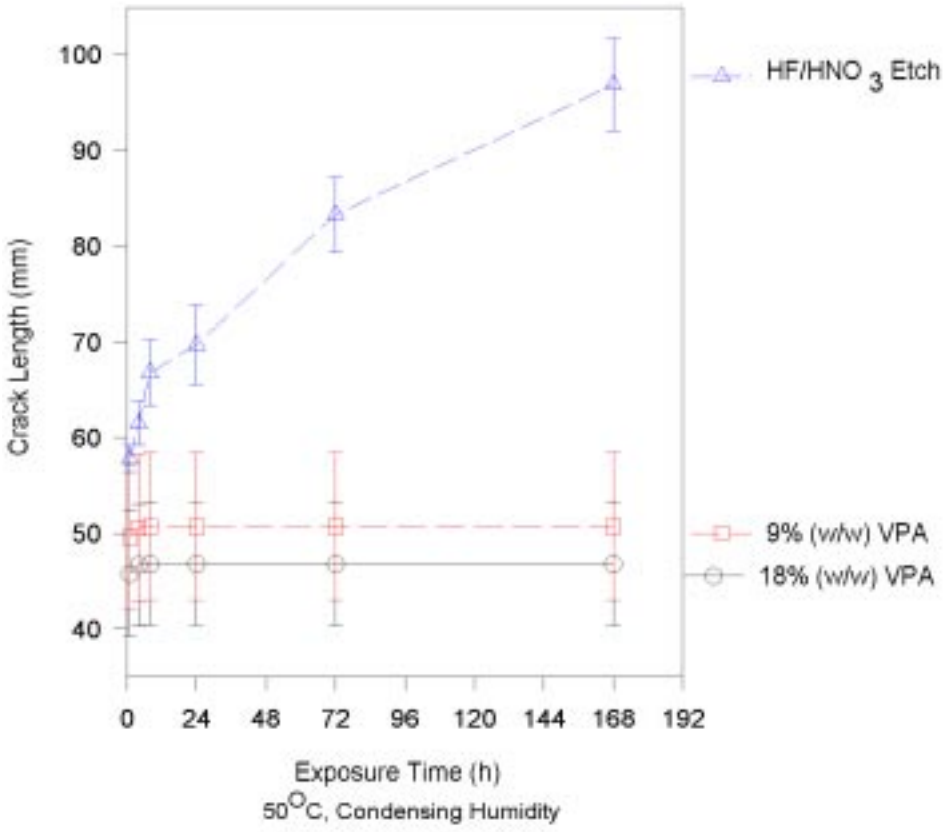

Figure 6.21. Comparison of Wedge Test Durability of 6061-T6 Anodized in Vinylphosphonic Acid Solution with Etched-Only 6061-T6 {40 V, 30 s, 23°C}

There is a dramatic difference in final crack lengths. The final crack lengths for bonds with VPA anodized[293] adherends averaged around 48 mm, whereas the average final crack length for bonds with etched-only adherends approached 100 mm. In addition the apparent failure mode for the VPA joints was thin cohesive, whereas it was interfacial for the etched-only systems.

Wedge tests were conducted to compare VPA anodization to phosphoric acid anodization. These wedge test data are presented in Figure 6.22. (Note: The initial crack lengths for all of the pretreated adherends bonded with XA-3498 epoxy paste adhesive are larger than when similarly treated substrates were bonded with the AF163-2k epoxy film adhesive (see for example Figure 4.6). The AF163-2k adhesive is a higher strength structural adhesive compared to the XA-3498 adhesive (see the lap shear breaking strengths found in Table 4.1 and Table 5.3). The lower strength of the XA-3498 adhesive is manifested in larger initial crack growths, compared with AF163-2k bonded aluminum.)

293. It should be noted that it was previously determined that simple adsorption of VPA onto clean oxidized aluminum surfaces, in lieu of anodization, may suffice to impart adhesive bond durability (*S. F. McCleary, G. A. Nitowski, J. M. Marinelli, and J. T. Siemon, U. S. Pat. 5,463,804* (1995)). For the purposes of this mechanistic study, however, it was felt that anodizing provides a more uniform and continuous layer of organophosphonate on the substrate surface. It is presumed that for barrier oxide formation to occur in these acidic ($pH \leq 1$) electrolytes, all of the available surface bonding sites must be occupied by organophosphonate. Otherwise, oxide dissolution would occur, with ensuing porous oxide formation.

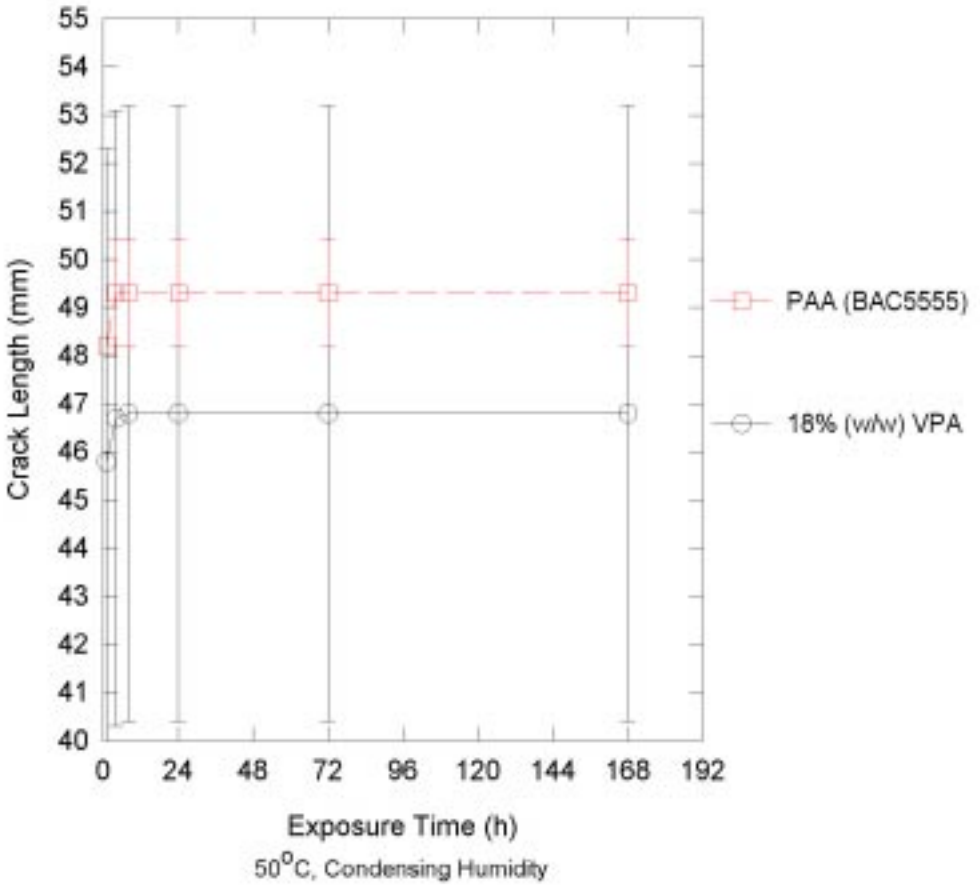

Figure 6.22. Comparison of Wedge Test Durability of Vinylphosphonic Acid Anodizing {18% (w/w) 40V, 30 s} to BAC5555 Phosphoric Acid Anodizing, 6061-T6, XA3498 Epoxy

The average final crack length for joints with 30 s VPA anodized adherends was not significantly different than the crack lengths for bonds prepared using adherends anodized for 20 min according to the BAC5555 potentiostatic PAA process. There was more scatter in the VPAA data than for the PAA pretreatment (the VPAA data represent 20-25 wedge specimens). The cause of this scatter was not determined. However, the microscopically flat VPA anodized adherends provided hydrothermal durability to the bonded systems that was comparable with that of a porous anodic oxide.

As with the functionalized hydroxide films, the importance of the organofunctional group can be empirically assessed by anodizing in solutions of other organophosphonic acids. Solutions of 0.1 M and 1 M ϕPA[294] and nitrilotris(methylene)triphosphonic acid (NTMP) (see Figure 2.8) were prepared. Alloy 6061-T6 was anodized in these solutions at 20 V and 23°C for 30s. Anodization in the 1 M solution of NTMP resulted in the formation of a white powder on the metal coupons. Because of this, no joining tests were done on these samples. Anodization in the 0.1 M NTMP solution resulted in a duplex barrier film, with no evidence of powder on the surface. The results for lap shear testing are in Table 6.7. No lap shear data were collected for 0.1 M ϕPA.

Table 6.7. Average Lap Shear Breaking Strengths for Joints with Adherends Anodized in Phenylphosphonic (ϕPA), Nitrilotris(methylene)triphosphonic acid (NTMP), and Vinylphosphonic Acid (VPA) Solutions

Electrolyte	Average Breaking Strength (MPa)	Standard Deviation (MPa)	Dry Failure Mode
0.1 M NTMP	7.9	1.3	Interfacial
1.0 M ϕPA	18.2	2.6	Cohesive
1.0 M VPA	22.0	2.1	Cohesive

The average joint strengths for the bonds with VPA and the ϕPA anodized adherends are similar, perhaps with a trend, although not statistically significant, for higher strength for adhesive bonds with VPA adherends. For the dry, initial strength, both of these systems failed cohesively in the adhesive. For VPA, this is the same result obtained for the VPA functionalized hydrothermal films. The initial bond strength when using NTMP anodized adherends was less than half of that

294. 1 M solutions of ϕPA were only attainable from one specific lot of ϕPA. An analysis for impurities in this lot of ϕPA was inconclusive. The supplier, Aldrich Chemical Co., did not have an explanation. Other lots of ϕPA were not soluble enough to prepare a 1 M solution.

of the other systems. The poor initial joint strength provided by NTMP anodizations was also observed when one of the wedge assemblies with NTMP anodized adherends fractured (interfacially) during machining of the wedge specimens. Wedge test results for these adherends bonded with the epoxy paste adhesive are found in Figure 6.23.

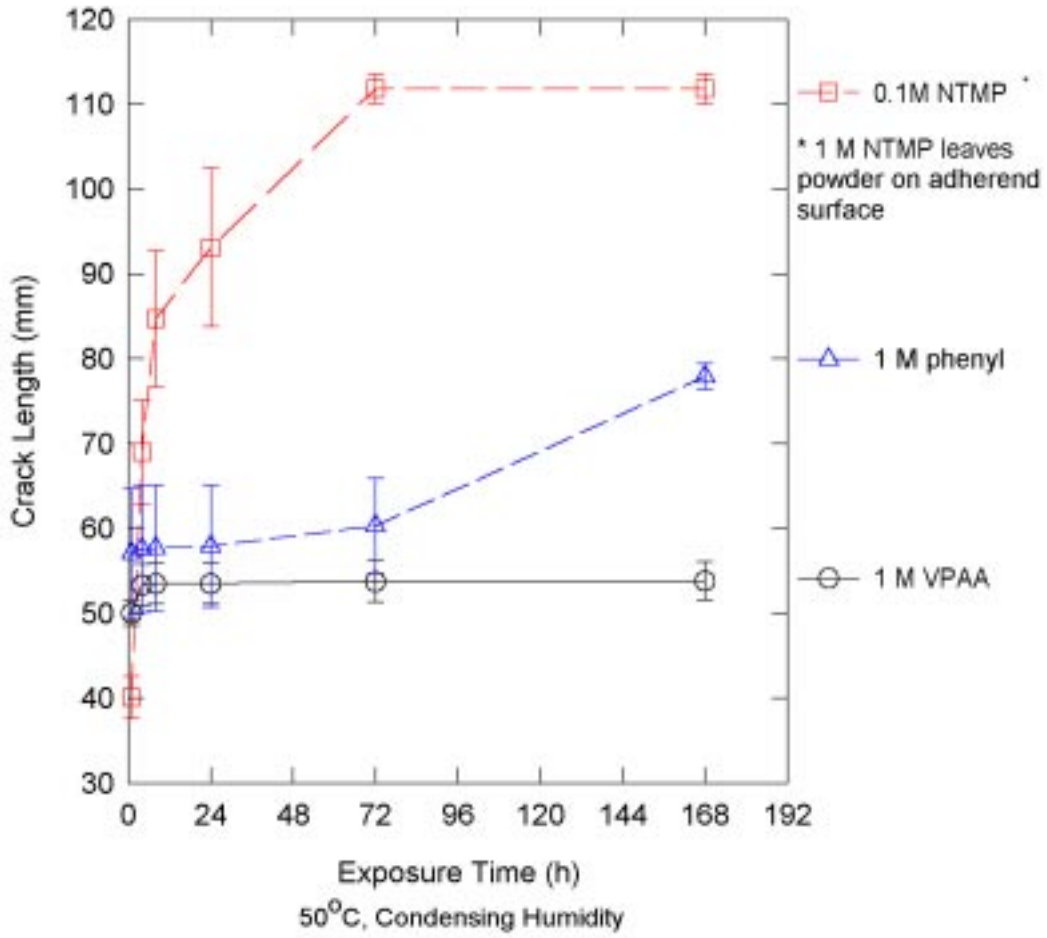

Figure 6.23. Effect of Surface Functionalization with Chemically Unreactive Functional Groups on Adhesive Bond Durability - 20 V, 30 s, 6061-T6, XA3498 Epoxy

The NTMP anodized adherends provided the least hydrothermally stable joints, with the ϕPA yielding intermediate performance. Adhesive bonds with both, NTMP and ϕPA adherends, failed interfacially. Again, the VPA anodization gave superior bond durability to these epoxy-

bonded systems, and failed predominantly as thin cohesive failure. These data, together with the lap shear results suggest that interfacial chemistry does affect bond durability.

The topography of VPA anodic oxide formed in 1 M VPA solution (Figure 6.13), while not exhibiting classical porosity (Figure 4.3), does exhibit slight roughening due to incipient porosity. It is seen in the TEM of Figure 6.15 that a rough surface also results from incipient porosity on allylphosphonic acid (APA) anodized 6061-T6 alloy. Any contribution of this scale of roughness to adhesive joint durability can be discounted by the wedge test results of adhesive bonds with APA anodized adherends (Figure 6.24).

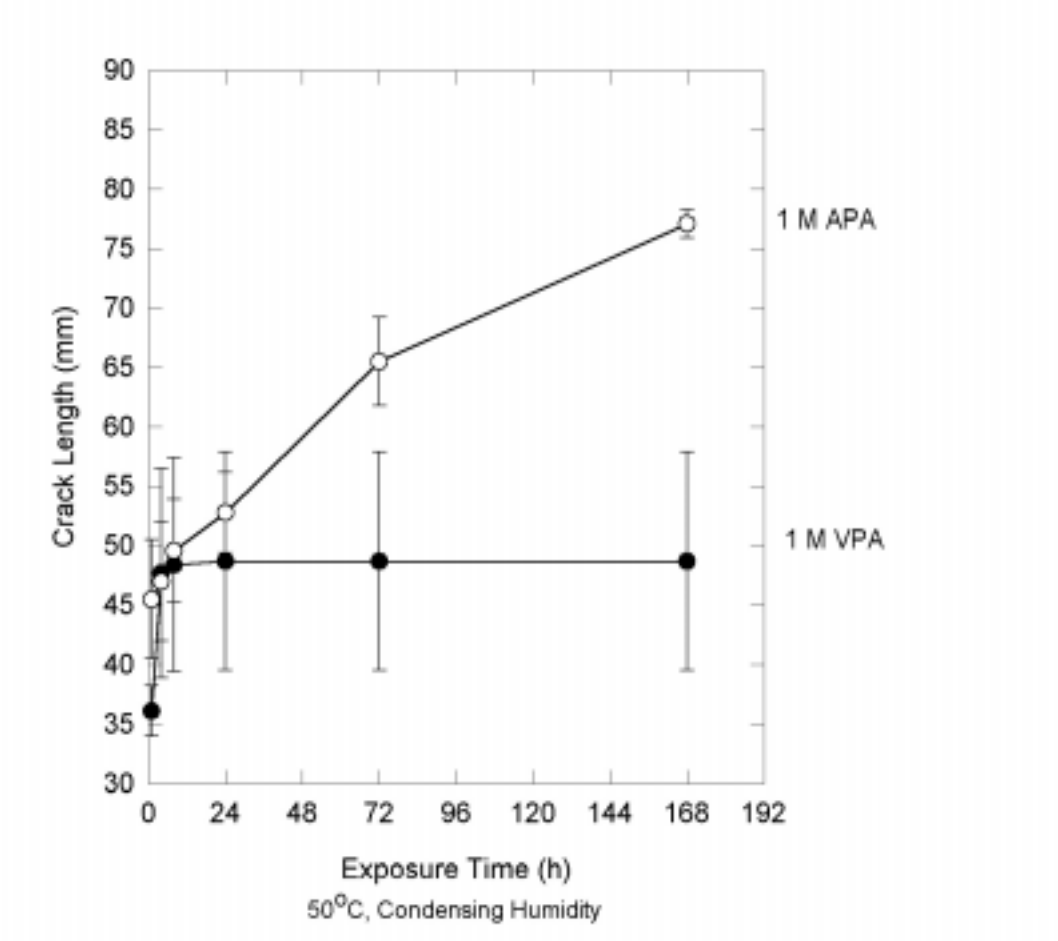

Figure 6.24. Wedge Test Comparison of Adherends Anodized in Vinylphosphonic Acid and Allylphosphonic Acid - 6061-T6, 20 V, 5 min, 23°C, XA3498 Epoxy

Joints with APA anodized adherends exhibit poor hydrothermal stability as is evidenced by the wedge test crack lengths in Figure 6.24. The wedge test results indicate the environmental durability does not correlate with surface roughness, since the VPA and APA anodized surfaces are both almost microscopically smooth.

A FT-IR transmission spectrum of 15 mg of APA in a KBr pellet is shown in Figure 6.25.

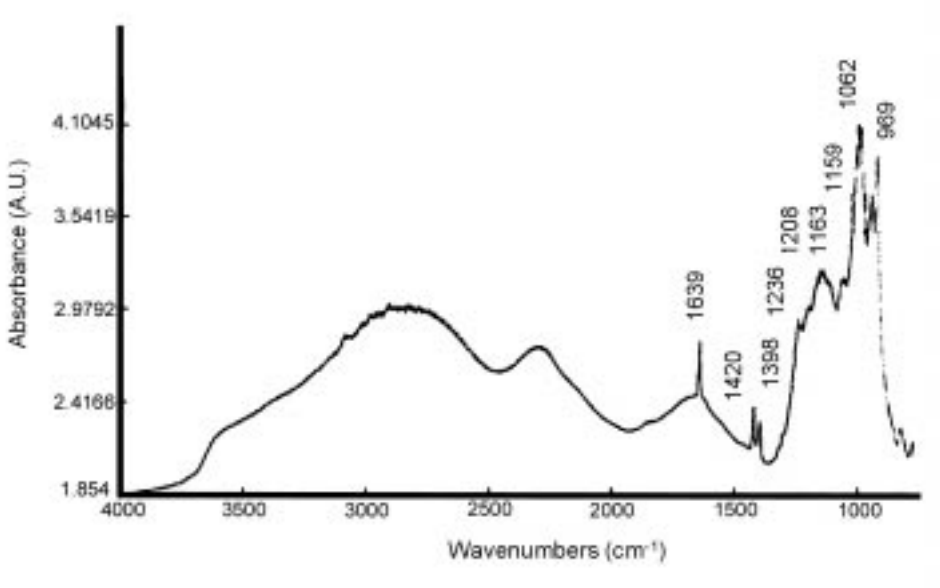

Figure 6.25. FTIR Transmission Spectrum of ~15 mg of Allylphosphonic Acid in a KBr Pellet

The C=C stretch band for APA is found at 1639 cm^{-1}, which is expected for an isolated vinyl-group.[269] It is recalled the frequency of the C=C stretch vibration for VPA was observed at 1613 cm^{-1} (Table 5.2).

The empirical and spectroscopic data support the argument that VPA acts as a chemical coupling agent between the adhesive and the adherend to impart environmental durability. Hydrolytically stable Al-O-P bonds are formed between VPA and aluminum oxide/hydroxide (Figure 5.9).

Determination of bonding of VPA with the adhesive in a joint is not easily accomplished since this is a buried interface, which is inaccessible to spectroscopic analysis, and since the analysis of fracture surfaces is encumbered by artifacts generated during the fracturing process.

Attempts were made to react VPA treated surfaces with low molecular weight analogues of epoxy resin components, for subsequent XPS examination of the surface reactant products. These attempts were unsuccessful. Finally, it was decided to model the VPA/adhesive reaction using bulk chemical. This is the subject of the next Chapter.

Chapter 7. Simulation of Interfacial Chemistry by Bulk Reactions

The reaction mechanism of vinylphosphonic acid with oxidized aluminum was spectroscopically identified in the preceding chapters. Empirical adhesive bonding data suggested that there was a further chemical reaction of VPA on the surface of aluminum oxide/hydroxide with components of the epoxy adhesives. The nature of this reaction was intractable due to inaccessibility of the intact interface to spectroscopic analysis.

Bulk compounds were used to simulate reactions that could occur at the interface of VPA treated aluminum and the epoxy adhesive. Propylene oxide was used to simulate the epoxide components of the adhesive. A latent curing agent of the adhesives (AF163, XA3498) that were used in the preceding accelerated durability testing, dicyandiamide (DICY), was also used in the bulk reaction simulation. Dimethylvinylphosphonate (DMVP) represented the reaction product that forms on the oxidized aluminum that has been treated with VPA. The ester, DMVP, does not facilitate salt formation, as could occur with DICY and the acidic protons of VPA. Neat DMVP and PPO are liquids in ambient laboratory conditions; DICY is a solid. The molecular structures of the compounds used in this simulation are found in Figure 7.1.

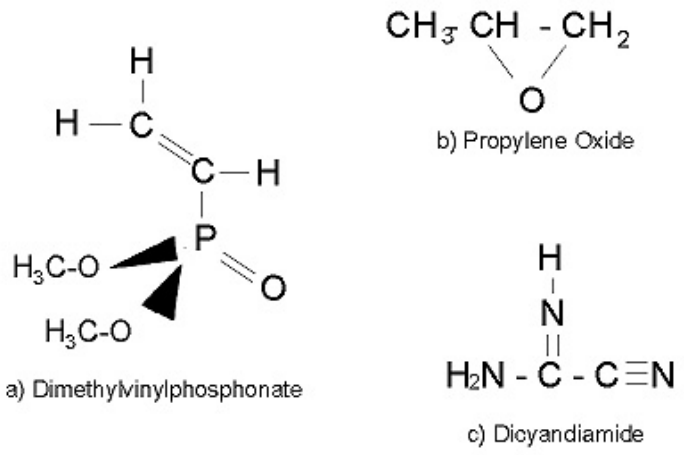

Figure 7.1. Molecular Structure of Bulk Reactants

Stoichiometric ratios of DICY or PPO were mixed with DMVP. The ratios are found in Table 3.1. The stoichiometric mixtures and the neat compounds were placed into individual Teflon-lined stainless steel reactor bombs, and heated at 150°C for 24 h. This temperature represents a curing temperature for epoxy adhesives that use DICY as a latent-hardening agent. At the end of the 24 h the bombs were allowed to cool, and were opened. The reaction products of all of the mixtures, except 1 DMVP**:**2 DICY, were liquids of various viscosity. The 1 DMVP**:**2 DICY product was a hard solid. The neat compounds maintained their original physical state after heating.

For ^{13}C NMR analysis, the liquid samples were dissolved in d_6-dimethylsulfoxide (d_6-DMSO). ^{13}C NMR analysis showed that neat PPO and mixtures of PPO and DMVP did not decompose or react during heating. The spectrum of heated PPO was identical to the spectrum of PPO taken directly from the manufacturer's bottle. The spectrum of the PPO / DMVP mixture was a mixture of the neat spectra of the two compounds. Since no literature was uncovered regarding the reaction of carbon double bonds and epoxide rings, no further work was done with PPO.

The ^{13}C spectrum of 300 mg of DICY dissolved in DMSO was also identical to the ^{13}C spectrum of DICY heated to 150°C. This indicates that neat DICY does not decompose at 150°C. A representative ^{13}C NMR spectrum of DICY is presented in Figure 7.2. The experimental DICY spectra matched one obtained from the Aldrich NMR Library.

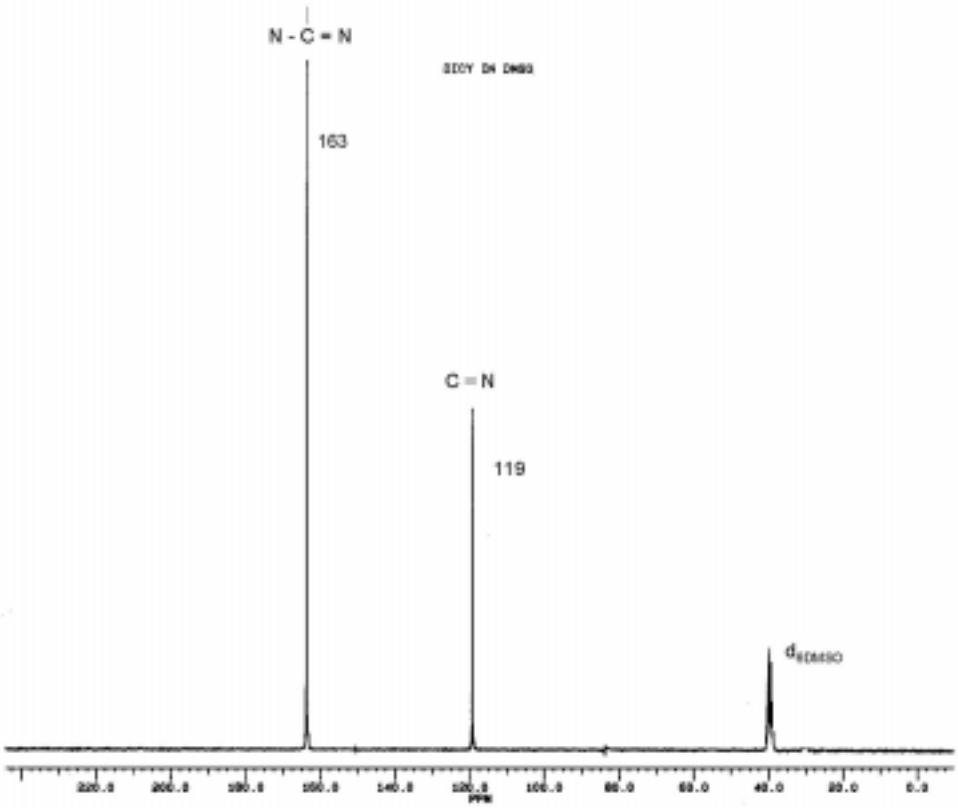

Figure 7.2. ^{13}C NMR Spectrum of 300 mg Dicyandiamide Dissolved in d_6-DMSO

The ^{13}C NMR spectra of DMVP and DMVP heated to 150°C were also identical. Neat DMVP does not decompose when heated to 150°C. A representative ^{13}C NMR spectrum of 600 mg DMVP dissolved in d_6-DMSO is presented in Figure 7.3.

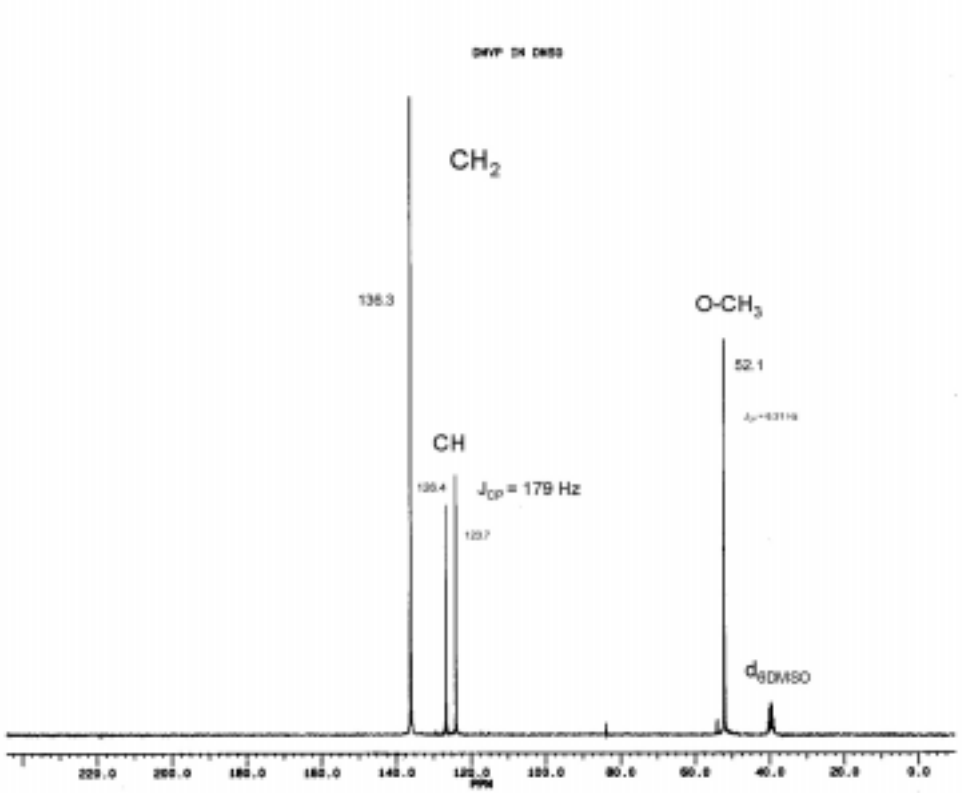

Figure 7.3. ^{13}C NMR Spectrum of 600 mg Dimethylvinylphosphonate Dissolved in d_6-DMSO

When the 1 DMVP**:**1 DICY mixture was heated to 150°C a semi-solid material was obtained. The ^{13}C NMR spectrum of this material in DMSO is presented in Figure 7.4. Peaks attributed to vinylic-CH_2 (137 ppm) and vinylic-CH (doublet around 124 ppm) are still present, but their intensity is substantially diminished. The peaks attributed to C≡N (119.5 ppm) and N-C=N (163.5 ppm) are completely absent from the spectrum. These data indicate that the groups from the dicyandiamide have been consumed in the reaction sequence, and that the vinyl-groups are present in excess in the 1**:**1 sample.

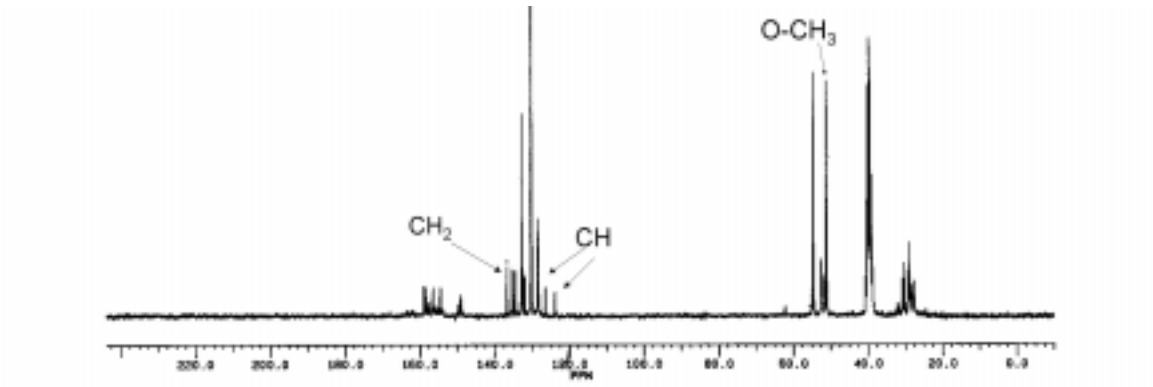

Figure 7.4. ^{13}C NMR Spectrum of 1 mole Dimethylvinylphosphonate : 1 mole Dicyandiamide Reaction Product in d_6-DMSO

The ^{13}C NMR spectrum for all other ratios of DMVP to DICY that are greater than 1, showed the same trends. In these spectra, the signals due to the vinylic carbons increased in intensity with increased concentration of DMVP. There was no evidence of the original DICY peaks in any of the spectra of reaction products with ratios of DMVP to DICY equal to one or greater. The ^{13}C NMR spectrum of the reaction product of the 6 DMVP **:** 1 DICY sample is presented in Figure 7.5.

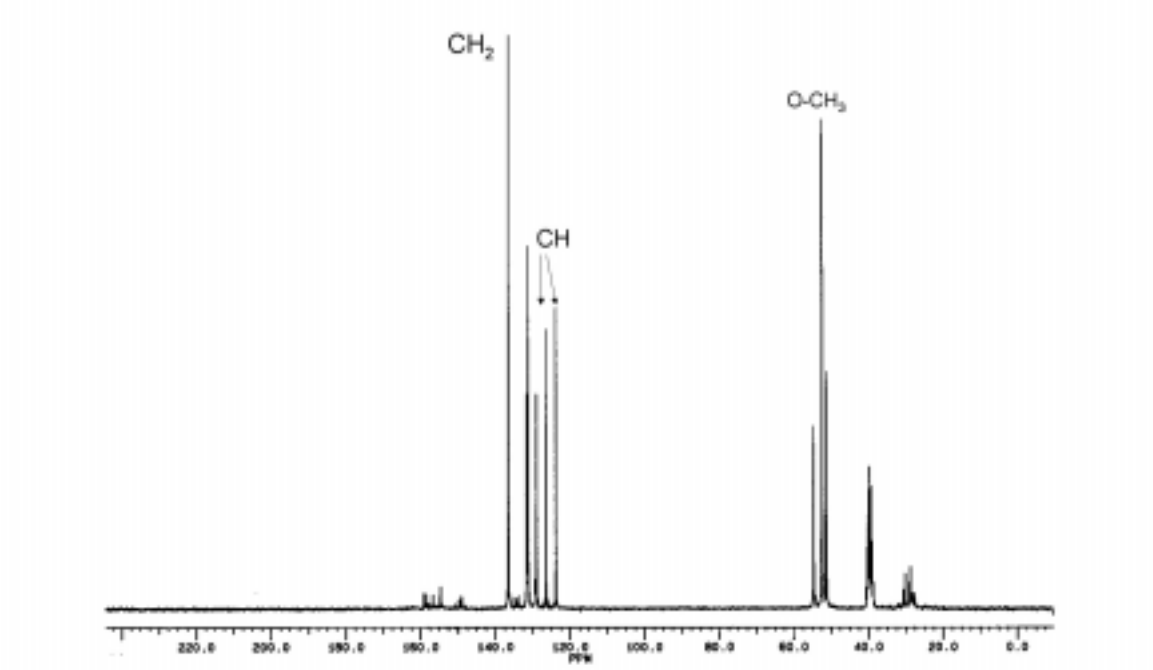

Figure 7.5. ^{13}C NMR Spectrum of the Reaction Product of 6 Moles of Dimethylvinylphosphonate and 1 Mole of Dicyandiamide

Lastly, it is recalled that the reaction product of 1 DMVP **:** 2 DICY was a hard solid. The solid was insoluble in common solvents. 600 mg of the solid material was placed in d_6-DMSO and was ultrasonically agitated and warmed to facilitate dissolution. After 24 h, a substantial amount of solid remained in the beaker. The d_6-DMSO was pipetted off of the solid, and a ^{13}C spectrum was obtained. After 1000 scans, only peaks from the solvent were observed. Therefore, the solid sample was analyzed using solid-state Cross Polarized Magic Angle Spinning-NMR. The CPMAS-NMR ^{13}C spectrum for 1 DMVP **:** 2 DICY is presented in Figure 7.6. Of note in this spectrum is that the peak for vinylic CH_2 (137 ppm) is absent. There is no substantial evidence that the original vinyl group is present in this sample. A small peak at about 122 ppm is present, and is attributed to C≡N. The large peak around 167 ppm is assigned to the C=N group.

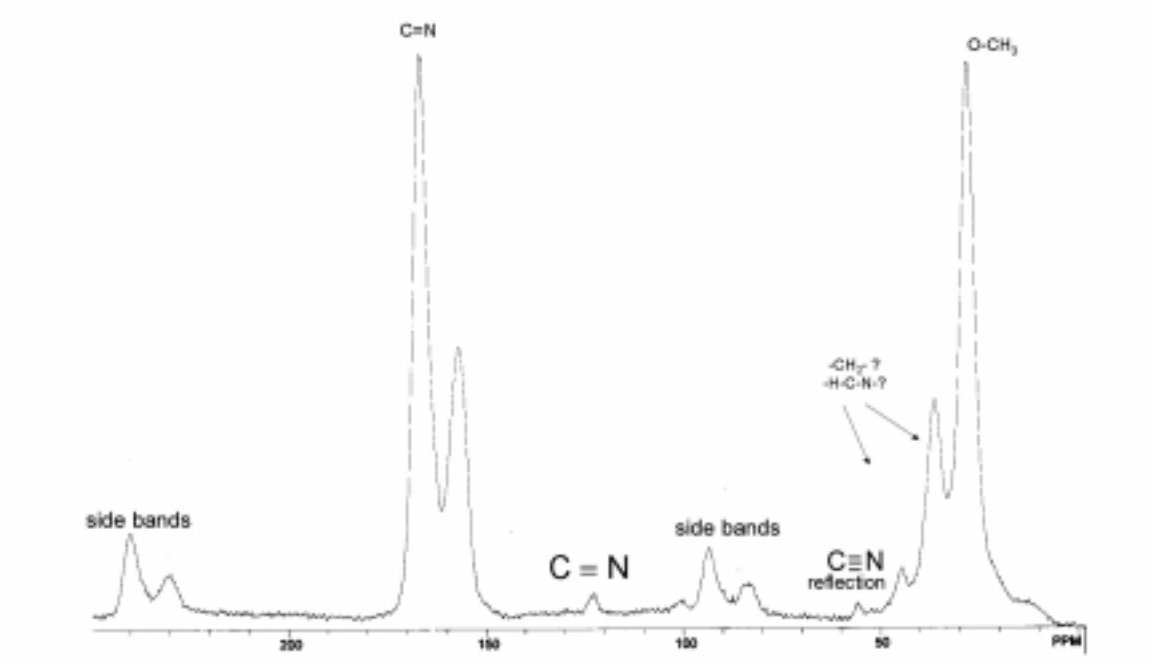

Figure 7.6. ^{13}C CPMAS-NMR Spectrum of the Reaction Product of 1 Mole Dimethylvinylphosphonate and 2 Moles Dicyandiamide

All of the vinyl- groups of the dimethylvinylphosphonate have reacted with the dicyandiamide. Since signals from C≡N and C=N are present, it is reasoned that the vinyl groups most likely reacted with the primary amine present on the dicyandiamide molecule (Figure 7.1). This reaction scheme involving a Michael Addition was proposed and schematically presented in Figure 4.16.

Chapter 8. Discussion

The wedge test data presented in the previous chapters provide an empirical correlation between the chemical state of adherend surfaces and bond durability. The data support the proposition that the formation of hydrolytically stable chemical bonds between the adhesive and the adherend is the dominant requirement for bond durability. Mechanical interlocking, as a major mechanism in controlling the durability of epoxy-bonded aluminum structural joints, is not supported by these data.

This wedge test does not provide a rigorous measurement of mechanical or chemical properties of a metal-polymer bond; it only allows a relative comparison of performance under standard conditions.[209] The analyses presented herein and interpretations of experimental results should be viewed in the context of the limitations of this test.

It is recalled that the crack lengths and failure mode for the bonded specimens with adherends anodized for 2 min or longer in phosphorous acid solution were comparable to the CAA and 20 min PAA results (Figure 4.6). However, this was not the case for the oxide formed in 2 min in phosphoric acid solution. The thickness of the HPAA oxide grown in 2 min was less than half of the thickness of the oxide formed in the 20 min PAA process. Also, cell and pore diameters of the anodic oxide on the 2 min HPAA adherend (Table 4.2) were the same as those on the 20 min PAA adherend. Therefore, the pore volume and bonded surface area of the 20 min-PAA oxide are at least twice as large as those of the 2 min-HPAA oxide films. It was suggested that if the crack propagation rate in the wedge test is influenced by the chemical state of the surface, the effect of HPAA oxides on the environmental durability of the adhesive bond must be significantly greater than that of the PAA oxide.

An effect of interfacial chemistry on joint durability is suggested by a comparison of the crack propagation in adhesive bonds made with geometrically identical anodic oxides formed in

solutions of the two inorganic phosphorus oxo acid electrolytes. Adhesive bonds prepared with substrates that were anodized in H_3PO_3 solutions exhibited lower wedge test crack growth compared to those prepared with adherends that were anodized in H_3PO_4 solutions. The NMR results revealed a higher density of coordinatively unsaturated aluminum (tetrahedral Al-O) in the bulk of the HPAA oxides, compared with the PAA oxides. As with γ-alumina, which has considerable tetrahedral coordination and a highly reactive (catalytic) surface, it is reasonable to assume that the higher degree of tetrahedral coordination detected in the HPAA oxides translates into a higher reactivity for the surface of the HPAA oxide, compared to the PAA oxide. Since surface topographies of the anodic oxides are practically identical, the difference in wedge test crack growths is attributed to the differing surface chemistry (acid-base sites), and the subsequent type and density of interactions with the adhesive resin.

The failure mode for *both* PAA and HPAA topographically identical anodic oxides was thin cohesive. It is speculated that thin cohesive failure is affected by the morphology and composition of the polymer interphase, which is in turn affected by the chemical state of the adherend surface. Different acid-base chemistry at the anodic oxide surface could influence the curing and subsequent morphology of the resin in the interphase, similar to the effect of surface treatment on interphase resin morphologies observed by Kötting.[215] The survey of the literature provided examples of low molecular weight components of the adhesive,[218] particularly amine curing agents,[219-222] that were present in excess in the interphase. A different stoichiometry of resin components in the polymer interphase, compared with bulk polymer, should result in an interphase polymer composition that is different from the bulk polymer composition. By purely entropic considerations, the presence of a surface would reduce the number of conformations available to the growing oligomers and polymers adjacent to the surface. Therefore, in addition to differences in composition, the interphase polymer could have a different morphology (cross-linking density) than the structure of the bulk polymer. Interphase polymer composition and morphology were not determined in this investigation. However, the observation that joints with HPAA and PAA adherends both exhibited thin cohesive failures, but at different rates, strongly suggests that the properties, and therefore the composition and morphology of the polymer

interphase for these bonded systems are different from each other and different from the bulk adhesive.

It is to be expected that interactions occurring between the adhesive and the adherend, particularly primary bond formation as depicted in Figure 4.16, would alter the morphology of the interphase polymer. Adhesive resins that are highly reactive with the adherend surface should form a cured polymer interphase structure that is different from resins that do not react strongly with the adherend surface. Functional groups of the resin that would normally be involved in curing reactions can instead react with functional groups on the adherend surface. Depending upon the chemical compatibility, or reactivity, of the adhesive and the surface, the number of functional groups reacting *across* the interface would be different, resulting in different polymer interphase structures.

Determination of the actual differences in composition and morphology of the polymer interphase that result from varying degrees of reactivity and type of interaction between the adherend and the adhesive is beyond the scope of this dissertation. However, one can speculate that these could include differences in cross-linking density and free volume. In the presence of moisture and stress, it is reasonable to assume that interphases of differing morphology will respond differently. The swelling behavior and response to stress will be different, and could account for the observed thin cohesive failure at different failure rates that was observed in the wedge test.

In the experiment where oxalic acid anodic oxides were functionalized with VPA and NTMP, it is proposed that VPA functions as a chemical coupling agent between the oxide and the resin. It was demonstrated that VPA forms hydrolytically stable bonds with the aluminum oxide/hydroxide surface (Figure 5.10). The electronic configuration of the VPA molecule provides the possibility of nucleophilic addition of resin nucleophiles to the carbon double bond (see Figure 4.16). It was suggested in Chapter 4 that the potential exists for the amine group of the dicyandiamide curing agent to add to surface carbon double bonds on VPA treated aluminum

(nucleophilic Michael addition, see Figure 4.16). A condition for nucleophilic addition is that there is electron withdrawal from the carbon double bond by a vicinal electronegative group. The FTIR and IETS analyses of VPA (Table 5.2) demonstrated that the PO_3^{2-} group does distort the electron cloud towards the α-carbon. The C=C stretching vibration was observed approximately 30 cm^{-1} lower than what is observed for isolated C=C bonds (1613 cm^{-1} versus 1640 cm^{-1}, respectively). This shift in vibrational frequency indicates that electrons are withdrawn from the carbon double bond of VPA. Hernández-Laguna, et al.,[295] using *ab initio* quantum mechanical calculations and ^{13}C-NMR data show that electrons in the C=C double bond of VPA are strongly polarized toward the phosphorus, and that the β-carbon (farthest from the phosphorus atom) is less shielded than the α-carbon. Electron withdrawal from the vinyl group on the VPA molecule is most likely due to induction effects due to the vicinal PO_3^{2-} group, but UV absorption spectroscopy data indicate that the C=C/P=O system in VPA has weak conjugation, which could also account for electron delocalization.[295]

Electron withdrawal does not occur when the C=C double bond is separated from the phosphonate group by a methylene group, as is the case with allylphosphonic acid. APA is not activated for nucleophilic addition by inductive electron withdrawing effects. The C=C stretch band for APA is found at 1639 cm^{-1}, which is expected for an isolated vinyl- group.[269] It is recalled the frequency of the C=C stretch vibration for VPA was observed at 1613 cm^{-1} (Table 5.2). The C=C on APA bond is shielded from the electronegative PO_3^{2-} by a methylene group (Figure 6.14). The observation that APA anodization does not extend environmental durability to adhesive bonds supports the mechanism of nucleophilic addition (Michael Addition, Figure 4.16) of the amine-group of the dicyandiamide curing agent to activated vinyl-groups of the surface VPA, and not to isolated C=C bonds. The lack of electron withdrawal from the allyl-carbon double bond correlated with poor durability, and the correlation of electron withdrawal on VPA and good durability, provides strong evidence that nucleophilic addition of an epoxy

---

295. A. Hernández-Laguna, C. I. Sainz-D•az, Y. G. Smeyers, J. L. G. de Paz, and E. Gálvez-Ruano, *J. Phys. Chem., **98*** (1994) 98.

adhesive component, presumably an amine-group from the dicyandiamide curing agent, is providing a hydrolytically stable linkage of the VPA treated surface with the adhesive.

The bulk chemical reactions proved that nucleophilic Michael Addition of the amine group of the DICY curing agent is possible, and most likely occurs at the epoxy resin/VPA bonded interface during curing. There is strong evidence that the primary amino- group on the DICY molecule adds to the surface VPA double bond. In the ^{13}C NMR spectrum of the 1 DMVP**:**2 DICY reaction product (Figure 7.6) the ratio of the C=N to C≡N peaks is much larger than the same ratio for neat DICY (Figure 7.2). The spectra were collected using cross polarization. This means that the signals from carbon nuclei that are in close proximity to protons will be amplified. In the proposed structure of the reaction product (see Figure 4.16 for analogous product reacted to surface VPA), the closest proton to the carbon nucleus of C≡N is separated by two atoms, whereas the closest proton to the C=N is only separated from the C nucleus by one atom. Due to cross polarization, and considering the proposed reaction product, one would expect the signal from C≡N to be small, compared to that from C=N.

After addition of the primary amine of the DICY to the surface vinyl group, the multifunctional DICY curing agent could then further react with epoxide groups of the adhesive. This would provide a cross-linked and hydrolytically stable interface. This reaction scheme supports the wedge test data for joints with VPA treated adherends, regardless of the surface topography. VPA surface treatment consistently provided durable adhesion, whether the topography was that of porous oxides, gelatinous boehmite or the non-porous, relatively flat barrier anodic oxides.

A lack of chemical bond formation is responsible for poor results when using NTMP-coated surfaces. Because the literature states[262] that tertiary amines do not react with epoxides, but do catalyze their cure, and because adhesion durability is decreased from that of anodized-only, it is reasonable to assume that a lack of chemical bonding at the NTMP-adhesive interface resulted in poor joint durability for the NTMP porous oxides. These results conflict with those of Hardwick,

et al.,[173] but NTMP coating, as practiced in this dissertation, consistently resulted in poor adhesive joint durability, irrespective of the surface topography.

The wedge test study on inorganic phosphorus oxo acid functionalized hydroxide films, presented in Chapter 5 corroborate the intrinsic role of interfacial chemistry in determining joint durability. It was observed that wedge test durability of bonds with functionalized hydroxide films with identical topography could be changed from good to poor by changing the functionality on the surface.

As with the porous anodic oxides, functionalizing the hydroxide film with phosphoric or phosphorous acid resulted in acceptable performance, but a significant difference was observed in the final crack lengths, with the phosphorous acid joints exhibiting lower crack lengths than the phosphoric acid joints. For the acid-modified gelatinous boehmite films, the difference could be attributed to inherent differences in reactivity of the acid complexes that form on the surface after rinsing of the acid dipped surfaces. Based on the IETS results of phosphorous acid adsorption on aluminum oxide presented by Ramsier, et al.,[258] it is reasonable to suggest that dipping the hydrothermally formed hydroxide films in H_3PO_3 solution, versus H_3PO_4 solution will result in different species on the outer surface of the hydroxide film. For H_3PO_3, Ramsier, et al. [258] demonstrated that phosphorous acid bonds with the oxidized surface by an acid-base reaction involving the three phosphonate oxygens and hydroxyl groups on the oxide surface. This orientation results in a resonance structure on the surface with a P-H bond extended away from the surface. It is not unreasonable to assume that phosphoric acid reacts with hydroxylated aluminum in a similar fashion. The resulting ligand that extends away from the surface for the case of the H_3PO_4 / hydroxyl reaction would either be P-OH or P=O. The interactions of adhesive resins with P-H, P-OH, or P=O are not well documented, but intuitively, one would expect these interactions to be vary in bond strength and resistance to hydrolysis.

Hydroxide films treated with vinylphosphonic acid provided strong and durable joints. However, when the surface films were functionalized with ethylphosphonic acid, joint durability was found

to be deficient. Considering that the hydroxide films exhibit a rough surface, if mechanical interlocking were the dominant mechanism in determining durability, even the ethylphosphonic functionalized films should have yielded joints with some degree of hydrothermal stability. This was not the case. The aliphatic ethyl- group only provided secondary bonding (dispersion forces) of the substrate with the adhesive. Thus, as described previously, when water diffuses to the adherend/adhesive interface of joints with EPA treated adherends, W_A becomes negative, and without hydrolytically stable primary bonds between the adhesive and the substrate, the joint fails. This was exhibited in the wedge test as high crack lengths and interfacial failure for joints with EPA treated adherends when exposed to applied stress and humidity.

With boiled-only gelatinous boehmite films or with oxalic acid anodized-only porous oxides, the adhesive can interact with surface hydroxyl groups. In terms of chemical interactions, the hydroxyl surface groups can form chemical bonds with functional groups in the adhesive. Surface hydroxyl groups can act as Brönsted acid sites and donate a proton to epoxide groups resulting in aluminum alkoxide bonds,[296] hydroxyl groups in the adhesive can react in a acid-base (condensation) reaction with Brönsted acid surface hydroxyls to form surface alkoxide linkages.[296] Amines in curing agents can react with Lewis acid sites, by transfer of electrons from the nitrogen atoms in the amine to coordinatively unsaturated aluminum sites on the surface, or with Brönsted acid sites on the surface, by transfer of a proton from a surface hydroxyl to the amine group of the curing agent.[55] None of these interactions is as hydrolytically stable as the proposed reaction product of the nucleophilic addition of the amine- group of dicyandiamide with the carbon double bonds of surface VPA, and this is macroscopically expressed in less durable adhesive bonds for joints with boiled only (and anodized only) adherends, compared with VPA treated adherends.

The most convincing evidence that surface roughness (porosity) and mechanical interlocking are

---

296. secondary reference, M. Nishio, K. Usa, and U. Hasegawa, *Sumitomo Keikinzoku Giho, **30*** (1989) 36, in M. Imai and M. Nishio, *Sumitomo Keikinzoku Giho, **30*** (1989) 22.

not required for the formation of durable joints, was presented in the chapter on organophosphonic acid anodizing. For these systems, adherends possessing microscopically flat, barrier anodic oxides formed in vinylphosphonic acid solution yielded joints that were as durable as those formed with adherends with porous anodic oxides formed by the standard phosphoric acid anodizing process. Furthermore, by changing the functional group on the organophosphonic acid, the durability, and initial bond strength could be manipulated from extremely good to extremely poor. The durability and initial strength decrease in the order: VPA > ϕPA > NTMP.

The correlation of adhesive bonding data with oxide structure and composition presented in this dissertation do not support the idea of mechanical interlocking as a mechanism for enhancing adhesive bond durability. The data present a consistent picture that chemical bond formation at the interface is the controlling factor in adhesive bond durability. In particular, forming a hydrolytically stable interphase by establishing hydrolytically stable, primary chemical bonds between the adherend, and in this case, the adhesive curing agent is the controlling factor in maintaining adhesive joint strength in the presence of stress and humidity. This is attained with the VPA treatments by the ability of VPA to form hydrolytically stable bonds with the adherend oxide film and with adhesive components.

The reaction of the curing agent with the surface in a manner suggested above provides many perceived benefits for adhesive bond durability. Firstly, a hydrolytically stable bond is formed between the curing agent and the VPA treated surface. Secondly, since the dicyandiamide molecule is multifunctional, the surface species can participate in cross-linking of the epoxide groups in the adhesive. This would create a strong, hydrolytically stable interphase region of polymer that may be more resistant to swelling and other effects of moisture. Thirdly, it was previously shown[12] that a possible cause of adhesive bond failure in humid environments is a result of dissolution of the oxide substrate caused by a stoichiometric excess of amine curing agents and localized high alkalinity at the oxide/adhesive interface.[220,221] By chemically reacting the amine curing agent with the surface, the possibility of the alkaline failure mechanism is diminished.

The current thesis can be summarized by saying that durable adhesion is obtained when a hydrolytically stable interphase is formed between the adhesive and the adherend. A hydrolytically stable interphase is achieved when hydrolytically stable, primary bonds are formed between the adherend and the adhesive. While it is not argued that an inherently hydration resistant surface film will add to durability, the current results indicate that surface hydration resistance, alone, does not guarantee bond durability. The literature shows that NTMP treated surfaces are extremely hydration resistant.[172] However, when the oxide surface is fully covered with NTMP, as during anodizing in NTMP, or with NTMP functionalized porous oxides, joint durability is not provided because of lack of chemical bonding with the adhesive. As described earlier, tertiary amines catalyze the reaction of epoxide- groups with each other, but do not react with epoxides.[262]

Surfaces that are not highly resistant to hydration, such as those obtained with phosphorous acid (HPA) anodizing, provide highly durable bonds. The increased reactivity of the HPA anodized surface with the epoxy adhesive, compared with PAA surfaces, provided durable bonds without the prerequisite of inherent oxide hydration resistance. Furthermore, morphological changes of the aluminum oxide surface, which are suggested to be responsible for joint failure,[229] require water in liquid form, while the aluminum oxide - organic adhesive bonds (Al-O-R) can be attacked by molecularly dispersed water. Therefore, bond durability is enhanced by the formation of hydrolytically stable Al-O-R bonds. Even if the substrate oxide is not inherently resistant to hydration, a high density of hydrolytically stable aluminum oxide - adhesive bonds limits the sites (capillary gaps) where liquid water can form, and change the composition, morphology, and consequently, the strength of the adherend oxide and the bonded joint.

The combination of the chemical interaction of the VPA treated surface to form hydrolytically stable bonds with the adhesive, and the hydrolytically stable $(Al\text{-}O)_3$-P bonds that are formed with the aluminum oxide result in the formation of a *hydrolytically stable interphase*, regardless of the topography of the surface. Durable adhesion is obtained on microscopically flat surfaces,

as well as with porous oxides.

Analyses of all of the data provided in this dissertation support the thesis statement presented initially, which is rephrased, and presented again as a conclusion. The data presented indicate that the chemical state of the aluminum surface film, and the resulting interaction with the adhesive resin, are the dominant factors in determining the environmental durability of epoxy-bonded aluminum joints. It is not argued that surface topography has an effect on the initial "dry" joint strengths. However, in the presence of moisture and stress, epoxy-bonded aluminum requires a chemically coupled, hydrolytically stable interphase to maintain "wet" joint strengths that are comparable to initial dry strengths.

A chemically coupled, hydrolytically stable interphase can be attained when hydrolytically stable primary bonds are formed between the aluminum oxide and the organic adhesive, and when the aluminum oxide is chemically converted to increase the hydration resistance of the oxide. The second requirement is necessary to prevent chemical and physical changes of the substrate surface in the event that water, molecularly diffusing through the polymeric adhesive, would be able to form a liquid phase by capillary condensation in areas of the adherend not wet by the adhesive, that is, in capillary gaps. Condensed water could change the oxide into a hydroxide, with a concomitant increase in volume, a decrease in the mechanical strength, and subsequent joint rupture.

Morphological changes of the aluminum oxide surface require water in liquid form, while the aluminum oxide - organic adhesive bonds (Al-O-R) can be attacked by molecularly dispersed water. Therefore, the more resistant the Al-O-R bond is to hydrolysis, and the higher density of bonding sites per unit area, the better is bond durability. The durability enhancement observed with certain, but not all, porous anodic aluminum oxides can be explained by the increase in the total surface area per unit geometric that porosity provides, and the potential to form more hydrolytically stable bonds between the adhesive and the oxide. Also, because there are few capillary gaps in the interphase of a properly prepared joint, even if the substrate oxide is not

hydrolytically stable, a high density of hydrolytically stable aluminum oxide - adhesive bonds limits the sites where liquid water can form, and change the composition, morphology, and consequently, the strength of the adherend oxide and the bonded joint.

These conclusions can be drawn from the analysis of the test results for the aluminum alloy / epoxy systems under investigation. It is likely that the conclusions drawn here could be applicable to other metal / adhesive systems.

Chapter 9. Summary

- The wedge test data provide an empirical correlation between the chemical state of adherend surfaces and bond durability.
- Mechanical interlocking as a major mechanism in controlling durability of epoxy-bonded aluminum structural joints is not supported by the preceding data.
- The phosphorous acid anodizing data demonstrate that intrinsic hydrolytic stability of the surface oxide is not an absolute prerequisite for durable adhesion, but could add to durability in flawed areas, or capillary gaps of the bond line where condensed water would cause the transformation of oxide to hydroxide resulting in stresses at the bond line.
- Adhesive bonds prepared with adherends that were anodized in H_3PO_4 and H_3PO_3 electrolytes to form porous oxides with identical topographies exhibited significantly different crack growth rates.
- NMR results revealed a higher density of coordinatively unsaturated alumina (tetrahedral Al-O) in the bulk of HPAA oxides compared to PAA oxides.
- As with γ-alumina, which has a high degree of tetrahedral coordination and a highly reactive (catalytic) surface, it is reasonable to assume that the bulk tetrahedral coordination observed with the HPAA oxide translates into higher surface reactivity for HPAA oxides compared to PAA oxides, and influences the type and density of interaction with the adhesive.
- Regardless of the surface topography, specific chemical functional groups on the adherend surface affected bond durability either positively or negatively.

- Non-reactive surface groups, such as phenyl- and ethyl-, provided only secondary bonding (dispersion forces) with the adhesive and resulted in adhesive joints that exhibited poor durability in the presence of moisture.
- The tertiary amine of NTMP apparently catalyzed the reaction of epoxides in the adhesive, without chemical interaction *across* the interface, resulting in poor initial joint strengths and poor durability.
- Adherends functionalized with vinylphosphonic acid resulted in improved durability regardless of the surface topography.
- VPA anodized adherends consist of a microscopically flat surface oxide reacted with a single layer of VPA, and yielded durability comparable to joints with porous PAA adherends.
- Excellent durability of VPA treated adherends is attributed to the nucleophilic addition (Michael addition) of amine curing agents to the surface carbon double bond, which is made possible by electron withdrawal by the adjacent electronegative phosphonate group.
- VPA surface functionalization promotes adhesive bond durability by formation of a hydrolytically stable interphase, which includes:
    - hydrolytically stable Al-O-P bonds of VPA to the oxide,
    - hydrolytically stable P-C bonds inherent in the organophosphonates,
    - hydrolytically stable addition of the dicyandiamide to surface VPA
    - subsequent cross linking of remaining reactive groups of the multifunctional curing agent with epoxide
    - reduction in excess free amine at the interface that could result in alkaline dissolution of the adherend oxide

Appendix A. Aluminum Alloy Compositions

Registered Compositions of Aluminum Alloys (w/w)

Registered Designation	Si	Fe	Cu	Mn	Mg	Cr	Zn	Ti	Others Each[297]	Others Total	Al
1050A[298]	0.25	0.4	0.05	0.05	0.05	…	0.07	0.05	0.03	…	99.50
1199[299]	0.006	0.006	0.006	0.002	0.006	…	0.006	0.002	0.002	…	99.99
2014A[298]	0.50-0.9	0.50	3.9-5.0	0.40-1.2	0.20-0.8	0.10	0.25	0.15300	0.05	0.15	remainder[301]
2024[299]	0.50	0.50	3.8-4.9	0.3-0.90	1.2-1.8	0.10	0.25	0.15	0.05	0.15	remainder
2219[299]	0.20	0.30	5.8-6.8	0.2-0.40	0.02	…	0.10	0.02-0.10	0.05	0.15	remainder[302]
5251[298]	0.40	0.50	0.15	0.1-0.50	1.7-2.4	0.15	0.15	0.15	0.05	0.15	remainder
6061[299]	0.40-0.8	0.7	0.15-0.4	0.15	0.8-1.2	0.04-0.35	0.25	0.15	0.05	0.15	remainder
7075[299]	0.40	0.50	1.2-2.0	0.3	2.1-2.9	0.18-0.28	5.1-6.1	0.20	0.05	0.15	remainder

297. "Others" includes listed elements for which no specific limit is shown as well as unlisted metallic elements. The producer may analyze samples for trace elements not specified in the registration or specification. However, such analysis is not required and may not cover all metallic "other" elements. Should any analysis by the producer or the purchaser establish that an "others" element exceeds the limit of "Each" or that the aggregate of several "others" elements exceeds the limit of "total", the material shall be considered non-conforming.*

298. *Registration Record of International Alloy Designations and Chemical Composition Limits for Wrought Aluminum and Wrought Aluminum Alloys*, The Aluminum Association, Washington, D.C., Revised June 1, 1985.

299. *Registration Record of Aluminum Association Designations and Chemical Composition Limits for Wrought Aluminum and Wrought Aluminum Alloys*, The Aluminum Association, 900 19th Street N.W., Washington, D.C. 20006, Revised December 1993.

300. total Zr + Ti = 0.20

301. also → 0.10 Ni

302. also → 0.05-0.15 V; 0.10-0.25 Zr

Appendix B. A Listing of Organophosphonic Acids Used in This Investigation

Name	Supplier	Purity (w/w)
Allylphosphonic Acid	Specialty Organics, Inc.	99.9%
Ethylphosphonic Acid	Aldrich Chemical Company	99.0%
Methylphosphonic Acid	Specialty Organics, Inc.	99.9%
Nitrilotris(methylene) triphsophonic acid	Aldrich Chemical Company	undetermined
Phenylphosphonic Acid	Aldrich Chemical Company	99.0%
Vinylphosphonic Acid	Hoechst-Celanese (Clariant)	65-70%

Appendix C. ^{31}P NMR Analysis of Technical Grade Vinylphosphonic Acid Solution

VINYL PHOSPHONIC ACID TECHNICAL

$CH_2 H_5 O_3 P$

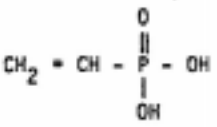

Product Data are as follows:

		Typical Dilutions Used in Experiments	
Vinyl Phosphonic Acid	65% m/m (weight percentage)		
		17.6%	9.2%
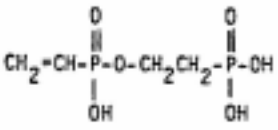	6% m/m	1.6%	0.8%
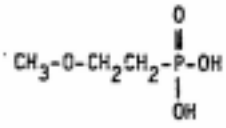	6% m/m	1.6%	0.8%
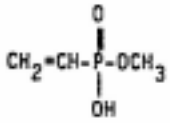	4% m/m	1.1%	0.6%
Polyvinylphosphonic acid	6% m/m	1.6%	0.8%
H_3PO_4	7% m/m	1.9%	1.0%
unknown	5% m/m	1.3%	0.7%

Method: "Phosphorus NMR"

Vita

Gary Alan Nitowski

The author was born in Natrona, PA on November 22, 1956, and graduated from Highlands High School in 1974. He attained a Bachelor of Science degree in Biochemistry from the Pennsylvania State University in 1979. In 1980 he was hired by the Aluminum Company of America (Alcoa) as a research technician in the Surface Science Group of the Alloy Technology Division. After attending evening classes, he received a Master of Science degree in Colloids, Polymers, and Surfaces from Carnegie-Mellon University in 1985. In 1986, he was promoted to the position of scientist and became the principal investigator in Alcoa's adhesion and surface pretreatment program. In 1993, with the sponsorship of Dr. Karl Wefers - Alcoa, he enrolled in and was resident at Virginia Polytechnic Institute & State University studying under the direction of Dr. John G. Dillard. After completion of the residency requirement, he returned to Alcoa as program manager for the corporate surface pretreatment program. His current interests are in the area of aluminum corrosion resistance, electrochemistry, and organic/inorganic interfaces. He is co-author of eleven U.S. patents dealing with surface treatments of aluminum. He is a member of the Adhesion Society, the American Chemical Society, SAE, and Sigma Xi. Gary is married to Vicki Larraine Craig, has three children Tony, Joshua, and Elizabeth, and resides in Lower Burrell, Pa.